



**ANALYSIS OF METHODS FOR
DETERMINING HIGH CYCLE FATIGUE
STRENGTH OF A MATERIAL WITH
INVESTIGATION OF Ti-6Al-4V GIGACYCLE
FATIGUE BEHAVIOR**

DISSERTATION

Randall D. Pollak, Major, USAF

AFIT/DS/ENY/06-07

**DEPARTMENT OF THE AIR FORCE
AIR UNIVERSITY**

AIR FORCE INSTITUTE OF TECHNOLOGY

Wright-Patterson Air Force Base, Ohio

APPROVED FOR PUBLIC RELEASE; DISTRIBUTION UNLIMITED

The views expressed in this dissertation are those of the author and do not reflect the official policy or position of the United States Air Force, Department of Defense, or the United States Government.

AFIT/DS/ENY/06-07

ANALYSIS OF METHODS FOR DETERMINING HIGH CYCLE FATIGUE
STRENGTH OF A MATERIAL WITH INVESTIGATION OF Ti-6Al-4V
GIGACYCLE FATIGUE BEHAVIOR

DISSERTATION

Presented to the Faculty of the
Graduate School of Engineering and Management
Air Force Institute of Technology
Air University
Air Education and Training Command
in Partial Fulfillment of the Requirements for the
Degree of Doctor of Philosophy

Randall D. Pollak, B.S., M.S.

Major, USAF

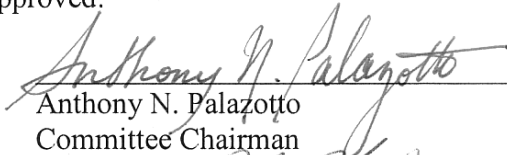
October 2005

APPROVED FOR PUBLIC RELEASE; DISTRIBUTION UNLIMITED

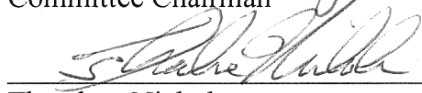
ANALYSIS OF METHODS FOR DETERMINING HIGH CYCLE FATIGUE
STRENGTH OF A MATERIAL WITH INVESTIGATION OF Ti-6Al-4V
GIGACYCLE FATIGUE BEHAVIOR

Randall D. Pollak, B.S., M.S.
Major, USAF

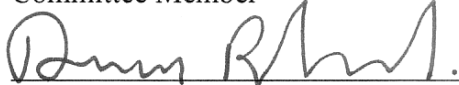
Approved:


Anthony N. Palazotto
Committee Chairman

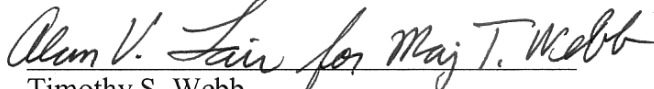
13 Oct 05
Date


Theodore Nicholas
Committee Member

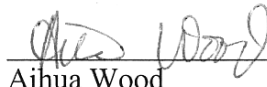
13 Oct 05
Date


Dursun A. Bulutoglu
Committee Member

19 Oct 05
Date



Timothy S. Webb
Committee Member

6 Dec 05
Date


Aihua Wood
Dean's Representative

19 Oct 05
Date

Accepted:


Robert A. Calico, Jr.
Dean, Graduate School of Engineering and Management

Dec 05
Date

ACKNOWLEDGEMENTS

The work presented in this document would not have been possible without the guidance, assistance, and support of others. First, I would like to thank Dr. Ted Nicholas for agreeing to work with me and helping to scope a suitable research project which tapped both my interest and expertise. In addition, his technical guidance and contributions throughout the project were invaluable. It was truly an honor and a privilege to work with such a world-renowned leader in the field of materials testing. Next I'd like to thank Dr. Anthony Palazotto for his leadership, guidance, and support throughout my research. Dr. Palazotto was instrumental in leading me through the details necessary to complete this work and my degree. I'd also like to thank Dr. Ryan Morrissey of the Air Force Research Laboratory's Materials and Manufacturing Directorate for his technical contributions and for ensuring the testing necessary for this research was completed accurately and on time. Without his experiments, there would be no dissertation. I'd also like to thank Dr. Dursun Bulutoglu, Dr. Tim Webb, and Dr. Aihua Wood from AFIT's Department of Mathematics and Statistics for their review of my work. Last but certainly not least, I'd like to thank my wife for her unlimited patience and understanding throughout this research and my program.

Ty Pollak

TABLE OF CONTENTS

List of Figures	viii
List of Tables	xiv
Nomenclature	xvii
Abstract	xxi
I. Introduction	1
II. Preliminaries	12
An Introduction to Fatigue	12
Definition of Key Terms	13
Stress-Life (S-N) Curves	13
Fatigue Crack Growth	16
Mean Stress Effects	17
Scatter in Fatigue Data	19
Statistical Analysis of Fatigue Experiments	20
Introduction to Probability and Statistics	20
Probabilistic Approach to Fatigue Strength Testing	26
Conventional S-N Testing	29
Quantal Response Tests	30
Accelerated Stress Tests	35
Advanced Statistical Methods	36
Ultra High Cycle Fatigue Research	39
Ultrasonic Fatigue Testing	39
Fatigue Limit Behavior in the Gigacycle Regime	41
Air Force Research Laboratory Research	45
Titanium and Titanium Alloys	46
Introduction to Titanium and Titanium Alloys	47
Heat Treatment	48
Conclusion	49
III. Investigation of the Staircase Method	50
Dixon-Mood Analysis of Staircase Data	50
Modifications of the Dixon-Mood Estimate for Mean	55
Modifications of the Dixon-Mood Estimate for Standard Deviation	60

	Svensson-Lorén Correction for Small-Sample Tests	62
	Braam and van der Zwaag Correction	63
	Fang et al Approach	68
	Rabb's Investigation of Staircase Settings	69
	Summary of Standard Deviation Methods	71
	Investigation of Staircase Parameters using Numerical Simulation	72
	Selection of the Number of Simulation Runs	72
	Effect of Starting Stress on Dixon-Mood Standard Deviation	73
	Effect of Step Size on Dixon-Mood Standard Deviation	75
	Correction for Dixon-Mood Standard Deviation	80
	Bootstrapping to Reduce Standard Deviation Scatter	85
	The Bootstrap and the Dixon-Mood Estimate	86
	Use of Bootstrapping in Conjunction with Bias Correction	91
	Iteration to Improve Standard Deviation Estimates	94
	Summary	97
IV.	Use of the Modified Staircase Method for Ti-6Al-4V Gigacycle Test Data	99
	Introduction	99
	Experimental Background	101
	Material Processing and Properties	101
	Ultrasonic Fatigue Testing Machine	102
	Test Specimens	103
	Experimental Data	104
	Reworking the Data	106
	Staircase Analysis	108
	Assumption of Normality	109
	Standard Deviation Analysis	112
	Summary	117
V.	Investigation of Test Design using the Random Fatigue Limit Model	119
	Staircase Testing at Multiple Numbers of Cycles	119
	Methodology of the RFL Model	124
	Genealogy of the RFL Model	124
	RFL Model Formulation	127
	Estimating the Model Parameters	129

Test Design using the RFL Model	130
Scoping the Problem	131
Three Approaches to Consider	132
Simulation Scenarios	135
Simulation Process	136
Simulation Results	140
Summary	145
VI. Analysis of Beta Annealed Ti-6Al-4V Test Data using RFL Modeling and Alternative Means	146
Experiment Objective	146
Experimental Background	146
Material Microstructure	146
Test Machine and Specimen Design	148
Test Strategy	149
Experimental Data	149
Analysis with the RFL Model	151
RFL Model Applied to α - β Ti-6Al-4V Data	153
Alternative Models for Representing Knee-shaped <i>S-N</i> Curves	155
Bilinear “Hockey Stick” Model	155
Nishijima Hyperbolic Model	156
Fatigue Strength Distribution	157
Maximum Likelihood Method for Model Fitting	159
Analysis of α - β Ti-6Al-4V Data	160
Beta Annealed Ti-6Al-4V Analysis	166
Bilinear Model	166
Hyperbolic Model	167
Quantal Response Analysis	167
Summary	168
VII. Summary and Conclusions	169
Problem Restatement	169
Summary of Findings	170
Investigation of the Staircase Method	170
Experimental Investigation of α - β Ti-6Al-4V	172

Test Strategies and the Random Fatigue Limit (RFL) Model	175
Beta Annealed Ti-6Al-4V Data Analysis	177
Areas for Further Research	180
Staircase Investigation	180
Bootstrapped P-S-N Plots	180
Mean Stress Effects	180
Residual Stress Effects	181
Conclusions.....	181
Appendix A. Experimental Stress-Life Data Collected from Ti-6Al-4V Tests.....	182
Appendix B. Detailed Results for Comparison of Methods for Mean Fatigue Strength Estimation	185
Appendix C. Overview of Rabb's Use of Size Effect for Estimating Fatigue Strength Standard Deviation.....	188
Appendix D. Staircase Simulation Code	191
Appendix E. Staircase Simulation Data for Mean Fatigue StrengthH using the Dixon- Mood Method.....	208
Appendix F. Simulation Results for Staircase Parameter Investigation	213
Appendix G. Simulation Results for Staircase Bootstrapping Analysis.....	235
Appendix H. Probabilistic Stress-Life Curves using the Random Fatigue Limit Model Based on Simulated Data	237
Bibliography	247
Vita	254

LIST OF FIGURES

Figure 1. Materials Damage Tolerance Action Team's research schedule (from National HCF S&T Program's 2002 Annual Report [5]).	5
Figure 2. Typical $S-N$ curve (from Dowling [30]).	14
Figure 3. Fatigue limit and fatigue strength on typical $S-N$ curves.	15
Figure 4. Stress-life curves for various stress ratios (from Dowling [30]).	17
Figure 5. Constant life diagram for 7075-T6 aluminum (from Dowling [30]).	18
Figure 6. Normalized amplitude-mean diagram for 7075-T6 aluminum (from Dowling [30]).	19
Figure 7. Histogram showing lognormal fatigue life based on Sinclair and Dolan's data (from Sobczyk and Spencer [80]).	24
Figure 8. Conceptual $S-N$ curves for specified P values (from Little and Jebe [46]).	27
Figure 9. $P-S-N$ surface showing $P-S$ trace (from Little and Jebe [46]).	27
Figure 10. $P-S-N$ surface showing $P-N$ trace (from Little and Jebe [46]).	28
Figure 11. $P-S$ curve for typical quantal response data (from Little and Jebe [46]).	32
Figure 12. Illustration of the staircase test method (from Little [46]).	33
Figure 13. Fatigue life and fatigue strength distributions (from Nelson [58]).	37
Figure 14. Probabilistic $S-N$ curves based on random fatigue limit modeling of nickel superalloy data (from Meeker and Escobar [50]).	37
Figure 15. Schematic view of a particluar ultrasonic test apparatus (from Bathias and Ni [16]).	40
Figure 16. Conceptual $S-N$ curves using the concept of a bimodal model (from Shiozawa et al [77]).	43
Figure 17. Schematic illustration of bimodal $S-N$ behavior (from Mughrabi [54]).	44
Figure 18. $S-N$ test data generated from HCF S&T program for Ti-6Al-4V under fully-reversed loading [4].	46
Figure 19. Notional staircase data for illustration of the Dixon-Mood method.	54
Figure 20. Notional staircase data for illustration of the Brownlee <i>et al</i> method.	56
Figure 21. Graphical solution of the Braam and van der Zwaag standard deviation equation for the staircase data shown in Figure 19.	65
Figure 22. Effect of starting stress on Dixon-Mood standard deviation estimates for underlying Normal(400,5) with $s/\sigma = 1$.	74
Figure 23. Effect of step size and number of specimens on Dixon-Mood standard deviation estimates for underlying Normal(400,5).	77

Figure 24. Effect of step size and number of specimens on Dixon-Mood standard deviation estimates for underlying Normal(400,15).	77
Figure 25. Standard deviation bias for $S_{init} = \mu$ using the Dixon-Mood method.	78
Figure 26. Standard deviation scatter for $S_{init} = \mu$ using the Dixon-Mood method.	79
Figure 27. Svensson-Lorén standard deviation correction applied to normalized $\bar{\sigma}_{DM}$ estimates.	80
Figure 28. Proposed standard deviation correction applied to normalized $\bar{\sigma}_{DM}$ estimates.	82
Figure 29. Comparison of normalized standard deviations for Dixon-Mood mean, Svensson-Lorén correction, and proposed correction for $N = 20$ specimens. ..	83
Figure 30. Bootstrap results sorted by Dixon-Mood standard deviation for 120 staircases with $N = 15$ and $s = 1.5\sigma$	88
Figure 31. Bootstrap results sorted by Dixon-Mood standard deviation for 50 staircases with $N = 12$ and $s = 1.0\sigma$	88
Figure 32. Bootstrap results sorted by Dixon-Mood standard deviation for 100 staircases with $N = 8$ and $s = 1.7\sigma$	89
Figure 33. Bootstrap results sorted by Dixon-Mood standard deviation for 50 staircases with $N = 20$ and $s = 1.7\sigma$	89
Figure 34. Frequency histograms for Dixon-Mood standard deviation and bootstrapped standard deviation for 50 staircases with $N = 12$ and $s = 1.0\sigma$	90
Figure 35. Convergence of mean of fatigue strength mean estimates using Dixon-Mood statistics for 8-specimen subtests with 1.7σ step, initial standard deviation estimate of 15 and initial mean estimate of 390 for true underlying distribution Normal($\mu = 400, \sigma = 5$).	95
Figure 36. Convergence of mean of fatigue strength standard deviation estimates using Dixon-Mood statistics for 8-specimen subtests with 1.7σ step, initial standard deviation estimate of 15 and initial mean estimate of 390 for true underlying distribution Normal($\mu = 400, \sigma = 5$).	96
Figure 37. Distribution of standard deviation estimates using Dixon-Mood statistics after 50 iterations of 8-specimen subtests for both high and low initial estimates of standard deviation using step size 1.74σ	97
Figure 38. Schematic of possible dual-phase $S-N$ behavior.	99
Figure 39. Thermal image of Ti-6Al-4V gage section during 200 MPa test using the 20-kHz ultrasonic fatigue machine (provided by AFRL/MLLM).	100
Figure 40. Schematic drawing and photograph of the 20-kHz ultrasonic fatigue testing apparatus (provided by AFRL/MLLM).	103
Figure 41. Specimen geometry (provided by AFRL/MLLM).	104

Figure 42. Fatigue data for α - β Ti-6Al-4V at both conventional and 20 kHz frequencies at $R = -1$.	105
Figure 43. Initial staircase data for 10^9 -limited tests of α - β Ti-6Al-4V under $R = -1$ loading using the 20 stress-relief annealed (SRA) specimens.	106
Figure 44. Ti-6Al-4V data transformed into a single staircase.	108
Figure 45. Dixon-Mood calculations for 23-specimen Ti-6Al-4V staircase data.	109
Figure 46. Bilinear curve fit using least squares for Ti-6Al-4V data.	110
Figure 47. Residuals in the HCF region for Ti-6Al-4V data at $R = -1$ for a horizontal fatigue limit.	111
Figure 48. Probability plot for normal distribution fit of Ti-6Al-4V residuals.	112
Figure 49. Probability plot for extreme value distribution fit of Ti-6Al-4V residuals.	112
Figure 50. Bootstrap input and output for the 23-specimen Ti-6Al-4V staircase.	114
Figure 51. Standard deviation results using modified staircase analysis for 30 runs using Ti-6Al-4V fatigue strength estimates as inputs.	115
Figure 52. Simulated Dixon-Mood standard deviation results for 23-specimen staircase starting at 400 MPa with 10 MPa step for underlying Normal(406.4,12.45).	116
Figure 53. Several 30-specimen histograms randomly generated using the same conditions as Figure 52.	117
Figure 54. Probabilistic stress-life curve with constant standard deviation in fatigue life as a function of stress.	124
Figure 55. Probabilistic stress-life curve with non-constant standard deviation in fatigue life as a function of stress.	125
Figure 56. P - S - N curve exhibiting a bend-back effect.	126
Figure 57. Illustration of test designs used with the RFL model.	134
Figure 58. Nishijima S - N model.	135
Figure 59. Coarse P - S - N plot of scenario #1 material behavior.	137
Figure 60. Fine P - S - N plot of scenario #1 material behavior.	137
Figure 61. Coarse P - S - N plot of scenario #2 material behavior.	138
Figure 62. Fine P - S - N plot of scenario #2 material behavior.	138
Figure 63. Coarse P - S - N plot of scenario #3 material behavior.	139
Figure 64. Fine P - S - N plot of scenario #3 material behavior.	139
Figure 65. RFL analysis for scenario #1 using the traditional staircase and balanced strategy for random number set #1.	141
Figure 66. RFL analysis for scenario #3 using the traditional staircase and balanced strategy and random number set #1.	141

Figure 67. Comparison of mean fatigue strength results for scenario #1.	143
Figure 68. Comparison of mean fatigue strength results for scenario #3.	143
Figure 69. Comparison of mean fatigue strength results for scenario #2.	144
Figure 70. Microstructure for beta annealed Ti-6Al-4V specimens as used in 20-kHz fatigue testing (provided by AFRL/MLLM).	147
Figure 71. Comparison of microstructure for (a) an α - β (solution treated and overaged, STOA) Ti-6Al-4V alloy, and (b) a lamellar beta annealed Ti-6Al-4V alloy (from Nalla <i>et al</i> [57]).	148
Figure 72. Stress-life data for beta annealed Ti-6Al-4V tests at $R = -1$	150
Figure 73. Stress-life data for Ti-6Al-4V α - β (bimodal) and beta annealed (lamellar) microstructures at $R = -1$	151
Figure 74. Analysis of beta annealed Ti-6Al-4V data using the RFL model.	152
Figure 75. Simulated data set for a linear S - N curve with horizontal fatigue limit.	153
Figure 76. RFL model applied to the α - β Ti-6Al-4V data.	154
Figure 77. Bilinear (hockey stick) S - N model.	155
Figure 78. Sample S - N curve shapes using the Nishijima hyperbolic model.	156
Figure 79. Probability functions for the extreme value distribution.	158
Figure 80. Maximum likelihood analysis of fully-reversed α - β Ti-6Al-4V data using the bilinear model with extreme value distribution for fatigue strength.	161
Figure 81. P - S - N plot of α - β Ti-6Al-4V data using the bilinear model with extreme value distribution for fatigue strength.	162
Figure 82. Sensitivity plots based on log-likelihood for parameter settings using the bilinear model for the α - β Ti-6Al-4V data.	163
Figure 83. Maximum likelihood analysis of fully-reversed α - β Ti-6Al-4V data using the hyperbolic model with extreme value distribution for fatigue strength.	164
Figure 84. P - S - N plot of α - β Ti-6Al-4V data using the hyperbolic model with extreme value distribution for fatigue strength.	165
Figure 85. Bilinear model with extreme value distribution applied to beta annealed Ti- 6Al-4V data.	166
Figure 86. Hyperbolic model with extreme value distribution applied to beta annealed Ti-6Al-4V data.	167
Figure 87. Initial staircase data for 10^9 -limited tests of α - β Ti-6Al-4V under $R = -1$ loading using the 20 stress-relief annealed (SRA) specimens (numbers in parentheses indicate number of runouts).	173
Figure 88. AFRL/MLLM's α - β Ti-6Al-4V data reworked into a single staircase.	174

Figure 89. Experimental results for beta annealed Ti-6Al-4V tests at $R = -1$ (number of runouts in parentheses).....	177
Figure 90. $P-S-N$ plot of α - β Ti-6Al-4V data ($R = -1$) using the bilinear model with extreme value distribution for fatigue strength with constant standard deviation.	178
Figure 91. $P-S-N$ plot of α - β Ti-6Al-4V data ($R = -1$) using the Nishijima model with extreme value distribution for fatigue strength with constant standard deviation.	179
Figure 92. Effect of starting stress on calculated fatigue strength mean for a Normal(400,5) underlying fatigue strength distribution.	209
Figure 93. Effect of starting stress on scatter of fatigue strength mean for a Normal(400,5) underlying fatigue strength distribution.	209
Figure 94. Effect of step size on calculated mean fatigue strength using the Dixon-Mood method for a Normal(400,5) underlying fatigue strength distribution.	211
Figure 95. Effect of step size on scatter of mean fatigue strength using the Dixon-Mood method for a Normal(400,5) underlying fatigue strength distribution.	212
Figure 96. Histogram of staircase simulation results for 0.1σ step and 8 specimens....	214
Figure 97. Histogram of staircase simulation results for 0.25σ step and 8 specimens..	215
Figure 98. Histogram of staircase simulation results for 0.5σ step and 8 specimens....	216
Figure 99. Histogram of staircase simulation results for 0.75σ step and 8 specimens..	217
Figure 100. Histogram of staircase simulation results for 1.0σ step and 8 specimens..	218
Figure 101. Histogram of staircase simulation results for 1.5σ step and 8 specimens..	219
Figure 102. Histogram of staircase simulation results for 2.0σ step and 8 specimens..	220
Figure 103. Histogram of staircase simulation results for 0.1σ step and 20 specimens.	221
Figure 104. Histogram of staircase simulation results for 0.25σ step and 20 specimens.	222
Figure 105. Histogram of staircase simulation results for 0.5σ step and 20 specimens.	223
Figure 106. Histogram of staircase simulation results for 0.75σ step and 20 specimens.	224
Figure 107. Histogram of staircase simulation results for 1.0σ step and 20 specimens.	225
Figure 108. Histogram of staircase simulation results for 1.5σ step and 20 specimens.	226
Figure 109. Histogram of staircase simulation results for 2.0σ step and 20 specimens.	227
Figure 110. Histogram of staircase simulation results for 0.1σ step and 100 specimens.	228
Figure 111. Histogram of staircase simulation results for 0.25σ step and 100 specimens.	229

Figure 112. Histogram of staircase simulation results for 0.5σ step and 100 specimens.	230
Figure 113. Histogram of staircase simulation results for 0.75σ step and 100 specimens.	231
Figure 114. Histogram of staircase simulation results for 1.0σ step and 100 specimens.	232
Figure 115. Histogram of staircase simulation results for 1.5σ step and 100 specimens.	233
Figure 116. Histogram of staircase simulation results for 2.0σ step and 100 specimens.	234
Figure 117. Mean standard deviation estimates for 15-specimen staircase test with step 1σ resulting in 4 stress levels.	235
Figure 118. Standard deviation of standard deviation estimates for 15-specimen staircase test with step 1σ resulting in 4 stress levels.	235
Figure 119. Mean standard deviation estimates for 20-specimen staircase test with step 0.75σ resulting in 4 stress levels.	236
Figure 120. Standard deviation of standard deviation estimates for 20-specimen staircase test with step 0.75σ resulting in 4 stress levels.	236
Figure 121. Scenario #1 using traditional staircase.	238
Figure 122. Scenario #1 using balanced strategy.	239
Figure 123. Scenario #1 using adaptive approach.	240
Figure 124. Scenario #2 using traditional staircase.	241
Figure 125. Scenario #2 using balanced strategy.	242
Figure 126. Scenario #2 using adaptive approach.	243
Figure 127. Scenario #3 using traditional staircase.	244
Figure 128. Scenario #3 using balanced strategy.	245
Figure 129. Scenario #3 using adaptive approach.	246

LIST OF TABLES

Table 1. Various methods of experimental design for fatigue strength testing.	28
Table 2. Summations for illustration of the Dixon-Mood method.	54
Table 3. Comparison of various methods of determining fatigue strength mean for simulated data sets with true mean of 400 MPa starting at 380 MPa (5 MPa step).	59
Table 4. Comparison of Dixon-Mood and Braam-van der Zwaag standard deviation estimates for 12-specimen staircase tests at $s = \sigma = 5$ MPa.	66
Table 5. Comparison of Dixon-Mood and Braam-van der Zwaag standard deviation estimates for 20-specimen staircase tests at $s = \sigma = 5$ MPa.	67
Table 6. Comparison of results for different simulation sizes.	73
Table 7. Constants used in proposed standard deviation correction.	81
Table 8. Comparison of normalized standard deviations using Dixon-Mood, Svensson- Lorén, and the proposed correction for individual random samples.	84
Table 9. Comparison of normalized standard deviations using Dixon-Mood, Braam-van der Zwaag, and the proposed correction for data from Table 5.	85
Table 10. Bootstrap data for $N = 15$ and $s = 1.5\sigma$	87
Table 11. Bootstrap data with bias correction for 4-level staircases using $N = 15$	92
Table 12. Validation runs for proposed bootstrapping rules.	93
Table 13. Transformation of real staircase data.	107
Table 14. P - S data for the 23-specimen Ti-6Al-4V staircase.	113
Table 15. Ti-6Al-4V (stress-relief annealed with no cooling, $R = -1$) fatigue data for 10^8 and 10^9 staircase tests from Morrissey and Nicholas [4; 52].	120
Table 16. Ti-6Al-4V (stress-relief annealed with cooling, $R = -1$) fatigue data for 10^8 and 10^9 staircase tests from Morrissey and Nicholas [4; 52].	121
Table 17. Nishijima S - N model constants for the three S - N scenarios.	136
Table 18. A set of sample simulation runs for scenario #3.	140
Table 19. Summary of simulated results for each strategy/scenario combination.	142
Table 20. Fatigue data for beta annealed Ti-6Al-4V tests at $R = -1$	150
Table 21. RFL model parameters for best fit to beta annealed Ti-6Al-4V data.	152
Table 22. RFL model parameters for best fit to α - β Ti-6Al-4V data.	154
Table 23. Comparison of modeled output using the RFL, bilinear, and hyperbolic models for the α - β Ti-6Al-4V data.	165
Table 24. Fatigue data for α - β Ti-6Al-4V using conventional fatigue machines.	182

Table 25. Fatigue data for α - β Ti-6Al-4V with stress-relief annealing and no cooling for 10^8 and 10^9 staircase tests using 20 kHz ultrasonic machine.	183
Table 26. Fatigue data for α - β Ti-6Al-4V with stress-relief annealing and with cooling for 10^8 and 10^9 staircase tests using 20 kHz ultrasonic machine.	183
Table 27. Fatigue data for α - β Ti-6Al-4V without stress-relief annealing and no cooling for 10^8 staircase tests using 20 kHz ultrasonic machine.	183
Table 28. Fatigue data for additional α - β Ti-6Al-4V tests used to supplement the stress-relief annealed staircase data.	184
Table 29. Fatigue data for beta annealed Ti-6Al-4V using 20-kHz ultrasonic machine.	184
Table 30. Comparison of various methods of determining fatigue strength mean for simulated data sets with true mean of 400 MPa starting 4 steps below the true mean.	185
Table 31. Comparison of various methods of determining fatigue strength mean for simulated data sets with true mean of 400 MPa starting 3 steps below the true mean.	186
Table 32. Comparison of various methods of determining fatigue strength mean for simulated data sets with true mean of 400 MPa starting 3 steps above the true mean.	186
Table 33. Comparison of various methods of determining fatigue strength mean for simulated data sets with true mean of 400 MPa starting 4 steps above the true mean.	187
Table 34. Summary statistics for simulation with 0.1σ step and 8 specimens.	214
Table 35. Summary statistics for simulation with 0.25σ step and 8 specimens.	215
Table 36. Summary statistics for simulation with 0.5σ step and 8 specimens.	216
Table 37. Summary statistics for simulation with 0.75σ step and 8 specimens.	217
Table 38. Summary statistics for simulation with 1.0σ step and 8 specimens.	218
Table 39. Summary statistics for simulation with 1.5σ step and 8 specimens.	219
Table 40. Summary statistics for simulation with 2.0σ step and 8 specimens.	220
Table 41. Summary statistics for simulation with 0.1σ step and 20 specimens.	221
Table 42. Summary statistics for simulation with 0.25σ step and 20 specimens.	222
Table 43. Summary statistics for simulation with 0.5σ step and 20 specimens.	223
Table 44. Summary statistics for simulation with 0.75σ step and 20 specimens.	224
Table 45. Summary statistics for simulation with 1.0σ step and 20 specimens.	225
Table 46. Summary statistics for simulation with 1.5σ step and 20 specimens.	226
Table 47. Summary statistics for simulation with 2.0σ step and 20 specimens.	227

Table 48. Summary statistics for simulation with 0.1σ step and 100 specimens.	228
Table 49. Summary statistics for simulation with 0.25σ step and 100 specimens.	229
Table 50. Summary statistics for simulation with 0.5σ step and 100 specimens.	230
Table 51. Summary statistics for simulation with 0.75σ step and 100 specimens.	231
Table 52. Summary statistics for simulation with 1.0σ step and 100 specimens.	232
Table 53. Summary statistics for simulation with 1.5σ step and 100 specimens.	233
Table 54. Summary statistics for simulation with 2.0σ step and 100 specimens.	234

NOMENCLATURE

α	location parameter of the extreme value distribution
β	scale parameter of the extreme value distribution
β_x	parameters of the random fatigue limit model
$\alpha\text{-}\beta$	designates the two-phase Ti-6Al-4V microstructure
Δ	lookup parameter for Little method of correcting for initial string of survivals or failures in staircase data
$\Delta\sigma$	stress range during cyclic loading
δ_i	delta term designating runout (0) or failure (1)
ε	error term between a data point and the $S\text{-}N$ model
γ	fatigue limit as used in random fatigue limit model
μ	true mean of a distribution
μ'	estimate for mean fatigue strength using the Brownlee <i>et al</i> method
$\hat{\mu}$	estimated mean fatigue strength
μ_γ	mean of the distribution for random fatigue limit
$\overline{\mu}_{DM}$	mean of mean fatigue strength estimates using the Dixon-Mood method
μ_{DM}^σ	standard deviation of mean fatigue strength estimates using the Dixon-Mood method
σ	true standard deviation of a distribution
$\hat{\sigma}$	estimated standard deviation of fatigue strength
σ_γ	standard deviation of the distribution for random fatigue limit
σ_a	stress amplitude during cyclic loading (equals half the stress range)
σ_{ar}	stress amplitude corresponding to fully-reversed loading
σ_{BZ}	standard deviation estimate using the Braam-van der Zwaag correction for staircase data

σ_{BZ}^{mod}	standard deviation estimate using the modified method for the Braam-van der Zwaag correction for staircase data
σ_{DM}	standard deviation estimate using the Dixon-Mood method for staircase data
$\bar{\sigma}_{DM}$	mean of standard deviation estimates using the Dixon-Mood method
σ_{DM}^{σ}	standard deviation of standard deviation estimates using the Dixon-Mood method
$\bar{\sigma}_{DM}^B$	mean of the bootstrapped standard deviation distribution where standard deviation is based on the Dixon-Mood equation
σ_m	mean stress during cyclic loading
σ_{max}	maximum stress during cyclic loading
σ_{min}	minimum stress during cyclic loading
σ_N	standard deviation of fatigue life
σ_{PC}	standard deviation estimate using the proposed non-linear correction for staircase data
$\bar{\sigma}_{PC}$	mean of standard deviation estimates using the proposed non-linear correction for staircase data
$\bar{\sigma}_{PC}^B$	mean of the bootstrapped standard deviation distribution where standard deviation is based on the proposed correction
$\tilde{\sigma}_{PC}^B$	average of the 60 th and 65 th percentiles of the bootstrapped standard deviation distribution where standard deviation is based on the proposed correction
σ_{SL}	standard deviation using the Svensson-Lorén correction for staircase data
$\bar{\sigma}_{SL}$	mean of standard deviation estimates using the Svensson-Lorén correction for staircase data
$\bar{\sigma}_{SL}^B$	mean of the bootstrapped standard deviation distribution where standard deviation is based on the Svensson-Lorén correction
$\tilde{\sigma}_{SL}^B$	average of the 60 th and 65 th percentiles of the bootstrapped standard deviation distribution where standard deviation is based on the Svensson-Lorén correction

σ_{UTS}	ultimate tensile strength
σ_y	yield strength
θ	designates a set of parameters in the maximum likelihood approach
A	constant used in proposed non-linear correction for Dixon-Mood standard deviation; or Nishijima hyperbolic $S-N$ model constant
B	constant used in proposed non-linear correction for Dixon-Mood standard deviation; or Nishijima hyperbolic $S-N$ model constant
C	Nishijima hyperbolic $S-N$ model constant
C'	sum of the stress levels over the last $n - 1$ trials and the $(N + 1)$ st trial using the Brownlee <i>et al</i> method
cdf	cumulative density function
$D(x)$	mathematical expression for cumulative density function
E	Young's modulus; Nishijima hyperbolic $S-N$ model constant
FLS	fatigue limit strength
i	counter; may designate specimen number, iteration number, run number, or stress level depending on context
i_{max}	highest stress level as used in Dixon-Mood equations
k	lookup parameter for Dixon method of correcting for initial string of survivals or failures in staircase data
L	likelihood function
\mathcal{L}	log-likelihood function
LPS	log pseudo-stress
LPS^*	mean of log pseudo-stress values
m	power constant used in proposed non-linear correction for Dixon-Mood standard deviation; slope parameter used in the bilinear model
m_i	number of survivals or failures at stress level i using the Dixon-Mood equations
n	number of specimens which mean fatigue strength estimate will be based on using the Brownlee <i>et al</i> method; or number of simulation runs

N	number of specimens; or number of cycles
N^*	number of cycles at which the bilinear S - N model becomes horizontal
P	probability of failure
$P(x)$	mathematical expression for probability density function
pdf	probability density function
p_i	probability of failure on stress level i
R	fatigue stress ratio
s	step size for the staircase test
S	stress (or pseudostress if a stress parameter is used)
S_0	$i = 0$ stress level for the staircase test
S_f	final stress level tested
S_{init}	initial stress level for the staircase test
Ti-6Al-4V	titanium alloy with 6% aluminum and 4% vanadium, commonly used in aerospace applications and testing
V	log of fatigue limit as used in the random fatigue limit model
W	log of fatigue life as used in the random fatigue limit model

ABSTRACT

The onset of mechanical failures due to metal fatigue has been a constant source of concern for engineers ever since the initial discoveries of fatigue-related phenomena in the early 1800s. Today, aerospace engineers still grapple with the qualitative and quantitative understanding of fatigue behavior in the design and testing of turbine-driven jet engines. The Department of Defense has taken a very active role in addressing this problem with the formation of the National High Cycle Fatigue Science & Technology Program in 1994. The primary goal of this program is to further the understanding of high cycle fatigue (HCF) behavior and develop methods in order to mitigate the negative impact of HCF on aerospace operations. This research supports this program by addressing the fatigue strength testing guidance currently provided by the DoD to engine manufacturers, with the primary goal to investigate current methods and recommend a test strategy to characterize the fatigue strength of a material at a specified number of cycles, such as the 10^9 design goal specified by MIL-HDBK-1783B, or range of cycles.

The research utilized the benefits of numerical simulation to initially investigate the staircase method for use in fatigue strength testing. The staircase method is a commonly used fatigue strength test, but its ability to characterize fatigue strength variability is extremely suspect. A modified staircase approach was developed and shown to significantly reduce bias and scatter in estimates for fatigue strength variance. Experimental validation of this proposed test strategy was accomplished using a dual-phase Ti-6Al-4V alloy. The HCF behavior of a second material with a very different microstructure (beta annealed Ti-6Al-4V) was also investigated. The random fatigue limit (RFL) model, a recently developed analysis tool, was investigated to characterize stress-life behavior but found to have difficulty representing fatigue life curves with sharp transitions. Two alternative models (bilinear and hyperbolic) were developed based on maximum likelihood methods to better characterize the Ti-6Al-4V fatigue life behavior. These models provided a good fit to the experimental data for the dual-phase Ti-6Al-4V and were applied to the beta annealed variant in order to estimate stress-life behavior using a small-sample approach. Based on this research, designers should be better able to make reliable estimates of fatigue strength parameters using small-sample testing.

ANALYSIS OF METHODS FOR DETERMINING HIGH CYCLE FATIGUE STRENGTH OF A MATERIAL WITH INVESTIGATION OF Ti-6Al-4V GIGACYCLE FATIGUE BEHAVIOR

I. INTRODUCTION

Engineering structures are designed to withstand a variety of in-service loading and environmental conditions specific to their intended application. For turbine components used in jet aircraft engines, this operating environment is a harsh regime characterized by high temperatures, high mean loads, and high-frequency vibrations. Materials selected for use under these conditions must be resistant to a variety of damage mechanisms to include yielding, creep deformation, fatigue crack growth, fretting fatigue, and oxidation. The hazards posed by these damage mechanisms have been a constant source of concern to designers throughout the jet aircraft age. With the development and use of high-strength, creep-resistant, oxidation-resistant alloys, a remaining challenge to the turbine designer becomes fatigue resistance – i.e., the ability of a component subjected to cyclic loading below the material’s ultimate strength to operate without functional or catastrophic failure due to the accumulation of microscopic damage.

The engineering community’s efforts to prevent mechanical failures due to fatigue pre-date the aviation era by some eighty years. The first study of metal fatigue is believed to be the work of German mining engineer W. A. J. Albert around 1829 [6], with the introduction of the term *fatigue* as a mechanism of metal failure credited to Poncelet in 1838 [70]. This era saw a rise in fatigue-related research across several countries in response to the increasing use of ferrous materials in engineering structures, and the resulting fatigue failures of components such as stagecoach and railway axles, shafts, gears, beams, and bridge girders [30; 83]. The German engineer August Wöhler is credited by many as the “grandfather” of fatigue due to his exhaustive fatigue tests of smooth and notched railway axles beginning in the 1850s. In addition to the introduction of the widely-used *S-N* diagram (a plot of the number of cycles to failure at a given stress or strain level), Wöhler developed design strategies for avoiding fatigue failure and demonstrated that fatigue was affected by not only cyclic stresses but also the

accompanying steady (mean) stresses [91]. His work also led directly to the concept of a fatigue (or endurance) limit which represents the theoretical maximum cyclic load a material can withstand indefinitely without risk of fatigue failure [83]. As the golden age of the railroads gave way to the automobile era, significant advances in fatigue research continued, to include the mean stress effect studies by Gerber and Goodman, the development of fatigue safety diagrams by Haigh, investigation of reversed loading phenomena by Bauschinger, investigation of the notch effect on fatigue limit by Heyn, formulation of empirical laws to characterize fatigue limit by Basquin, the introduction of the crack growth energy balance by Griffith, life estimation under variable loading by Palmgren, and the recognition of the statistical nature of fatigue by Weibull [30; 83; 88]. Fatigue-related research accelerated as the aviation industry grew, with the formation of the International Committee on Aeronautical Fatigue in 1951. Following the catastrophic failure of three de Havilland Comet airliners in 1953 and 1954, metal fatigue received even greater attention by the aerospace industry. Countless researchers from across the globe have since devoted immeasurable amounts of time and money for the purpose of characterizing and preventing fatigue failures, with an estimated ten fatigue-related publications per day now being published around the world [88].

Despite this enormous amount of research, fatigue failures continue to be a major problem in engineering design. The U.S. Department of Commerce, National Institute of Standards and Technology (formerly National Bureau of Standards), reported in a 1983 study that the total economic impact of fracture of materials was \$119 billion in 1982 dollars, representing 4% of the gross national product [30]. Approximately 80% of these costs were related to fatigue under cyclic loading. The costs to the United States Air Force are equally staggering, in particular those related to high cycle fatigue (HCF). HCF is the crack growth phenomenon related to components subjected to low stresses relative to the material's ultimate strength but very large numbers of cycles, either due to extremely long service life or very high frequency loads, or both. HCF is a particular concern in gas turbine engine design due to the very high frequency aeromechanical vibratory loads. Air Force statistics show that between 1982 and 1996, 56% of Class A (the most serious) engine-related failures were due to HCF [5]. HCF continues to be a major safety concern, leading to increased maintenance and inspections, affecting engine

reliability, availability, and maintainability. In fiscal year 1994, approximately 850,000 maintenance man-hours were expended as part of HCF risk management inspections, with annual cost of HCF to the Air Force and Navy estimated to be over \$400 million [5]. Reducing the impact of HCF-related failures and maintenance is currently a major goal of Department of Defense research.

To help eliminate HCF as a major cause of engine-related failures, the U.S. Government officially began the National HCF Science and Technology (S&T) Program in December 1994 [5]. This program is directed by an Air Force-led steering group with representatives from the Air Force, Navy, Army, and National Aeronautics and Space Administration (NASA) along with an adjunct advisory panel made up of industry members. In addition, a parallel committee was established in 2000 to share data and technology development with the United Kingdom. Since its inception, the HCF S&T Program has made considerable strides in the understanding of HCF and methods to mitigate its negative impacts. Significant cost savings are already being realized by the Air Force due to these efforts. However, HCF is still a very difficult design challenge. Currently, one of the major efforts of the program is to utilize the technology advancements and research discoveries to update the HCF-related portions of the Engine Structural Integrity Program (ENSIP) documentation. The ENSIP guidance, found in MIL-HDBK-1783B, provides engine manufacturers with recommended design considerations to ensure a structurally-reliable final product. The current guidance recommends a design life goal of 10^9 cycles for engine components subjected to high-frequency vibratory loads, as the following excerpt shows:

“All engine parts should have a minimum HCF life of 10^9 cycles. This number is based on the observation that an endurance limit does not exist for most materials. If it can be shown through analysis or test that a given part will not experience 10^9 cycles during its design life, a number lower than 10^9 may be used... It should be shown that the total time of exposure to any frequency and amplitude is less than 10^9 cycles or that the amplitude is less than the material allowable at 10^9 cycles. An alternate approach is to use a life of 10^9 cycles based on data obtained at shorter lives, but not less than 10^7 cycles, and a demonstrated valid method to extrapolate to 10^9 cycles to establish an endurance limit. Cycles which have vibratory stress amplitudes less than the endurance limit at 10^9 cycles can be considered to have no detrimental effect on pristine material and

can be ignored in damage accumulation evaluation, provided no other damage is present.” (MIL-HDBK-1783B, 15 Feb 2002 [3])

Although the ENSIP guidance provides the 10^9 -cycle design goal, there are no proposed means given within the documentation to validate a material’s ability to withstand these cycles with reasonable statistical confidence. In addition, the mention of alternative approaches for incorporating tests at lower numbers of cycles is not followed up with any recommendations for such an approach. In short, the guidance currently does not address how an engine manufacturer can adequately test to ensure compliance with material HCF design goals. This void is not unintentional but is due to the fact that there has been a very limited amount of research related to the development of efficient yet reliable test methods to characterize fatigue strength in the ultra high cycle regime ($\sim 10^9$ cycles) where test data points are extremely limited. Development of a means to predict the life of a material subjected to high-frequency, small-amplitude loads is one of the objectives of the Materials Damage Tolerance Action Team as part of the HCF S&T Program, as indicated by product 2.6 on the schedule shown in Figure 1. Validating a methodology to test fatigue strength at 10^9 cycles is part of this team’s overall effort.

Approaches to characterizing the fatigue strength of a material must statistically account for the scatter in fatigue data. This scatter is generally due to a variety of factors, some more controllable than others. Some of the relatively controllable factors include inconsistencies in surface finish, deviations in specimen alignment, differences in applied loading conditions, and inconsistent residual stresses. These sources of scatter are generally mitigated through proper experimental procedures. However, scatter in fatigue data is still observed due to the random nature of the microstructure of each specimen, which produces slightly different conditions for crack initiation and growth within each specimen. In the high cycle regime, fatigue life is dominated by the crack initiation phase, which is heavily dependent on microstructural phenomenon related to localized conditions. Thus, the scatter in fatigue data tends to be magnified in the high cycle regime. This behavior has been confirmed by numerous researchers through the years [78; 80]. Based on these and similar findings, any experiment designed to test fatigue strength in the high cycle regime must account for significant scatter in results.

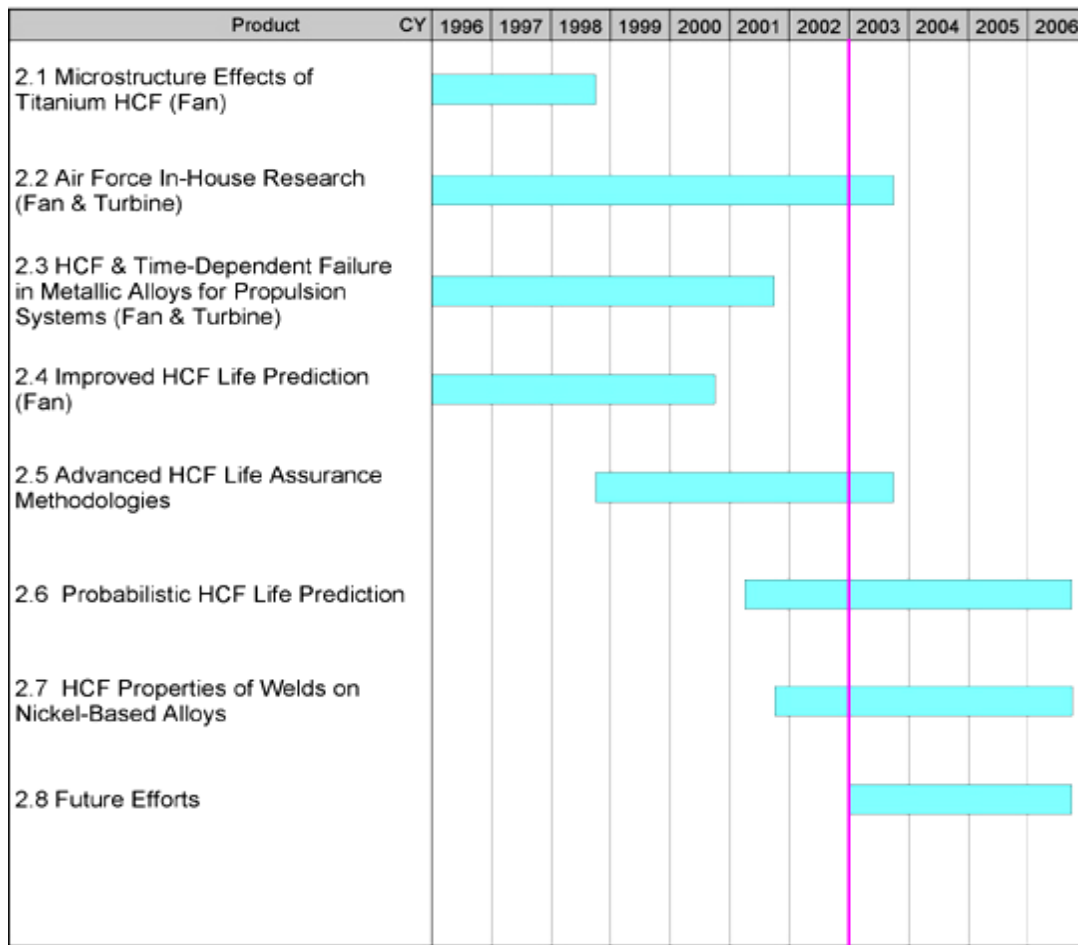


Figure 1. Materials Damage Tolerance Action Team’s research schedule (from National HCF S&T Program’s 2002 Annual Report [5]).

Currently, a variety of test approaches have been used to estimate the fatigue strength of a material. In general, these methods allow a means to deal with the scatter in fatigue data and provide an estimate for the median fatigue strength at a specified number of cycles. For simplicity, one can sort these methods into four broad categories: (1) conventional $S-N$ tests, (2) quantal response tests, (3) accelerated stress tests, and (4) more advanced statistical methods.

The conventional $S-N$ test approach prescribes a series of tests to determine the stress-life curve. Ever since the work of Wöhler, development of these curves for various materials and loading conditions has been the “backbone” of fatigue data generation. In a conventional $S-N$ test approach, a range in fatigue life for each load level can be estimated to produce a family of $S-N$ curves at various levels of probability of failure.

These curves then allow an estimate of fatigue strength at any specified number of cycles. This method has some major drawbacks, however. For one, runouts (specimens which do not fail before the test is concluded) cannot be handled using standard analysis methods since it is unknown when the specimen actually would have failed. For high cycle testing there is often a large number of specimens which do not fail in the allotted test time. This is especially true in the gigacycle regime; i.e., on the order of 10^9 cycles, also called the ultra high cycle fatigue (UHCF) regime. It is simply not practical to test every specimen to failure in this long-life regime where fatigue life has a large scatter and test times would be extraordinarily long. In addition to being unable to handle runout test data, the conventional $S-N$ approach has another major drawback. Although it allows an estimate of the scatter in fatigue life, it is more difficult using conventional $S-N$ analysis to estimate the scatter in fatigue strength for a given number of cycles. For these reasons, a conventional $S-N$ approach becomes impractical for the determination of fatigue strength and its dispersion in the high cycle regime. However, Spindel and Haibach looked at a modified $S-N$ approach to better represent the true shape of the $S-N$ curve as well as provide a better estimate of fatigue limit [81]. For the most part, their analysis was rather incomplete in describing a means to better estimate the fatigue limit using $S-N$ data, but it is significant in that it introduced the concept of maximum likelihood estimation as a means to handle runout data from $S-N$ tests.

As opposed to the conventional $S-N$ approach, quantal response tests are by their nature a “pass/fail” test and are thus better suited to handle runout test data. In a quantal response test, specimens are tested at a certain load level and they either survive the specified number of cycles or they fail. Thus, quantal response analysis methods generally do not need to consider the exact number of cycles to failure. Analysis allows an estimate of median and standard deviation of the fatigue strength at the specified number of cycles based on the proportion of failed specimens at each load level. Four methods of quantal response testing have been applied to fatigue strength testing: (1) the probit method, (2) the staircase (or “up-and-down”) test, (3) the two-point method, and (4) the $\arcsin\sqrt{P}$ method. Quantal response methods show some significant promise in allowing a relatively accurate estimate of fatigue strength (and to a lesser degree, fatigue strength dispersion) in an efficient manner so long as the test parameters are chosen

wisely. Unfortunately, there has been limited research since the widespread availability of computer-based numerical simulation to investigate these tests to determine the optimum set of test parameters for a given fatigue strength distribution.

Another approach to fatigue limit testing is the use of accelerated stress tests. This term essentially includes tests in which the stress level is increased during the test of a specimen in order to ensure the specimen fails in a reasonable number of cycles. This approach differs from the tests discussed so far which utilize a constant stress level for each individual specimen. Two such accelerated stress methods are the Prot method and the step-loading method [61; 72]. Although these methods show some promise in providing an estimate for fatigue strength, they are not developed enough at this time to provide estimates for the dispersion in fatigue strength.

The final group of fatigue limit test approaches are lumped together under the banner of advanced statistical methods. Three such approaches which show some initial promise include random fatigue limit (RFL) modeling, Bayesian methods, and bootstrapping methods. RFL modeling explicitly assumes that each specimen has its own fatigue strength at a given number of cycles based on its unique microstructure. Pascual and Meeker proposed a method incorporating maximum likelihood estimation to produce probabilistic $S-N$ curves which account for the uncertainty in both fatigue life as well as fatigue strength [66]. Their work takes a bold step in better modeling observable characteristics of $S-N$ data using a manageable mathematical formulation. Specifically, the Pascual-Meeker method accounts for the increase in standard deviation of fatigue life at lower stress levels as well as the curvature and flattening of the $S-N$ curve in the HCF regime. As an alternative approach, Bayesian statistical methods are an established means of estimation which utilize prior information, whether qualitative or quantitative in nature, to augment and enhance real test data to provide a better estimate of population parameters [38]. In a Bayesian approach applied to fatigue strength testing, additional sources of information such as fatigue strength distribution parameters at a lesser number of cycles may be used to augment the test data in the gigacycle regime in order to improve the strength distribution parameter estimates. However, Bayesian methods can be quite difficult to implement in practice as the weighting of prior data tends to be a subjective input that can greatly skew the final results. In addition to Bayesian methods,

bootstrap methods may also provide some opportunities to more efficiently model fatigue limit behavior [12]. The bootstrap method is a data-based simulation which utilizes multiple random draws from real test data to make statistical inferences about the underlying population [31]. The main drawback to bootstrapping is the reuse of existing data which may skew the results depending on the presence of outliers as well as any other misrepresentation of the sample with respect to the true population. It is also a somewhat difficult method to explain and rationalize to decision makers.

These methods of fatigue strength evaluation allow a means to address the void in the ENSIP guidance with respect to determination of a material's fatigue strength at 10^9 cycles. The primary goal of the research described in this dissertation is to address this lack of guidance by investigating these methods and refining a test methodology to efficiently investigate the fatigue behavior of a material in the gigacycle regime. The staircase test and the RFL model were selected as two of the most promising analysis approaches. The staircase test offers a relatively simple test protocol and post-test analysis. However, it is very sensitive to test parameter settings, and is prone to a wide scatter for estimates of fatigue strength standard deviation. Recent work by a number of researchers, among them Braam and van der Zwaag [20], Svensson *et al* [84], and Rabb [73], have attempted to modify the staircase analysis method based on results of staircase simulation. The merits and limitations of these approaches are discussed herein. An exhaustive simulation study was undertaken in this study to better quantify the inherent bias and scatter within the staircase method and offer means of dealing with this bias.

The next phase of this research effort focuses on the experimental validation of the proposed test strategy. The objective of this phase is to use the recommended staircase test modifications in a real laboratory environment to assess both the feasibility of conducting the test protocol and the accuracy of the analysis results using a material with relatively well-known fatigue strength properties. The material chosen for this investigation is a dual-phase titanium alloy, or α - β Ti-6Al-4V. Ti-6Al-4V is a commonly used aerospace metal found in turbine blades and other engine components requiring high strength-to-weight ratio, high temperature performance, and corrosion resistance. A significant number of Ti-6Al-4V data points were tested in earlier phases of the National

HCF S&T Program, making it an ideal choice for assessing the results using the recommended test strategy.

The next phase of the research focuses on experimental investigation. With the tests conducted for the validation phase, a significant opportunity exists to conduct some additional research on the gigacycle fatigue behavior of another Ti-6Al-4V variant. Gigacycle fatigue behavior has in the last decade become a very hot topic in the HCF community with the greater availability of data in the gigacycle regime made possible by new ultrasonic test equipment. These test machines, such as the 20-kHz machine operated by the Air Force Research Laboratory's Materials Directorate (AFRL/ML), reduce the time required to conduct a test of 10^9 cycles down to hours rather than days, weeks, or even months using lower frequency machines. Some very interesting findings have been made by various researchers around the world in the last decade or so which directly challenge some long-held beliefs regarding high cycle fatigue behavior. As Bathias *et al* describe in their editorial on gigacycle fatigue,

“Although high-cycle fatigue is one of the most common reasons for failure of components and structures, most experimental investigations are limited to testing periods of between 10^7 and 10^8 cycles, though failures may indeed occur at much higher numbers of cycles, especially in nonferrous materials. However, during the last few years several unexpected failures have been recorded, even in ferrous materials which were assumed to have a fatigue limit in the range of 10^6 - 10^7 cycles... Consequently, extensive research is now required to develop new experimental methods and lifetime prediction theories. Unfortunately very few experimental data exist despite many requests from failure analysts...” (Bathias, Miller, and Stanzl-Tschegg, 1999 [18])

As this excerpt reveals, recent research raises the question of whether a fatigue limit even exists in materials previously thought to exhibit one, such as ferrous metals and most titanium alloys. Several researchers have discovered a bi-modal shape to the stress-life curve which indicates a decrease in fatigue strength in and beyond the gigacycle regime [1; 13; 15; 51; 54; 55; 64; 65; 77; 86]. These investigations indicate that there is a second fatigue failure mechanism due to subsurface crack initiation at these very long fatigue lives which produces the drop in fatigue strength. Prior testing in the gigacycle regime by AFRL/ML using Ti-6Al-4V with an α - β microstructure did not

show this behavior which has been found by other researchers [4]. However, the use of an alloy with alternative microstructure provides an opportunity to investigate the presence of this second failure mechanism in a material with little data in the gigacycle regime. The beta annealed Ti-6Al-4V alloy is such a material. An investigation of the very high cycle fatigue behavior of beta annealed Ti-6Al-4V is presented. In order to investigate this material, an initial study of the RFL model was made to determine a recommended test strategy for fatigue life characterization over a range of cycles.

In summary, the research outlined in this dissertation is captured by the problem statement below:

Investigate and recommend a test methodology to efficiently evaluate the ultra high cycle fatigue behavior of materials, specifically to estimate the median and variance of the fatigue strength in the gigacycle regime based on a limited amount of failure and runout test data. This methodology may serve to support design guidance provided by the Air Force to engine manufacturers. This methodology will be used in conjunction with data from gigacycle fatigue tests of dual-phase Ti-6Al-4V to validate its applicability. Testing will be accomplished using AFRL/MLLM's 20-kHz ultrasonic fatigue testing apparatus. Additional investigation into the nature of fatigue failures in the gigacycle regime will be accomplished through testing of a beta annealed Ti-6Al-4V alloy. Namely, the crack initiation mechanism (surface versus subsurface) will be investigated. Use of the RFL model will be investigated to characterize fatigue life behavior. Alternative analysis methods will be developed as required.

The rest of this dissertation presents the research to address this problem. Chapter II discusses the preliminary background necessary for understanding the probabilistic approach to fatigue strength testing and gigacycle research. Chapter III presents the staircase simulation study, which results in a recommended test strategy for fatigue strength testing with limited samples. Chapter IV presents an experimental application of the test strategy outlined in Chapter III using the α - β Ti-6Al-4V alloy. Chapter V presents an investigation of the random fatigue limit (RFL) model for use in small-sample testing to characterize fatigue life behavior in the very high cycle regime. Chapter VI presents the experiments using beta annealed Ti-6Al-4V to characterize its HCF behavior. The RFL model is used to analyze the experimental data. An alternative analysis approach is developed using maximum likelihood analysis to better characterize

the Ti-6Al-4V data. This alternative approach is applied to both the α - β Ti-6Al-4V data and the beta annealed variant, allowing a characterization of stress-life behavior with a small-sample test. Chapter VII presents a summary of conclusions and areas for further research. Detailed results are outlined in the appendices.

II. PRELIMINARIES

In this chapter, the preliminary background pertinent to the study of high cycle fatigue and fatigue strength testing will be presented. The first part of this chapter presents a brief overview of the nature of fatigue and common means of relating fatigue testing data. The second part focuses on the statistical analysis of fatigue experiments, with an introduction to probability and statistics and an overview of the most applicable methods used to determine the fatigue strength of a material. The third part of this chapter summarizes previous studies of high cycle and ultra high cycle fatigue (HCF/UHCF) which are relevant to this research effort. Finally, the chapter concludes with a short overview of materials processing for Ti-6Al-4V.

An Introduction to Fatigue

It is quite common for components of engineering structures to be subjected to repeated loads, also called cyclic loads. These loads induce cyclic stresses within the material which result in microscopic physical damage, even when the gross stresses are well below the material's ultimate strength. This microscopic damage accumulates over time as the cyclic stressing continues until eventually a macroscopic crack or other damage becomes evident. This process of damage accumulation due to cyclic loading is known as *fatigue*.

Fatigue as a branch of study encompasses a range of scientific and engineering disciplines and offers a variety of interesting phenomena to explore as basic research or for use in engineering applications. It has been a source of study for over 170 years, with an ever-growing body of knowledge which has been analyzed primarily using three major approaches [30]. The traditional approach bases analysis on the mean stresses and associated alternating stresses in the region of the component under investigation. The effects of stress raisers such as grooves, holes, or notches are included in this analysis. This approach, known as the stress-based approach, is considered the traditional method, and was developed to near maturity by 1955. The strain-based approach, on the other hand, involves a more detailed analysis of the deformation near stress raisers. Analysis centers on the localized yielding in these regions. The last approach is the adaptation of

fracture mechanics to fatigue crack growth. Typically, the stress-based approach is used in the analysis of fatigue strength.

Definition of Key Terms

Many practical applications involve the cycling of a component between a minimum stress level and a maximum stress level. Using the stress-based approach, this constant amplitude stressing can be described using some common definitions. Stress range, $\Delta\sigma$, is defined as the difference between the maximum stress (σ_{\max}) and minimum stress (σ_{\min}). The mean stress, σ_m , is defined as the average of the maximum and minimum stresses. The stress amplitude, σ_a , is taken as half the stress range. Mathematically, these definitions are expressed as [30]:

$$\Delta\sigma = \sigma_{\max} - \sigma_{\min}, \quad \sigma_m = \frac{\sigma_{\max} + \sigma_{\min}}{2}, \quad \sigma_a = \frac{\Delta\sigma}{2} \quad (1)$$

The ratio of minimum stress to maximum stress is a very important value used when describing fatigue test results. This ratio, known as the stress ratio, is denoted by R as shown below:

$$R = \frac{\sigma_{\min}}{\sigma_{\max}} \quad (2)$$

Some useful relationships based on these definitions include:

$$\begin{aligned} \Delta\sigma &= 2\sigma_a = \sigma_{\max}(1 - R) \\ \sigma_m &= \frac{\sigma_{\max}}{2}(1 + R) \end{aligned} \quad (3)$$

Notice that when the minimum stress is the negative of the maximum stress, the mean stress is obviously zero, and the associated stress ratio R equals -1. This condition is known as fully-reversed (or completely-reversed) loading. The definitions in Equations 1 through 3 can also be applied to other variables of interest such as strain (ϵ), load (P), bending moment (M), and nominal stress (S).

Stress-Life (S-N) Curves

A stress-life curve relates the nominal stress level (S) to the number of cycles until a specimen fails (N , or N_f) – i.e., catastrophic failure or a crack develops and reaches

some critical length. The nominal stress is usually expressed in terms of stress amplitude although other fatigue parameters are often used as well. The curve is usually drawn with linear S and log N scales as shown in Figure 2, although log S and log N curves are also frequently encountered. Ever since the work of Wöhler, development of these curves for various materials and loading conditions has been the “backbone” of fatigue data generation. As Yen describes, the S - N curve can be interpreted as the progressive structural deterioration and gradual breaking of interatomic bonds under repeated stresses and may be analyzed as a statistical process [47]. The same principles and mathematical approach can be applied to the development of strain-life (ϵ - N) curves as well.

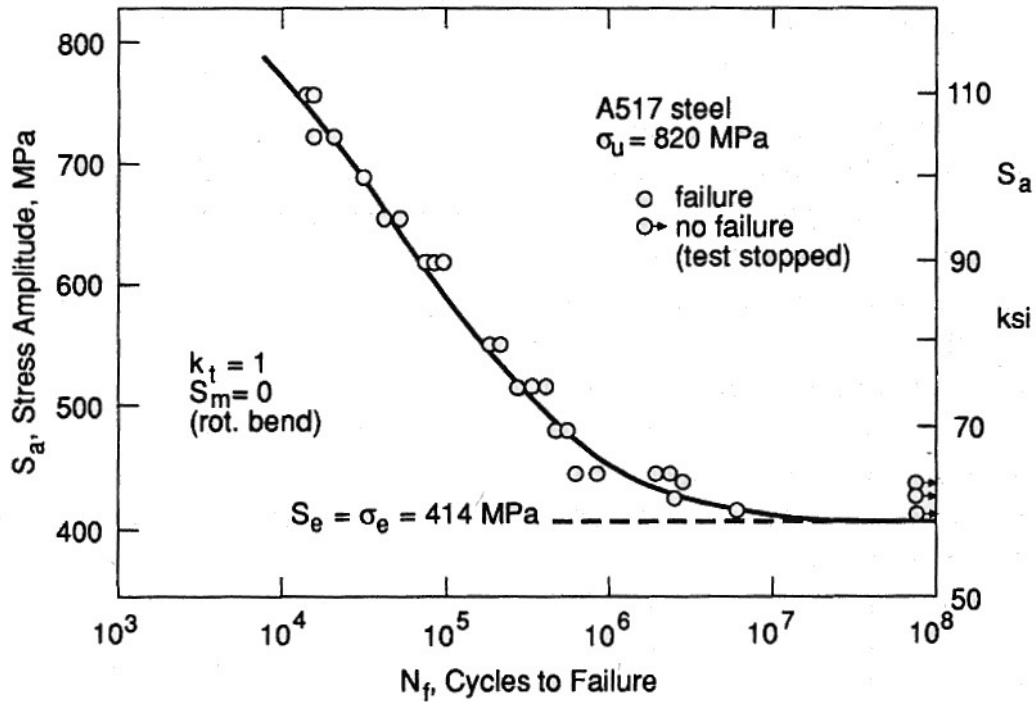


Figure 2. Typical S - N curve (from Dowling [30]).

When S - N data are found to be approximately linear on a log-linear plot, the curve may be modeled using the following expression over the linear region [30]:

$$\sigma_a = C + D \log N_f \quad (4)$$

where C and D are fitting constants. For linear regions on a log-log plot, the following expression is often used (also called Basquin's equation):

$$\sigma_a = A N_f^B \quad (5)$$

where A and B are fitting constants. This equation is more commonly expressed in the following form [30]:

$$\sigma_a = \sigma_f' (2N_f)^b \quad (6)$$

In some materials, there appears to be a noticeable stress level such that fatigue failure does not occur at stresses below this level. This stress level is known as the *fatigue limit*. The term *endurance limit* as used by Nelson [58] specifies the stress level at which the fatigue life becomes a prescribed long but finite life. The term *fatigue strength* specifies the stress amplitude corresponding to a particular fatigue life of interest, as defined by Collins [23] and Dieter [25]. Thus, the fatigue strength at 10^9 cycles is merely the stress level corresponding to failure at 10^9 cycles on the $S-N$ diagram. For materials which do not exhibit a clear fatigue limit, fatigue strength is used to specify the stress level corresponding to a specific long life. In practice, the terms fatigue limit and fatigue strength at a very high number of cycles (such as 10^9) are often used interchangeably. In this work, the term fatigue strength will be used when specifying the stress corresponding to a specific number of cycles. Figure 3 illustrates fatigue limit and fatigue strength on typical $S-N$ curves.

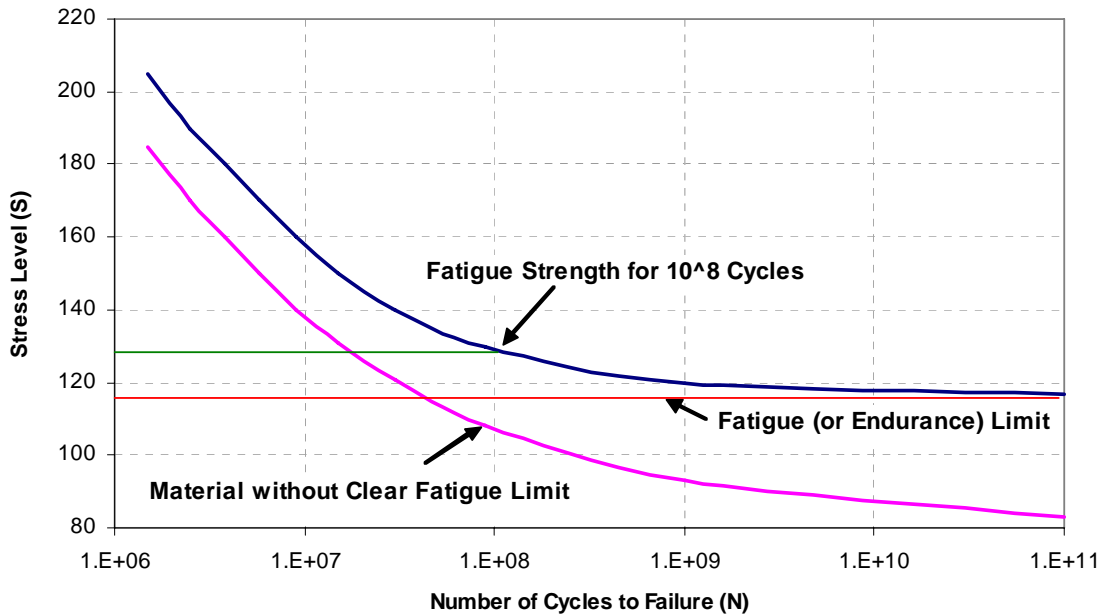


Figure 3. Fatigue limit and fatigue strength on typical $S-N$ curves.

The $S-N$ curve is often conceptually divided into two regions: the low cycle fatigue (LCF) and the high cycle fatigue (HCF) regions. LCF corresponds to the region where failures occur at relatively short lives, typically less than 10^4 cycles. The HCF region corresponds to the part of the curve associated with higher fatigue lives. Note that this division between the LCF and HCF regions is somewhat arbitrary and varies by material. In the HCF region, fatigue life is dominated by the crack initiation phase, which transitions to crack propagation once the crack grows to some macroscopic length. LCF, on the other hand, is more dominated by the crack propagation phase, with a macroscopic crack, severe stress concentration, or other defect already initially present or quickly developed due to high stresses. The term very high cycle fatigue is occasionally used as well, typically referring to lives on the order of 10^6 - 10^9 cycles, although again this term is somewhat arbitrary. Ultra high cycle fatigue (UHCF) typically refers to fatigue at greater than 10^8 cycles. Gigacycle fatigue is a term often used when fatigue lives are on the order of 10^9 cycles.

Fatigue Crack Growth

As a property of crystalline solids (such as aerospace metals), the initiation of fatigue cracks is essentially a problem of dislocation physics, a result of the motion and interaction of dislocations acted upon by cyclic stresses. These dislocations represent discontinuities in the crystal lattice. Yen describes the mechanism of fatigue crack formation in a simplified three-stage manner [47].

In the first stage, the dislocations originally present in the crystal grains multiply, thus increasing the dislocation density. An irregular cell wall or subgrain begins to form. Fine slip bands that tend to appear initially along favorably oriented grains become more numerous as the number of stress cycles increases. Slip bands are regions of intense deformation due to the shear motion between crystal planes. Some of these slip bands remain localized, some broaden, and the very pronounced become persistent slip bands. The crystal grains begin to become distorted and strain-hardened. Then, dislocation motion in one direction may become fully reversed in synch with the stress. New dislocations and their movements are generated only in some local slip zones where microstructural features are not consistent in both directions of motion.

In the second stage, thin ribbon-like extrusions of metal are emitted from the free surface and internal fissures called intrusions develop as the persistent slip bands are matured. These fissures are the initiations of a crack, and tend to occur along the slip planes associated with maximum resolved shear.

In the final stage, the newly formed crack propagates in a zigzag manner along slip planes and cleavage planes from grain to grain, maintaining a general direction perpendicular to the maximum tensile stress. Many factors affect the rate of crack propagation at this point, but as much as 99% of the fatigue life may be spent in the development of these internal fissures and their coalescence into macroscopic cracks.

Mean Stress Effects

Consideration of the effect of mean stress ratio on fatigue life is a primary concern in many fatigue analyses. Presentation of this data is accomplished in several different manners. The most obvious manner is to develop a family of $S-N$ curves for tests run at various stress ratios. These curves are often drawn on the same diagram with different R ratios identified for each curve, as shown in Figure 4.

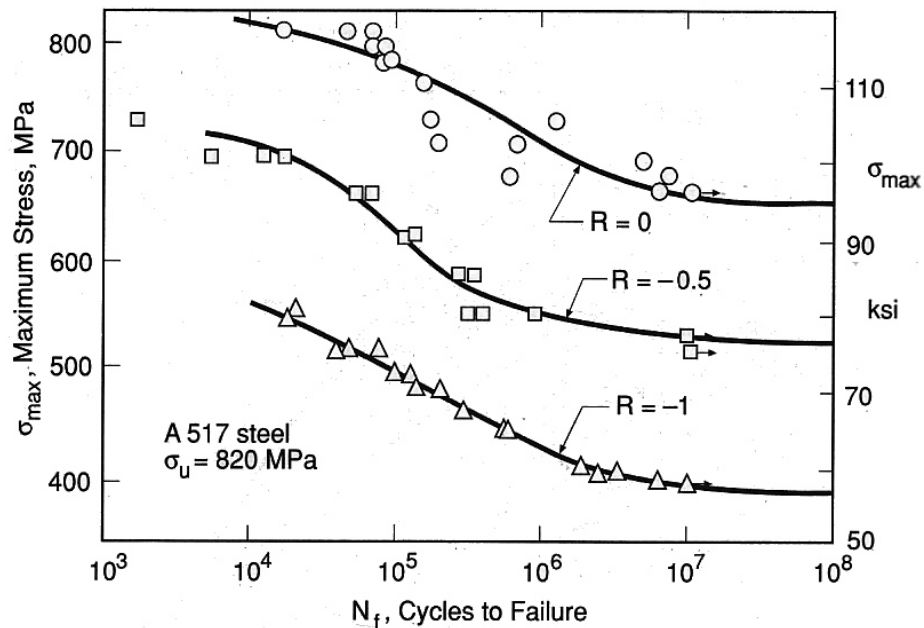


Figure 4. Stress-life curves for various stress ratios (from Dowling [30]).

An alternative means of expressing data at different mean stresses is to use a constant-life diagram. In this type of diagram, data from the various $S-N$ curves at

different stress ratios is replotted with each combination of mean stress and stress amplitude corresponding to a specified value of the number of cycles to failure. Various curves can then be drawn for different values of N , as illustrated by Figure 5. The stress amplitude at zero mean stress (denoted by σ_{ar}) is represented by the intercept ($\sigma_m = 0$) of the constant-life curve. A normalized constant life curve can be drawn using values of the ratio σ_a/σ_{ar} plotted against σ_m for a particular fatigue life. This plot, known as a normalized amplitude-mean diagram, is shown in Figure 6. Various relations have been developed to fit the normalized amplitude-mean data, such as the linear fit (Goodman curve) shown on Figure 6, to more elaborate means such as the Gerber parabola [30].

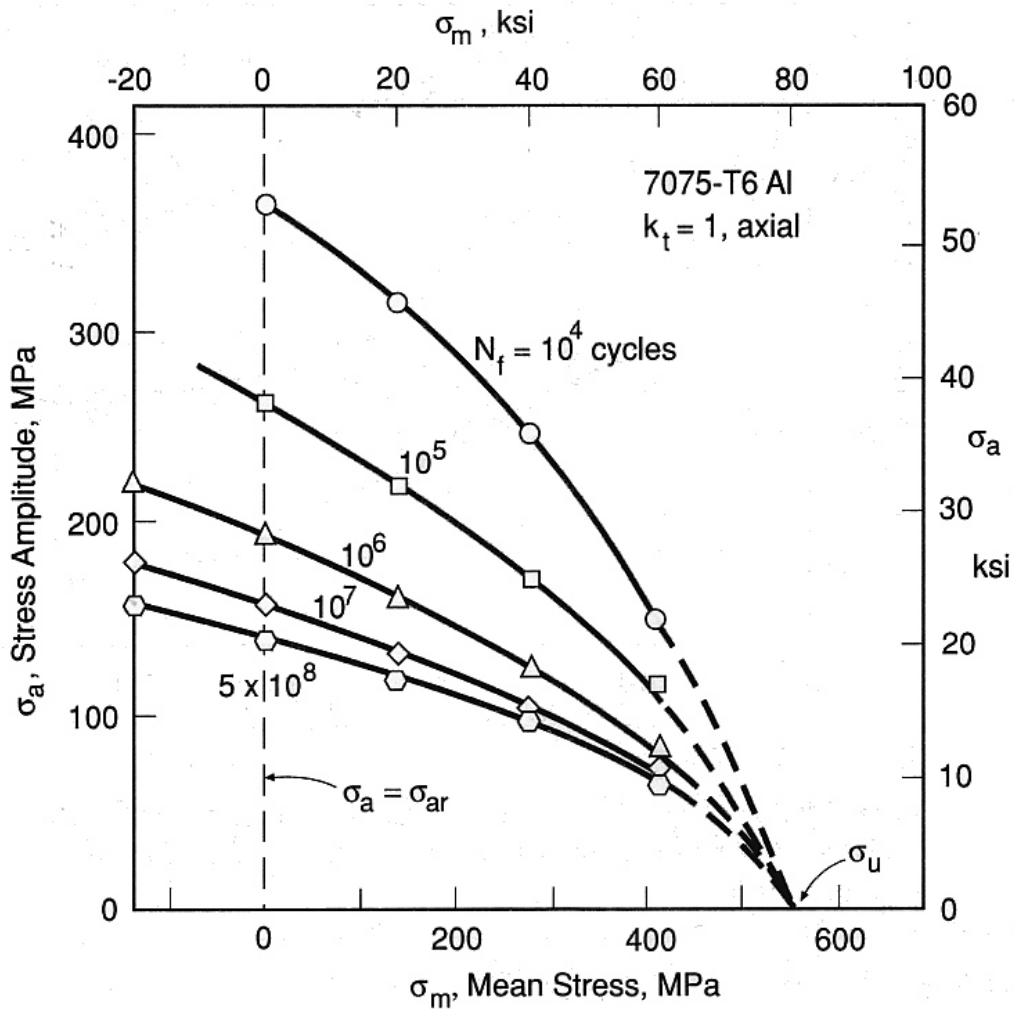


Figure 5. Constant life diagram for 7075-T6 aluminum (from Dowling [30]).

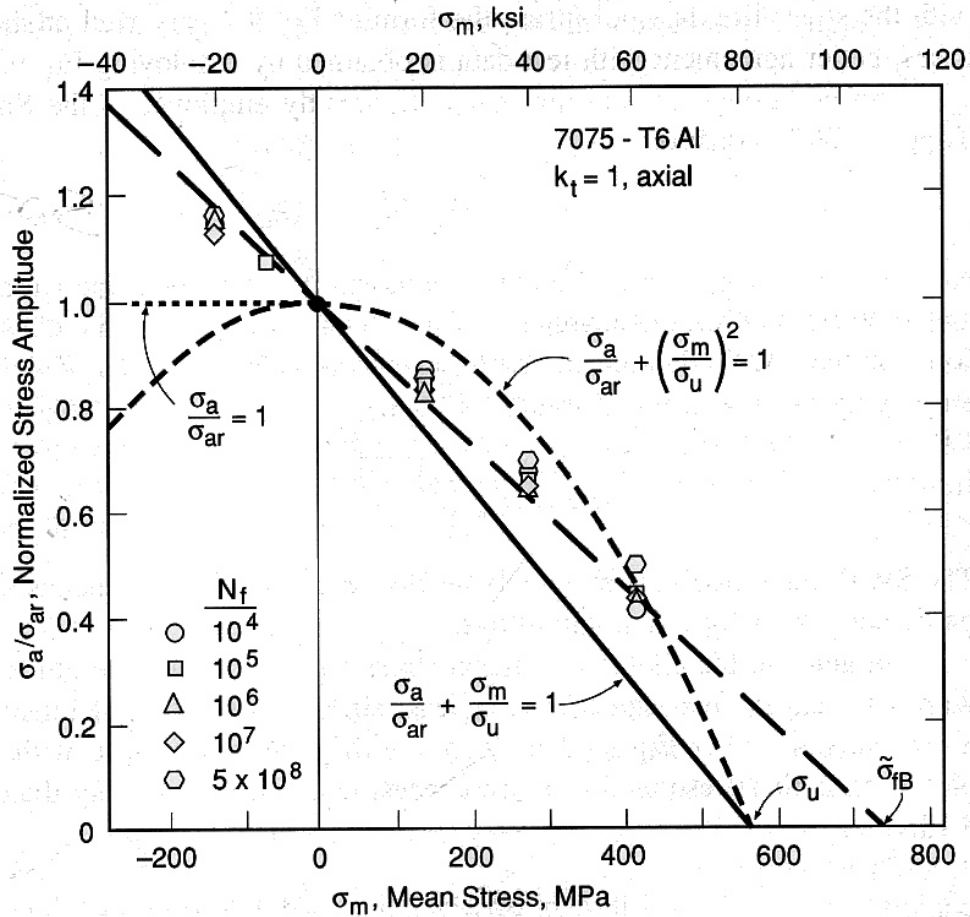


Figure 6. Normalized amplitude-mean diagram for 7075-T6 aluminum (from Dowling [30]).

Scatter in Fatigue Data

In any planned fatigue experiment, there is always some amount of scatter in the data, as depicted in Figure 4. This scatter is generally the cumulative effect of a variety of random factors. Some of the relatively controllable factors include inconsistencies in surface finish, deviations in specimen alignment, differences in applied loading conditions, and inconsistent residual stresses. These sources of scatter are generally mitigated through careful specimen preparation and handling, calibration of laboratory equipment, replicable experimental procedures, and use of identical specimens made from similar material from the same supplier. But even if these steps are taken, scatter in fatigue data is still observed due to slight differences in the microstructure of each specimen, which produces different conditions for crack initiation and propagation within each specimen.

Since crack initiation is a microstructural phenomenon dependent on localized conditions surrounding grain boundaries, inclusions, and other defects with a somewhat random distribution within the crystalline structure, one might expect the scatter in fatigue data to be magnified in the high cycle regime where fatigue life is dominated by the crack initiation phase. In fact, this phenomenon has been confirmed by numerous researchers through the years. In one such study, Sinclair and Dolan performed a lengthy experiment reported in 1953 using 174 identical highly-polished unnotched 7075-T6 aluminum alloy specimens tested to failure at six different stress levels [78]. Their results showed that greater scatter in fatigue life occurred at lower stress levels (corresponding to longer fatigue lives). This effect was also observed by Bastenaire using a variety of grades of steel [14]. Moreover, Sinclair and Dolan showed that fatigue life was distributed approximately lognormal at each stress level tested. Based on these and similar findings, any experiment designed to test fatigue strength in the high cycle regime must account for significant scatter in results.

Statistical Analysis of Fatigue Experiments

Before investigating various statistical methods used to analyze fatigue strength data, it is important to review some of the basics of probability and statistics to lay the groundwork for discussions to follow.

Introduction to Probability and Statistics

Although the subject of statistics is often perceived as murky and complex by engineers, the essential elements of probability and statistics relevant to fatigue testing are fairly straightforward. The goal of statistics is summarized below:

“The objective of statistics is to make an inference about a population based on information contained in a sample and to provide an associated measure of goodness for the inference.” (Wackerly *et al* [89])

This objective clearly cuts to the heart of the matter at hand as the primary objective of this research is to develop a means to estimate the fatigue limit and its dispersion (the inference) based on a limited amount of fatigue tests (the sample) with reasonable confidence (the measure of goodness).

As an introduction to probability theory, consider the roll of a die, with possible outcomes of 1, 2, 3, 4, 5, or 6. These outcomes together form the sample space – i.e., the range of all possible outcomes. Each roll of the die is a random event. The probability of any outcome assuming a fair die is obviously $1/6$. A random variable is defined as a real-valued function for which the domain is a sample space [89]. In the die example, one could define a random variable Z as a function equal to 1 if the roll is odd and 0 if the roll is even. In this case, Z would have an expected value of 0.5 since half the possible outcomes would be odd and half would be even. These concepts lead to the three basic axioms of probability theory, which define a probability function as follows [80]:

1. The probability of any random event is between 0 and 1; i.e., $0 \leq P(A) \leq 1$, where A is a random event.
2. The sum of all probabilities of random events within a sample space is 1; i.e., $\sum P(A) = 1$.
3. For a countable collection of mutually disjoint random events, the probability of any of these events occurring equals the sum of the probability for each individual event's occurrence; i.e., $P\{\cup A_j\} = \sum P(A_j)$.

There are two basic classes of random variables: discrete and continuous. Discrete random variables take on only a finite or countably infinite number of distinct values whereas continuous random variables take on a non-countable number of values. For example, the number of cycles to failure for a given test would be a discrete random variable as it must be an integer. Conversely, the stress level at which a specified portion of specimens fails to reach a given number of cycles would be a continuous random variable as it could be any positive real number.

The probabilistic behavior of a random variable is characterized by a cumulative distribution function (cdf) which is defined as

$$F_X(x) = P\{X(\gamma) \leq x\} \quad (7)$$

where $X(\gamma)$ is a random variable, γ is an event in the sample space, and x is a real number [80]. By this definition, the cdf is a nonnegative, nondecreasing function over the range $[0,1]$. If one denotes the probability of any discrete random event as p_i , then

$$F_X(x) = \sum_{i, x_i \leq x} p_i, \quad (8)$$

$$\sum_i p_i = 1.$$

For continuous random variables, a probability density function (pdf) is defined such that

$$F_X(x) = \int_{-\infty}^x f_X(\xi) d\xi. \quad (9)$$

Clearly, based on these definitions the following relations exist:

$$\begin{aligned} \frac{dF_X(x)}{dx} &= f_X(x), \\ f_X(x) &\geq 0, \\ \int_a^b f_X(x) dx &= F_X(b) - F_X(a), \\ \int_{-\infty}^{\infty} f_X(x) dx &= 1. \end{aligned} \quad (10)$$

Two random events are said to be independent if the occurrence of one event has no effect on the occurrence of another event. One must be careful during experimental design to ensure outcomes are independent of each other with respect to the random variables of interest. An example of dependent events in terms of fatigue testing concerns the reuse of specimens tested at other stress levels or shorter lives. Say that one is interested in determining the fatigue strength at both 10^7 and 10^8 cycles. If a series of pass/fail tests at 10^7 cycles were run and the surviving specimens were reused for the 10^8 cycle tests, a dependence has been introduced since the outcomes of the first test series affect the second test series. It would be impossible to have a specimen fail before 10^7 cycles in our second series of tests since all the specimens have already survived that duration. Note, however, that the probability of the specimens failing before 10^7 cycles may be so low for the second series of tests that one may be justified in ignoring this dependence (assuming there are no other effects due to stressing the specimens).

With this background, the expected value (i.e., mean value) of a random variable is defined in the following manner:

$$\mu = E(X) = \int_{-\infty}^{\infty} x dF_X(x) = \begin{cases} \sum_i x_i p_i & \text{discrete} \\ \int_{-\infty}^{\infty} x f_X(x) dx & \text{continuous} \end{cases} \quad (11)$$

which is simply an average value taken over all possible outcomes weighted by the probability of each outcome [80]. Another commonly used measure of central tendency is the median, which is just the value for which 50% of the random variable values lie above and 50% lie below; i.e., the value of x for which $F_X(x)$ equals 0.5.

The dispersion, or spread of a random variable about its mean, is generally measured using the variance which is defined as

$$\sigma_X^2 = \begin{cases} \sum_i (x_i - \mu)^2 p_i & \text{discrete} \\ \int_{-\infty}^{\infty} (x - \mu)^2 f_X(x) dx & \text{continuous,} \end{cases} \quad (12)$$

and σ_X (the positive square root of the variance) is the standard deviation [80].

Several probability distributions have proven to be of significant value in both theory and application over the years. These distributions are merely analytical expressions for $F_X(x)$ which are useful because of their ease in deriving analytical solutions to many problems and their applicability to represent a large number of random variables with reasonable accuracy. With respect to fatigue, some of the more relevant distributions include the Poisson, Gaussian (normal), lognormal, gamma, exponential, chi-square, inverse-Gaussian, and extreme value distributions [80]. A detailed description of each of the distributions commonly used in reliability analysis are presented by Elsayed [32], with a more complete overview given by Rice [75].

The goal of a statistical analysis of a fatigue experiment is generally to estimate some material property or behavior – fatigue limit, $S-N$ curve, etc. – based on a sample of test data. Generally, the property or behavior is modeled as a random variable using an appropriate probability distribution which fits the data reasonably well. Using this distribution or parameters of this distribution, one can test most any hypothesis regarding the underlying distribution related to the property or behavior of interest. Thus, it is important to be able to determine the key parameters of the population's underlying distribution – such as the mean and standard deviation of a fatigue limit at 10^9 cycles.

Estimators are rules (generally expressed as formulae) that define how to estimate values of a population based on sampled data.

It is important to differentiate between the population's underlying distribution and the sampling distribution. For example, the fatigue life at a certain stress level may be plotted using a histogram as shown in Figure 7. This plot shows that the fatigue life in Sinclair and Dolan's data set is distributed approximately lognormal. The sampling distribution, on the other hand, refers to the probability distribution associated with an estimator. The standard deviation of the sampling distribution for an estimator is generally known as the standard error of the estimator. If we defined a sampling statistic \hat{y} to be the mean fatigue life, then the sampling distribution would be the distribution associated with the mean fatigue life, not the distribution associated with individual fatigue life. For large samples, sampling distributions based on mean values tend to become normal according to the central limit theorem [89].

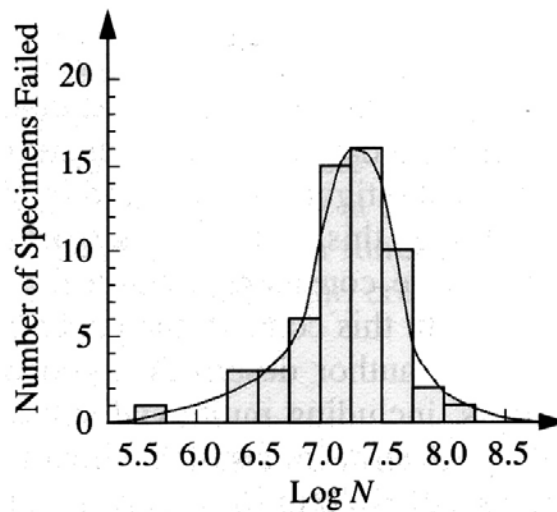


Figure 7. Histogram showing lognormal fatigue life based on Sinclair and Dolan's data (from Sobczyk and Spencer [80]).

Common, unbiased estimators valid for any underlying distribution are tabulated in most statistics texts. The most important of these estimators related to fatigue research are estimates for mean and proportion (e.g., a ratio such as fraction of survivals). As one would expect, the point estimates for mean and proportion are calculated by simply evaluating the sample mean and sample proportion, respectively. The standard error for mean and proportion are estimated using the following equations [89]:

$$\sigma_{\hat{\theta}} = \begin{cases} \frac{\sigma}{\sqrt{n}} & \text{for mean} \\ \sqrt{\frac{pq}{n}} & \text{for proportion,} \end{cases} \quad (13)$$

where σ is the true population standard deviation, n is the sample size, p is the true probability of survival, and q is the true probability of failure (i.e., $1-p$). Since the standard error estimates are based on true population parameters which are generally unknown, some initial estimates of the true population are needed in order to estimate standard error.

If a test series can provide a reasonably accurate estimate of the fatigue limit distribution parameters associated with a given number of cycles (such as 10^9), then a designer can easily specify the maximum loads that a component may be subjected to for an associated level of risk. For example, say a test series shows that the fatigue limit at 10^9 cycles can be estimated using a normal distribution with mean 400 MPa and standard deviation 5 MPa, then simple statistics may be used to determine the maximum allowable load for a given risk level, say 1% risk of failure before 10^9 cycles. To determine this maximum load, a standard normal probability table (such as Table 4 of Appendix 3 in Wackerly *et al* [89]) is used to find the Z value associated with the risk level 0.01. The Z value represents the standard normal variate (mean 0 and standard deviation 1) associated with a probability level α such that the probability of any value greater than Z is equal to α . In this case, the Z value associated with 0.01 would be -2.3267. We can then transform this standard normal variate to a specific normal distribution using the transformation law:

$$Z = \frac{Y - \mu}{\sigma} \quad (14)$$

where Y is a random normal variable with mean μ and standard deviation σ . Thus, for this example,

$$Z = \frac{Y - \mu}{\sigma} \Rightarrow -2.3267 = \frac{Y - 400}{5} \Rightarrow Y = 388.4 \text{ MPa.} \quad (15)$$

Therefore, the maximum allowable load associated with 1% risk of failure before 10^9 cycles would be 388.4 MPa for this fatigue strength distribution. If the fatigue loads on

this component are less than 388.4 MPa, then it would meet a design goal of 10^9 -cycle fatigue life with 1% risk of failure. This example represents the general idea in using a fatigue strength distribution to ensure compliance with ENSIP guidance. The assumption is that fatigue strength distribution could be reasonably estimated using fatigue test data.

Probabilistic Approach to Fatigue Strength Testing

Before discussing the methods to determine the parameters of a fatigue strength distribution, it is important to provide the conceptual model and terminology common to most all statistical analyses of fatigue data. In general, there are three fundamental variables applicable to fatigue analysis [46]:

1. S – the load level, generally a stress or strain index such as stress amplitude or Smith-Watson-Topper parameter; this parameter is generally the independent variable.
2. N – the number of cycles tested, usually to failure; this parameter is generally the dependent variable.
3. P – the proportion of specimens which fail before a specified number of cycles have been completed; this parameter is sometimes used as the dependent variable.

These three parameters taken together can be used to conceptually construct a P - S - N surface (sometimes referred to as the S - N - P surface in the literature) [46]. The P - S - N surface is visualized by adding a third axis to the S - N curve. This third axis represents the proportion of specimens which fail given a load level and number of cycles. From this surface, one can trace an S - N curve by fixing a specific value of P . Thus, one sees that any individual S - N curve has an implicit fixed value of P , and a family of S - N curves can be drawn together corresponding to different value of P as shown in Figure 8. The typical S - N curve shown without an associated probability level represents the mean (or centerline) curve, meaning that 50% of the specimens fail above this curve and 50% below it, but one could just as easily draw a curve where say 30% of the specimens fail above and 70% below so long as multiple tests are run at each stress level.

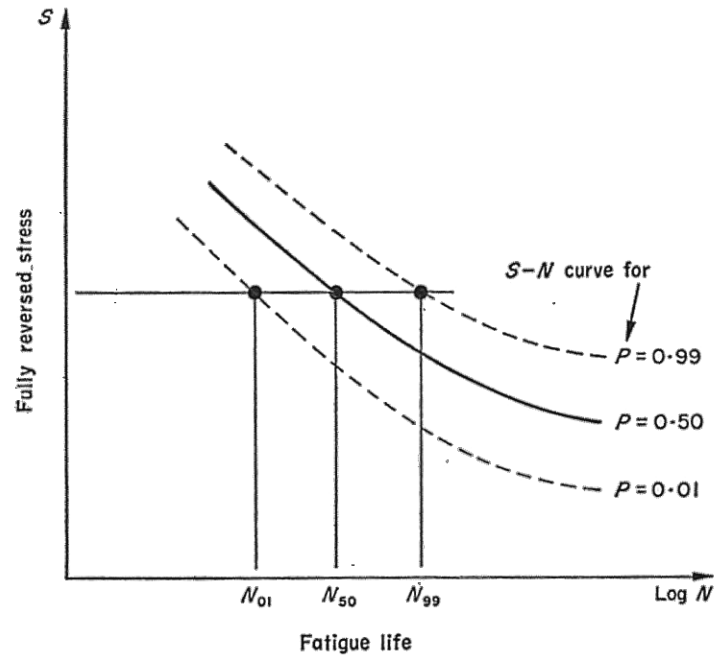


Figure 8. Conceptual S - N curves for specified P values (from Little and Jebe [46]).

Likewise, one can trace a P - S curve from the P - S - N surface by fixing a value of N (Figure 9) or a P - N curve by fixing a value of S (Figure 10). The P - S curve plays an important role in fatigue strength testing as it relates the proportion of failed specimens to the load level for a specified number of cycles.

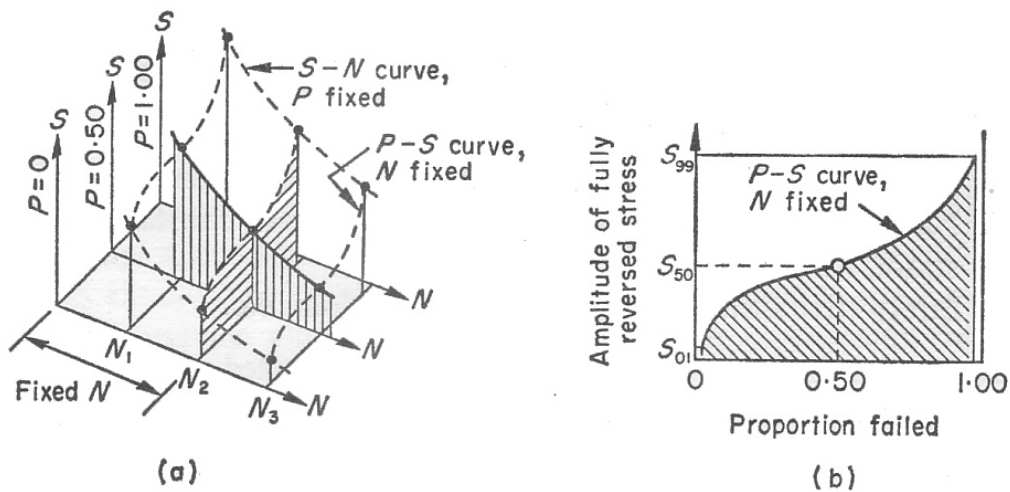


Figure 9. P - S - N surface showing P - S trace (from Little and Jebe [46]).

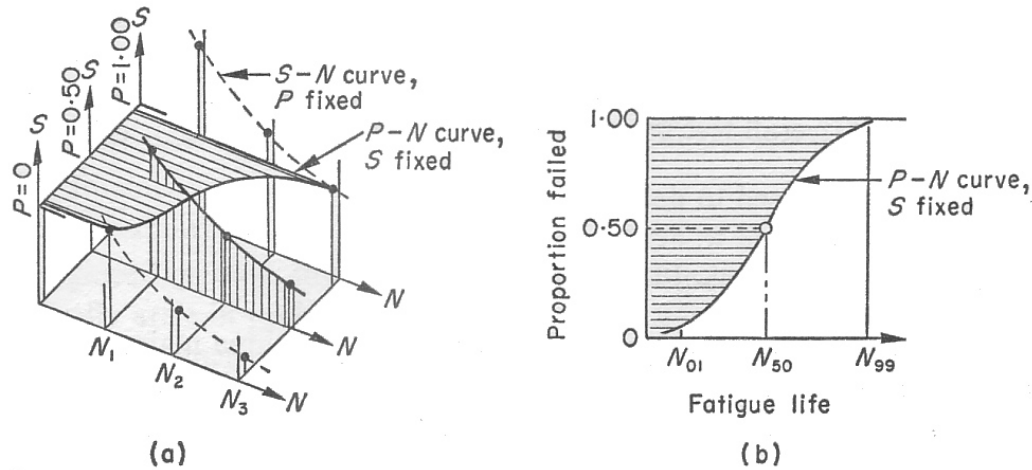


Figure 10. P - S - N surface showing P - N trace (from Little and Jebe [46]).

In the next several sections, a survey of current methods to statistically design and analyze experiments to determine a material's fatigue strength will be presented. These methods allow a means to deal with the stochastic nature of fatigue data and provide an estimate for the fatigue limit and its variance at a specified number of cycles. In general, one can sort these methods into four broad categories: (1) conventional S - N tests, (2) quantal response tests, (3) accelerated stress tests, and (4) more advanced statistical methods. Table 1 shows the various methods that will be considered in this study.

Table 1. Various methods of experimental design for fatigue strength testing.

Conventional S - N test method
Quantal response tests
<ul style="list-style-type: none"> • Probit method • Staircase method • Two-point method • $\text{Arcsin}\sqrt{P}$ method
Accelerated stress tests
<ul style="list-style-type: none"> • Prot method • Step-loading method
More advanced statistical methods
<ul style="list-style-type: none"> • Random fatigue limit model • Bayesian method • Bootstrap method

Conventional S-N Testing

The conventional *S-N* test approach requires a series of tests to be conducted at a range of stress levels, preferably with replication, in order to determine the stress-life curve. Using this approach, a range in fatigue life for each load level can be estimated to produce a family of *S-N* curves at various probability levels. Using multiple tests at the same set of load levels allows a means to describe this range in fatigue life using a probability distribution (such as the lognormal distribution used by Sinclair and Dolan). This distribution then allows an estimate for mean and standard deviation for fatigue life for any load level within the range of data. The details of how to draw the *S-N* curve using a mathematical model are generally straightforward for simple models. In particular, ASTM E739 describes the statistical analysis of linear (or linearized) *S-N* and ϵ -*N* fatigue data [8]. When all fatigue specimens fail, the most common method of determining the parameters of the *S-N* curve is to use ordinary least squares – the same method commonly used in curve fits of engineering data for the last 200 years since popularized by Gauss [8; 10]. This method has one serious drawback, however. Namely, runouts cannot be handled since an actual failure time is not known. Thus, a residual (i.e., the difference between the best-fit curve and the actual data point) cannot be calculated for runouts. Therefore, conventional *S-N* analysis using ordinary least squares (or a similar approach) must exclude runout test data. For high cycle testing – and especially testing in the gigacycle regime – there are often a large number of specimens which do not fail in the allotted test time since it is not feasible to test every specimen to failure in this long-life regime. However, if all (or the vast majority) of tests are run to failure, the conventional *S-N* approach would allow a graphical representation of the fatigue strength associated with a specified number of cycles, as well as the fatigue limit, if one exists.

In addition to being unable to handle runout test data, the conventional *S-N* approach has another limitation. Although it allows an estimate of the scatter in fatigue life, it is more difficult using this approach to estimate the scatter in fatigue strength. The reason for this difficulty should be rather obvious. Because the number of cycles to failure is the dependent rather than independent variable, the researcher cannot set about to collect a certain number of failed specimens at an arbitrary value of *N* due to the

stochastic nature of fatigue life. For these reasons, a conventional $S-N$ approach in its most simplified form becomes impractical for the determination of fatigue strength and its dispersion in the high cycle regime.

Spindel and Haibach looked at a more elaborate means of analyzing $S-N$ data to better represent the true shape of the $S-N$ curve as well as provide a better estimate of fatigue limit [81]. Their proposed approach allowed use of runouts by using maximum likelihood principles to deal with these data points in a statistically acceptable manner. Maximum likelihood estimation is a means to determine the best parameters to fit a data set using the principle that the best parameter estimates are those which would be most likely to produce the observed experimental data. Their aim was to determine the parameters of the most likely “parent” population common to a number of data sets using similar specimens along with the associated confidence intervals for these parameters. Their first task was to investigate the shape of the $S-N$ curve, looking at conventional linear fits (using linear S and $\log N$ or both $\log S$ and N) which include a horizontal portion beyond the fatigue limit, as well as S-shaped types of curves like those suggested by Weibull and others. Based on an analysis of available data sets, they made the following conclusions concerning basic assumptions used in traditional $S-N$ analysis: (1) straight-line approximations gave a generally poorer fit relative to S-shaped curves for larger data sets, and (2) the assumption of a normal distribution with constant standard deviation for the logarithm of fatigue life at all stress levels is generally untrue. Their analysis recommended a computer-based approach to determination of $S-N$ curve shape but was rather incomplete in describing a means to better estimate the fatigue limit using $S-N$ data. However, their work is significant in that it incorporated the concept of maximum likelihood estimation as a means to handle runout data from $S-N$ tests.

Quantal Response Tests

As opposed to the conventional $S-N$ approach, quantal response tests do not consider the actual time to failure, but rather they are by their nature a “pass/fail” approach. Thus, quantal response tests are designed to handle runout test data. In a quantal response test, specimens are tested at a certain load level and they either survive the specified number of cycles or they fail. Statistical analysis of test results allows an estimate of median and standard deviation of the fatigue strength at the specified number

of cycles based on the proportion of failed specimens at each load level. Although used in fatigue strength testing and other applications, quantal response methods are historically associated with biological assay. Biological assay is a set of techniques used in comparisons of alternative but similar biological stimuli – basically, the term means the measurement of the potency of any stimulus by observing the reaction that it produces in a living organism [35]. The objectives of biological assay and fatigue strength testing are quite similar. In both cases, one wishes to determine the appropriate stimulus level (either “stress” or “dose”) for which an acceptable proportion of specimens survive. Four methods of quantal response testing have been applied to fatigue strength testing: (1) the probit method, (2) the staircase (or “up-and-down”) test, (3) the two-point method, and (4) the $\arcsin\sqrt{P}$ method.

The probit method is a relatively well-known means of conducting fatigue strength testing [44]. In this approach, a group of specimens is tested at each of several uniformly-spaced test levels. The data from these tests are then plotted on a P - S curve, also known as a fatigue strength response curve. As previously mentioned, the P - S curve is simply a slice from a conceptual P - S - N surface with fixed N , as shown in Figure 11. According to Little, the probit method requires on the order of 30 or more specimens in order to provide an accurate estimate of median fatigue limit [44]. Little provides a chart to best allocate the specimens to each stress level based on the assumed true probability distribution for the probability of failure. He also notes that one may test at any arbitrary stress level with arbitrary spacing and arbitrary number of specimens so long as the true probability of failure at that stress level is between roughly 0.3 and 0.7 and the probability distribution is symmetrical (such as for normal distributions). Finney describes this same procedure from the biological assay perspective, using a dose-response curve, which is identical in principle to the P - S curve [35]. The primary drawbacks to the probit method are the number of specimens required for an accurate estimate and the overall complexity of the analysis. In addition, few data are available to recommend appropriate interval sizes, numbers of specimens for each stress level, and other key test parameters. Nishijima offers a modified probit approach which utilizes a small-sample strategy on the order of ten specimens, although analysis still requires a rather cumbersome iterative approach [62].

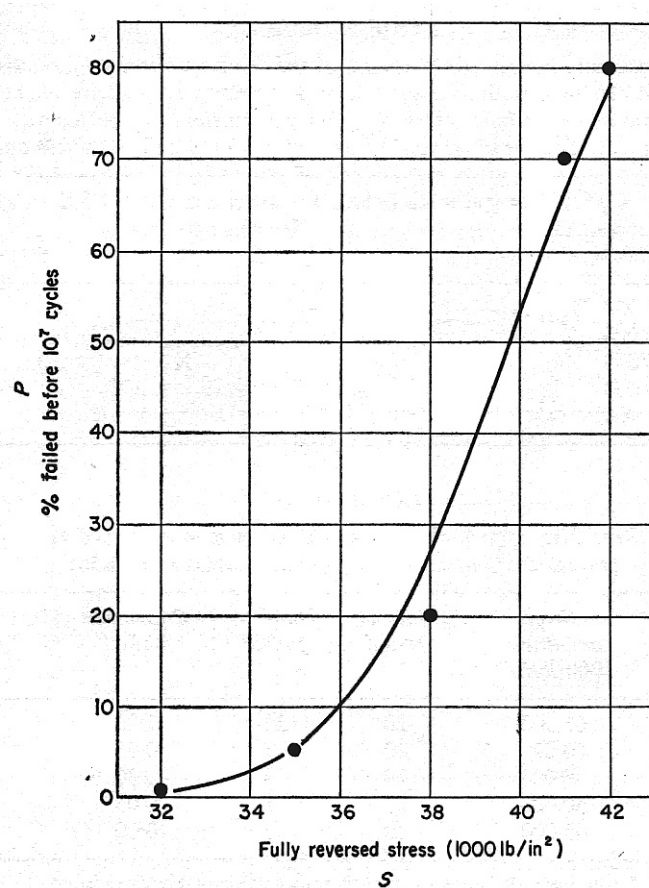


Figure 11. P - S curve for typical quantal response data (from Little and Jebe [46]).

The staircase (or up-and-down) test was first analyzed by Dixon and Mood in 1948 [27]. In a staircase test, specimens are tested sequentially, with the first specimen tested at an initial stress level, typically the best guess for median fatigue limit estimated from either experience or preliminary S - N data. The stress level for the next specimen is increased or decreased by a given interval depending on whether the first specimen survives or fails. This process is continued until all the specimens allocated for the experiment have been used. Typically, the step size between adjacent stress levels is held constant (approximately equal to the standard deviation of fatigue strength), in which case the statistics of Dixon and Mood may be applied directly to estimate mean and standard deviation of the fatigue strength [26]. Even though the true standard deviation in fatigue strength is one of the unknowns, Dixon notes that it is not too important if the interval is actually incorrect with respect to the true standard deviation by as much as 50%. However, Little notes that arbitrary spacing between stress levels may be used

when accompanied by a probit-type analysis [44]. In fact, tests conducted with non-uniform spacing may be more statistically efficient than uniform spacing; however, the analysis becomes much more tedious and the equations and tables derived for uniformly-spaced tests are no longer useful [42]. Figure 12 illustrates the staircase approach for a constant step size between stress levels.

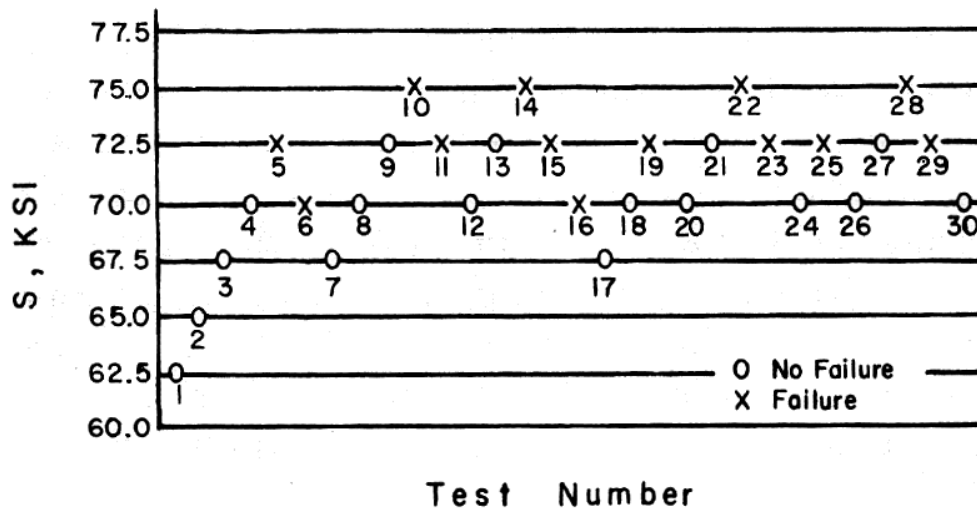


Figure 12. Illustration of the staircase test method (from Little [46]).

The primary advantage of the staircase method over the probit method is the improved efficiency. Originally, Dixon and Mood indicated that the staircase method may require forty to fifty specimens for accurate parameter estimates to be made [27]. However, Brownlee *et al* showed that a reasonably reliable estimate for mean effective dosage (fatigue strength) can be calculated from as few as five to ten samples [21]. They go on to make the following conclusions when comparing the two methods: (1) the probit method requires substantially more observations to obtain results similar to the staircase method, (2) small-sample performance of the staircase method is known whereas small-sample performance of the probit method is unknown and difficult to compute (note that this conclusion has since been addressed to some degree by Nishijima [62]), (3) staircase parameter estimates are easy to compute arithmetically whereas probit estimates require either a complex iterative method or graphical method involving judgment, and (4) staircase estimates can always be determined from the data whereas probit estimates may not exist. For these reasons, Brownlee *et al* recommend use of the

staircase method over the probit method for tests in which the arrangement of the sequence of trials is not prohibited by external considerations such as cost or difficulty in experimental setup. In fact, the Japan Society of Mechanical Engineers (JSME) standard method for determination of $S-N$ curves utilizes a 14-specimen strategy in which six specimens are devoted to determination of the horizontal portion of the curve (i.e., the fatigue limit) using a basic staircase strategy [56].

The two-point strategy outlined by Little is essentially a more efficient extension of the staircase strategy [44; 46]. The two-point method follows the staircase protocol up until the first test result in which two stress levels are observed with nonzero or nonunity proportions of survivals, after which specimens are tested only at these two stress levels. Thus, using Figure 12, the two-point method would be identical to the staircase method over the first nine specimens, after which tests would only be conducted at the 70.0 and 72.5 ksi levels – eliminating the four tests at the 75.0 ksi level and the one remaining test at 67.5 ksi where statistical weight is diminished. The analysis of the two-point method in essence reduces to a probit analysis with only two stress levels. Little provides an analytic expression for the estimation of the asymptotic variance of the median fatigue strength, allowing calculation of confidence limits for the median fatigue strength. Little recommends spacing between stress levels on the order of $2/3$ to $3/2$ the standard deviation of the underlying fatigue strength distribution.

The $\arcsin\sqrt{P}$ method utilizes a prescribed number of uniformly-spaced stress levels with a fixed number of specimens tested at each level [20]. Braam and van der Zwaag provide an analytical expression for the probability density function for the probability of failure (P) based on the observed proportion of failed specimens at each stress level tested (P_i). The method is known as the $\arcsin\sqrt{P}$ method due to the fact that the proportion of failed specimens at each stress level appears transformed in the parameter expressions as $\arcsin\sqrt{P_i}$. Thus, the test approach is basically similar to the probit approach whereas the analysis is much more straightforward and similar to the staircase approach. Braam and van der Zwaag found the staircase and $\arcsin\sqrt{P}$ methods to be relatively similar in accuracy and efficiency.

Accelerated Stress Tests

Another approach to fatigue limit testing is the use of accelerated stress tests. Accelerated stress testing includes those tests in which the stress level is increased during the test of a specimen in order to ensure it fails in a reasonable number of cycles. This approach differs from the other tests discussed which utilize a constant stress level for each individual specimen. Two such accelerated stress methods are the Prot method and the step-loading method.

In the Prot method, testing begins at a stress level below the estimated fatigue limit, with the stress level increasing at a constant rate until failure occurs [72]. Each successive test is accomplished at a reduced rate of stress increase resulting in a series of stress values corresponding to each rate of stress increase. One of the concerns regarding use of such a method is the influence of coaxing on the results. Coaxing, or “under-stressing,” refers to the phenomenon of raising the fatigue strength in a material by subjecting it to lower stresses relative to the fatigue strength. There is some debate over whether this phenomenon really occurs or is just the product of statistical skewing of the population [33; 61; 74]. Regardless, the Prot method has been found by Ward *et al* to be valid for welded SAE 4340 steel and applicable to ferrous metals with a well-defined fatigue limit, although some ferrous metals have been shown to display coaxing behavior [24; 90]. As for titanium alloys, some researchers have indicated that coaxing behavior is of little concern for high cycle testing. However, Bathias and Ni reported in a 1993 study that there indeed did appear to be a coaxing effect on Ti-6Al-4V samples tested using an ultrasonic apparatus at 20 kHz [16]. Overall, one of the primary disadvantages of the Prot method is the need to conduct a series of tests at non-constant stresses. This requirement adds significant complexity to the overall test approach. In general, the Prot method is not very widely used – if at all – for fatigue strength testing today.

The step-loading method demonstrated by Nicholas is similar in concept to the Prot method in that the stress is not held constant for each specimen [61]. In this procedure, specimens were tested to a given number of cycles (specifically, 10^7) and if they survived, the stress was increased by approximately 5% and the specimens were again retested up to 10^7 cycles. This process was repeated until each specimen failed. A linear interpolation scheme was used to calculate the fatigue limit stress for each

specimen. The procedure when applied to the titanium alloy Ti-6Al-4V produced data consistent with fatigue strength tests using conventional S - N testing.

Advanced Statistical Methods

The final group of fatigue strength test approaches are lumped together under the heading of advanced statistical methods. Three such approaches will be discussed: (1) random fatigue limit modeling, (2) Bayesian methods, and (3) bootstrapping methods.

Random fatigue limit (RFL) modeling explicitly assumes that each specimen has its own fatigue limit based on its unique microstructure. Thus, there is an associated fatigue strength distribution at each specified number of cycles [58]. Pascual and Meeker proposed a method incorporating maximum likelihood estimation to produce probabilistic S - N curves which account for the behavior visually represented by the distributions shown in Figure 13 [66]. There are two distributions which must be modeled using the RFL model – namely, the conditional distribution in fatigue life at a specified stress level given fatigue limit (the horizontal distributions in Figure 13) and the distribution in fatigue strength at a specified fatigue life (the vertical distributions in Figure 13). Pascual and Meeker considered several combinations of analytical distributions to model these random variables. Based on the findings of numerous researchers (such as Sinclair and Dolan [78]), the conditional distribution of fatigue life is generally assumed to have a lognormal distribution (although this assumption is not required). The distribution in fatigue strength (or, random fatigue limit) is a bit more of an unknown, but several reasonable distributions were investigated with the Weibull distribution showing significant promise [10]. The mechanics of the RFL model are rather detailed (and are discussed in depth in Chapter V) but have been simplified by the authors who offer available software to perform the necessary calculations.

Pascual and Meeker's work takes a bold step in better modeling observable characteristics of S - N data using a manageable mathematical formulation. This effort builds upon Nelson's work in fitting fatigue curves with nonconstant standard deviation associated with each stress level, which also utilized maximum likelihood methods to allow use of runout data [59]. Specifically, the RFL method accounts for the increase in standard deviation of fatigue life at lower stress levels as well as the curvature and flattening of the S - N curve in the HCF regime. This flattening effect is observed in the

probabilistic S - N curve shown in Figure 14. By treating fatigue limit as a property specific to each specimen rather than an overall material property, their approach also provides a better estimate of fatigue limit than conventional S - N analysis allows. Conventional analysis which assumes a single-valued constant fatigue limit for all specimens must by necessity result in an estimate of fatigue limit below the lowest stress tested, thus producing an unrealistically low value.

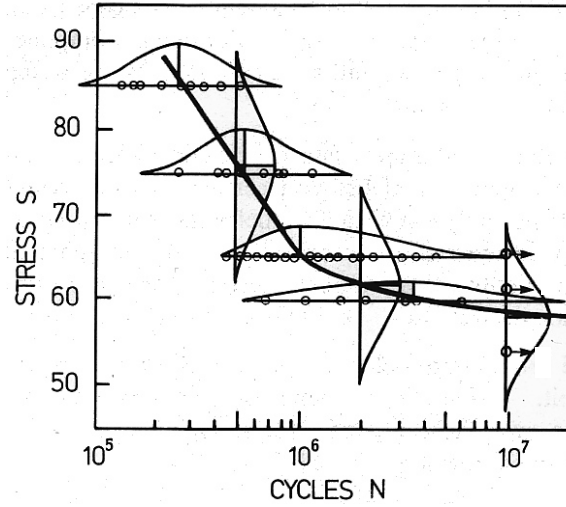


Figure 13. Fatigue life and fatigue strength distributions (from Nelson [58]).

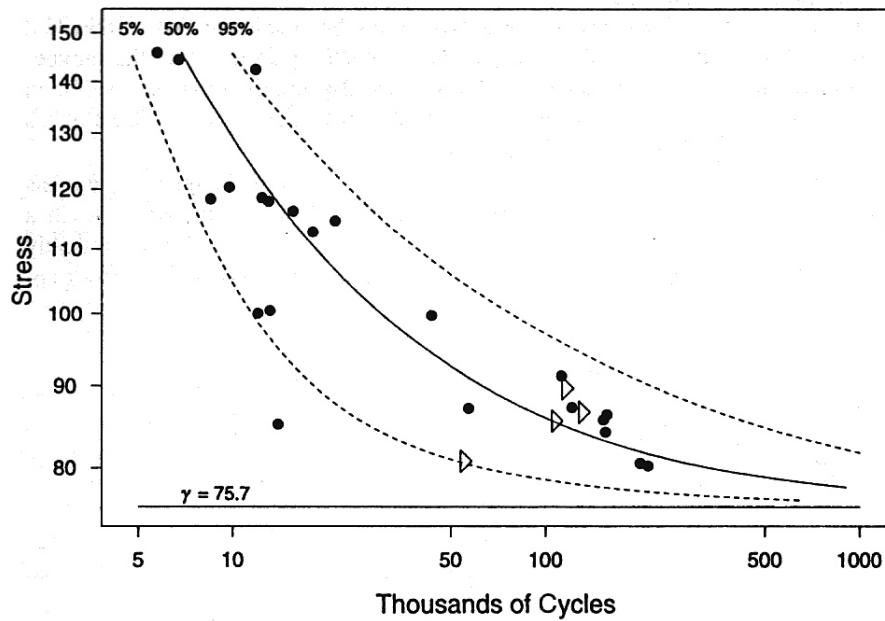


Figure 14. Probabilistic S - N curves based on random fatigue limit modeling of nickel superalloy data (from Meeker and Escobar [50]).

As an alternative approach, Bayesian statistical methods are an established means of estimation which utilize prior information, whether qualitative or quantitative in nature, to augment and enhance real test data to provide a better estimate of population parameters [38]. Estimation of a median fatigue strength and its associated dispersion is a means of statistical inference based on a small sample of test data in order to make conclusions based on the entire population of a particular material. The typical approach to statistical inference is to use hypothesis testing or confidence interval estimation using objective data in the form of independent samples from a similar population. In a Bayesian approach, additional sources of information of generally lesser quality are used to augment this objective data in order to improve the parameter estimates. For example, one may use prototype test data to augment limited test data on a full-up article in order to provide a more complete picture of real performance.

With respect to the RFL model, Johnson *et al* proposed incorporation of a hierarchical Bayesian approach to provide a means for parameter estimation (in lieu of Pascual and Meeker's maximum likelihood approach) [39]. The general approach is to specify prior distributions for each of the RFL model parameters. These prior distributions are used in conjunction with the observed fatigue test data to determine posterior parameter distributions which can then be used to draw statistical inferences on fatigue limit. Johnson *et al* claim that the primary advantage to this approach is the ability to use prior information in the analysis beyond that data collected in the fatigue test sample. Since development of new materials is generally evolutionary, a decent picture of what some of the parameter distributions will look like already exists based on tests of similar materials or preliminary analysis of the material under investigation. In addition, some numerical advantages are realized so long as the choices of prior distribution guarantee a proper posterior distribution which can be analyzed. Besides the disadvantage of having to choose suitable prior distributions which allow a proper posterior distribution, there is the standard pitfall of Bayesian analysis to contend with: namely, how to make generally subjective prior distribution estimates based on limited data without compromising the objectivity of the test program.

In addition to Bayesian methods, bootstrap methods may also provide some opportunities to more efficiently model fatigue strength behavior [12]. The bootstrap

method is a data-based simulation which utilizes multiple random draws from real test data to make statistical inferences about the underlying population [31]. Essentially, the repeated draws from the test data pool allow estimates of parameter confidence intervals which can be quite accurate. The main drawback to bootstrapping is the reuse of existing data which may skew the results depending on the presence of outliers as well as any other misrepresentation of the sample with respect to the true population. It is also a somewhat difficult method to explain and rationalize to decision makers.

Ultra High Cycle Fatigue Research

UHCF behavior has in the last decade become a very hot topic in the fatigue community as new testing methods have allowed considerably more test data to be generated at fatigue lives that were previously impractical to test. In this section, some of the major findings and current research thrusts related to UHCF research will be introduced in an overview manner.

Ultrasonic Fatigue Testing

Exhaustive testing in the gigacycle regime has only fairly recently been made possible by the introduction of ultrasonic test equipment. These test machines can operate at frequencies in the 20 kHz range (and beyond), thus reducing the time required to conduct a test of 10^9 cycles down to hours rather than days, weeks, or even months using lower frequency machines. These ultrasonic test machines operate based on the longitudinal vibration of the specimen at its resonant frequency in the axial loading mode. The specimen is mounted on an amplifying horn which is attached to a transducer which provides ultrasonic excitation at a frequency of approximately 20 kHz (for most current apparatus) – the resonant frequency of both the horn and specimen. Strain data can be measured through strain gages (so long as they do not fail), or through the use of an eddy current or laser sensor at the free end of the specimen. A schematic of a version of this system is depicted in Figure 15.

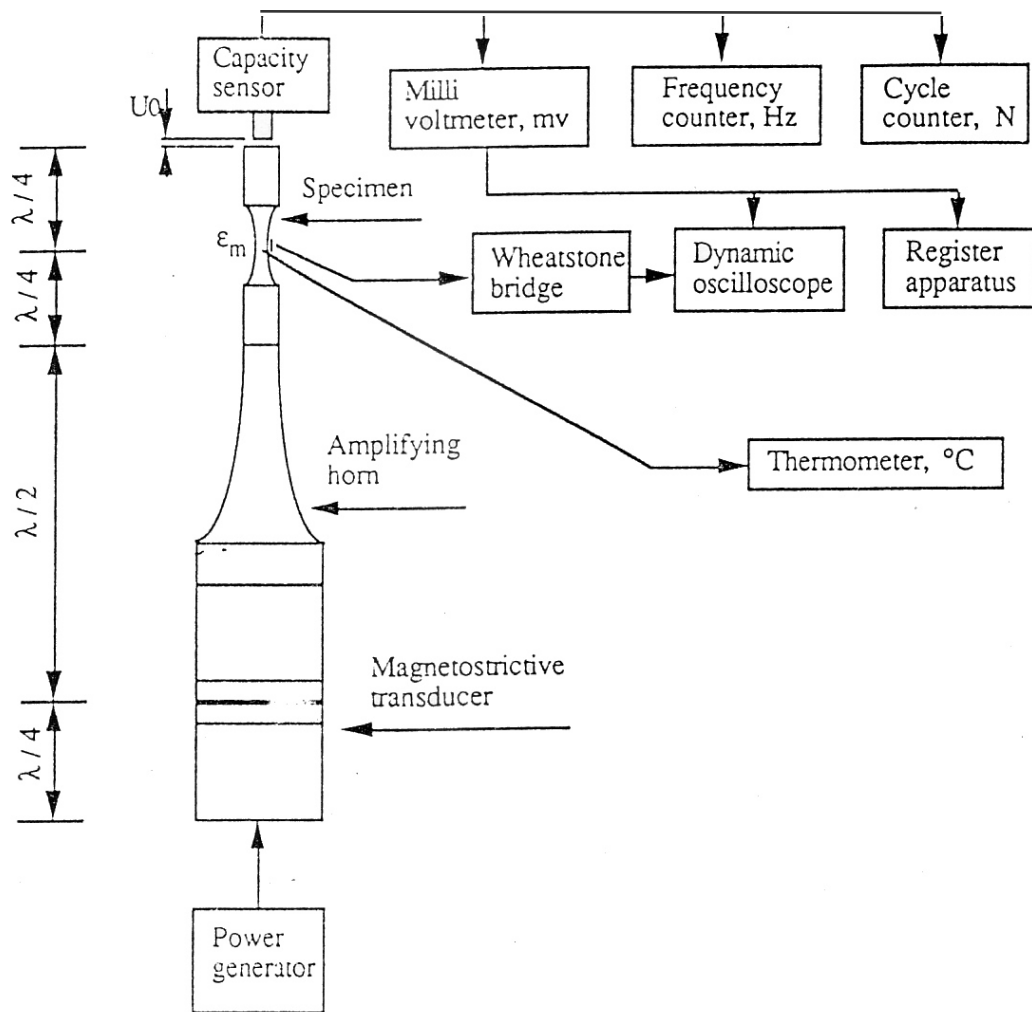


Figure 15. Schematic view of a particular ultrasonic test apparatus (from Bathias and Ni [16]).

Bathias and Ni performed a study comparing the fatigue limit behavior of three materials (Udimet 500, 17-4PH, and Ti-6Al-4V) using an ultrasonic test apparatus and conventional lower frequency machines [16]. Their results indicated that ultrasonic frequency excitation at lower stress amplitudes effectively increases the material's fatigue strength (thus, coxing appears to occur at these high frequencies). In addition, the nickel-based superalloy Udimet 500 appeared to exhibit similar fatigue limit behavior using either the ultrasonic high-frequency apparatus or conventional machines at much lower frequency. On the other hand, the 17-4PH and Ti-6Al-4V specimens appeared to exhibit slightly better fatigue resistance using the ultrasonic equipment. Thus, it appears

that different materials respond in different fashions to ultrasonic fatigue excitation. These results are consistent with the findings of other researchers comparing fatigue response at widely different frequencies [40; 79].

Fatigue Limit Behavior in the Gigacycle Regime

Many design and analysis approaches are based on the assumption that a fatigue limit exists for a material. This assumption allows the use of a component at stresses below the fatigue limit for a theoretical infinite number of cycles. However, recent research raises the question of whether a fatigue limit exists in materials previously thought to exhibit one, such as ferrous metals. As Stanzl-Tschegg describes in her editorial on the state of fatigue testing in the very high cycle regime,

“During the last few years, long life fatigue failures have been detected even in materials which were assumed to have an endurance limit, such as high strength steels.” (Stanzl-Tschegg, 2002 [82])

These failures in regimes thought to be free of fatigue failures are obviously of great concern for engineers who are designing components to withstand a very large number of cycles – more than can be adequately tested in a reasonably efficient manner with respect to time and cost. This is especially true given the longer and longer service lives expected of today’s products, to include aircraft, spacecraft, shipping vessels, high-speed trains, and the like.

Miller and O’Donnell discussed the elimination of the fatigue limit conceptual model [51]. They argue that research shows that under variable loading, the few higher stress cycles have a very significant impact in overcoming the fatigue resistance of a material. Thus, in general, fatigue limit is observable only under constant cyclic stress range conditions, which are rarely encountered under actual service conditions. They go on to point out that other factors also significantly deteriorate the fatigue resistance of a material in the very high cycle regime – such as corrosive environments and fretting. Thus, they appear to argue that fatigue limit is a concept that only adequately applies to pristine materials tested under laboratory conditions and should not be applied so liberally to the analysis of engineering materials operated under more dynamic conditions.

Bathias also concluded there was no infinite fatigue life in metallic materials based on his study of the UHCF behavior of aluminum matrix composites, high-strength steels, titanium alloys, and nickel-based superalloys [15]. His findings indicated that there was a marked decrease in fatigue strength from the 10^6 -cycle point to beyond 10^8 cycles for many materials. Results indicated that fatigue failures in the UHCF regime which occurred below the asymptotic fatigue limit in the HCF regime (based on statistical analysis of tests conducted at 10^6 - 10^7 cycles) were characterized by internal (subsurface) crack initiation. The reasons why this mechanism would occur were not immediately obvious, but the roles of inclusions, porosity, and grain size were recommended for further study.

Shiozawa *et al* also observed this phenomenon of subsurface crack initiation in the UHCF regime in their study of high carbon-chromium bearing steel using rotary bending fatigue tests [77]. They reported that,

“The remarkable shape of the S - N curve obtained in this study was different from a step-wise one reported in literature and was characterized as a duplex S - N curve which is composed of two different S - N curves corresponding to the respective fracture modes.” (Shiozawa, Lu, and Ishihara, 2001 [77])

This so-called duplex (or bimodal) S - N curve is depicted in Figure 16, which shows the two associated probability distributions for surface and subsurface failure modes and how these distributions affect the overall S - N curve.

Other researchers have also observed this bimodal behavior in the gigacycle regime using a variety of fatigue tests on different materials. Nishijima and Kanazawa documented bimodal S - N behavior in steels without hardened surfaces, also noting the same phenomenon of internal initiation in the gigacycle regime [64]. Mughrabi also investigated this theory of a two-stage S - N curve (see Figure 17) and proposed conditions for which the internal defects could become the life-controlling mechanism in the gigacycle regime [54]. These conditions relate to the following: (1) the geometrical roles of the size and volume density of inclusions, (2) internal fatigue cracks originating from internal inclusions, and (3) crack initiation at pores. However, he notes that there is still a need to investigate how these internal cracks form as the process is currently not well understood.

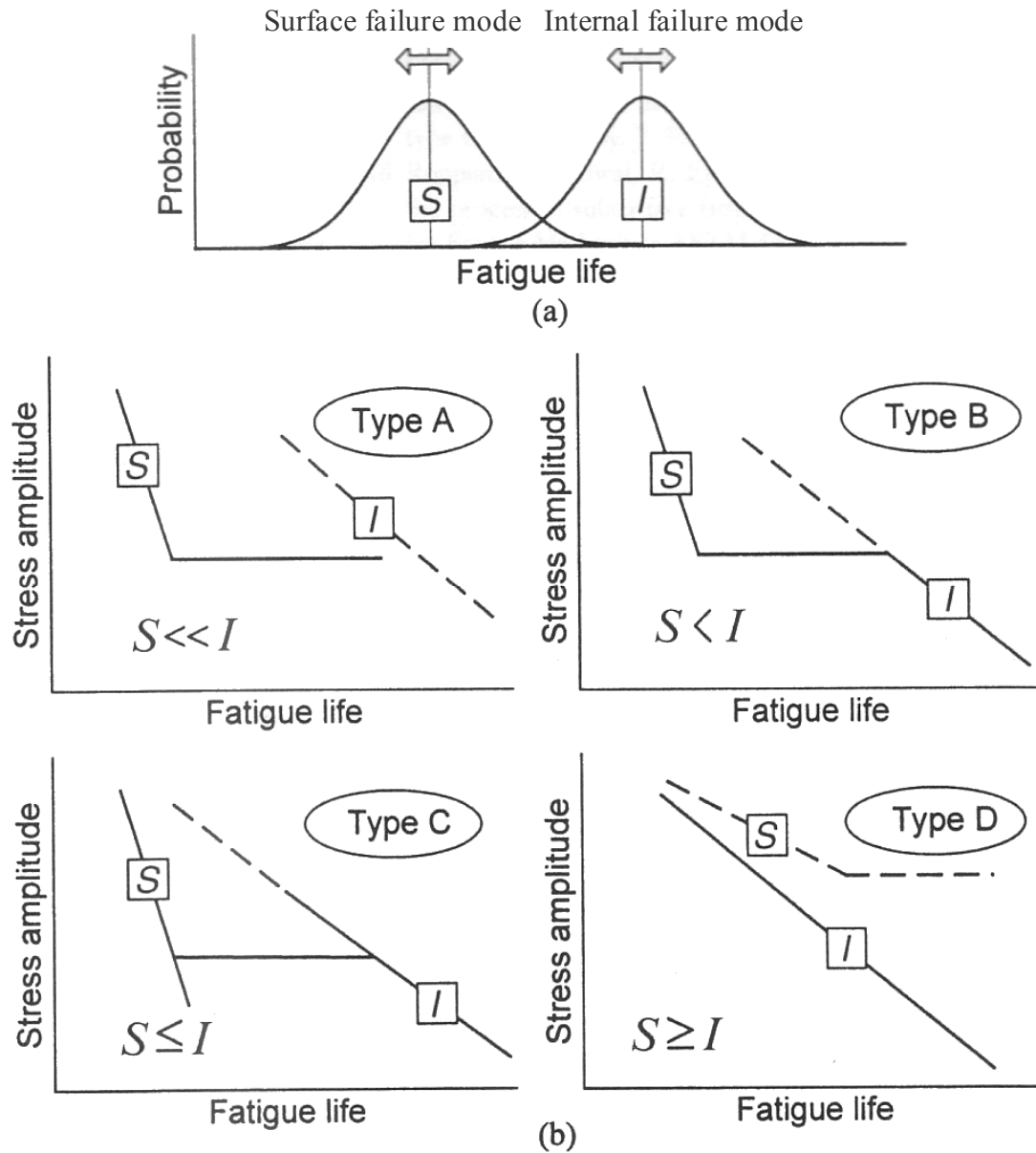


Figure 16. Conceptual S - N curves using the concept of a bimodal model (from Shiozawa et al [77]).

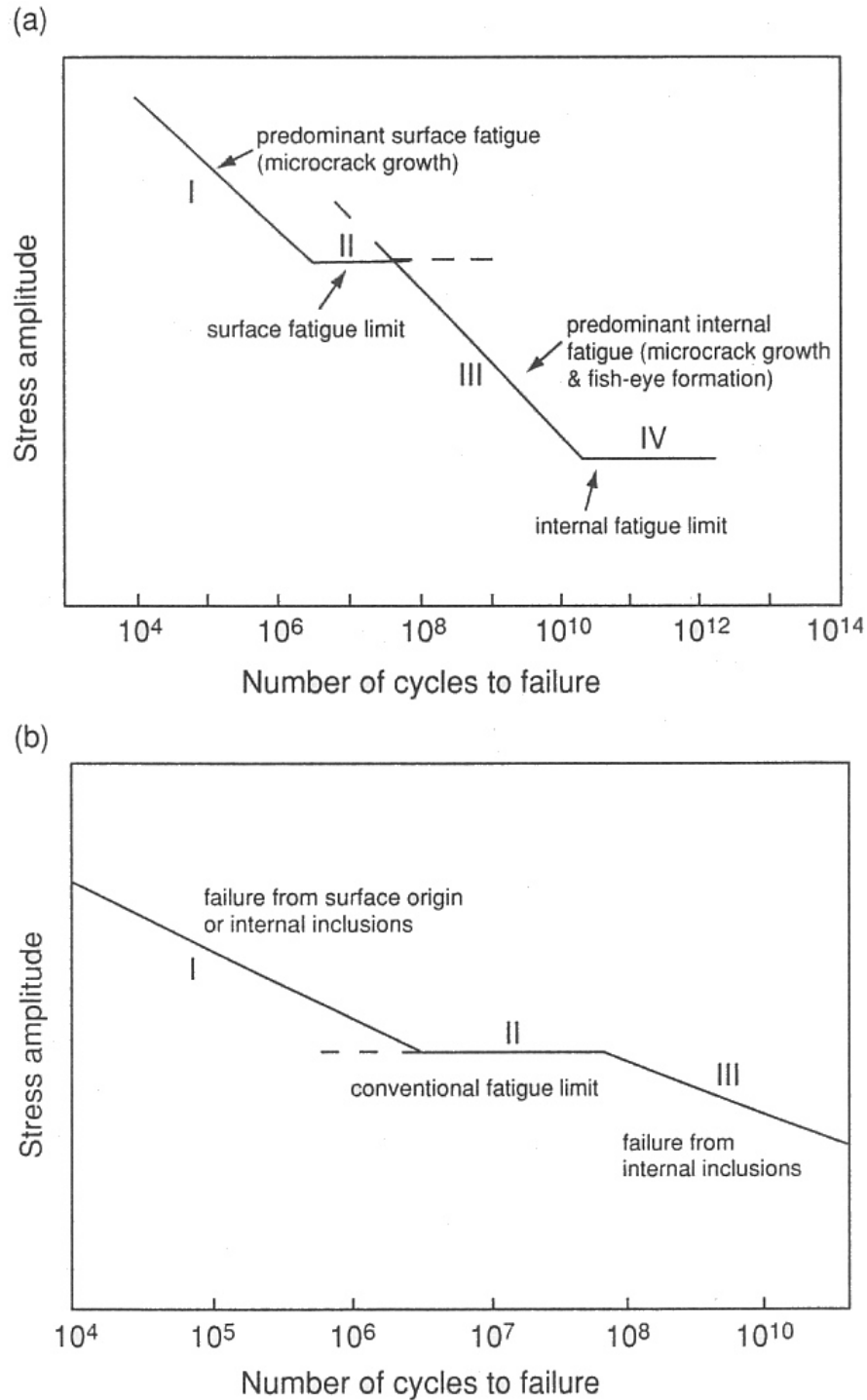


Figure 17. Schematic illustration of bimodal S - N behavior (from Mughrabi [54]).

The work of these researchers and others has led to the acknowledgement of a bimodal shape to the stress-life curve which indicates a decrease in fatigue strength in

and beyond the gigacycle regime. These investigations clearly indicate that there is a second fatigue failure mechanism due to subsurface crack initiation at these very long fatigue lives which produces the drop in fatigue strength. Chandran used Poisson defect statistics in conjunction with Monte Carlo simulation to represent this bimodal behavior [22]. However, a detailed understanding of how these internal cracks form is not yet well understood, although it is currently being explored, with particular fervor by a number of Japanese researchers interested in “fish-eye” (internally initiated) failures of ferrous metals. Characterization of this bimodal behavior using fatigue strength tests intended for application to a single mode fatigue strength distribution remains a challenge as well.

Air Force Research Laboratory Research

Preliminary test results in the UHCF regime collected by the Air Force Research Laboratory’s Materials and Manufacturing Directorate (AFRL/ML) using Ti-6Al-4V under fully-reversed loading conditions (shown in Figure 18, listed in Appendix A) does not seem to reveal the bimodal behavior discovered by other researchers [4]. However, it is quite possible that the very limited number of specimens tested in the UHCF regime have failure mode distributions characterized by Type A in Figure 16. Thus, the internal failure mechanisms may not have been encountered yet because the surface failure mode has a greater probability of being encountered at fatigue lives tested thus far. Atrens *et al* reported in a 1983 study of the fatigue strength of Ti-6Al-4V in the region of 10^7 - 10^8 cycles that a noticeable drop in the fatigue strength was observed [13]. Moreover, these failures at lower stress levels were characterized by subsurface crack initiation. To date, failures observed in AFRL/ML testing have all been characterized by surface initiation. The question remains as to whether this bimodal behavior observed by Atrens *et al* will be observable in future Ti-6Al-4V tests conducted by AFRL/ML.

AFRL/ML scientists are considering several approaches to determining if bimodal behavior in Ti-6Al-4V samples can be detected. One approach is the obvious idea of testing out to higher numbers of cycles at lower stress levels to see if reduced fatigue strengths will be encountered. Another avenue of approach is to use residual stresses to effectively increase the fatigue resistance of the surface material, thereby increasing the likelihood that the internally-initiated failure mode will be encountered. Both of these testing avenues are relatively feasible and likely to occur. AFRL/ML is also developing a

means to conduct gigacycle testing at stress ratios other than fully-reversed loading. Atrens *et al* reported that mean stress possibly plays a major role in the decrease in fatigue strength between 10^7 and 10^8 cycles [13]. Thus, use of stress ratios other than -1 may allow detection of the second failure mode within the UHCF regime. It is important to note that Ti-6Al-4V samples used in the tests to date have been machined from very high-quality material manufactured under very precise conditions. Thus, the material is generally free of major defects as compared to lesser quality samples. This comparative absence of defects in the material could account for the lack of internally initiated failures in the gigacycle regime (as these failures are initiated at internal defects).

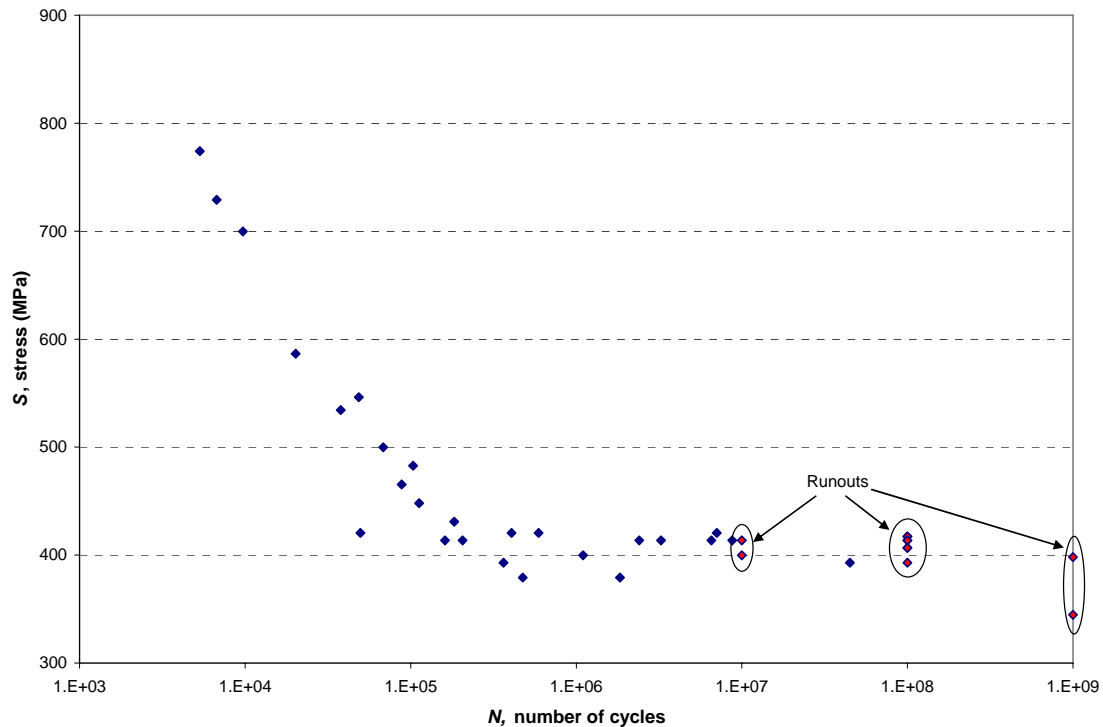


Figure 18. *S-N* test data generated from HCF S&T program for Ti-6Al-4V under fully-reversed loading [4].

Titanium and Titanium Alloys

The purpose of this section is to give the reader an introduction to titanium and titanium alloys, describe the differences in titanium alloy microstructures, and provide an overview of the various heat treatments of titanium alloys.

Introduction to Titanium and Titanium Alloys

Titanium is abundant in the earth's crust—the fourth most abundant metallic element, in fact [87]. In its natural state, it is generally found as an oxide ore, and it was not isolated with high purity until 1910. It first came into use as a structural material in the 1950s, stimulated by the aerospace industry. Specifically, the superiority of titanium alloys compared with steels (up to about 540°C) led to initial use in jet engines, and by the 1960s, over 90% of titanium production was for jet engine applications [28].

Aerospace applications continue to drive the titanium market, although titanium and its alloys are finding their way into ever more applications due to their many desirable properties. These properties include a relatively low density (about 60% of that of steel), high strength-to-weight ratios, corrosion resistance in many environments due to readily formed protective oxide layers, and relatively stable properties even at high temperatures.

Titanium has a high melting temperature (1668°C) but undergoes an allotropic transformation from a hexagonally close-packed (h.c.p.) lattice structure at lower temperatures to a body centered cubic (b.c.c.) structure at higher temperatures; specifically, this transformation occurs at about 882°C for commercially pure titanium [28]. This allotropic transformation allows more diverse strengthening opportunities, as compared to non-ferrous alloys such as those comprised chiefly of aluminum or copper. The thermal-mechanical processing of titanium alloys is the mechanism by which its microstructure and properties are controlled, and thus tailored for specific applications.

Titanium alloys are generally divided into three classes: alpha, alpha-beta, and beta alloys. The alpha phase corresponds to the h.c.p. structure, while the beta phase corresponds to the b.c.c. structure, and thus the alpha-beta phase occurs when both structures are present. Thermal treatments may be applied to an alloy to modify the phase structure. The addition of alloying elements may also be used to control the phase transitions. For example, the addition of aluminum stabilizes the alpha phase by raising the temperature of the alpha-beta transformation. Ti-6Al-4V is an alpha-beta type alloy, which incorporates 6% aluminum and 4% vanadium. It was first introduced in 1954 and is considered a general-purpose grade of titanium, recognized as the “workhorse titanium alloy” [87]. Typical applications of Ti-6Al-4V include aircraft turbine and compressor blades and disks, surgical implants, and pressure valves.

Heat Treatment

Titanium and its alloys are generally heat treated for several purposes: (1) to reduce residual stresses developed during fabrication, (2) to improve ductility, machinability, and dimensional and structural stability, (3) to increase material strength, and (4) to optimize special properties such as fracture toughness, fatigue strength, or creep strength [29].

Stress relieving (also called stress-relief annealing) is the process used to reduce residual stresses developed through fabrication. For fatigue testing purposes, removal of residual stresses is important in order to accurately calculate the true stress within a specimen under loading, and thus to remove variability in the fatigue life for a given applied stress due to residual stresses rather than material behavior. Stress relieving is accomplished by heating the metal over a period of time, with stress-relief treatments (time and temperature) specified based on the specific material. For Ti-6Al-4V, stress-relief treatment generally requires 1-4 hours at 480-650°C, with higher temperatures used for shorter times and lower temperatures used for longer times [29].

Process annealing is a fairly general term which applies to treatment techniques intended to increase toughness, ductility at room temperature, dimensional and thermal stability, and sometimes creep resistance [29]. Annealing, however, can be used as a general term to describe any softening of a metal through heating followed by gradual cooling, and therefore it is often used in conjunction with stress-relief treatment, solution treatment, and other processing treatments. Common process annealing treatments include mill annealing, recrystallization annealing, and beta annealing [29]. Mill annealing is a general-purpose heat treatment given to mill products. It is not a full anneal and may leave traces of cold or warm working in heavily worked products. Recrystallization annealing is used to improve material toughness by heating the metal to the upper end of the alpha-beta range, holding this temperature, and then slowly cooling. Beta annealing heats the metal to beyond the beta transus followed by a slow cool.

Solution treating and aging is used to improve strength characteristics of the material [28]. Solution treating typically requires heating to a temperature 28-83°C below the beta transus of the alloy in order to obtain high strength with adequate ductility (heating into the beta region may be desirable for improving fracture toughness or stress

corrosion resistance). Proper temperature control is important for solution treating in order to prevent accidental crossover into the beta region, which reduces tensile properties (especially ductility). The rate of cooling from solution-treating temperatures has a significant impact on the material's strength characteristics. If cooling occurs too slowly, appreciable diffusion may occur and decomposition of the beta phase material may reduce strengthening. Air or fan cooling may be adequate for alloys with a high content of beta stabilizers or for products of small section size, but in general a quenchant is required for alpha-beta alloys. The final step in the process requires reheating to an aging temperature. This reheating causes decomposition of the supersaturated beta phase which is retained during quenching. Aging at or near the annealing temperature results in overaging, resulting in material said to be solution treated and overaged (STOA), which allows modest increase in strength performance yet retains satisfactory toughness and dimensional stability.

Conclusion

This chapter has introduced some of the preliminary concepts and the literature survey necessary for an understanding of the research findings to follow. The next chapter presents a detailed investigation of the staircase method. This method is currently widely used to estimate fatigue strength at a given number of cycles, although the method's reliability in assessing fatigue strength variance has been a topic of considerable research in recent years. As discussed, the simplicity in test protocol, along with the straightforward data analysis, makes the method ideal for use, assuming deficiencies can be overcome. The results of the next chapter will be validated using the alpha-beta (α - β) Ti-6Al-4V alloy.

III. INVESTIGATION OF THE STAIRCASE METHOD

The purpose of this chapter is to provide a detailed investigation of the staircase method in order to assess its applicability to fatigue strength testing. In the first part of the chapter, details of the statistical method will be presented along with a survey of various means of improving fatigue strength parameter estimates using staircase analysis. Next, a numerical simulation study will be presented. This study analyzed the effects of staircase parameter settings on fatigue strength estimates using the Dixon-Mood method, and resulted in a new approach to calculating standard deviation estimates using staircase data. In addition, bootstrapping and staircase iteration were investigated as possible means of improving staircase results. The chapter culminates in a modified method of analyzing staircase test data in order to reduce both the bias and scatter inherent in fatigue strength estimates based on small-sample fatigue tests.

Dixon-Mood Analysis of Staircase Data

In the previous chapter, an overview of the staircase method was presented. Recall that in a staircase test, specimens are tested sequentially, with the first specimen tested in a fatigue testing apparatus set at an initial stress level (denoted as S_{init}). The specimen is fatigued until it either fails or reaches the maximum number of cycles at which the fatigue strength is to be estimated. If the specimen fails before reaching the maximum number of cycles, the stress level for the next specimen is decreased by a given interval (i.e., the step size, denoted as s). Conversely, if the specimen reaches the maximum number of cycles without failing (i.e., a runout), then the stress level for the next specimen is increased by s . This process is repeated until all the specimens allocated for the experiment have been used. In such a constant-step protocol, there are three parameters which the researcher must specify: (1) the starting stress, S_{init} , (2) the step size, s , and (3) the number of specimens, N .

In 1948, Dixon and Mood presented a means of analyzing data generated in such a fashion (then called the “up-and-down” method) [27]. Their objective was to analyze results from explosives tests conducted at various heights. Tests were conducted at an initial height h_0 , and if the weight exploded then the height for the next test would be

lowered by an interval, or it would be raised an interval if the weight did not explode. Such a protocol was popularized for the application of fatigue strength testing by Little in the 1970s [46]. Discussion of Dixon-Mood's approach will be couched in fatigue-related terms rather than their original explosives testing terminology.

Dixon and Mood noted several advantages for the use of the staircase method. First, the staircase test by its very nature tends to concentrate data near the mean, which increases the accuracy with which the mean can be estimated. Compared to use of a balanced test strategy such as the probit method (in which groups of equal size are tested at fixed stress levels), Dixon and Mood estimated a "30 to 40 percent" savings in the number of specimens required to estimate the mean with a given accuracy. Another advantage is the relative simplicity of the statistical analysis of staircase data. Unlike the probit method which requires iterative equations or graphical techniques involving subjective judgment, a set of simple arithmetic equations can be used to provide estimates of the fatigue strength mean and its standard deviation using staircase data, provided that certain conditions apply. Brownlee *et al* also recommended the staircase test over a probit-type method because of the staircase test's advantages in efficiency and simplicity, with the following conclusion:

"In summary, we believe that the up-and-down [staircase] method will prove superior to the probit method in any situation wherein the arrangement of the trials in series is not prohibited by experimental or cost considerations. Certainly there are many laboratories now using the probit method which would profit from a change to the up-and-down [staircase] design." [21]

The primary condition of the Dixon-Mood analysis is that the variate under consideration must be normally distributed. In the case of fatigue testing, this would imply that the fatigue strength distribution must be normally distributed. This condition would seem to be very restrictive and rule out staircase testing for many materials; however, a transformation of the stress values may be applied. For example, the fatigue strength distribution of some materials may be reasonably represented using a lognormal distribution, in which case the logarithm of stress values would be normally distributed. The staircase test would then be conducted using steps of equal intervals with respect to the natural logarithm of stress. Depending on the skewness of the distribution, other

transformations may be applied to make the distribution reasonably normal, although there is no guarantee that every distribution can be transformed to approach normality. In addition to logarithmic transformations, power transformations are often applied for such a purpose. Squared and cubic transformations (as well as other powers greater than 1) are used to reduce negative skewness, while logarithmic and powers less than 1 (such as a square-root transformation) as well as negative reciprocals ($-1/x$) are often used to reduce positive skewness [60]. Thus, the normality condition is not as restrictive as it first appears. However, it is likely to often be the case where there is not enough data to actually estimate the distribution shape prior to conducting a staircase test. Thus, one must either make a guess as to the shape based on data from a similar material and apply an appropriate transformation if non-normal, or simply accept the initial assumption of normality and conduct the test without a stress transformation and then use the data from the experiment itself to estimate the distribution.

Dixon and Mood's second condition of their staircase analysis is that the sample size must be large, on the order of 40 to 50 specimens or more. This condition ensures that large sample theory, on which the analysis is based, can be applied. However, additional research with respect to sample size has shown that this condition is actually unnecessary when testing for fatigue strength mean. Brownlee *et al* note that the distribution mean using Dixon-Mood analysis is "reasonably reliable even in samples as small as 5 to 10" [21]. In fact, the Japan Society of Mechanical Engineers (JSME) recommends a 6-specimen staircase for the determination of the fatigue limit [56]. In addition, several different researchers have proposed modifications to Dixon and Mood's original analysis to account for smaller sample sizes. These modifications will be discussed later in this chapter.

The final condition of the Dixon-Mood approach is that the standard deviation of the normal distribution must be roughly estimated prior to testing. This condition is necessary because the equations on which the standard deviation equations are based assume that the step size is on the order of 0.5σ to 2.0σ where σ is the true standard deviation. Thus, some knowledge of the standard deviation is required in order to specify the step size prior to testing. This requirement is not as severe as it may appear because

usually some data points are available from other testing of the material of interest or a similar material in order to provide a rough initial estimate of standard deviation.

With these assumptions, Dixon and Mood used maximum likelihood estimation techniques to analytically solve the problem of determining the mean and standard deviation of the variate of interest based on staircase test data. The results of their analysis are summarized by the equations below for estimated fatigue strength mean ($\hat{\mu}$) and standard deviation ($\hat{\sigma}$), which may be considered the “traditional” approach to interpreting staircase data [27]:

$$\text{Define } A = \sum_{i=0}^{i_{\max}} m_i, \quad B = \sum_{i=0}^{i_{\max}} i m_i, \quad C = \sum_{i=0}^{i_{\max}} i^2 m_i \quad (16)$$

$$\hat{\mu} = S_0 + s \cdot \left(\frac{B}{A} \pm 0.5 \right) \quad (17)$$

$$\hat{\sigma} = 1.62 \cdot s \cdot \left(\frac{A \cdot C - B^2}{A^2} + 0.029 \right) \text{ if } \frac{A \cdot C - B^2}{A^2} \geq 0.3 \quad (18)$$

$$\text{or, } \hat{\sigma} = 0.53 \cdot s \text{ if } \frac{A \cdot C - B^2}{A^2} < 0.3 \quad (19)$$

In these equations, the parameter i is an integer denoting the stress level, with i_{\max} corresponding to the highest stress level in the staircase. If the majority of specimens failed, then the lowest stress level at which a survival occurs (i.e., runout) corresponds to the $i = 0$ level and m_i corresponds to the number of specimens which survived each stress level. The next highest stress level would be the $i = 1$ level, and the stress level one above that would be $i = 2$, etc. If the majority of specimens survived the given number of cycles, then the lowest stress level at which a failure was observed is denoted as the $i = 0$ level and m_i corresponds to the number of specimens which failed at each stress level. S_0 is the stress value corresponding to the $i = 0$ stress level; note that this is not necessarily the same as the initial starting stress, S_{init} . As already defined, s is the step size. The plus sign in the equation for $\hat{\mu}$ is used when failures are the majority event, while the minus sign is used if survivals are the majority event.

Use of these equations can be clarified using Example 1, a notional staircase test based on underlying properties fairly similar to that of a Ti-6Al-4V alloy at very high

cycles. In this example, a 10-specimen staircase was simulated with S_{init} equal to 395 MPa and step size 5 MPa. The true underlying fatigue strength distribution was modeled as normal, with mean 400 MPa and standard deviation 5 MPa. Simulated staircase data for such an experiment are depicted in Figure 19. The simulated results included 4 failures and 6 survivals. Since survivals are the majority event, the $i = 0$ stress level corresponds to the lowest stress level at which a failure occurred, or 395 MPa in this case. Then the $i = 1$ stress level corresponds to 400 MPa, and $i = 2$ corresponds to 405 MPa, and $i = 3$ corresponds to 410 MPa. Table 2 tabulates the summations required for the Dixon-Mood equations. The summations from this table are used in the Dixon-Mood equations, as shown in the calculations which follow.

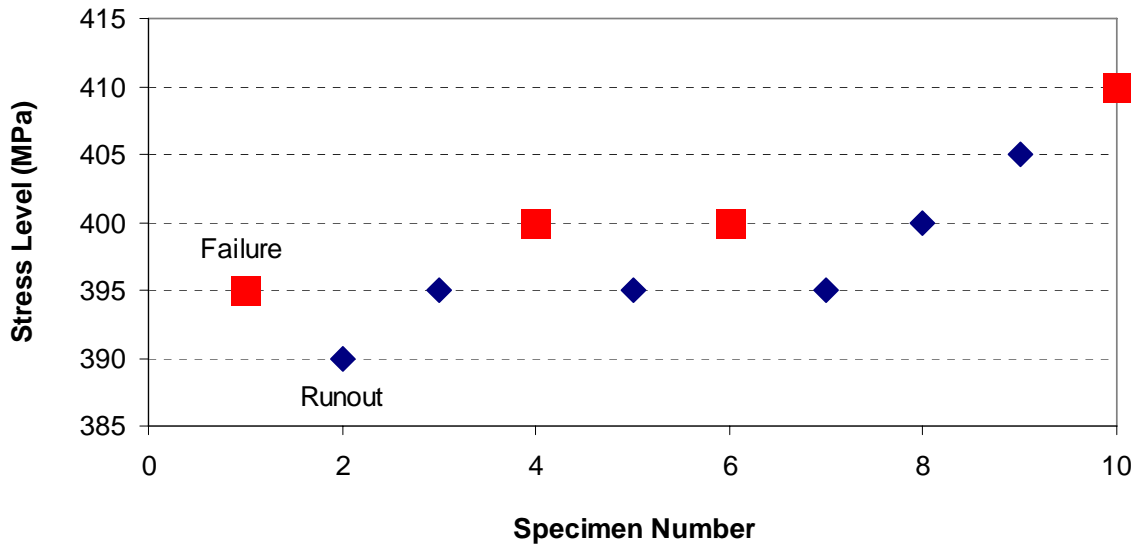


Figure 19. Notional staircase data for illustration of the Dixon-Mood method.

Table 2. Summations for illustration of the Dixon-Mood method.

Stress Level	Stress (MPa)	m_i (failures)	$i \cdot m_i$	$i^2 \cdot m_i$
$i = 0$	395	1	0	0
$i = 1$	400	2	2	2
$i = 2$	405	0	0	0
$i = 3$	410	1	3	9
Sum	--	A = 4	B = 5	C = 11

$$\hat{\mu} = S_0 + s \cdot \left(\frac{B}{A} \pm 0.5 \right) = 395 + 5 \cdot \left(\frac{5}{4} - 0.5 \right) = 398.75 \quad (20)$$

$$\frac{A \cdot C - B^2}{A^2} = \frac{4 \cdot 11 - 5^2}{4^2} = 1.19 \geq 0.3 \quad (21)$$

$$\hat{\sigma} = 1.62 \cdot s \cdot \left(\frac{A \cdot C - B^2}{A^2} + 0.029 \right) = 1.62 \cdot 5 \cdot (1.19 + 0.029) = 9.85 \quad (22)$$

Thus, using Example 1, the Dixon-Mood estimates for mean fatigue strength and the standard deviation of fatigue strength would be 398.75 MPa and 9.85 MPa, respectively, at the cycles tested for the simulated data set.

Modifications of the Dixon-Mood Estimate for Mean

There have been no less than three efforts to improve the Dixon-Mood estimate for mean for small sample tests. The first such effort was conducted by Brownlee *et al*, published in 1953 [21]. Their proposed changes for the calculation of mean were actually not required if one starts testing near the true mean, as they noted:

“In many experimental situations the experimenter will be able to guess the value of μ to within 2 steps, where the step is the guessed value of σ . In these situations the [Dixon-Mood] estimate [for μ] is quite satisfactory, being both simple and accurate.” [21]

Their proposed method is intended to handle situations in which the initial starting stress is more than a couple steps away from the true mean. In such a case, the initial data points will likely be a string of survivals (if the starting stress was too low) or failures (if starting too high). One could simply apply the Dixon-Mood equation over the entire set of data, or ignore those initial points with the same outcome and use the Dixon-Mood equation for the data starting at the first point where the result changes from survival to failure, or vice versa. In fact, this truncation of data is often done, with the Dixon-Mood equation applied to the smaller data set. However, the Brownlee *et al* method takes a different approach, as the following paragraph shows.

In the Brownlee *et al* method, one chooses a value n which represents the number of specimens which the mean value will be based upon, and the experiment is run until there have been $n - 1$ trials in addition to the initial run of constant sign (all survivals or

all failures). Thus, the total number of specimens (N) is a random variable, with $N \geq n$ (note that $N = n$ if the first and second trials have opposite outcomes). Each stress level is denoted by an integer, with the starting stress denoted as level 0. Thus, a trial two steps above the starting level would be at stress level 2. The value C' is defined as the sum of the stress levels over the last $n - 1$ trials and the $(N + 1)$ st trial (which is not performed). Then, the estimate for μ , in units of stress level, is given as:

$$\mu' = \frac{C'}{n} \quad (23)$$

Example 2 will help demonstrate the simplicity of this method. Consider a 9-specimen staircase conducted at starting stress 380 MPa with step size 5 MPa (equal to the true standard deviation σ). Figure 20 illustrates simulated data from such a test.

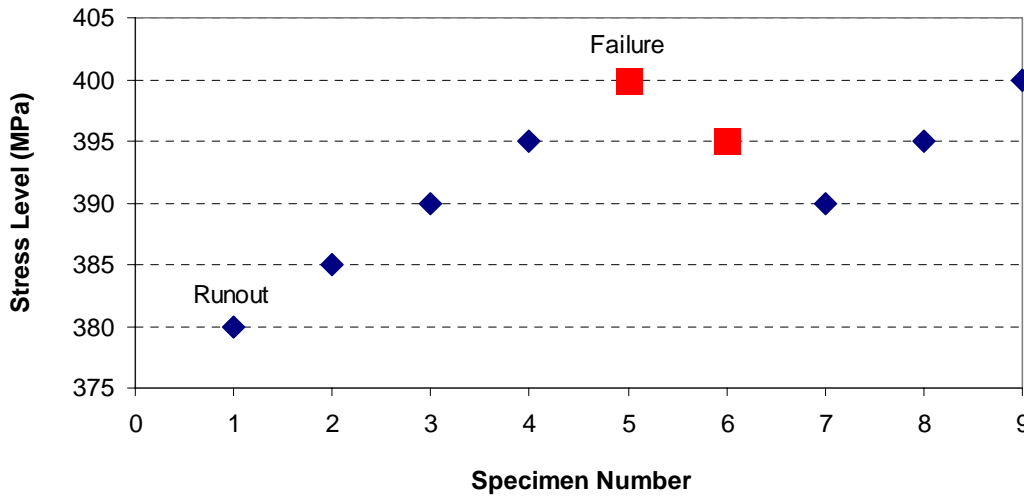


Figure 20. Notional staircase data for illustration of the Brownlee *et al* method.

For this example, $N = 9$ and $n = 6$ by the Brownlee *et al* definitions. Then, C' is determined by summing the stress levels over the last $n - 1$ trials and adding the stress level for the $(N + 1)$ st trial, which is not performed. In this case, since the last trial was a survival, the next trial, if performed, would be one step higher than the last trial. Thus, C' would be equal to $(4 + 3 + 2 + 3 + 4 + 5)$, or 21. Then, μ' would equal $21/6$, or 3.5. This value is expressed in stress levels, so the actual fatigue strength mean would be found using $S_{init} + s \cdot (\mu')$, or $(380 + 5 \cdot 3.5) = 397.5$ MPa. In this case, the estimated

mean from the Dixon-Mood equation (Equation 17) is 395.0 MPa. The true value of fatigue strength mean for this simulated data was 400 MPa. Thus, the Brownlee *et al* method provides an improved estimate for fatigue strength mean. In some cases, however, the two methods may yield the exact same or closely similar results.

Although the Dixon-Mood method is generally quite accurate for fatigue strength mean, the Brownlee *et al* method offers two significant advantages. First, it is more robust in that it corrects for data in which the first few trials all have the same outcome. Thus, one can start a staircase with less knowledge of the true mean and “walk” up or down to that mean with less error in calculated results. Dixon numerically calculated this benefit and noted that at initial stresses two or more steps from the mean, the Brownlee *et al* method results in less mean square error (approximately 23% less error beyond three steps), although there is slightly more error when tests are conducted starting near the mean [26]. The second major advantage is that the modified method makes calculation of the mean incredibly simple. Instead of the computations necessary for the Dixon-Mood method, one must simply add integers representing stress levels, and then perform a single division of two integers. The computational simplicity of such an approach, coupled with less sensitivity to starting stress, makes this method an effective way to calculate mean fatigue strength from a set of staircase data. As if this was not easy enough, Dixon offered another approach a decade later.

In 1965, Dixon published “The Up-and-Down Method for Small Samples” [26], very similarly titled to the Brownlee *et al* paper “The Up-and-Down Method with Small Samples.” Although the papers were similarly titled, the methods proposed were quite different. Like the Brownlee *et al* method, the Dixon method accounts for a sequence of similar outcomes at the start of a test until the staircase “walks” into the general vicinity of the mean, where opposite outcomes are encountered. Unlike the Brownlee *et al* method, Dixon used digital simulation to solve maximum likelihood equations to account for the initial series of same outcome results. Thus, the knowledge gained by these initial outcomes is more fully utilized in the actual analysis. Although more complex than the previous method, Dixon reduced these computations into simple lookup tables which can be used to translate staircase data into a mean fatigue strength estimate using the following equation:

$$\hat{\mu} = S_f + k \cdot s \quad (24)$$

In this equation, S_f is the final stress value tested, k is a parameter found using the lookup table based on the sequence of staircase results, and s is the step size. Trials are denoted by an “X” for a failure, and an “O” for a survival. Thus, the staircase data from Example 2 (Figure 20) would be represented by the sequence OOOOXXOOO. The value for k based on an initial sequence of OOOO followed by XXOOO is -0.263 according to the Dixon tables. Thus, for this simulated data, the estimated mean fatigue strength would be $(400 - 0.263 \cdot 5) = 398.7$ MPa. Recall that the true mean for this simulated data was 400 MPa, so the Dixon estimate is better than both the Brownlee *et al* (397.5 MPa) and original Dixon-Mood (395.0 MPa) estimates. Dixon’s calculations show that mean square errors when starting at or beyond two steps from the true mean are less than the Brownlee *et al* method, which are less than the Dixon-Mood method. When starting at the mean, the Dixon method produces similar mean square error to that of the Brownlee *et al* method. In addition, the Dixon method is obviously extremely simple, requiring just the use of a lookup table and one equation. However, his tables are only complete for up to four initial trials of the same result, followed by up to five more trials. But, this amount of data is shown to be more than adequate for a good estimate of the mean fatigue strength, so additional data points are generally unnecessary.

In 1972, Little expanded upon the work of Dixon by considering the use of minimum chi square analysis versus maximum likelihood analysis, using logistic and extreme value distributions versus the normal distribution, and considering step sizes of $s/\sigma = 2/3$ and $3/2$ versus 1 [42]. Like Dixon, his work resulted in a series of lookup tables. These tables use the sequence of results and assumed underlying distribution shape to lookup the scale factor Δ with which the following equation can be solved:

$$\hat{\mu} = S_{init} + \Delta \cdot s \quad (25)$$

Little’s tables are limited to up to four trials after the first crossover in outcomes, but may be extended to any number of initial trials of the same result. Thus, for the data from Example 2 (Figure 20), the sequence of results would be OOOOXXOO. Using Little’s table for an underlying normal distribution, Δ would be 3.38 using maximum likelihood analysis or 3.37 using minimum chi square analysis. Thus, the estimated mean

fatigue strength would be $(380 + 3.38 \cdot 5) = 396.9$ MPa. This estimate is better than Dixon-Mood alone. To fairly compare this method with the others, assume the last data point is removed so that each method is based on only 8 total specimens. Removing the last data point changes the Brownlee *et al* estimate from 397.5 MPa to 396.0 MPa, and changes the Dixon estimate from 398.7 MPa to 396.9 MPa. Thus, the Little estimate is the same as Dixon, which is slightly better than Brownlee *et al*.

To provide further comparison of the various methods for calculating the fatigue strength mean, a total of 40 unique simulated sets of staircase data were generated, each with step size 5 MPa, with an underlying normal fatigue strength distribution with mean 400 MPa and standard deviation 5 MPa. The staircases used differing starting stresses, with 10 sets of data starting 4 steps below the true mean, 10 sets starting 3 steps below, 10 starting 3 steps above, and 10 starting 4 steps above. Each staircase was terminated when four data points were collected beyond the initial series of similar outcomes. The estimates for fatigue strength mean for the simulated sets of data starting 4 steps below the true mean (i.e., starting at 380 MPa) are shown in Table 3. As the numbers show, the modified methods generally provide a slightly better estimate for fatigue strength mean compared to Dixon-Mood analysis. When one considers that these estimates are based on staircase tests using on average only 7.5 specimens and initiated at a starting stress 4 steps (and thus 4 standard deviations) below the true mean, the efficiency of the staircase test in providing estimates for the mean fatigue strength really becomes obvious.

Table 3. Comparison of various methods of determining fatigue strength mean for simulated data sets with true mean of 400 MPa starting at 380 MPa (5 MPa step).

	Sequence of Results	Dixon-Mood	Brownlee <i>et al</i>	Dixon	Little (MLE)	Little (min χ^2)
Run 1	OOXOOO	387.5	392.0	394.2	394.3	393.7
Run 2	OOXOOX	390.0	390.0	390.5	390.7	390.5
Run 3	OOOXOXO	392.5	393.0	393.7	393.7	393.3
Run 4	OOOXOOO	392.5	397.0	399.2	399.3	398.7
Run 5	OOOXOOX	395.0	395.0	395.7	395.7	395.5
Run 6	OOOXXOO	395.0	396.0	396.9	396.9	396.9
Run 7	OOOXXOXX	395.8	396.0	395.9	395.9	396.2
Run 8	OOOXXOOX	400.0	400.0	400.7	400.7	400.5
Run 9	OOOOXXOX	399.2	399.0	399.3	399.3	399.0
Run 10	OOOOXXOXX	400.8	401.0	400.9	400.9	401.2
Average	7.5 specimens	394.8	395.9	396.7	396.7	396.6

The data in Table 3, as well as data for the other starting stresses (shown in Appendix B), clearly show that the modified methods have more impact compared to Dixon-Mood analysis the farther one starts from the mean or the worse the Dixon-Mood analysis underestimates (if starting below the mean) or overestimates (if starting above the mean) the true mean. It is also apparent that Little's tables provide, in general, the best estimates for mean fatigue strength for tests with up to four trials after the first crossover in outcomes. Since they are also more robust in that they account for other interval sizes and underlying distributions, use of Little's tables is preferable for small sample tests in which the first few trials have the same outcome for tests with up to four trials after crossover. If more than four trials are available after crossover, then Dixon's tables should be used for underlying normal distributions with $s \cong \sigma$. If the first two trials result in opposite outcomes, then the original Dixon-Mood equation should be used without modification. For example, use Little's tables for a sequence of XXXOXOO, use Dixon's tables for XXXOXOOX, and use Dixon-Mood analysis for XOXOOX.

Modifications of the Dixon-Mood Estimate for Standard Deviation

As described in the previous section, the Dixon-Mood method is generally very efficient and accurate for calculation of mean fatigue strength when one starts near the true mean. In addition, there are adequate modifications to account for cases in which the trials begin significantly far from the true mean. Few, if any, additional works have been published since Little's work in the 1970s on the subject of improving the mean estimates, as that problem has been considered to be adequately solved.

Unfortunately, the standard deviation estimates provided by Dixon-Mood analysis are not nearly so reliable for small-sample tests. In fact, Brownlee *et al* dismissed the problem of determining the standard deviation with the following conclusion:

“We have not considered the problem of estimating the scale parameter σ . The reason for this is partly that μ is usually the parameter of greater interest, but primarily that with small samples no estimate for σ can be accurate enough to have much value. Even if μ were known, and even if the trials are conducted at stimuli giving the most efficient estimation, over 200 trials would be required to estimate σ within 20 percent with confidence of 95 percent.” [21]

Little also expressed this sentiment when he wrote the following as part of his study on mean fatigue strengths:

“Reliable estimation of the standard deviation σ of the underlying normal response distribution is quite a different matter however. The up-and-down strategy is quite inefficient in this regard. Consequently its σ estimates should be used only in the absence of more reliable prior information.” [42]

Standard deviation estimation is so difficult using staircase testing because of the very nature of the testing itself. By concentrating the majority of the data points near the mean, it is more difficult to get an accurate measure of dispersion, which of course is exactly what standard deviation represents. With few data points in the “tails” of the distribution (i.e., the areas of decreasing probability), standard deviation estimates become based on data near the center of the distribution. Therefore, slight differences in the central data can lead to very different measures of standard deviation as there is little data in the tails to help scope the dispersion. When there are very many data points, even if centrally located, the dispersion can be more accurately measured since the underlying distribution (normal) is fixed. For this reason, one can overcome the difficulties of standard deviation estimation using the staircase test if a very large number of specimens are available for testing. However, using a very large number of specimens would defeat the whole purpose of doing staircase testing in the first place, which is to realize gains in efficiency versus balanced test strategies such as the probit method.

After many years of apparently little work being published on the staircase test, there has recently been considerable effort in this area, specifically with respect to standard deviation estimation, by a number of different researchers. One can reasonably speculate that this increased emphasis is due to the following factors: (1) increasing interest in the probabilistic aspects of fatigue, primarily high cycle fatigue, (2) dramatically improved processing power of personal computers to handle more complex digital simulations, and (3) greater emphasis on efficient test strategies to provide reliable estimates due to the high cost of materials and components and longer test times in the ultra high cycle regime.

Some of the recent research in this area includes investigation of a correction factor for standard deviation in small sample tests conducted by Svensson *et al* in Sweden (1999-2000, [85-85]), Braam and van der Zwaag's modified standard deviation work from the Netherlands (1998, [20]), Griffiths and Annis's use of staircase testing in conjunction with RFL analysis for General Electric's contribution to the National HCF S&T Program (2001, [11]), the simulation work of Lin *et al* for DaimlerChrysler (2001, [41]), the modified standard deviation approach of Fang *et al* in China (2000, [34]), and the use of size effect to improve the reliability of staircase results by Rabb in Finland (2003, [73]). Clearly, there is currently a worldwide interest in improving the reliability of standard deviation estimates based on staircase data. Interestingly, none of these works reference any of the others and it appears that these recent efforts have emerged somewhat independently, and therefore represent unique approaches to the standard deviation problem. The following sections describe some of this work in more detail.

Svensson-Lorén Correction for Small-Sample Tests

In 1999, Svensson and Maré published an analysis of the random features of the fatigue limit [84]. In this paper, the results of simulation work from small-sample tests (≤ 30 specimens) were summarized. This simulation work suggested (or rather confirmed) that the standard deviation estimates using Dixon-Mood analysis are biased. In a follow-up paper summarizing the research conducted by Lorén and led by Svensson, Maré, and Wadman, it was stated that “we have not found any theoretical solution to the problem [of bias] for the general maximum-likelihood method...” [85]. However, a linear correction factor was proposed (here called the Svensson-Lorén correction) and found to be “an improvement in all maximum-likelihood evaluation procedures, including the staircase method.” Their equation is shown below, where σ_{SL} represents the Svensson-Lorén corrected standard deviation estimate, σ_{DM} is the standard deviation estimate based on Dixon-Mood analysis, and N is the total number of specimens:

$$\sigma_{SL} = \sigma_{DM} \frac{N}{N-3} \quad (26)$$

The correction is strictly a function of the sample size and has the effect of increasing the standard deviation estimate found from Dixon-Mood analysis, with the

increase greater for smaller sample sizes. Since the standard deviation estimate is merely multiplied by a constant greater than 1, this correction will yield slightly more scatter in results compared to Dixon-Mood. This correction factor will be analyzed in more detail using the simulation work presented later in this chapter.

Braam and van der Zwaag Correction

In 1998, Braam and van der Zwaag also used numerical simulation to address the adequacy of standard deviation estimates provided by Dixon-Mood analysis [20]. In addition, they compared the results of staircase estimates to those calculated using the $\arcsin\sqrt{P}$ method, which uses uniformly spaced stress levels with a prescribed number of specimens at each level. Like Svensson *et al*, they identified the bias inherent in small-sample staircase tests. They concluded:

“It has been shown that the staircase method and the $\arcsin\sqrt{P}$ transformation for determining the fatigue limit of engineering materials both yield a correct estimate of the average fatigue limit almost irrespective of the number of samples available. In contrast, the standard deviation of the fatigue limit is seriously underestimated by both methods, especially in the case of small sets of samples. For a given set size, the error in the standard deviation depends on the ratio of s to σ , where σ is unknown by definition. Both testing methods yield comparable accuracy for the average value and both methods suffer from the same problem considering the standard deviation.” [20]

To address this standard deviation bias, they proposed a correction to the Dixon-Mood estimate which they claim “gives better results, especially for small data sets” [20]. Unlike the Svensson-Lorén correction, Braam and van der Zwaag’s proposed correction accounts for both the number of specimens as well as the step size. Their equation is shown below, with σ_{BZ} denoting their modified standard deviation and other terms as previously defined:

$$\frac{\sigma_{BZ} - \sigma_{DM}}{s} = \left(\frac{\sigma_{BZ}}{s} - 0.95 \right) \cdot \exp \left(- \frac{N}{4.93 \cdot \frac{\sigma_{BZ}}{s} + 24.48} \right) \quad (27)$$

This equation can be solved iteratively, graphically, or with the help of a solver. One can see that for cases in which there are a very large number of specimens, the

exponential term goes to zero, and therefore σ_{BZ} is approximately equal to σ_{DM} . This result is qualitatively satisfying since the Dixon-Mood standard deviation estimate improves as the number of samples becomes very large. Also, when the step size is approximately equal to the standard deviation, the pre-exponential term then goes to zero, and again σ_{BZ} is approximately equal to σ_{DM} . Braam and van der Zwaag appear to accept this as qualitatively satisfying as well. It is not obvious, however, that a good correction should behave in this manner. The scatter inherent in Dixon-Mood estimates may result in some standard deviation estimates approximately equal to the step size in spite of, and not because of, the true standard deviation of the material. It is also worth noting that this correction was developed based on simulations with step sizes ranging from 0.1σ to 1σ and sample sizes ranging from 20 to 100 specimens.

Braam and van der Zwaag claim that the distribution of standard deviation estimates using their proposed correction is less dependent on the step size when compared to Dixon-Mood estimates, although they noted a disadvantage in that the modified estimate has a broader distribution (i.e., more scatter) than the Dixon-Mood approach, especially for smaller sample sizes. Consider the data depicted previously by Figure 19 in which a 10-specimen staircase test was simulated with $s = 5$ MPa using a normally distributed fatigue strength with $\sigma = 5$ MPa. Recall that Dixon-Mood analysis resulted in an estimated standard deviation of $\sigma_{DM} = 9.85$ MPa. The corrected standard deviation estimate using the Braam and van der Zwaag approach can be found using Figure 21, where the y -axis represents the difference between the left and right sides of the Braam-van der Zwaag equation. Thus, σ_{BZ} is found as the point where the curve passes through the x -axis, or approximately 40 MPa in this case. This corrected standard deviation estimate is in fact much worse than the original Dixon-Mood estimate (700% error versus 97% error, respectively). This seemingly surprising result will be shown to be a real issue, and not a statistical anomaly, in the next paragraph.

In the present investigation, a more rigorous comparison of the Dixon-Mood and Braam-van der Zwaag estimates was accomplished using additional simulations of 12-specimen staircase tests conducted under similar assumptions ($s = \sigma = 5$ MPa, $\mu = 400$ MPa, $S_{init} = 395$ MPa), for 10 cases resulting in unique Dixon-Mood standard deviation estimates (more than 10 simulations were run, but results using Dixon-Mood are

discretized and the simulations were stopped once 10 unique outcomes were observed). These runs are summarized in Table 4. The results of this comparison show that the Braam-van der Zwaag estimates (σ_{BZ}) were in fact worse than the Dixon-Mood estimates (σ_{DM}) in almost every case (only being a slight improvement for the one case where the Dixon-Mood estimate was already very close to the true value). For the lowest values of Dixon-Mood standard deviation (2.65 MPa), the correction even produced nonsensical results of negative standard deviation. The σ_{DM} value of 2.65 MPa is no statistical outlier, either. On the contrary, this result is the most frequent outcome for standard deviation using Dixon-Mood analysis for a staircase test under these conditions.

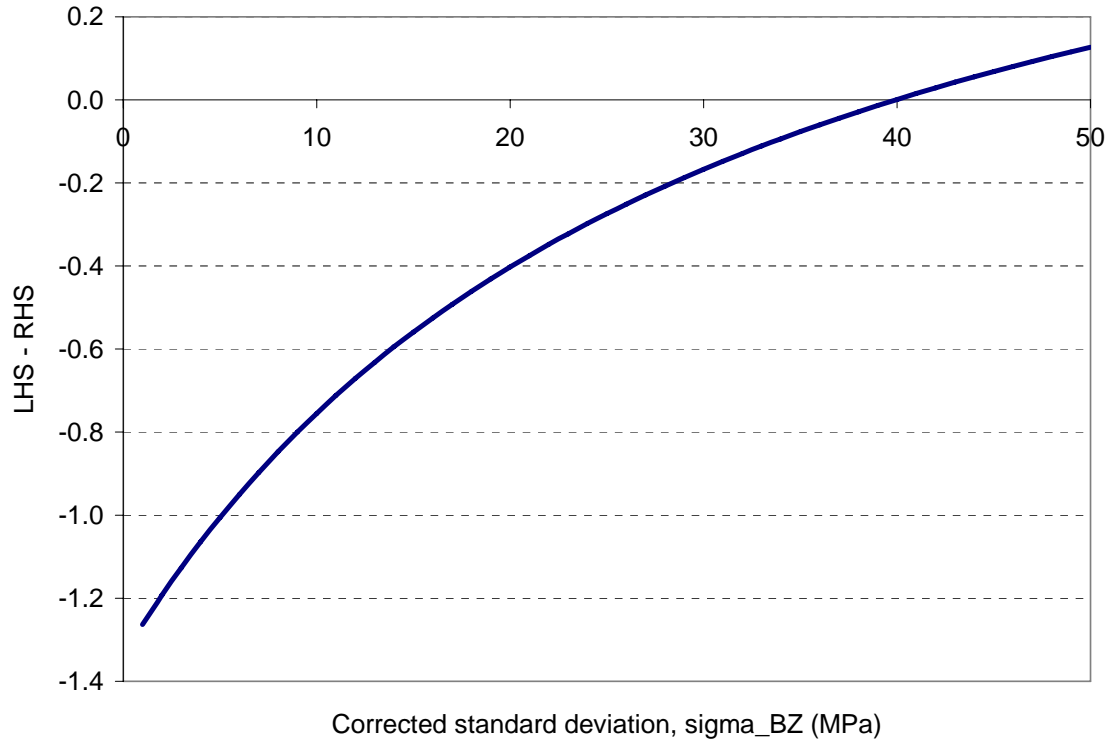


Figure 21. Graphical solution of the Braam and van der Zwaag standard deviation equation for the staircase data shown in Figure 19.

Table 4. Comparison of Dixon-Mood and Braam-van der Zwaag standard deviation estimates for 12-specimen staircase tests at $s = \sigma = 5$ MPa.

	Sequence of Results	Standard Deviation (MPa)		
		Dixon-Mood (σ_{DM})	Braam-van der Zwaag (σ_{BZ})	Braam-van der Zwaag, modified (σ_{BZ}^{mod})
Run 1	OOXXOXOOXXOX	2.65	N/A (< 0)	1.3
Run 2	XOOXOXOXOOXX	2.94	0.07	1.8
Run 3	OOXXOXOXOOXOO	3.48	1.3	2.6
Run 4	OXOOXXOXOOXX	4.06	2.8	3.6
Run 5	OOXOXOXOXOOO	4.77	4.8	4.8
Run 6	OOXOXOXOXOXOX	5.64	7.5	6.2
Run 7	OXOXOOXOXOXO	6.72	11.5	8.0
Run 8	OXOXOOXOXOXOX	7.44	14.9	9.3
Run 9	OOXXOXOXOXOXO	7.66	16.0	9.8
Run 10	XOOXOXOXOXOX	11.90	55.0	17.0

The Braam-van der Zwaag correction appears to break down when sample sizes are very small (a minimum of 20 specimens were used in their initial work). A small change to their original equation was made by replacing σ_{BZ} with σ_{DM} in the right-hand side of the equation. Making this modification, the following equation results, where the modified Braam-van der Zwaag standard deviation estimate is denoted by σ_{BZ}^{mod} . Estimates using this equation are also shown in Table 4. These estimates appear better than the estimates obtained using the original equation, although they are still generally worse than the Dixon-Mood estimates.

$$\frac{\sigma_{BZ}^{mod} - \sigma_{DM}}{s} = \left(\frac{\sigma_{DM}}{s} - 0.95 \right) \cdot \exp \left(- \frac{N}{4.93 \cdot \frac{\sigma_{DM}}{s} + 24.48} \right) \quad (28)$$

Thus, this method does not appear to deliver better fatigue strength estimates compared to Dixon-Mood analysis for tests using very few samples. Additional simulations were run with $s = \sigma = 5$ MPa, $S_{init} = 395$ MPa, $\mu = 400$ MPa, and $n = 20$ specimens. The results are presented in Table 5, sorted in ascending order of standard deviation. The use of 20 specimens versus the previous simulations with 12 specimens has eliminated cases where σ_{BZ} is less than zero. However, the standard deviation

estimates using the Braam-van der Zwaag correction are still worse than Dixon-Mood in each case, even if the modified correction is used. However, the average standard deviation estimate is better using Braam-van der Zwaag versus Dixon-Mood over this small set of data. This result could explain how the correction appears to reduce the bias inherent in the Dixon-Mood method, although with greater scatter. However, it appears that it is only in an average sense that bias is removed. Standard deviation estimates which are too low are even lower using the correction, and estimates which are too high are even higher using the correction, for the cases investigated. Thus, the method does not appear to be a viable alternative to Dixon-Mood analysis for very small sample sizes (smaller than those originally investigated by Braam and van der Zwaag, $N \leq 20$).

Table 5. Comparison of Dixon-Mood and Braam-van der Zwaag standard deviation estimates for 20-specimen staircase tests at $s = \sigma = 5$ MPa.

Run	Standard Deviation (MPa)		
	Dixon-Mood (σ_{DM})	Braam-van der Zwaag (σ_{BZ})	Braam-van der Zwaag, modified (σ_{BZ}^{mod})
1	2.65	0.9	1.6
2	2.65	0.9	1.6
3	2.65	0.9	1.6
4	3.15	1.7	2.3
5	3.15	1.7	2.3
6	3.15	1.7	2.3
7	3.47	2.3	2.8
8	3.56	2.4	2.9
9	3.80	2.8	3.3
10	3.83	2.9	3.4
11	3.83	2.9	3.4
12	4.20	3.6	3.9
13	4.63	4.4	4.5
14	5.42	6.1	5.7
15	5.63	6.5	6.0
16	5.83	7.0	6.3
17	6.80	9.3	7.8
18	7.04	9.8	8.2
19	7.43	10.9	8.8
20	8.65	14.4	11.8
Average	4.58	4.66	4.53
Std Dev	1.78	3.86	2.83

Fang et al Approach

In 2000, Fang, Zhang, Zhao, and Liu also investigated standard deviation estimation using staircase data for the Zhengzhou Research Institute of Mechanical Engineering in China [34]. Like Braam and van der Zwaag, they noted that standard deviation is a function of both the stress increment s as well as the true standard deviation σ . Unlike Svensson-Lorén and Braam-van der Zwaag, they did not include the effects of sample size in their equation. They characterized the relationship between the ratio of estimated standard deviation to true standard deviation and the ratio of step size to true standard deviation using the following formula (variables as previously defined):

$$\left(\frac{\sigma_{DM}}{\sigma}\right)^2 = 0.87478 \cdot \left(\frac{s}{\sigma}\right)^{1.58885} \quad (29)$$

This formula was developed using the following abbreviated rationale. First, the S - N behavior of a material was modeled as linear on a log-log plot so that fatigue life was lognormally distributed for a given stress level. Thus, fatigue life and its standard deviation (σ_N) are modeled as:

$$\log N_p = c + m \log(S - S_0) + u_p \sigma_N \quad (30)$$

$$\sigma_N = a + b \log(S - S_0) \quad (31)$$

where: c, m, a, b, S_0 are material constants,

σ_N is the standard deviation of $\log N$ for a given stress,

u_p is the standard normal distribution value for probability P ,

N_p is the fatigue life with probability P for a given stress.

Next, several different steels (40Cr and 42CrV) were tested under various conditions (smooth and notched, ambient and under water) with sample sizes for each condition ranging from 36 to 62 specimens (for a total of 392 data points). These data were used to create P - S - N plots from which best-estimate σ_N values could be calculated at the fatigue strength associated with the number of cycles of interest. It is not clear based on their paper what method was used to develop these P - S - N curves, but one can assume that conventional S - N analysis was used since there is no reference to more elaborate methods such as those based on maximum likelihood methods. Of greater

concern, it is not specified how the σ_N values (which are measures of standard deviation in life, not stress) translate into estimates for fatigue strength standard deviation (which are associated with stress, and not life). The paper omits this key step with the following:

“With these best fitting parameters [for $\log N$ and σ_N], we can give out the standard deviations of the fatigue strengths for the fatigue lives that the staircase methods selected.” [34]

It can only be speculated that σ estimates are interpreted from the P - S - N data by analyzing the vertical distribution at the number of cycles of interest. These P - S - N curves were then used to replicate simulated staircase tests from which sets of Dixon-Mood standard deviation estimates and step sizes could be found.

In short, the Fang *et al* method is another approach to improving standard deviation estimates based on staircase data but will not be investigated in more detail.

Rabb's Investigation of Staircase Settings

In 2003, Rabb also conducted a simulation-based investigation of the staircase test, noting that “due to the nature of the staircase test, it is very difficult to obtain a correct value of the sample standard deviation” [73]. He conducted a simulation of 10,000 runs to analyze the staircase estimates obtained using a modified maximum likelihood method. His simulations were run with $\mu = 195.5$ MPa and $\sigma = 17.6$ MPa, which corresponded to the sample values obtained from a 25-specimen staircase test of nodular cast iron under fully-reversed loading conducted at $S_{init} = 213.8$ MPa and $s = 18.25$ MPa. Instead of the Dixon-Mood equations for these estimates, he used the following maximum likelihood equation for the conditional probability that there are n failures and m survivals in a staircase test:

$$P(n, m | S_{init}) = K \prod_{i=1}^{\infty} p_i^{n_i} q_i^{m_i}, \text{ with } p_i = \frac{1}{\hat{\sigma} \sqrt{2\pi}} \cdot \int_{-\infty}^{S_{init}} \exp\left(-\frac{(x - \hat{\mu})^2}{2\hat{\sigma}^2}\right) dx, q_i = 1 - p_i \quad (32)$$

where: n_i and m_i are the failures and survivals on stress level i ,

p_i is the probability of failure on level i ,

K is a constant,

$\hat{\mu}$ is the estimated mean fatigue strength,

$\hat{\sigma}$ is the estimated standard deviation.

Rabb's approach requires the following stipulations as to what was an "acceptable" set of staircase data: (1) data from tests resulting in only 2 or 3 stress levels were unacceptable, (2) the probabilities of failure must increase as stress level increases, and (3) for cases in which there were 4 stress levels, there must be at least two failures on level 2 and two runouts on level 3. With these stipulations, the 10,000 runs resulted in 2423 acceptable tests with 4 levels, and 2123 acceptable tests with 5 levels; thus only 45.5% of the 25-specimen tests resulted in "acceptable" outcomes allowing evaluation by his method. The simulation data indicated that standard deviation was generally underestimated for tests resulting in 4 stress levels, and overestimated for those resulting in 5 stress levels.

Rabb conducted additional simulations to investigate the effects of various staircase parameter settings on calculated mean and standard deviation estimates. He looked at three different step sizes ($s/\sigma = 0.85, 1.00, \text{ and } 1.15$), two different sample sizes ($N = 25 \text{ and } 30$), and two different starting stresses ($S_{init} = \mu \text{ and } \mu + s/2$). Several conclusions were drawn from the simulation results. First, use of the smaller step size resulted in a higher frequency of acceptable tests, but also resulted in a poorer estimate for standard deviation. It is rather intuitive that the smaller step would yield more acceptable tests as a smaller step should allow more tests with more than 2 or 3 stress levels. As for the smaller step resulting in poorer standard deviation estimates, this effect is quantified in more detail in the simulation work presented later in this chapter. He also noted that a higher frequency of acceptable results occurred for cases with the starting stress offset higher than the true mean strength. It also seems intuitive that an offset starting stress may result in more stress levels, thus leading to more acceptable tests. The offset starting stress did not have much effect on standard deviation estimates except for the 4-level results using the largest step size. Lastly, the number of specimens had relatively little impact on results, although the number of acceptable tests increased for the larger sample size. This conclusion is also intuitive as use of more specimens should result in a higher probability of meeting the acceptability conditions. It is worth noting that the conclusion that the number of specimens has little effect on standard deviation is only based on his simulations using 25 or 30 samples – this generalization should not imply that there would be little difference between say 12 and 30 specimens.

In addition to his investigation of the staircase test, Rabb proposed another means to investigate the fatigue strength scatter of a material. Rabb used the concept of a size factor to develop a method of evaluating the standard deviation of the fatigue strength. His premise is summarized by the following:

“The statistical size factor is basically determined by the effective stress area, or in some cases, the effective stress volume, and the standard deviation of the fatigue limit. ... It is therefore possible to evaluate a reliable estimate of the standard deviation by calculating it from the observed statistical size effect from two staircase tests with different specimen sizes.” [73]

This approach would require a different test strategy with considerations not required by staircase testing (such as the use of specimens with different geometries). The use of this approach was not explored further in this study, although Rabb’s approach is summarized in Appendix C.

Summary of Standard Deviation Methods

In the previous sections, several different standard deviation methods were introduced, all of which are based on recent research papers (1998-2003). The methods all address the same fundamental issue: the unreliability of the standard deviation estimates obtained from staircase data, especially for small-sample tests. However, they approached this problem from very different angles, some being more general in scope (such as the corrections of Svensson *et al* and Braam-van der Zwaag) and some more specific (such as the empirical relation of Fang *et al* for 40Cr and 42CrV steels). It is clear, however, that this problem is in no way completely solved. The Svensson *et al* method only increases standard deviation estimates based on small sample sizes by a constant greater than 1, and does not address the scatter produced by the Dixon-Mood method. Likewise, the Braam-van der Zwaag method does not address this scatter, but on the contrary significantly increases scatter in results. In addition, this method appears to produce estimates which may be worse than Dixon-Mood alone for very small samples. Neither the Svensson *et al* nor Braam-van der Zwaag methods have been applied to real staircase test data in the literature to date. The approach of Fang *et al* has some holes in detail and in its current form, it is not applicable to general materials.

Lastly, the size effect method of Rabb requires a reliable means of estimating effective stress areas and the capability to conduct testing with different specimen sizes. Use of this method for other materials beyond nodular cast iron has not been documented.

In the next section, the problem of standard deviation estimation will be addressed through the use of numerical simulation. Results of this analysis address some of the deficiencies of the methods previously described.

Investigation of Staircase Parameters using Numerical Simulation

A computer simulation was designed to analyze the effects of staircase parameter settings on standard deviation estimates using the Dixon-Mood analysis method. The simulation allows the user to specify the true fatigue strength distribution (modeled as normal in all cases) by specifying the mean and standard deviation of the fatigue strength at the number of cycles of interest. The staircase test parameters (starting stress, step size, and number of specimens) are specified for each simulation run. For each specimen, the simulation calculates a random fatigue strength based on the specified underlying distribution and compares this value to the current stress level (starting with the initial stress, S_{init}) to determine if the specimen failed or survived. The stress level is increased or decreased for the next specimen according to the staircase protocol. This procedure is repeated until the total number of specimens is reached. Next, the standard deviation of the fatigue strength is calculated according to Dixon-Mood statistics using the simulated staircase data. This represents one run of a simulation case. This whole procedure is then repeated a large number of times (default 1000 runs) in order to provide a distribution of calculated standard deviations from which to draw conclusions.

The simulation was coded using the MATLAB programming language. Appendix D shows the underlying code for the staircase simulation. Various modifications to the code were developed for different tasks as needed, including the use of a bootstrapping algorithm and various staircase iteration schemes. The programs used for these purposes are also shown in Appendix D.

Selection of the Number of Simulation Runs

When drawing conclusions from simulated data, one would obviously prefer a very large number of simulation runs to smooth out any variance in results due solely to

statistical error related to sample size. However, depending on the complexity of the simulation and capability of the machine processor on which the digital simulation is performed, a very large number of simulation runs may require unnecessarily long run times. To address this tradeoff, an initial comparison of results was accomplished for simulations made with 1000 runs versus 10,000 runs. The PC-based MATLAB program was usually able to accomplish the 1000-run simulations in less than 2 minutes, whereas a 10,000-run simulation case could take on the order of 15 minutes or more (which may not sound like much, but when dozens of different parameter settings are being simulated at once, this run time becomes many hours). Table 6 shows the simulation results for a particular staircase scenario simulated at both 1000 and 10,000 runs. Clearly, statistics based on 1000-run simulations appear to have adequate significance. Thus, an iteration limit of 1000 runs was used as the default simulation setting.

Table 6. Comparison of results for different simulation sizes.

	Distribution Statistic	Runs = 1,000	Runs = 10,000
Dixon-Mood Std Dev (σ_{DM})	Mean	8.40	8.39
	Median	7.60	7.60
	Std deviation	3.24	3.31
	90% conf. interval	(5.30, 14.16)	(5.30, 14.87)
Note: Using true distribution normal with $\mu = 200$ and $\sigma = 10$, and staircase test with $S_{init} = 200$, $s = 10$, and 20 specimens.			

Effect of Starting Stress on Dixon-Mood Standard Deviation

As previously discussed, the staircase test efficiently provides a fairly accurate estimate of the mean fatigue strength even for small sample sizes when testing starts near the true mean. In addition, it has already been shown that there are adequate means of correcting for initial starting stress when calculating mean fatigue strengths (through use of the Brownlee *et al*, Dixon, or Little methods). Since further investigation of staircase parameter settings on mean fatigue strength estimates is thus unnecessary, simulated results for fatigue strength means are relegated to Appendix E. The effect of staircase settings on standard deviation estimates requires further investigation, however.

The first question of interest is what effect the initial starting stress has on standard deviation estimates using the Dixon-Mood method. Rabb's simulation work,

although using a different maximum likelihood method from the Dixon-Mood method, showed that initial starting stress has little influence on standard deviation estimates [73]. However, his simulations only used starting stresses at the mean or half a step higher than the mean. The simulation work in this section considers a wider range of possible starting stresses.

To address this question, simulations were accomplished using an underlying Normal(400,5) distribution (i.e., $\mu = 400$, $\sigma = 5$). The step size was equal to the true standard deviation. Three starting stresses were used: μ , $\mu + 2\sigma$, and $\mu - 2\sigma$. The mean standard deviation estimate is plotted as a function of sample size in Figure 22 for each starting stress value.

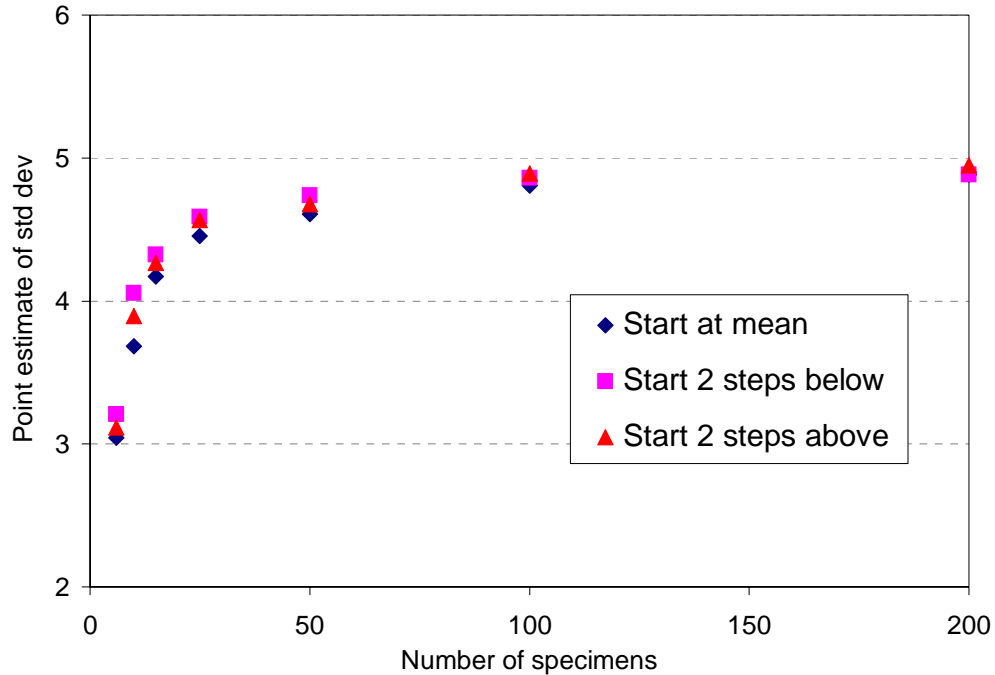


Figure 22. Effect of starting stress on Dixon-Mood standard deviation estimates for underlying Normal(400,5) with $s/\sigma = 1$.

The data show that as sample size increases, starting stress really becomes a non-factor in determining standard deviation, as one would expect. Even for small sample sizes, the effect of starting stress is rather small. However, use of offset starting stresses does have some beneficial effect for small sample sizes by alleviating some of the standard deviation bias. This result is due to the fact that when one starts above or below

the mean, it is statistically more likely that a failure will be observed below the mean (if starting below) or a survival will be encountered above the mean (if starting above), simply because one is conducting more testing above or below the mean, on average. In a small-sample test, just one of these outcomes can lead to a higher estimate of standard deviation, and therefore on average, there is a slight reduction of the standard deviation underestimating bias for small-sample tests. This effect is not overwhelming enough to eliminate the bias altogether, but does provide some means of softening it. For the data in Figure 22, the mean standard deviation for $N = 10$ samples is 3.68 (26.3% error) when starting at the mean, but 4.06 (18.9% error) when starting two steps below the mean. The traditional approach of using $S_{init} = \mu$ for staircase tests in order to maximize accuracy of the estimate for mean fatigue strength may be modified in order to improve standard deviation estimation, especially since adequate means of handling offset starting stresses exist for mean fatigue strength estimation.

Effect of Step Size on Dixon-Mood Standard Deviation

The long pole in the tent, so to speak, of standard deviation estimation is clearly the choice of step size. Step size plays a direct role in Dixon-Mood's standard deviation calculation, as Equations 18 and 19 show. It has been commonly understood, stemming from Dixon and Mood's original work, that step sizes should be on the order of 0.5σ to 2σ when using the staircase method. Use of steps greater than 2σ results in staircases which tend to bounce back and forth across the mean but do not include enough stress level data with non-zero or non-unity probabilities of survival. When this situation occurs, Equation 19 becomes applicable, and then the standard deviation estimate becomes a strict function of step size alone ($0.53s$). Use of steps much smaller than 0.5σ risk requiring too many initial data points in order to walk up to or down to the mean in case the starting stress is significantly offset. In addition, use of very small steps results in significantly underestimated standard deviations, as this simulation work will confirm. There has been some prior work in investigating the choice of step size, as Rabb used step sizes ranging from 0.85σ to 1.15σ [73], while Braam and van der Zwaag investigated steps from 0.1σ to 1σ [20]. Neither work really recommended a step size, but left the impression that a 1σ step size is generally adequate. Both works, along with

that of Svensson *et al* [84-85], confirmed that the standard deviation estimate is biased for small-sample tests, although this bias was not specifically quantified in the papers. But bias does not represent the whole story, as the next paragraph describes.

There are two primary considerations when evaluating the standard deviation estimate. The first is assessing how accurate the test is on average. In this sense, the goal is obviously to have a test method which provides a mean (or median) standard deviation estimate as close to the true value of σ as possible – i.e., a test with little bias in results. The second consideration involves the scatter in results. Because a designer or researcher must make conclusions based on a limited set of data, it is important that a test should not be subject to a wide dispersion in results due to statistical scatter alone. In addition, the test should not be overly sensitive to step size. Because the true standard deviation is one of the very unknowns the test is intended to estimate, it is impossible to be sure whether a test is conducted at step 0.8σ or 1.2σ until after the test is already complete (and even then, there is still a great deal of uncertainty as to the true standard deviation). Thus, scatter due to step size should also be minimized, if possible. In short, one prefers a test method with estimates as tightly grouped as possible around the true distribution parameter without impractical step size constraints. Recent investigations of the staircase standard deviation do not address means of reducing this scatter.

The first problem to address, therefore, is quantifying the standard deviation bias. Simulations were run for both Normal(400,5) and Normal(400,15) underlying fatigue strength distributions. For each simulation, the starting stress was set at the true mean, so $S_{init} = \mu = 400$. The following sample sizes were used: $N = 8, 10, 12, 15, 20, 30, 50, 100$, and 1000 specimens. For each sample size, 1000 runs were made for each of the following step sizes: $s/\sigma = 0.1, 0.25, 0.5, 0.75, 1, 1.5$, and 2. Thus, a total of 126 ($2 \times 9 \times 7$) simulation cases were investigated. Figure 23 and Figure 24 show the mean standard deviation estimates ($\bar{\sigma}_{DM}$) for each of these 126 cases. Simulation data for some of these data points are detailed in Appendix F.

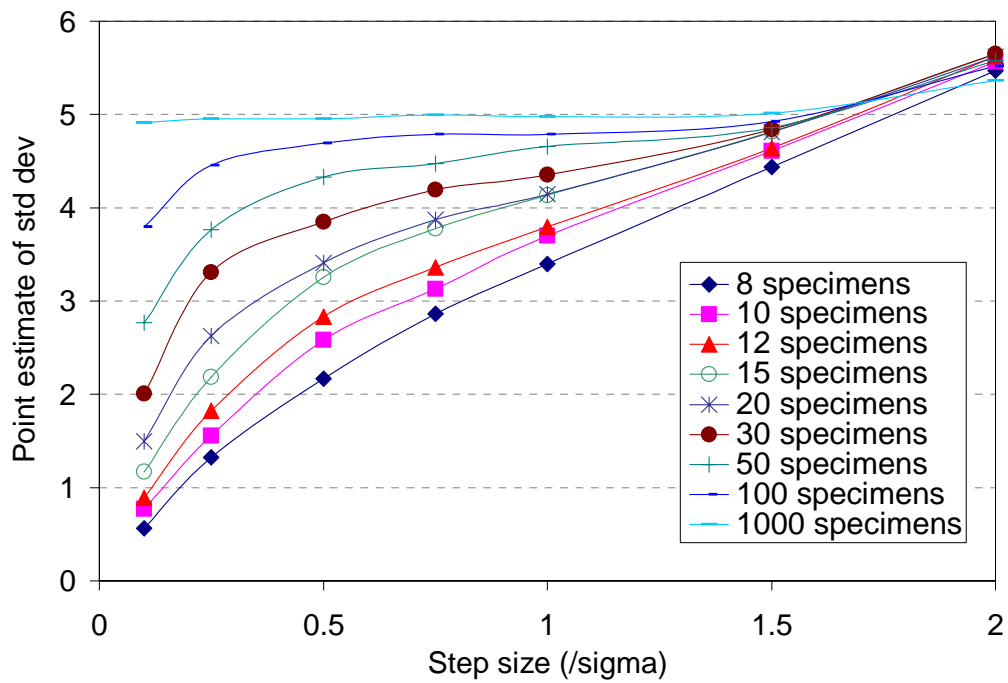


Figure 23. Effect of step size and number of specimens on Dixon-Mood standard deviation estimates for underlying Normal(400,5).

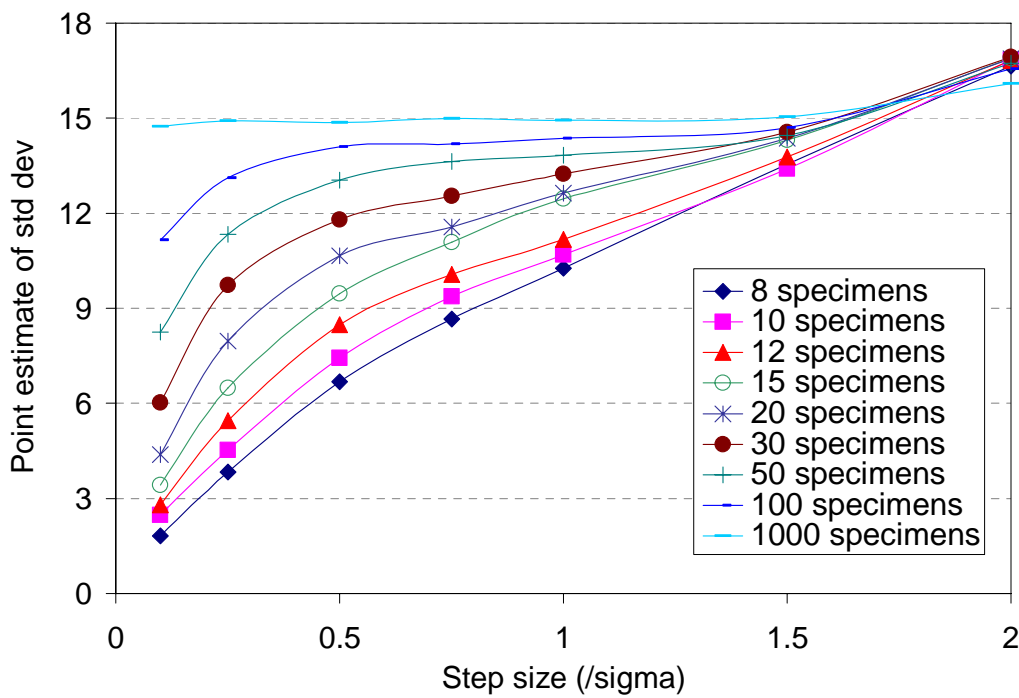


Figure 24. Effect of step size and number of specimens on Dixon-Mood standard deviation estimates for underlying Normal(400,15).

When the standard deviation estimates are divided by the true standard deviation (i.e., normalized), the same outcome results irrespective of σ . The normalized mean standard deviations for both the Normal(400,5) and Normal(400,15) cases were averaged to create Figure 25. This figure therefore gives the expected value of standard deviation using the Dixon-Mood method (for starting stresses at the true mean) for any combination of sample size (≥ 8) and step size (0.1σ to 2σ). For example, if one were to conduct a staircase test at $s = 1\sigma$ using 12 specimens, the average standard deviation estimate would be 0.75σ , or 25% too low. This figure clearly shows that the Dixon-Mood method underestimates the standard deviation as sample size or step size is reduced. Thus, if a correction were to be made, it should account for both these biasing factors. Note that in the limit (represented by 1000 specimens), the Dixon-Mood method is unbiased regardless of step size (in the 0.1σ to 1.7σ region). Also, the method is generally unbiased for step sizes in the 1.6σ to 1.75σ region. This result is significant in that it shows that use of larger steps than currently recommended in the literature would result in less standard deviation bias. Beyond 1.5σ , Equation 19 begins to dominate as step sizes get large and the curves converge to the $0.53s$ line.

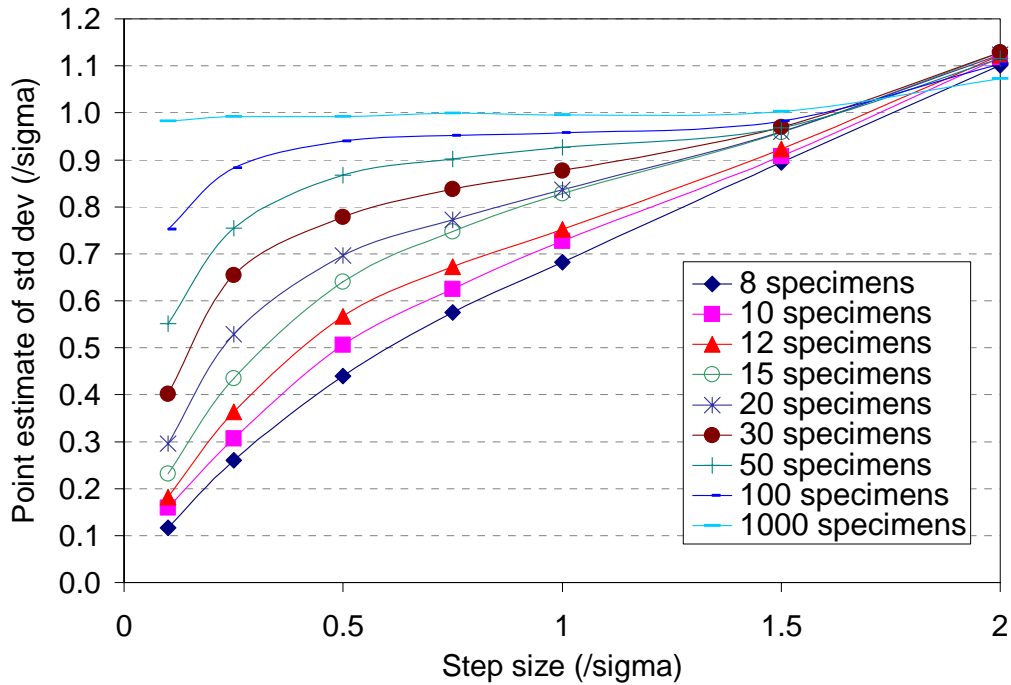


Figure 25. Standard deviation bias for $S_{init} = \mu$ using the Dixon-Mood method.

Next, the scatter in standard deviation is addressed. Like $\bar{\sigma}_{DM}$, the standard deviation of the standard deviation estimates (σ_{DM}^σ) is independent of σ when normalized by σ . In other words, both the Normal(400,5) and Normal(400,15) produced similar results. Figure 26 shows the average values of the normalized σ_{DM}^σ estimates. Based on this data, it is clear that step sizes in the unbiased region of 1.6σ to 1.75σ produce less scatter in results than more traditional steps in the 0.5σ to 1.5σ range. This effect is due in part to the larger steps producing more results requiring analysis by Equation 19, which is constant for a given step size. In general, it appears that use of steps in the 1.6σ to 1.75σ range will result in both less bias and less scatter than smaller step sizes.

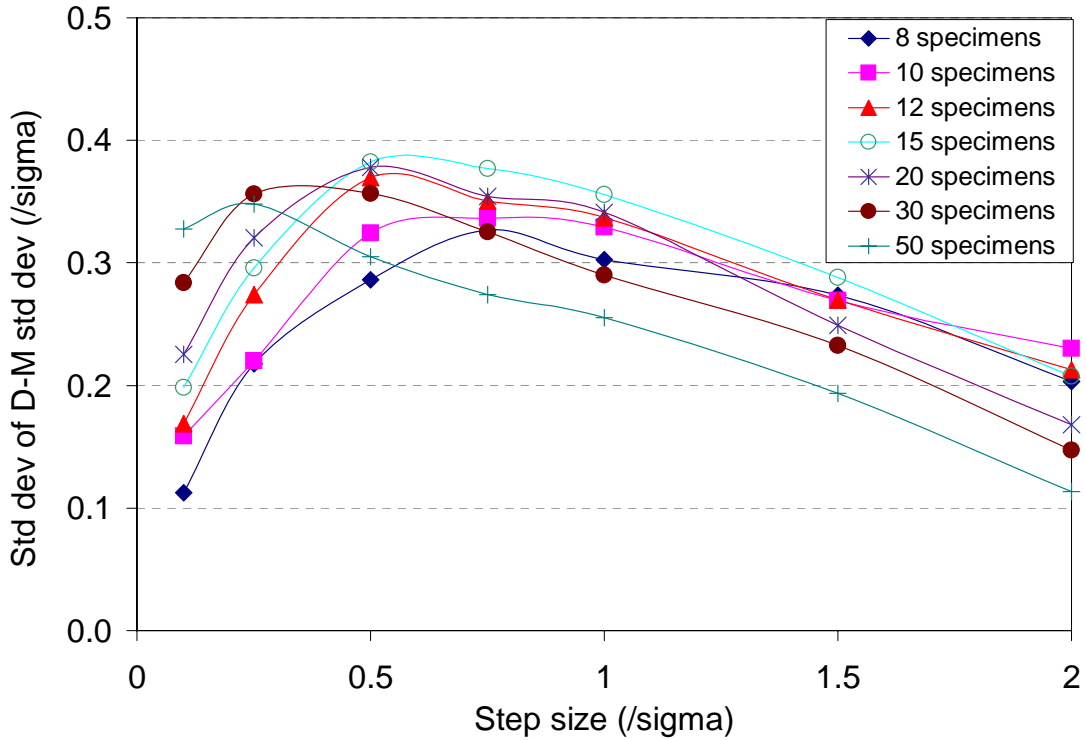


Figure 26. Standard deviation scatter for $S_{init} = \mu$ using the Dixon-Mood method.

By quantifying the standard deviation bias as well as its scatter for small-sample tests, the groundwork has been laid for developing methods to alleviate both the bias and the scatter in standard deviation. In the next section, a modified correction for bias will be explored. In the section after that, a method to reduce scatter using the bootstrapping technique will be proposed.

Correction for Dixon-Mood Standard Deviation

Development of an approach to reduce standard deviation bias started with the Svensson-Lorén correction (Equation 26). The correction was applied to the normalized $\bar{\sigma}_{DM}$ estimates shown in Figure 25. This resulted in the normalized means of standard deviation using the Svensson-Lorén correction ($\bar{\sigma}_{SL}$) shown in Figure 27.

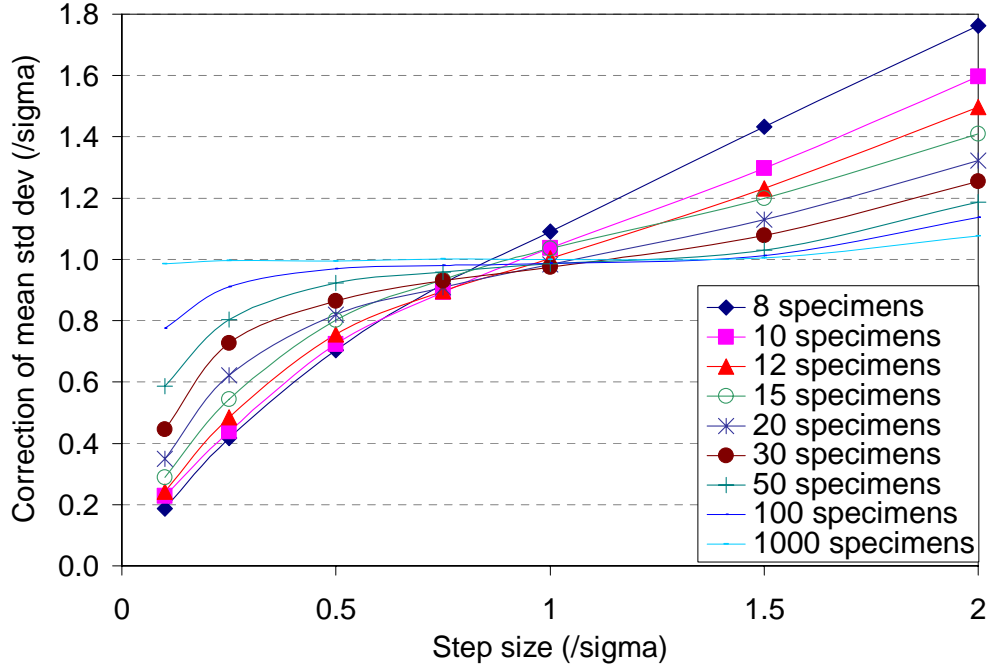


Figure 27. Svensson-Lorén standard deviation correction applied to normalized $\bar{\sigma}_{DM}$ estimates.

These results show a significant shift in the unbiased region from the 1.6σ – 1.75σ range to the 0.85σ – 1.0σ range. This shift is advantageous for three reasons: (1) it allows relatively unbiased standard deviation estimates at 1σ , which is more consistent with recommendations made in prior works, (2) use of smaller steps reduces scatter in mean fatigue strength estimates ($\bar{\mu}_{DM}$), and (3) it provides a more balanced bias because high initial σ estimates remain high, and low estimates remain low, on average. Thus, although the correction is still rather sensitive to step size based on the initial estimate of σ , at least it is not skewed to consistently underestimate standard deviation in the 0.1σ – 1.6σ range, like the Dixon-Mood estimate does.

Consider the case in which the standard deviation is initially overestimated, where the actual σ is 10, but the experimenter assumes 15 (50% too high). Thus, when the staircase is conducted at a planned 1σ step of 15, it is actually a 1.5σ step. According to Figure 27, if a 15-specimen staircase is conducted with the Svensson-Lorén correction applied, the mean result is 1.2σ , or in this case 12. If the same test were run with an initial σ estimate of 5 (50% too low), rather than 15, then the 1σ step actually becomes a 0.5σ step, and the mean outcome is 0.8σ , or 8. Thus, the mean result is 20% high or 20% low when the initial σ estimate is 50% high or 50% low, respectively. This result demonstrates the balance in bias using the Svensson-Lorén correction, and based on the curve shapes from Figure 27 this bias is lessened for larger sample sizes and worsened for smaller sample sizes.

A modified correction was developed which attempted to allow a greater range of unbiased estimation than the Svensson-Lorén correction. Like the Braam-van der Zwaag correction, this proposed correction included the ratio of the standard deviation to step size. The Svensson-Lorén sample size factor was included in order to retain the advantage of centering the unbiased region around the $s = \sigma$ step size. The form of the proposed correction is shown below, where A , B , and m are constants dependent on the number of samples (values are displayed in Table 7). For sample sizes not listed in the table, use of linear interpolation is adequate to obtain values of $A(N)$ and $m(N)$.

$$\sigma_{PC} = A\sigma_{DM} \left(\frac{N}{N-3} \right) \left(B \frac{\sigma_{DM}}{s} \right)^m \quad (33)$$

Table 7. Constants used in proposed standard deviation correction.

Sample Size (N)	A	B	m
8	1.30	1.2	1.72
10	1.08	1.2	1.10
12	1.04	1.2	0.78
15	0.97	1.2	0.55
20	1.00	1.2	0.45
30	1.00	1.2	0.22
50	1.00	1.2	0.15
> 50	Use Svensson-Lorén correction.		

The proposed correction is applied to the normalized $\bar{\sigma}_{DM}$ estimates in Figure 28. Compared to the Svensson-Lorén correction shown in Figure 27, the proposed correction has a much broader unbiased region with respect to step size when applied to the mean Dixon-Mood estimate. A comparison of normalized values of $\bar{\sigma}_{DM}$, $\bar{\sigma}_{SL}$, and the proposed correction is shown in Figure 29 for $N = 20$ specimens. These figures suggest that the proposed correction strongly reduces standard deviation bias over a wide range of step sizes and therefore represents a significant improvement in standard deviation estimation. Unfortunately, the effectiveness of this correction is not as significant as these figures would indicate, due to the effects of statistical scatter, as described next.

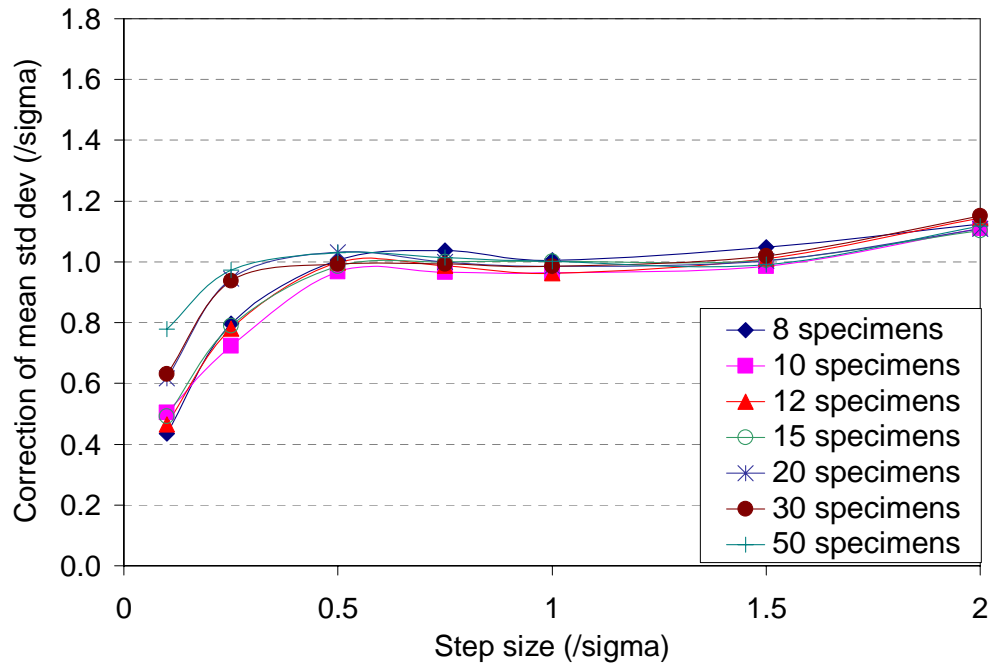


Figure 28. Proposed standard deviation correction applied to normalized $\bar{\sigma}_{DM}$ estimates.

Although the proposed correction appears to remove bias over a greater range of step sizes, it must be understood that these results are only valid when applied to the “average” outcome—despite Figure 28, there is still no guarantee that the proposed correction is any better on a case-by-case basis (a similar situation was previously shown for the Braam-van der Zwaag correction). In order to assess the adequacy of the correction, the scatter in results must be considered.

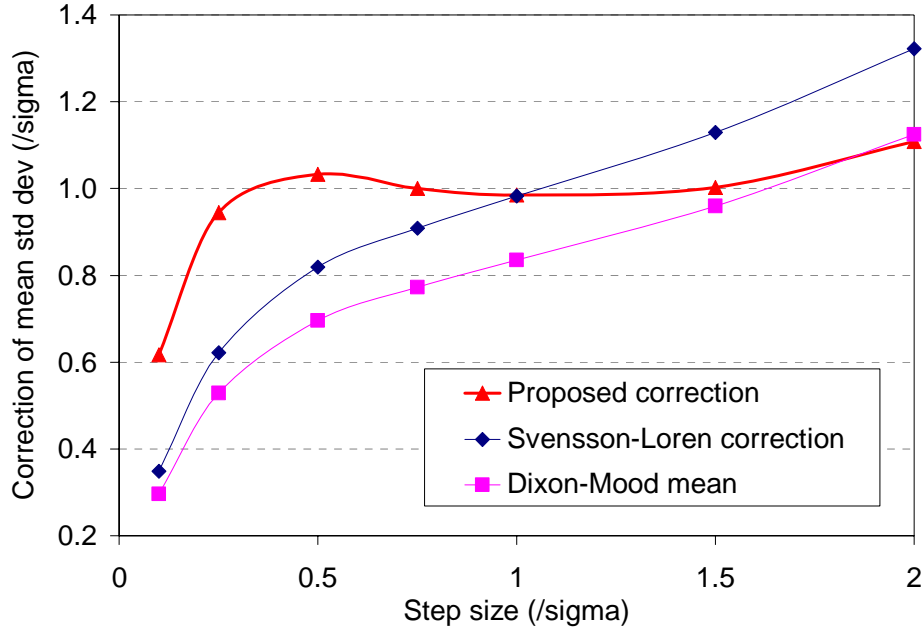


Figure 29. Comparison of normalized standard deviations for Dixon-Mood mean, Svensson-Lorén correction, and proposed correction for $N = 20$ specimens.

A comparison of the Svensson-Lorén correction and the proposed correction was made for the same conditions as those used in the Braam-van der Zwaag analysis summarized in Table 4—namely, $S_{init} = 395$, $\mu = 400$, $\sigma = 5$, and $N = 12$. Random samples of twenty runs were selected for each of the following step sizes: $s/\sigma = 0.5$, 1, and 1.5. The results for three sets of samples are shown in Table 8 (normalized by σ). The trends identified in this data are generally consistent for any staircase scenario, but are magnified at smaller sample sizes. As expected, σ_{SL} has slightly more scatter (higher standard deviation) than σ_{DM} , but is generally more accurate, except at bigger step sizes (which have already been shown to produce less bias using Dixon-Mood). When Dixon-Mood overestimates the result, σ_{SL} is obviously worse than σ_{DM} (since Svensson-Lorén always multiplies the estimate by a number greater than 1). Compared to both Dixon-Mood and Svensson-Lorén, the proposed correction tends to have more scatter (though less than Braam-van der Zwaag). Unlike Braam-van der Zwaag, the proposed correction does produce better estimates than Dixon-Mood for step sizes on the order of 1σ , especially when the Dixon-Mood estimate is near its mean value. In fact, the correction generally produces better results than Dixon-Mood whenever the results are near their

mean value. Table 9 shows the proposed method compared to Dixon-Mood and Braam-van der Zwaag for the 20-specimen data originally shown in Table 5. Note how the proposed method is more accurate than Braam-van der Zwaag when Dixon-Mood underestimates, but behaves similarly to Braam-van der Zwaag when Dixon-Mood overestimates the true standard deviation.

Overall, despite less bias when based on average values, the proposed correction suffers from increased scatter in results, primarily due to slight underestimation when results are on the very low end of the distribution and large overestimation when they are on the high end. In short, the proposed correction, without further modification, is generally a poorer estimator than the Svensson-Lorén correction.

Table 8. Comparison of normalized standard deviations using Dixon-Mood, Svensson-Lorén, and the proposed correction for individual random samples.

Run	$s = 1\sigma$			$s = 0.5\sigma$			$s = 1.5\sigma$		
	Dixon-Mood (σ_{DM})	Svensson-Lorén (σ_{SL})	Proposed Correction (σ_{PC})	Dixon-Mood (σ_{DM})	Svensson-Lorén (σ_{SL})	Proposed Correction (σ_{PC})	Dixon-Mood (σ_{DM})	Svensson-Lorén (σ_{SL})	Proposed Correction (σ_{PC})
1	0.53	0.71	0.52	0.27	0.35	0.15	0.80	1.06	1.07
2	0.53	0.71	0.52	0.27	0.35	0.15	0.80	1.06	1.07
3	0.53	0.71	0.52	0.27	0.35	0.15	0.80	1.06	1.07
4	0.53	0.71	0.52	0.29	0.39	0.18	0.80	1.06	1.07
5	0.53	0.71	0.52	0.41	0.54	0.32	0.80	1.06	1.07
6	0.53	0.71	0.52	0.48	0.64	0.43	0.80	1.06	1.07
7	0.53	0.71	0.52	0.48	0.64	0.43	0.80	1.06	1.07
8	0.53	0.71	0.52	0.48	0.64	0.43	0.80	1.06	1.07
9	0.53	0.71	0.52	0.48	0.64	0.43	0.80	1.06	1.07
10	0.59	0.78	0.62	0.48	0.64	0.43	0.80	1.06	1.07
11	0.69	0.93	0.83	0.54	0.72	0.54	0.88	1.17	1.27
12	0.69	0.93	0.83	0.56	0.75	0.58	0.88	1.17	1.27
13	0.69	0.93	0.83	0.58	0.77	0.61	0.88	1.17	1.27
14	0.81	1.08	1.10	0.58	0.77	0.61	1.04	1.39	1.72
15	0.81	1.08	1.10	0.74	0.99	0.94	1.22	1.62	2.27
16	0.95	1.27	1.47	0.87	1.15	1.24	1.22	1.62	2.27
17	0.95	1.27	1.47	0.87	1.15	1.24	1.22	1.62	2.27
18	0.95	1.27	1.47	1.01	1.35	1.64	1.43	1.91	3.03
19	1.08	1.45	1.85	1.51	2.02	3.34	1.63	2.17	3.80
20	1.35	1.80	2.73	1.77	2.37	4.43	2.40	3.21	7.62
Average	0.72	0.96	0.95	0.65	0.86	0.91	1.04	1.38	1.87
Std Dev	0.24	0.31	0.59	0.40	0.53	1.11	0.41	0.54	1.56
Note: Using Normal(400,5) distribution with $S_{init} = 395$ and $N = 12$ specimens.									

Table 9. Comparison of normalized standard deviations using Dixon-Mood, Braam-van der Zwaag, and the proposed correction for data from Table 5.

Run	Dixon-Mood (σ_{DM})	Braam-van der Zwaag (σ_{BZ})	Proposed Correction (σ_{PC})
1	0.53	0.18	0.51
2	0.53	0.18	0.51
3	0.53	0.18	0.51
4	0.63	0.34	0.65
5	0.63	0.34	0.65
6	0.63	0.34	0.65
7	0.69	0.46	0.75
8	0.71	0.48	0.78
9	0.76	0.56	0.86
10	0.77	0.58	0.87
11	0.77	0.58	0.87
12	0.84	0.72	0.99
13	0.93	0.88	1.14
14	1.08	1.22	1.44
15	1.13	1.30	1.52
16	1.17	1.40	1.60
17	1.36	1.86	1.99
18	1.41	1.96	2.10
19	1.49	2.18	2.27
20	1.73	2.88	2.83
Average	0.92	0.93	1.17
Std Dev	0.36	0.77	0.67

Bootstrapping to Reduce Standard Deviation Scatter

Obviously, one of the biggest problems inherent in small-sample testing is that statistical scatter can greatly impact results. However, it has been shown that the Braam-van der Zwaag, Svensson-Lorén, and proposed corrections all increase the scatter in σ_{DM} estimates. The bootstrapping method (introduced in Chapter II) was investigated as a possible means to reduce this variance. The bootstrap is a data-based simulation which utilizes multiple random draws from real test data to improve statistical inferences about the underlying population [31]. Essentially, the bootstrap method can be summed up by the following conjecture: *Assuming the test data collected accurately represents the true distribution, what other results could have been obtained if the test were repeated?*

The bootstrap algorithm for the staircase application is based on the associated probabilities of failure computed using the number of survivals and failures at each stress level (i.e., P - S data). Using these data, simulated staircase tests can be generated numerically using the same starting stress, step size, and number of specimens. For the first specimen, a random number is drawn and compared to the probability of failure associated with the initial stress level. The stress level is increased or decreased depending on the result of this draw (if the random number is less than the probability of failure, the result is considered a failure, otherwise it is a survival). Another random number is then drawn for the second specimen and compared to the probability of failure for its associated stress level, with the stress level increased or decreased based on this comparison, and the process is repeated until all specimens are used. Note that test data must be bounded by both $P(\text{failure}) = 0$ and $P(\text{failure}) = 1$ stress levels or the staircase may walk to a stress level where no data exists. Through this algorithm, a set of “virtual” staircase tests is generated for the one “real” staircase test. For each virtual staircase, the Dixon-Mood method can be applied to provide a standard deviation estimate. The result is a distribution of standard deviation estimates. Lastly, the revised point estimate can then be taken as the mean of this distribution, or another statistic such as the median or other percentile point. The staircase simulation was modified to accommodate this bootstrapping algorithm by simulating a “real” staircase using an assumed underlying fatigue strength distribution, and then using the P - S data from this simulated staircase to bootstrap additional staircases from which a distribution of standard deviation estimates can be analyzed. Simulation code is contained in Appendix D.

The Bootstrap and the Dixon-Mood Estimate

The first phase of the bootstrap investigation addressed the effects of the bootstrap on Dixon-Mood estimation. Four different scenarios were considered: (1) 120 staircases with $N = 15$ and $s = 1.5\sigma$, (2) 50 staircases with $N = 12$ and $s = 1.0\sigma$, (3) 100 staircases with $N = 8$ and $s = 1.7\sigma$, and (4) 50 staircases with $N = 20$ and $s = 1.7\sigma$. These four scenarios were chosen as they provided a range in number of specimens (8 to 20) and they used larger step sizes as the parameter investigation recommended (1.0σ to 1.7σ). The number of staircases for each scenario varied in order to ensure an adequate cross-section of standard deviation estimates resulted (7 to 10 distinct values, except for the

case with $N = 8$ in which only three unique distinct results occurred). For each of these 320 staircases, the Dixon-Mood standard deviation estimate was calculated. P - S data for each staircase were then used to generate 5000 bootstrap iterations, each resulting in a Dixon-Mood standard deviation estimate. A revised estimate was calculated as the mean standard deviation from the 5000 estimates for each staircase, designated as $\bar{\sigma}_{DM}^B$.

For the first scenario ($N = 15$ and $s = 1.5\sigma$), the 120 staircases resulted in 8 unique standard deviation estimates (normalized by σ). Thus, the data can be grouped by Dixon-Mood estimate into 8 bins, as shown in Table 10. For the staircases in each bin, a $\bar{\sigma}_{DM}^B$ value was calculated. For example, 5 of the 120 staircases resulted in a σ_{DM} value of 2.05σ (the 3rd row from the bottom in Table 10), which resulted in $\bar{\sigma}_{DM}^B$ values of 1.48σ , 1.48σ , 1.49σ , 1.49σ , and 1.56σ , for a mean of 1.50σ . The data from this table are displayed graphically in Figure 30, where group numbers refer to the bins of data with the same σ_{DM} result, and expected value for the standard deviation estimate is taken from Figure 25. Data for the other three scenarios are shown in the following figures.

Table 10. Bootstrap data for $N = 15$ and $s = 1.5\sigma$.

Dixon-Mood Std Dev ($/\sigma$)	Outcome Frequency	Mean Bootstrap Std Dev	Min Bootstrap Std Dev	Max Bootstrap Std Dev
0.80	75	0.80	0.80	0.94
1.06	11	1.01	0.97	1.12
1.26	13	1.10	1.08	1.11
1.36	9	1.21	1.14	1.33
1.46	5	1.20	1.18	1.28
2.05	5	1.50	1.48	1.56
2.45	1	1.86	1.86	1.86
2.65	1	1.76	1.76	1.76

Based on the data from these figures, it appears that the bootstrap algorithm has the satisfying effect of reducing errors due to overly large standard deviation estimates. In fact, this is exactly what the bootstrap is doing in that it smoothes out the statistically unlikely results by performing the many virtual replications using the P - S data. Using this method, the $\bar{\sigma}_{DM}^B$ value is closer to the expected value of σ_{DM} , or $E(\sigma_{DM})$, than individual σ_{DM} estimates—nearly every one of the 320 σ_{DM} estimates from the four

scenarios was closer (or as close) to its expected value after bootstrapping. Figure 34 shows the distribution of standard deviation estimates for the second scenario. The bootstrap's ability to reduce statistical scatter of Dixon-Mood estimates is clearly evident.

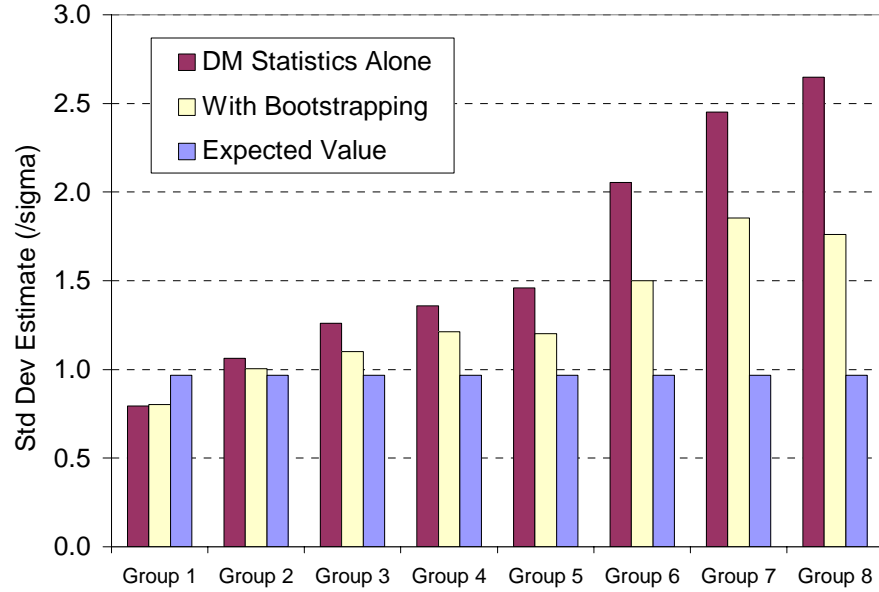


Figure 30. Bootstrap results sorted by Dixon-Mood standard deviation for 120 staircases with $N = 15$ and $s = 1.5\sigma$.

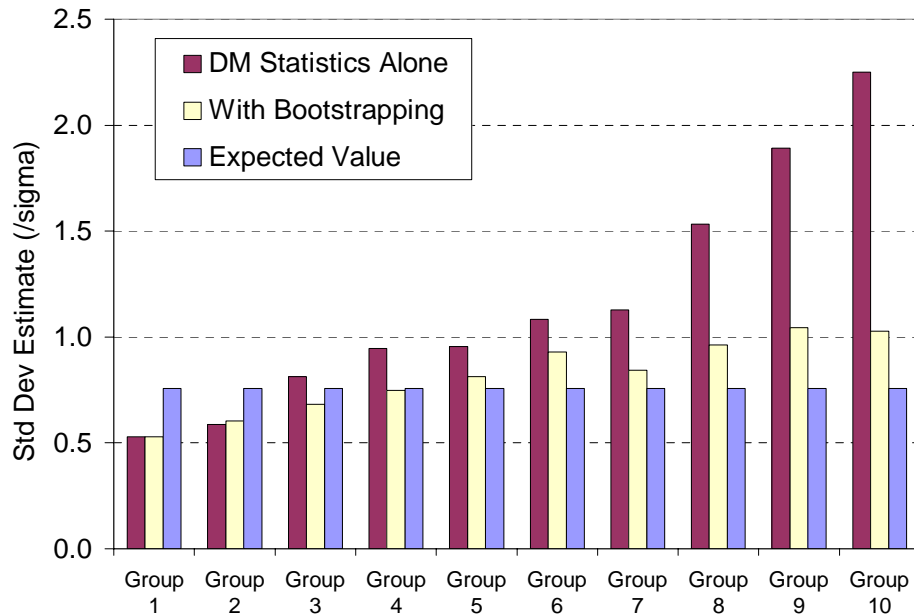


Figure 31. Bootstrap results sorted by Dixon-Mood standard deviation for 50 staircases with $N = 12$ and $s = 1.0\sigma$.

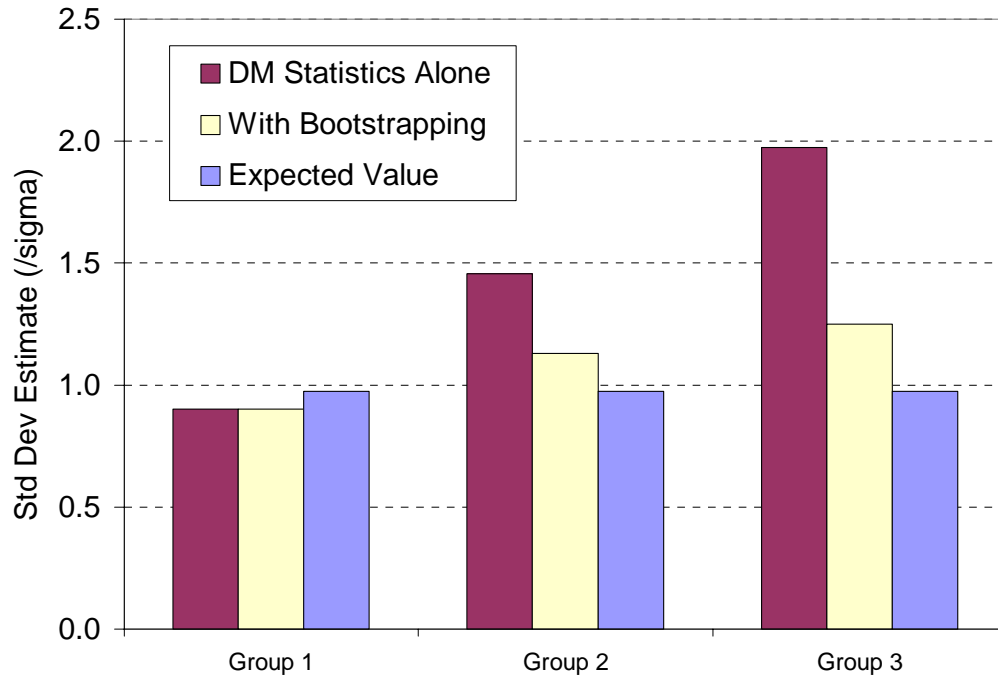


Figure 32. Bootstrap results sorted by Dixon-Mood standard deviation for 100 staircases with $N = 8$ and $s = 1.7\sigma$.

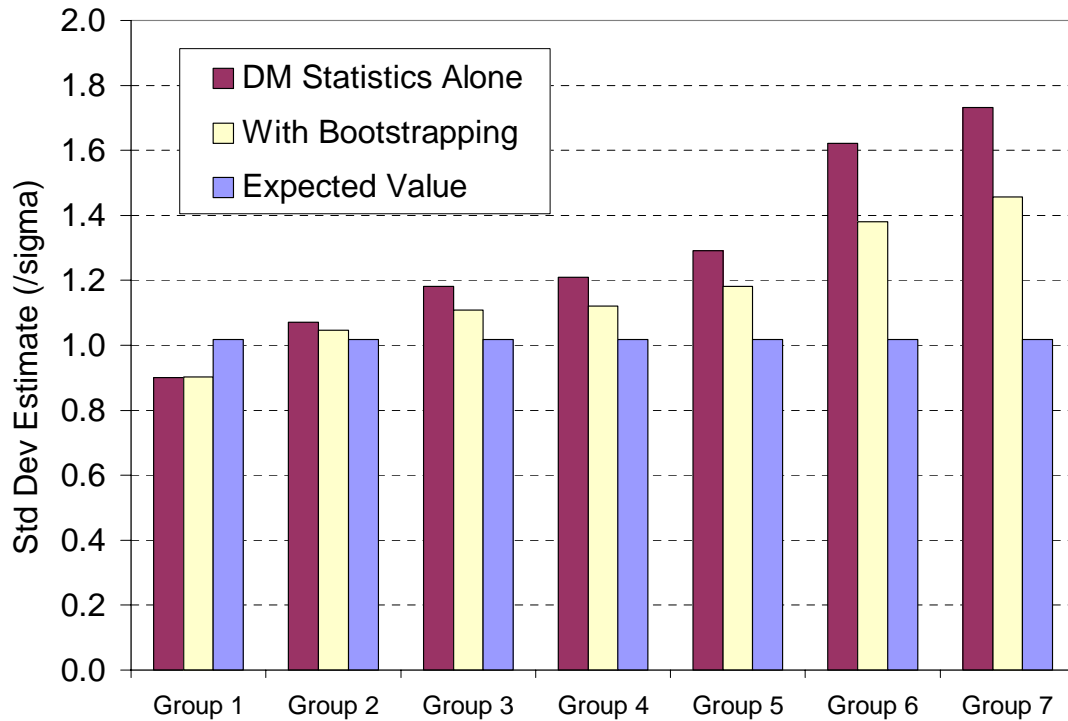


Figure 33. Bootstrap results sorted by Dixon-Mood standard deviation for 50 staircases with $N = 20$ and $s = 1.7\sigma$.

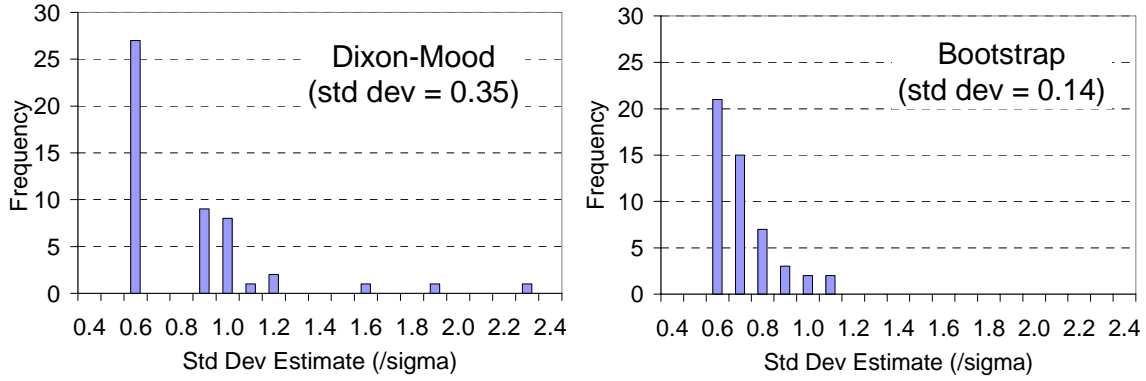


Figure 34. Frequency histograms for Dixon-Mood standard deviation and bootstrapped standard deviation for 50 staircases with $N = 12$ and $s = 1.0\sigma$.

One of the remarkable outcomes of the bootstrap analysis is that it is actually possible to get better standard deviation estimates with smaller sample sizes than with larger ones in some cases, assuming a step size with little bias is used. The data from the two scenarios using $s = 1.7\sigma$ support this conclusion—recall that for uncorrected estimates, this step size is generally unbiased. For the $N = 20$ case, the 50 σ_{DM} values ranged from 0.90 – 1.73σ . For the $N = 8$ case, the 100 σ_{DM} values ranged from 0.90 – 1.97σ . Thus, without the use of bootstrapping, the larger sample size produced better estimates on average, as would be expected. But with bootstrapping, the 20-specimen results ranged from 0.90 – 1.46σ , which is less of an improvement than the 0.90 – 1.25σ range of the 8-specimen bootstrapped data. It seems logical that this result is due to the fact that larger-specimen tests may result in more stress levels, which tends to increase standard deviation estimates. Thus, when there is little bias or positive bias (expected value under the test conditions is greater than the true value), using a smaller-sample test with bootstrapping may yield better results than a test with more specimens. However, if testing under negative bias conditions, $E(\sigma_{DM}) < \sigma$, the smaller-specimen test would on average yield worse results than a larger-specimen test. One must keep in mind that the bootstrap does not drive the standard deviation estimate towards the true value, but rather drives it towards the expected value given the test parameters. This effect is clearly shown in Figure 31 for groups 3–7, where bootstrapping drives the standard deviation estimate towards 0.75σ rather than 1σ . Note that Figure 25 shows that the expected value of σ_{DM} is 0.75σ for $N = 12$ and $s = 1\sigma$.

The bootstrap provides the first real tool to reduce the scatter inherent in the Dixon-Mood standard deviation method. It has been shown to adjust Dixon-Mood estimates towards their expected value. Thus, if one tests in an unbiased region, such as the $s = 1.7\sigma$ region, then the bootstrap should drive Dixon-Mood estimates towards the true standard deviation. But, can a correction such as the Svensson-Lorén correction be used in conjunction with the bootstrap to alleviate bias and still provide less overall scatter? This question is addressed in the next section.

Use of Bootstrapping in Conjunction with Bias Correction

In this section, the use of bootstrapping is investigated in conjunction with the Svensson-Lorén correction (σ_{SL}) and the proposed correction (σ_{PC}). The bootstrap was performed in the same manner as in the last section, except that the two corrections were made to each of the Dixon-Mood estimates during the bootstrap, thus leading to three bootstrap distributions—one each for Dixon-Mood, Svensson-Lorén, and the proposed correction. The primary scenario of interest was the $N = 15$ specimen case with $s = 1\sigma \pm 0.25\sigma$, since this seems to be a reasonable small-sample test scenario. It was determined that the number of stress levels used in the test (i.e., resulting from the test protocol) plays a critical role in determining the effectiveness of bootstrapping in general, as well as in selecting the specific statistic for use from the bootstrap distribution. A considerable number of simulations were run to investigate various bootstrap distribution statistics in order to determine a general set of rules to recommend for analysis of staircase data using the bootstrap method.

For the $N = 15$ specimen case using $s = 1\sigma$, it was found that bootstrapping had no effect when the staircase only included 3 stress levels. For every case, the σ_{DM} estimate was 0.53σ , leading to estimates of $\sigma_{SL} = 0.66\sigma$ and $\sigma_{PC} = 0.50\sigma$. Bootstrapping did not change these results. This situation occurs for other sample sizes as well. Like Rabb alluded to with his acceptability criteria, a 3-level staircase generally provides too little data to make any useful standard deviation estimates [73]. However, in the absence of additional data, the σ_{SL} estimate can be used as an estimate for σ . For 4-level staircases, the bootstrap had a considerable effect. A sample of 15 runs each using $N = 15$ and $s = 1\sigma$

$\pm 0.25\sigma$, led to the data shown in Table 11. Observations from these data include the following:

- Without the bootstrap, Svensson-Lorén and the proposed correction have less bias than Dixon-Mood, although more scatter.
- Estimates based on bootstrap data have less scatter than the corresponding estimates without bootstrapping, and are also less biased in most cases.
- Basing the bootstrap estimate on the average of the 60th and 65th percentiles of the bootstrap distribution generally reduces bias compared to use of the bootstrap distribution mean or median for steps on the order of 1σ or less. This finding was shown to generally be true over a range of different sample sizes. For 5-level tests, however, the bootstrap based on the mean appears more accurate.
- The Svensson-Lorén estimate using the average of the 60th and 65th percentiles ($\tilde{\sigma}_{SL}^B$) was better than or equal to the non-bootstrapped Svensson-Lorén estimate in 100% of the cases at $s = 1\sigma$, 47% of the cases at $s = 0.75\sigma$, and 87% of the cases at $s = 1.25\sigma$. Likewise, the proposed correction with bootstrapping using these percentiles ($\tilde{\sigma}_{PC}^B$) was better than or equal to the correction without bootstrapping in 87% (1σ), 73% (0.75σ), and 87% (1.25σ) of the cases.
- The $\tilde{\sigma}_{PC}^B$ estimate is better than $\tilde{\sigma}_{SL}^B$ in 80% of the cases when $s = 1.25\sigma$, but just 20% of the cases at 1σ , and 24% of the cases at 0.75σ . Thus, it appears that the proposed correction is superior when larger steps are used, but slightly worse than Svensson-Lorén at smaller steps.

Table 11. Bootstrap data with bias correction for 4-level staircases using $N = 15$.

Statistic ($/\sigma$)	$s = 1\sigma$		$s = 0.75\sigma$		$s = 1.25\sigma$	
	Avg	StDev	Avg	StDev	Avg	StDev
Dixon-Mood (no bootstrap), σ_{DM}	0.83	0.13	0.67	0.19	1.02	0.20
Svensson-Lorén (no bootstrap), σ_{SL}	1.04	0.16	0.84	0.24	1.28	0.25
Proposed correction (no bootstrap), σ_{PC}	1.01	0.23	0.87	0.37	1.25	0.40
Svensson-Lorén correction based on mean of bootstrap distribution, $\bar{\sigma}_{SL}^B$	0.92	0.09	0.71	0.13	1.14	0.13
Svensson-Lorén correction based on average of the 60 th and 65 th percentiles of bootstrap distribution, $\tilde{\sigma}_{SL}^B$	1.00	0.11	0.76	0.17	1.23	0.13
Proposed correction based on mean of bootstrap distribution, $\bar{\sigma}_{PC}^B$	0.87	0.14	0.69	0.20	1.07	0.20
Proposed correction based on average of the 60 th and 65 th percentiles of bootstrap distribution, $\tilde{\sigma}_{PC}^B$	0.96	0.17	0.74	0.26	1.16	0.20

Based on the results of this section, and the detailed results shown in Appendix G, the following rules are recommended for small-sample tests:

- If the test results in three stress levels, bootstrapping is generally ineffective and the non-bootstrapped σ_{SL} estimate may be used to estimate σ . However, any standard deviation estimate based on 3-level staircase data should be used with caution and additional testing is recommended.
- If the test results in four stress levels, the 60th- and 65th-percentile points of the bootstrap distribution for σ_{PC} (i.e., $\hat{\sigma}_{PC}^B$) should be averaged to estimate σ for larger step sizes. If the step size is known to be on the order of standard deviation or smaller, then the 60th- and 65th-percentile points of the bootstrap distribution for σ_{SL} (i.e., $\hat{\sigma}_{SL}^B$) should be averaged to estimate σ .
- If the test results in five or more stress levels, then the mean of the Svensson-Lorén bootstrap distribution for (i.e., $\bar{\sigma}_{SL}^B$) should be used to estimate σ .

To demonstrate the utility of these rules, they were applied to the scenarios shown in Table 12 using a random sample of 5 staircase tests for each scenario. The normalized standard deviation estimates for each run are shown in Table 12.

Table 12. Validation runs for proposed bootstrapping rules.

Scenario	Sample Size (N)	Step Size ($/\sigma$)	Run 1	Run 2	Run 3	Run 4	Run 5
A	8	1	0.85 (0.53)	0.85 (0.53)	0.85 (0.53)	0.85 (0.53)	0.85 (1.16)
B	10	1	0.76 (0.53)	0.76 (0.53)	0.99 (0.95)	0.76 (0.53)	0.76 (0.53)
C	12	1	1.17 (0.95)	0.71 (0.53)	0.71 (0.53)	0.71 (0.59)	0.93 (0.81)
D	15	0.5	0.55 (0.45)	0.66 (0.68)	0.33 (0.27)	1.06 (0.95)	0.57 (0.45)
F	20	0.75	1.15 (3.76)	0.67 (0.58)	0.95 (0.96)	1.38 (1.51)	1.43 (1.42)
G	20	1.25	0.78 (0.66)	2.08 (2.19)	0.78 (0.66)	1.12 (0.97)	0.78 (0.66)
H	30	1	0.88 (0.80)	0.88 (0.80)	1.09 (1.06)	1.72 (1.73)	0.95 (0.87)
For each run, the normalized standard deviation estimate using the bootstrap rules is given above, and the Dixon-Mood estimate is below.							

The combination of bias correction and bootstrapping provides an effective “one-two punch” for evaluating staircase standard deviation by reducing both bias and scatter and providing a measure of protection against extreme results, allowing relatively efficient estimation even at small sample sizes using the Dixon-Mood analysis method.

Iteration to Improve Standard Deviation Estimates

Another alternative to reducing dependence on initial estimates for standard deviation is the use of iteration. An iterative staircase algorithm would perform a staircase test at a given step size based on the initial assumption of true standard deviation (σ). An estimate for standard deviation would be calculated from the staircase data using the methods previously discussed. A second staircase could then be performed using the result of the first staircase as an initial estimate for standard deviation. This process could be repeated a number of times. For example, suppose that the standard deviation of the fatigue strength at a specified number of cycles for a material was initially estimated to be 15 MPa. Rather than perform a 30-specimen staircase test at a fixed step size (e.g., 1.5σ), one could perform a 10-specimen staircase at $1.5\sigma_0$, where σ_0 represents the initial estimate for standard deviation. This staircase would result in an estimate for standard deviation given by σ_1 . Another 10-specimen staircase could be run at a step of $1.5\sigma_1$, resulting in an estimate denoted by σ_2 . Finally, a third staircase would be run at a step of $1.5\sigma_2$, with the resulting standard deviation estimate denoted by $\hat{\sigma}$. The question is whether this iterative means would provide a better answer than just testing all 30 specimens in one staircase. Would such an approach reduce the dependence on initial standard deviation estimates? If so, this could be a useful approach for staircase testing of materials with very little existing data in the regime of interest.

The first issue for such a method is to determine whether an iterative approach would converge to the true fatigue strength mean and the true fatigue strength standard deviation in the limit of an infinite number of iterations. The staircase simulation code was modified to handle such an iterative algorithm (as shown in Appendix D) in order to address this issue. Iterative staircases were run for a sample size fixed at 8 specimens per staircase subtest. This sample size would allow several iterations while still maintaining a reasonably small sample size (e.g., three iterations would require 24 samples). In

addition, the sample size is not so small that staircases almost always result in 3-level results. The 8-specimen staircases were iterated using a step size of 1.7σ as this step size provides generally unbiased results using the Dixon-Mood method, as previously shown. The starting stress was slightly lower than the true fatigue strength mean, in order to help mitigate standard deviation bias, which was also shown previously. The initial standard deviation estimate ranged from too low ($0.5x$) to far too large ($3x$). Each scenario was simulated for 1000 replications.

The results of this simulation work showed that the iteration scheme converged in an average sense. Consider the convergence results for an initial standard deviation estimate significantly too high ($3x$). Figure 35 shows that the mean of the 1000 fatigue strength means is quite close to the true value after just a couple iterations, and remains close to the true value as the number of iterations increases. This result is of course of no surprise as the Dixon-Mood estimate for mean fatigue strength has been shown to be extremely efficient and accurate. Figure 36 shows the mean of the 1000 standard deviation estimates as a function of iterations. Although the Dixon-Mood analysis for standard deviation (in its original form) is biased, the iteration scheme results in convergence of the mean of the estimates to the true value.

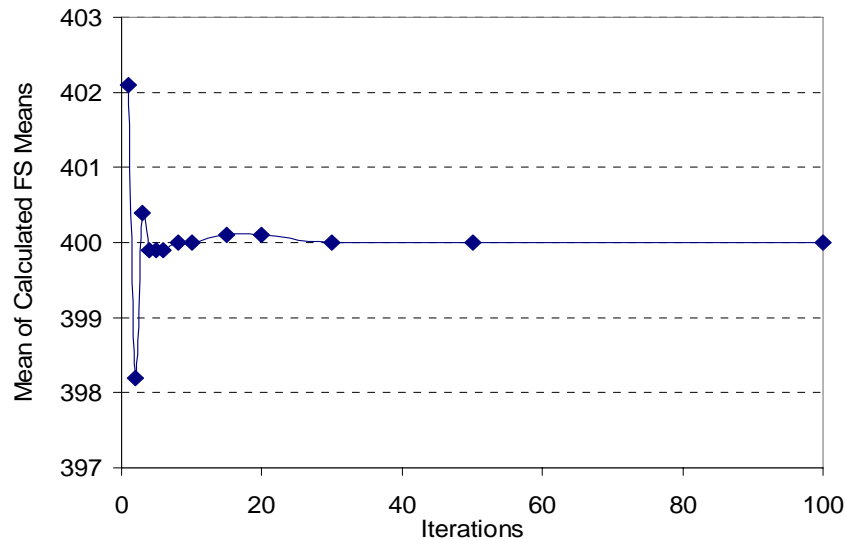


Figure 35. Convergence of mean of fatigue strength mean estimates using Dixon-Mood statistics for 8-specimen subtests with 1.7σ step, initial standard deviation estimate of 15 and initial mean estimate of 390 for true underlying distribution $\text{Normal}(\mu = 400, \sigma = 5)$.

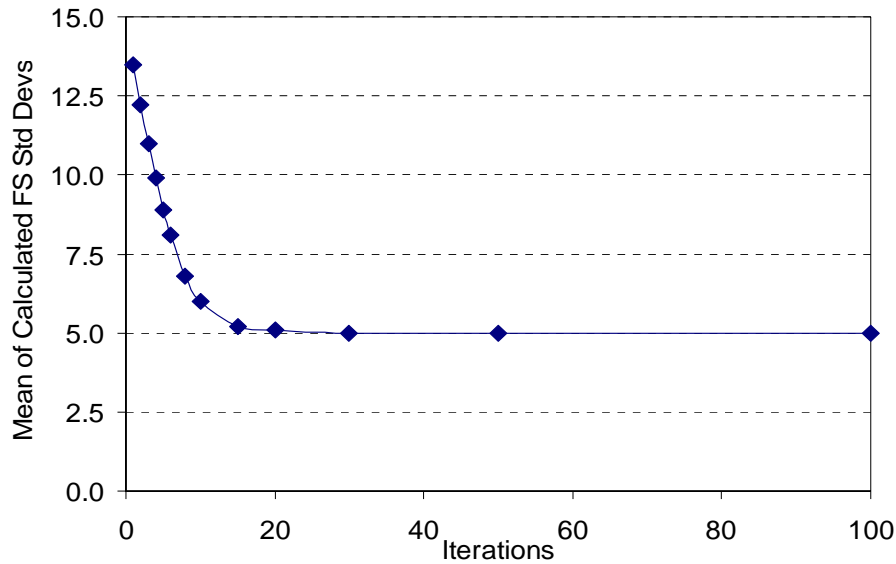


Figure 36. Convergence of mean of fatigue strength standard deviation estimates using Dixon-Mood statistics for 8-specimen subtests with 1.7σ step, initial standard deviation estimate of 15 and initial mean estimate of 390 for true underlying distribution $\text{Normal}(\mu = 400, \sigma = 5)$.

So far, it appears that the iteration algorithm produces convergence to true fatigue strength parameters. However, in the case of the standard deviation estimate, this result was shown to only be the case in an average sense, but not on an individual basis for any particular replication of staircase iterations. Figure 37 shows the distribution of standard deviation estimates after 50 iterations of 8-specimen subtests with step 1.74σ for both a low initial estimate ($0.5x$) and a high initial estimate ($2x$) for true standard deviation. Note that for both the low and high cases, the mean value for standard deviation was quite close to the true standard deviation (5.2 in this case, or 1.04σ). However, the figure shows that the scatter in the standard deviation estimates is quite large. For both the low and high cases (in terms of initial standard deviation estimate), the standard deviation in the Dixon-Mood standard deviation estimates was 0.42σ . This is an extremely large scatter in standard deviation for a test using 400 (50×8) specimens. If one were to just run a single 8-specimen test, the results from earlier simulation (see Figure 26) show that the scatter is approximately 0.23σ . The use of iterated subtests actually produced much more scatter in results rather than performing a single staircase. This result was apparent over a range of sample sizes and step sizes.

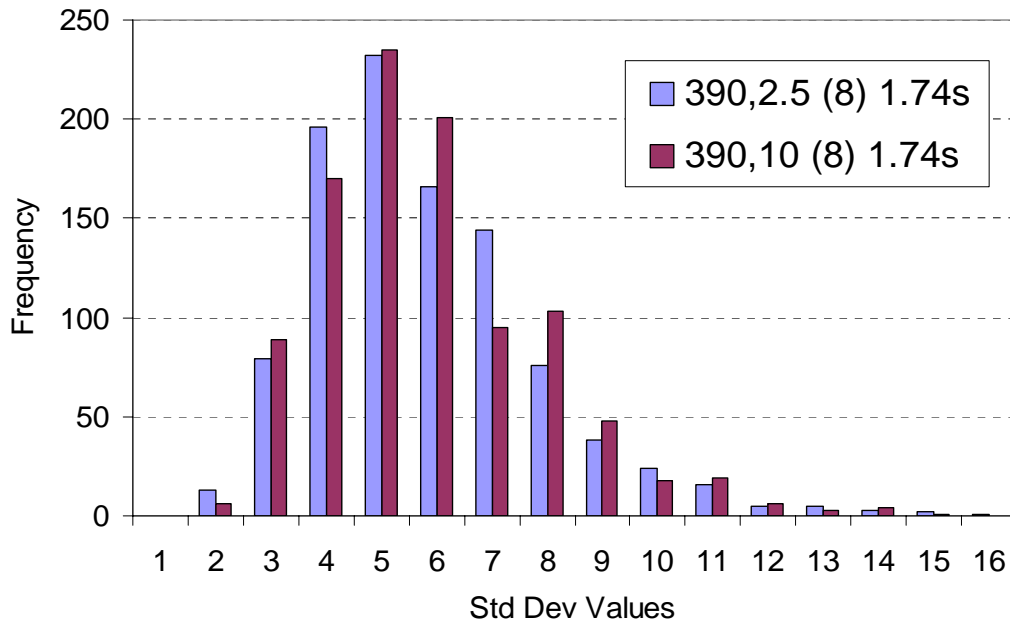


Figure 37. Distribution of standard deviation estimates using Dixon-Mood statistics after 50 iterations of 8-specimen subtests for both high and low initial estimates of standard deviation using step size 1.74σ .

Thus, although the use of staircase iteration may allow convergence of standard deviation estimates to true values in an average sense, there is no guarantee that the results will converge on an individual basis. Use of bias correction and bootstrapping in conjunction with iteration was attempted, but results generally did not improve as compared to cases in which a single staircase was used. In short, if given the choice between a single staircase of N specimens with some initial standard deviation estimate or a series of back-to-back staircases of $N/2$ specimens each, it appears that the single staircase produces better results.

Summary

In this chapter, several important strides were made in the understanding and characterization of the staircase test as applied to fatigue strength testing. The ability of the Dixon-Mood analysis method to accurately and efficiently characterize mean fatigue strength using very few specimens was demonstrated. A comparison of the various methods (Brownlee *et al*, Dixon, and Little) of correcting for a string of failures or survivals at the beginning of the test was accomplished, and it was shown that the Little

method was generally a more robust and accurate technique. A comparison of the very recent (1998-2003) research into improving fatigue strength standard deviation estimates using staircase testing was also completed, showing that these new methods were less than complete and did not fully characterize the bias and scatter inherent in standard deviation estimates based on staircase data. An exhaustive simulation study was undertaken which was able to completely characterize this bias and scatter for a range of sample sizes (≥ 8) and step sizes ($\geq 0.1\sigma$). Findings of interest included (1) use of an initial starting stress offset from the true fatigue strength mean slightly reduced standard deviation bias, and (2) use of larger step sizes in the $1.6\text{--}1.75\sigma$ range more significantly reduced this bias. A non-linear correction to Dixon-Mood standard deviation was developed to further eliminate bias as a function of sample size and step size. These bias reduction techniques tended to amplify scatter in results, however. Use of a bootstrapping algorithm applied to the P - S data from a staircase test was shown to reduce this scatter and provide protection against “outlier” standard deviation estimates. The use of iteration was also explored as a means to reduce the importance of initial standard deviation estimates. This iterative staircase algorithm was shown to provide convergence to true fatigue strength parameters in an average sense, but not on an individual basis, and was thus shown to be ineffective.

In the next chapter, an experimental validation of the proposed staircase methodology will be presented using Ti-6Al-4V tests conducted on a 20-kHz ultrasonic test machine. The data from these tests will be analyzed using the results of this chapter—i.e, larger step sizes will be used, the non-linear bias correction formulation will be investigated, as well as the use of bootstrapping the results.

IV. USE OF THE MODIFIED STAIRCASE METHOD FOR TI-6AL-4V GIGACYCLE TEST DATA

In this chapter, the staircase method is used to estimate the gigacycle fatigue strength distribution of Ti-6Al-4V specimens tested on a 20-kHz ultrasonic fatigue testing machine. The objective is to demonstrate the use of larger step sizes and staircase bootstrapping for a real engineering problem. Existing experimental data from AFRL's HCF program were utilized, with additional tests requested to fill in a complete staircase.

Introduction

There is significant interest in the HCF community regarding the existence of internally-initiated fatigue cracks in the very high cycle regime. As discussed in Chapter II, numerous researchers have identified this failure mechanism and proposed that two *S-N* curves actually exist for each material. One curve is associated with the surface-initiated cracking mechanism. The second curve is associated with internally-initiated (subsurface) cracks, as shown by Figure 38. Data from the National HCF S&T Program using conventional fatigue testing machines (up to 1000 Hz) do not reveal the presence of this internal cracking mechanism for tests up to 10^9 cycles conducted using Ti-6Al-4V under fully-reversed loading, although only two of the 37 data points at $R = -1$ went beyond 10^8 cycles [4].

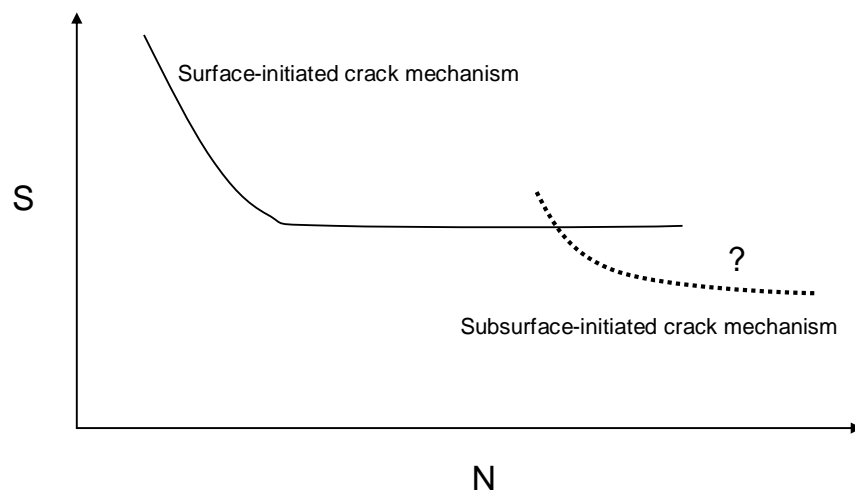


Figure 38. Schematic of possible dual-phase *S-N* behavior.

The staircase testing of Morrissey and Nicholas [52] addressed this void in experimental results for Ti-6Al-4V data points beyond 10^8 cycles. Their testing was meant to probe several issues: (1) any frequency effect when testing at 20 kHz, (2) any subsurface initiations observed in the gigacycle regime, and (3) any effect due to cooling specimens during testing. Their results showed that tests conducted using a 20-kHz ultrasonic fatigue testing machine matched up well with those observed using a conventional 60-Hz machine. There was no observable frequency effect for Ti-6Al-4V specimens under fully-reversed loading using the ultrasonic apparatus. As for subsurface initiation, no such phenomenon was observed in the 28 specimens tested, with the maximum fatigue failure occurring at 6.0×10^8 cycles [4]. Lastly, the thermal response of the material when tested at room temperature indicated that temperatures remained low enough such that specimen heating during loading had no significant effect on material behavior. Figure 39 shows a thermal image generated during their testing for the investigation of thermal response.

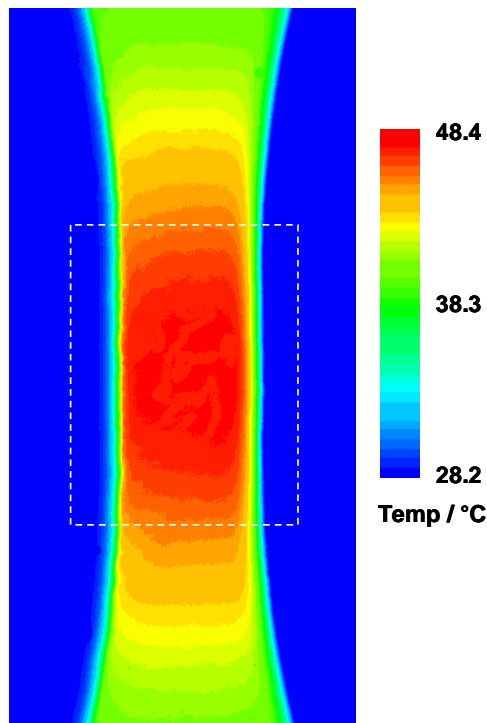


Figure 39. Thermal image of Ti-6Al-4V gage section during 200 MPa test using the 20-kHz ultrasonic fatigue machine (provided by AFRL/MLLM).

The work of Morrissey and Nicholas provided two sets of 10-specimen staircase data, each with a runout limit of 10^9 cycles, and one set of 8-specimen staircase data with a runout limit of 10^8 cycles [4; 52]. The objective of this chapter was to use the 10^9 staircase data to validate the simulation work of Chapter III. Ideally, one would prefer to perform a validation experiment with the freedom to choose the starting stress, step size, and the number of specimens. But with existing staircase data already provided, it was decided that it would be advantageous to use these existing data and perform minimal additional tests if needed.

Experimental Background

Before discussing the data analysis of the Ti-6Al-4V staircase tests, this section presents the necessary background related to the laboratory experiments.

Material Processing and Properties

The material used for the analysis in this chapter is a titanium alloy, specifically Ti-6Al-4V, which is a common aerospace engineering material, often used in turbine engine components. Much of the fatigue testing conducted by the National HCF S&T Program used this particular material [3]. The details of the material processing are provided in a number of papers [48; 52-53], but will be summarized here from Morrissey and Nicholas [52]. The material was produced in accordance with AMS 4928, being forged into flat plates of dimensions 406 mm x 150 mm x 20 mm (approximately). The forged plates were then solution heat treated at 932°C for 1 hour, vacuum annealed at 705°C for 2 hours, and then argon fan cooled. The resulting microstructure is of two-phase design, with approximately 60% by volume consisting of the primary α phase (hexagonally close-packed lattice, or h.c.p.), with the remaining volume consisting of transformed β phase (body-centered cubic lattice, or b.c.c.). This type of Ti-6Al-4V microstructure is often called “two-phase,” “dual phase,” “duplex phase,” “bimodal,” or simply “ α - β .” The material processed in this manner is known to metallurgists as solution treated and overaged (STOA). Average grain size was approximately 15-20 μm . Longitudinal tensile properties (along the loading axis) at room temperature in an ambient environment were $E = 116$ GPa (Young’s modulus), $\sigma_y = 930$ MPa (yield strength), and $\sigma_{UTS} = 968$ MPa (ultimate tensile stress).

Ultrasonic Fatigue Testing Machine

The original design of an ultrasonic fatigue testing apparatus goes back to the work of Mason in the late 1940s and 1950s [49]. The principle of operation is based on a transducer which converts input signals at a given frequency into a mechanical displacement at the same frequency [16; 52]. This displacement is mechanically amplified and vibrates the specimen at its resonant frequency. The vibration of the specimen at its resonant frequency produces the alternating strain field which leads to an alternating stress field in the gage section of the specimen. In this manner, a specimen is fatigued until failure or the specified number of cycles has been reached.

The ultrasonic fatigue testing machine used for this testing was the property of AFRL/MLLM, and used a piezoelectric transducer to convert electronic signals generated by a power supply at a frequency of 20 kHz (± 500 Hz) into displacements [52]. The power supply is automatically tuned to the natural frequency of the system, and when the frequency falls outside the 19.5-20.5 kHz range, the system will automatically shut off. Branson Ultrasonics Corporation is the manufacturer of the power supply and transducer, which were originally designed for ultrasonic welding applications [52]. A titanium booster and horn are attached to the transducer. These components are designed to amplify the mechanical displacement provided by the transducer. The horn is attached to the specimen, which has a threaded end which screws into a female receptor in the horn. Specimens must be designed to have an axial natural frequency of 20 kHz in order to achieve the resonant condition.

All tests for this study were conducted under fully-reversed loading conditions so that mean loads were not applied. Thus, the end of the specimen not connected to the amplifying horn was a free surface. An eddy current sensor was mounted opposite this free surface and provided a means of measuring displacement of the specimen end during its load cycle. At the beginning of each test, a resistance strain gage was mounted on the gage section and the free end displacement as read by the eddy current sensor was calibrated with the strain values obtained from the strain gage [52]. Once calibrated, a control loop is used by the machine to ensure that gage section strains are controlled by measuring the calibrated eddy current sensor data. Knowing the elastic properties of the specimen, the gage section strain can be converted to stress, and thus the stress amplitude

of the fatigue test is controlled. Strain gages are not mounted throughout testing because they are not durable at such high frequencies and quickly fall off. Thus the eddy current sensor calibration is crucial to providing accurate stress amplitude data. Test control software is displayed on a computer and monitors and records displacement data and controls the power supply. Fatigue failure is detected by the change in natural frequency, causing the system to shut down. Figure 40 shows the ultrasonic fatigue testing setup as used by AFRL/MLLM.

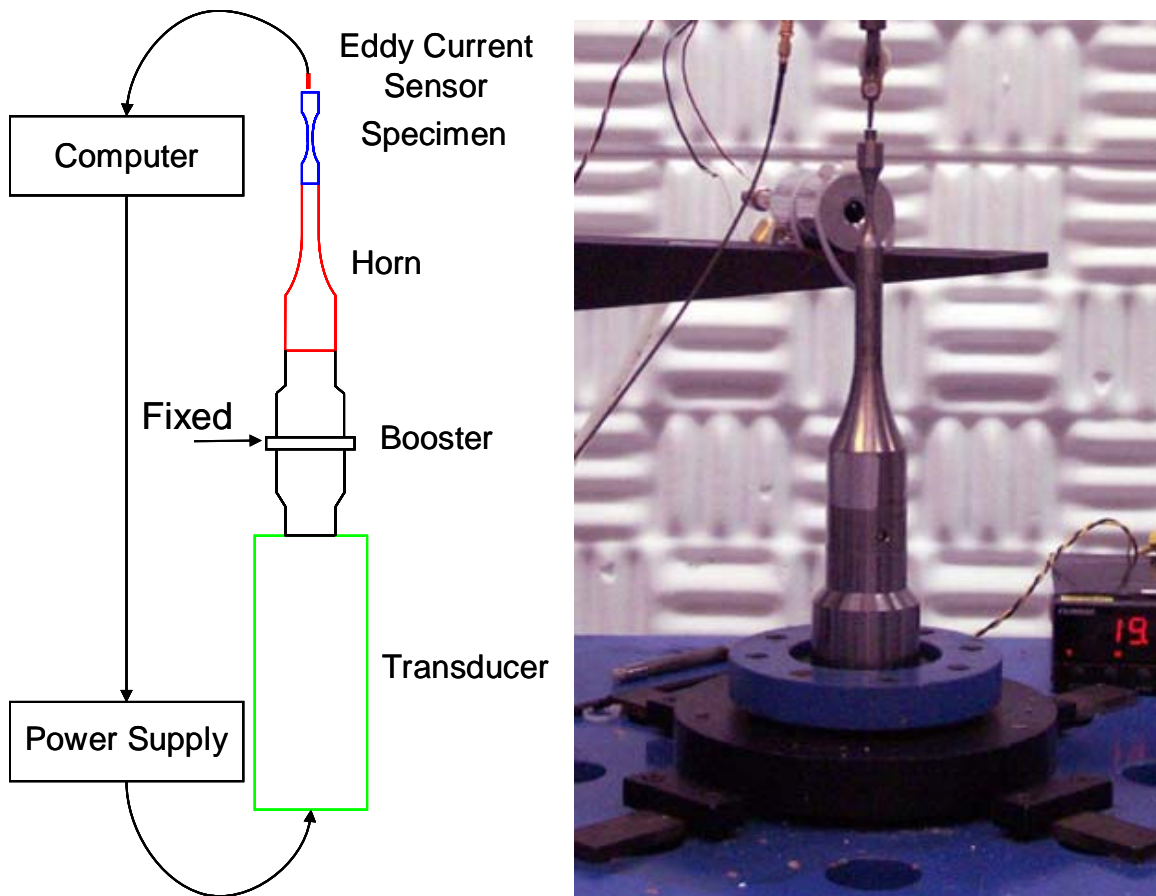


Figure 40. Schematic drawing and photograph of the 20-kHz ultrasonic fatigue testing apparatus (provided by AFRL/MLLM).

Test Specimens

The specimens designed for this experiment used a cylindrical dog-bone geometry with a gage section diameter of 4 mm and an outer end diameter of 12.7 mm. The gage

section had a length of 6 mm. Figure 41 shows the details of the specimen geometry along with a photograph of the specimen mounted to the horn.

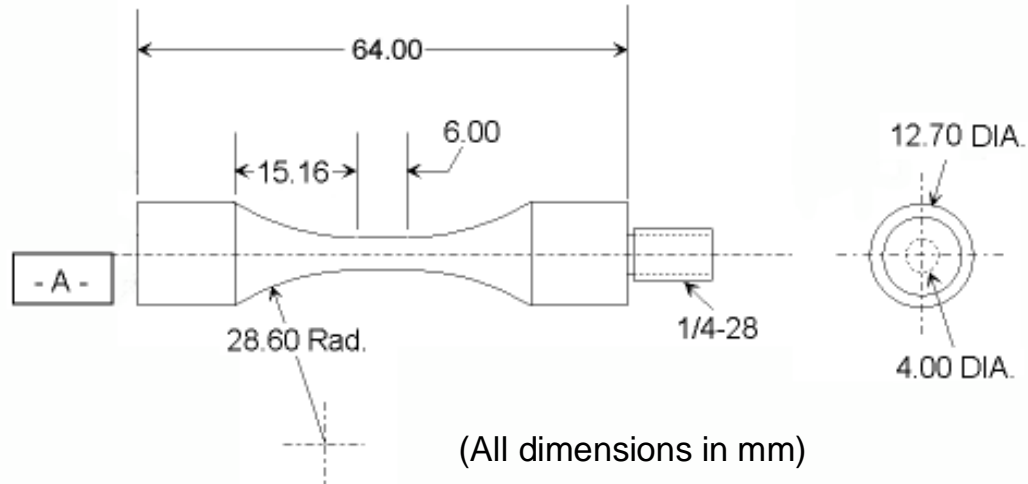


Figure 41. Specimen geometry (provided by AFRL/MLLM).

All specimens were prepared using a low stress grinding technique [52]. Of the 28 specimens initially tested, 8 were tested as received after machining and 20 were stress relief annealed (SRA) prior to testing. As the name implies, the SRA method is an annealing procedure which alleviates residual stresses at the surface due to machining. For the 20 SRA specimens, half were tested with two air jets mounted on opposite sides of the specimen blowing 0°C air, and half were tested without cooling.

Experimental Data

The tests were conducted by AFRL/MLLM in three separate staircases, with an 8-specimen staircase for the as-received specimens, and two 10-specimen staircases for the SRA specimens with cooling and without cooling, respectively. Each staircase used a 10

an $S-N$ format in Figure 43. Use of the SRA-only data also allowed the data to be combined into one “super staircase” permitting analysis as described in Chapter III.

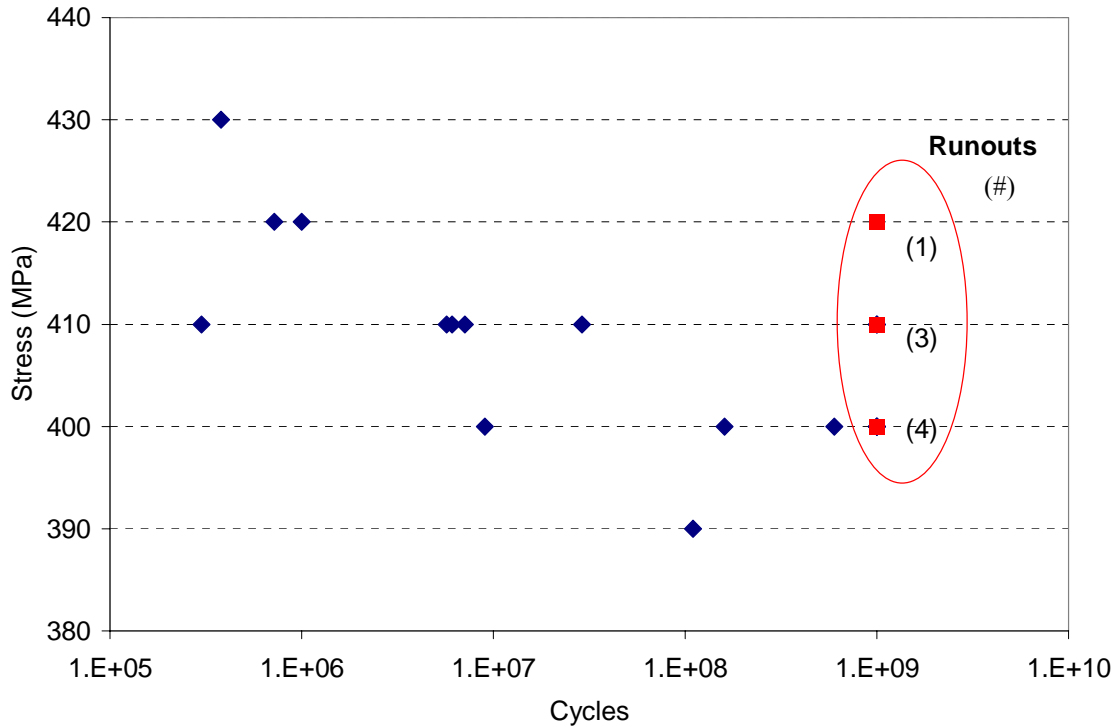


Figure 43. Initial staircase data for 10^9 -limited tests of α - β Ti-6Al-4V under $R = -1$ loading using the 20 stress-relief annealed (SRA) specimens.

Reworking the Data

In order for the data from the Morrissey and Nicholas tests to be used to provide a validation example of the staircase procedures developed in Chapter III, the data must conform to the staircase protocol. Since the data come from separate staircase tests, they must be reorganized to fit into a single staircase format. In order to make a single staircase out of the data, some changes were necessary. Note that if a specimen fails at a given stress, it would also have failed at a higher stress. Conversely, if a specimen survives at a given stress, it would also have survived at a lower stress. These statements lead to the following rules which were used to transform staircase data from one stress level to another stress level:

- A real failure at stress level X is also a failure at stress level Y if $Y > X$.
- A real survival at stress level X is also a survival at stress level Y if $Y < X$.

Using these rules, the 20 staircase data points can be transformed from a 10 MPa step to a 20 MPa step, as shown in Table 13. These transformed staircase data almost make a complete staircase, as shown by Figure 44. In order to be a complete staircase, three additional data points are needed at 380 MPa, and they must be runouts. If these data points were available, then all 20 points from the SRA staircases may be utilized. Three additional tests were thus conducted at 380 MPa. Each of these tests did, in fact, result in a runout at 10^9 cycles (as shown in Table 28 in Appendix A). Thus, a complete 23-specimen staircase with step size 20 MPa and starting stress 400 MPa and four resulting stress levels was available for analysis using the three additional tests.

Table 13. Transformation of real staircase data.

Staircase Data Set	Specimen	Real Results		Transformed Results	
		Stress (MPa)	Result	Stress (MPa)	Result
SRA with no cooling	1	400	Survival	400	Survival
	2	410	Survival	400	Survival
	3	420	Failure	420	Failure
	4	410	Survival	400	Survival
	5	420	Failure	420	Failure
	6	410	Failure	420	Failure
	7	400	Survival	400	Survival
	8	410	Survival	400	Survival
	9	420	Survival	420	Survival
	10	430	Failure	440	Failure
SRA with cooling	11	410	Failure	420	Failure
	12	400	Failure	400	Failure
	13	410	Failure	420	Failure
	14	400	Failure	400	Failure
	15	390	Failure	400	Failure
	16	400	Survival	400	Survival
	17	410	Failure	420	Failure
	18	400	Survival	400	Survival
	19	410	Failure	420	Failure
	20	400	Failure	400	Failure

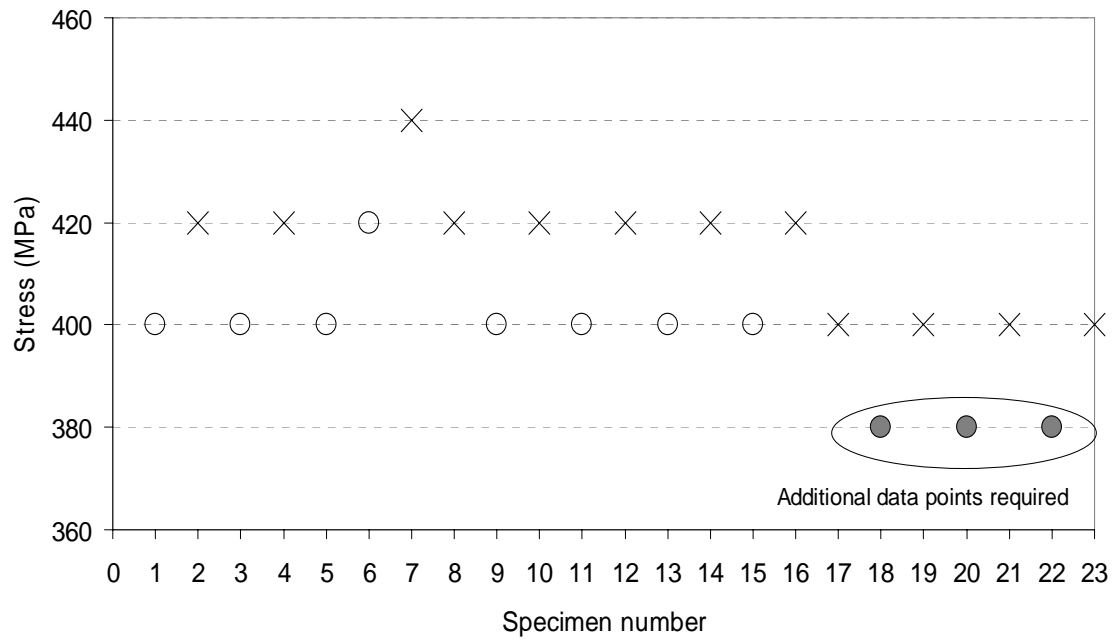


Figure 44. Ti-6Al-4V data transformed into a single staircase.

Staircase Analysis

The staircase analysis could now be accomplished on a complete set of real test data. The first step of the analysis was to apply the Dixon-Mood equations in order to estimate the mean fatigue strength and its standard deviation. A spreadsheet-based staircase analysis tool built using the Dixon-Mood equations was used to calculate the mean fatigue strength and standard deviation of fatigue strength at 10^9 cycles. Figure 45 shows the calculations and results from the Dixon-Mood analysis. Since the first two trials are of opposite sign, no adjustment to the Dixon-Mood estimate for mean fatigue strength is needed. Thus, the mean fatigue strength for the Ti-6Al-4V data based on these 23 specimens is 406.4 MPa. The Dixon-Mood estimates for mean fatigue strength are generally very accurate so long as assumptions are not grossly violated.

Staircase test parameters						Staircase test statistics		Summation terms for Dixon-Mood equations							
Stress 0	400					Number failed	12	Level	Count	Count_S	Count_F	m_i	i*m_i	(i^2)*m_i	
Step size	20					Test to be based on	Survivals	0	3	3	0	3	0	0	
Specimen #	Staircase Stress	Result (S/F)	Formula Counter	Stress Values	Stress Levels	Stress (i = 0)	380	1	11	7	4	7	7	7	
	1	400	S	1	400	1	StDev condition	0.33	2	8	1	7	1	2	4
	2	420	F	1	N/A	2	Mean fatigue limit	406.36	3	1	0	1	0	0	0
	3	400	S	1	400	1	StDev fatigue limit	11.65	4	0	0	0	0	0	0
	4	420	F	1	N/A	2	* Statistics using Dixon-Mood	5	0	0	0	0	0	0	0
	5	400	S	1	400	1		6	0	0	0	0	0	0	0
	6	420	S	1	420	2		7	0	0	0	0	0	0	0
	7	440	F	1	N/A	3		8	0	0	0	0	0	0	0
	8	420	F	1	N/A	2		Sum	23	11	12	11	9	11	
	9	400	S	1	400	1									
10	420	F	1	N/A	2										
11	400	S	1	400	1										
12	420	F	1	N/A	2										
13	400	S	1	400	1										
14	420	F	1	N/A	2										
15	400	S	1	400	1										
16	420	F	1	N/A	2										
17	400	F	1	N/A	1										
18	380	S	1	380	0										
19	400	F	1	N/A	1										
20	380	S	1	380	0										
21	400	F	1	N/A	1										
22	380	S	1	380	0										
23	400	F	1	N/A	1										

Figure 45. Dixon-Mood calculations for 23-specimen Ti-6Al-4V staircase data.

Assumption of Normality

Before going onto the standard deviation analysis, the assumption of normality should at least be checked to ensure that gross deviation is not observed. In order to assess the shape of the fatigue strength distribution (which is an unknown), several analysis techniques may be employed that go beyond staircase data analysis. First, using the data from Figure 42, a bilinear curve fit model (in stress-log cycle coordinates) was developed using a least squares approach. The least squares approach is used to find a linear curve fit to a set of x - y data, thus providing the best line of the form $y = ax + b$, where a and b are constants based on the sample points. The solution to the least squares linear curve fit is a classic mathematics problem and is given by:

$$a = \frac{n \sum_i xy - \sum_i x \sum_i y}{n \sum_i x^2 - \left(\sum_i x \right)^2} \quad (34)$$

$$b = \frac{\sum_i y \sum_i x^2 - \sum_i x \sum_i xy}{n \sum_i x^2 - \left(\sum_i x \right)^2} \quad (35)$$

where n is the number of x - y data points and $\sum_i = \sum_{i=1}^n (\cdot)$.

The data from Figure 42 were divided into two sets, one corresponding to the sloped region at lower fatigue lives ($< 2 \times 10^5$ cycles) and one corresponding to the relatively flat region for fatigue lives greater than 2×10^5 cycles. Only failure points were included as x - y data. For this scenario, x corresponded to $\log(N)$ and y corresponded to S . With the two sets of S - N data, the best fits for each region of the S - N curve were calculated as:

$$S = -226.6 \log(N) + 1588.7 \text{ (sloped region) } N \leq 2 \times 10^5 \quad (36)$$

$$S = -4.0 \log(N) + 433.7 \text{ (horizontal region) } N > 2 \times 10^5 \quad (37)$$

These linear fits were then plotted over the Ti-6Al-4V S - N data points as shown in Figure 46. The data points in Figure 46 and Figure 42 are identical except for the addition of the three runouts at 380 MPa.

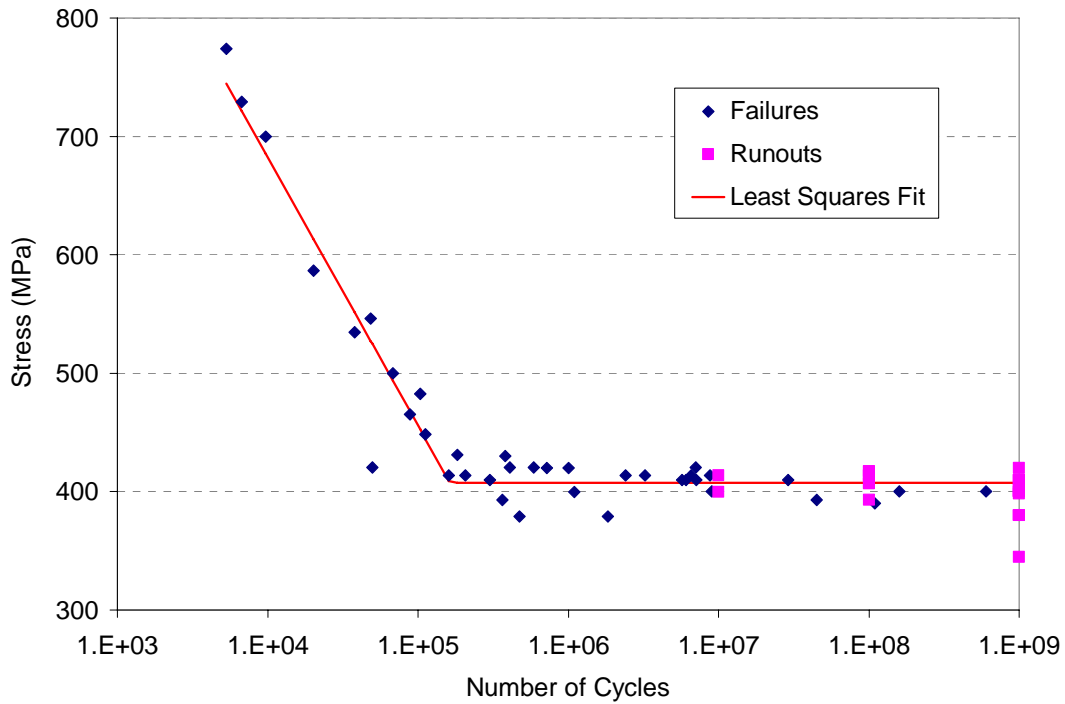


Figure 46. Bilinear curve fit using least squares for Ti-6Al-4V data.

The next step was to measure the residuals from the failure points to the curve fit. These residuals thus provide a quantification of the scatter about the mean S - N curve. As suggested by Hanaki *et al* [36], the fatigue data may be transformed into a “normalized fatigue strength” which groups the data with differing fatigue life into a single

distribution, thus allowing a means of estimating the fatigue strength distribution with much less data than if only points with similar fatigue lives were used. Of course, for this approach to be applicable, no discernible trend in fatigue strength scatter as a function of fatigue life should be apparent. Looking at Figure 46, the assumption of constant fatigue strength scatter about the mean fatigue strength line is indeed reasonable.

The residual errors in the fatigue-limit regime ($> 2 \times 10^5$ cycles) were analyzed using distribution-fitting software. A histogram of the residuals is shown in Figure 47 along with a normal and an extreme value distribution fit. Clearly, there is some skewness in the data towards lower stress values and the extreme value distribution appears to represent the scatter in fatigue strength rather well. Although the fatigue strength distribution appears to be non-normal based on Figure 47, the probability plot shown in Figure 48 is not so far from normality that the Dixon-Mood analysis cannot be used with caution. Figure 49 shows the probability plot for data fitted with an extreme value distribution, which again appears to yield a good fit.

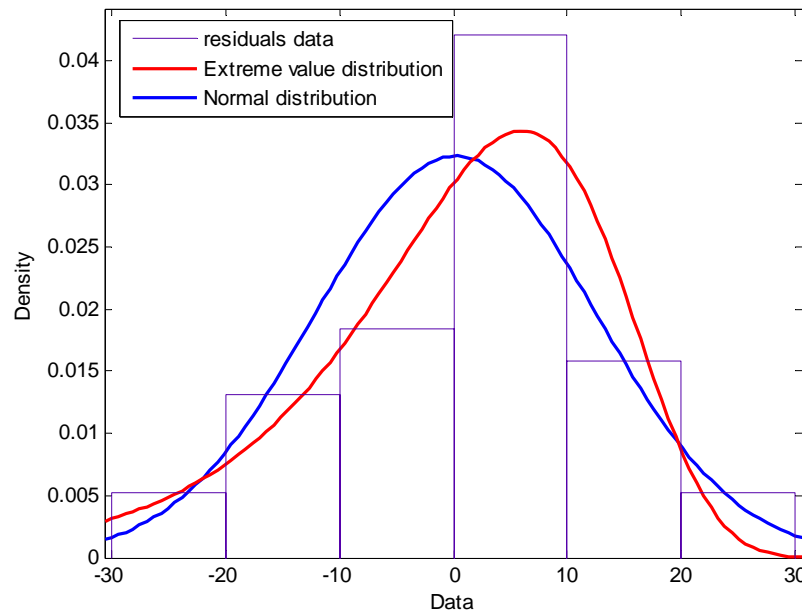


Figure 47. Residuals in the HCF region for Ti-6Al-4V data at $R = -1$ for a horizontal fatigue limit.

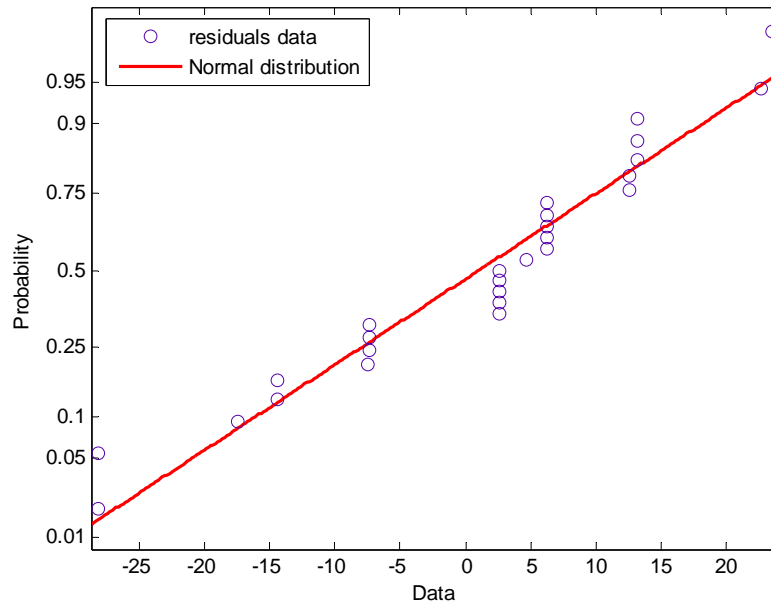


Figure 48. Probability plot for normal distribution fit of Ti-6Al-4V residuals.

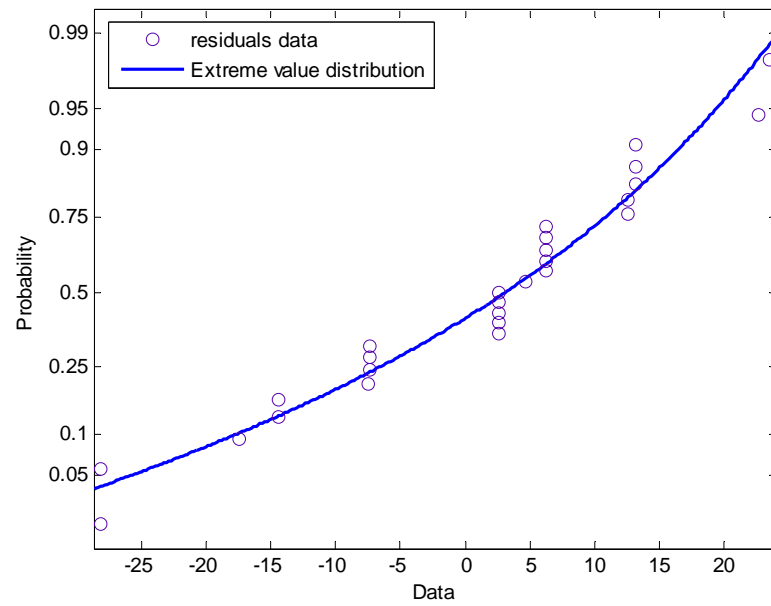


Figure 49. Probability plot for extreme value distribution fit of Ti-6Al-4V residuals.

Standard Deviation Analysis

The Dixon-Mood standard deviation estimate (shown in Figure 45) is 11.65 MPa. As discussed in Chapter III, the standard deviation estimate should be adjusted using

either the Svensson-Lorén or the proposed non-linear correction. For the 23-specimen data, the standard deviation using the Svensson-Lorén correction is given by:

$$\sigma_{SL} = \sigma_{DM} \frac{N}{N-3} = 11.65 \cdot \left(\frac{23}{23-3} \right) = 13.40 \text{ MPa} \quad (38)$$

To use the newly proposed non-linear correction for 23 specimens, the values for the constants used in Equation 3-18 can be interpolated from Table 7. Interpolating between 20 and 30 specimens yields $A = 1.0$, $B = 1.2$, and $m = 0.381$, so that the proposed correction is calculated as:

$$\sigma_{PC} = A \sigma_{DM} \left(\frac{N}{N-3} \right) \left(B \frac{\sigma_{DM}}{s} \right)^m = 1 \cdot 11.65 \cdot \left(\frac{23}{23-3} \right) \left(1.2 \frac{11.65}{20} \right)^{0.381} = 11.69 \text{ MPa} \quad (39)$$

Thus, the proposed correction is very close to the uncorrected Dixon-Mood standard deviation for this case. If the 11.69 MPa estimate is considered close to the true standard deviation, then the 20 MPa interval corresponds to a 1.71σ step, which was earlier shown to be in the unbiased region for the Dixon-Mood standard deviation estimator. Thus, a “good” Dixon-Mood standard deviation estimate may have resulted from using a step size that was appropriately large relative to the true standard deviation.

Since the staircase data resulted in four stress levels, it is appropriate to use the bootstrapping algorithm to reduce any potential for an outlier standard deviation estimate. Recall that the average of the 60th- and 65th-percentiles of the bootstrapped distribution worked well for estimating the standard deviation for a 4-level staircase. The bootstrap algorithm requires the P - S data from the staircase test as an input. In this case, the P - S data can be read from Figure 44 and are summarized in Table 14.

Table 14. P - S data for the 23-specimen Ti-6Al-4V staircase.

Stress Level	Survivals	Failures	$P(\text{failure})$
380	3	0	0
400	7	4	0.364
420	1	7	0.875
440	0	1	1

These *P-S* data were bootstrapped using the simulation-based algorithm discussed in Chapter III, with input parameters and output statistics shown in Figure 50. The Svensson-Lorén bootstrapped percentiles were 13.40 MPa (60th) and 14.63 MPa (65th), for a mean of 14.02 MPa. The proposed correction percentiles were 11.69 MPa (60th) and 13.20 MPa (65th), for a mean of 12.45 MPa. Because the bootstrapped values are so close to the non-bootstrapped values, it suggests that these estimates are quite near their expected value. The estimate based on the proposed correction should be used due to the large step, as discussed in Chapter III.

Bootstrap Input	Bootstrap Output
<code>initstress = 400;</code>	DIXON-MOOD STD DEV
<code>step = 20;</code>	Bootstrap sigma mu = 12.4737
<code>n = 23;</code>	Bootstrap sigma 60 = 11.6503
<code>Pstar = [0 0.363636 0.875 1];</code>	Bootstrap sigma 65 = 12.7214
<code>Sstar = [380 400 420 440];</code>	SVENSSON-LOREN CORRECTED STD DEV
	Bootstrap sigma mu = 14.3447
	Bootstrap sigma 60 = 13.3979
	Bootstrap sigma 65 = 14.6296
	POLLAK CORRECTED STD DEV
	Bootstrap sigma mu = 12.9856
	Bootstrap sigma 60 = 11.6893
	Bootstrap sigma 65 = 13.1989
	FATIGUE STRENGTH MEAN
	Bootstrap mean = 404.8778

Figure 50. Bootstrap input and output for the 23-specimen Ti-6Al-4V staircase.

An additional means of validating the standard deviation estimates would be to calculate the standard deviation of the best normal distribution fitted to the fatigue strength residuals shown in Figure 47. The standard deviation of this normal fit is calculated to be 13.38 MPa by the MATLAB `dfittool` command. This value is very close to that determined by the modified staircase analysis.

A final means of validating the standard deviation estimate would be to simulate a number of staircase tests using the same staircase settings ($S_{init} = 400$ MPa, $s = 20$ MPa, and $N = 23$ specimens) as the Ti-6Al-4V staircase analysis, but using the calculated fatigue strength parameters as fatigue strength inputs ($\mu = 406.4$ MPa, $\sigma = 12.45$ MPa)

and investigate the distribution of results. This process was accomplished for 30 runs of 23 specimens each. Twelve of these simulation runs resulted in a 3-level staircase, for which the Svensson-Lorén corrected standard deviation was used as the calculated standard deviation. The remaining 18 runs resulted in a 4-level staircase for which the bootstrap algorithm was used on the P - S data to calculate the average of the 60th- and 65th percentiles of the bootstrap distribution using the proposed standard deviation correction (with $A = 1.0$, $B = 1.2$, and $m = 0.381$). A histogram of the results of these 30 runs is presented in Figure 51. For these conditions, 26 of the 30 runs resulted in standard deviations within ± 2.2 MPa (18%) of the “true” value of 12.45 MPa. The mean of the standard deviation estimates from the 30 runs was 12.74 MPa, with just a 1.76 MPa standard deviation. Thus, these simulation data support the 12.45 MPa estimate obtained from the analysis developed in Chapter III to be a fairly accurate measure of the fatigue strength distribution of Ti-6Al-4V.

Another way to evaluate the modified analysis (larger steps, use of the Svensson-Lorén correction for 3-level data, and use of the bootstrap with bias correction for data with more than 3 stress levels) would be to assume that the 12.45 MPa estimate for

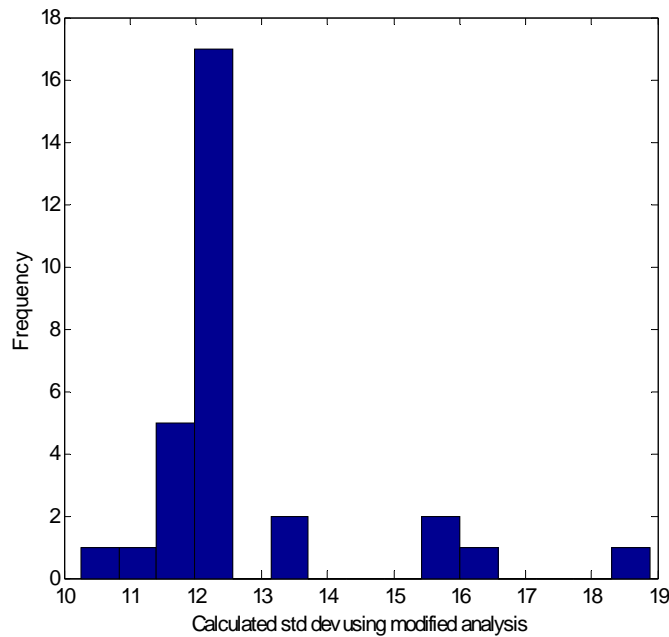


Figure 51. Standard deviation results using modified staircase analysis for 30 runs using Ti-6Al-4V fatigue strength estimates as inputs.

standard deviation is equal to σ , the true fatigue strength standard deviation. With this input, the staircase simulation can be used for a 23-specimen test run at 10 MPa (the original step size) using just the Dixon-Mood method. Thus, this effort simulates possible test results as originally tested and analyzed before reworking the data into 20 MPa steps. The simulation was run for a material with underlying fatigue strength normally distributed with $\mu = 406.4$ and $\sigma = 12.45$ using a 23-specimen staircase with $S_{init} = 400$ MPa and step 10 MPa. Figure 52 shows the simulated results for 1000 replications. Note that a larger number of simulation runs can be easily made here as the manual steps required by the bootstrap algorithm are not necessary.

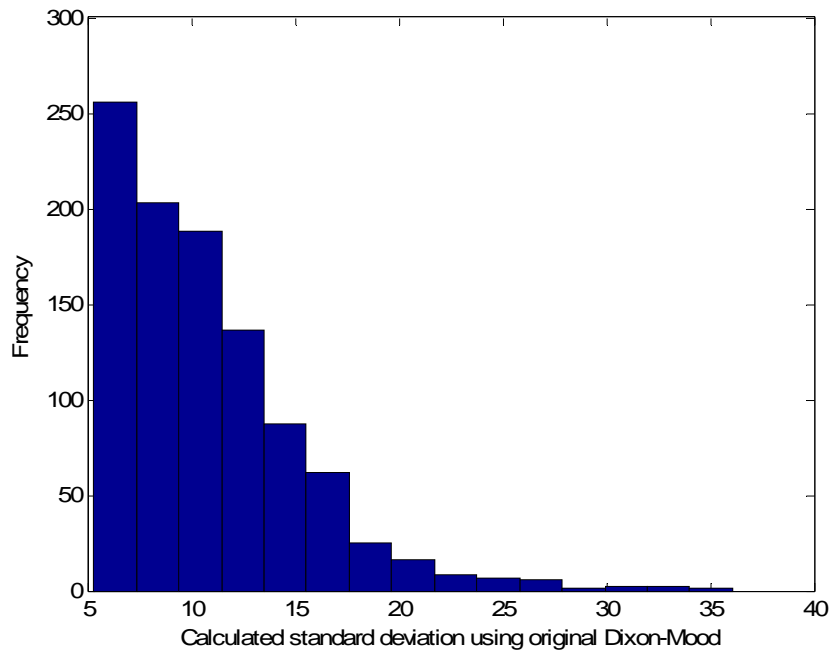


Figure 52. Simulated Dixon-Mood standard deviation results for 23-specimen staircase starting at 400 MPa with 10 MPa step for underlying Normal(406.4,12.45).

Based on Figure 52, the mode of this distribution is on the order of 6 MPa (about half the true value), versus the mode on the order of 12 MPa using the modified analysis. The 6 MPa estimate clearly does not match well with the observed standard deviation of 13.38 MPa based on the physical scatter of residuals about the S - N curve. The mean of the Dixon-Mood distribution was 10.67 MPa with a 4.60 MPa standard deviation, thus the scatter in results is significantly larger than for the modified method. Instead of a

large 1000-replication simulation, several 30-replication runs could also be made for comparison. Such runs are shown in Figure 53. Comparing the results obtained using the modified method in Figure 51 to those shown in Figure 53, it is clear that for this set of test conditions, the modified method provides a result which is much more accurate on average and has significantly reduced scatter when compared to the uncorrected Dixon-Mood analysis.

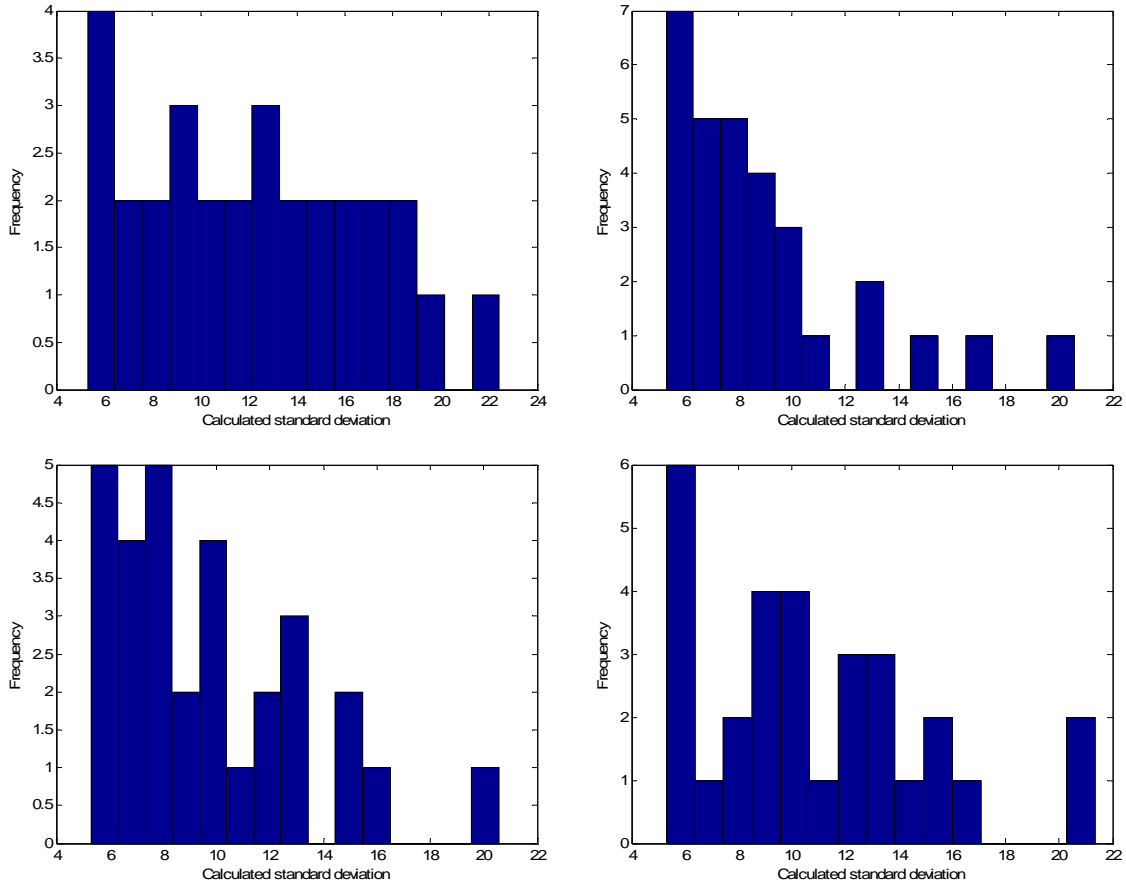


Figure 53. Several 30-specimen histograms randomly generated using the same conditions as Figure 52.

Summary

In this chapter, the staircase analysis methods developed in Chapter III were applied to a real-world set of Ti-6Al-4V data generated on a 20-kHz ultrasonic test machine. The analysis suggests that the larger step size, standard deviation corrections, and use of bootstrapping were able to estimate the fatigue strength parameters of the Ti-

6Al-4V data quite well using a small-sample staircase test. Validation of the standard deviation estimate was accomplished in two ways, one being an investigation of the physical scatter in fatigue strength from a larger number of Ti-6Al-4V tests, and the other being a simulation-based investigation which showed that tests conducted at the given staircase settings were likely to give results using the modified staircase method very close to those observed when the parameter estimates are used as true distribution parameters. Reworking the data into 20 MPa steps versus the original 10 MPa steps allowed not just a means of creating a continuous staircase, but allowed larger step sizes which reduced standard deviation bias. Using the new staircase analysis methods, the fatigue strength distribution of Ti-6Al-4V at 10^9 cycles was determined to have a mean fatigue strength of 406.4 MPa with a standard deviation of 12.45 MPa when approximated by a normal distribution. However, the distribution was not quite normal and was better fit using an extreme value distribution. Additionally, the fatigue strength scatter does not appear to vary significantly with fatigue life in the HCF regime. Thus, the 12.45 MPa standard deviation estimate should provide a reasonable estimate at any number of cycles beyond 2×10^5 . Note that all failed specimens showed failure due to surface-initiated cracking.

In the next chapter, the RFL model will be introduced in more detail for characterizing HCF behavior when more than just the fatigue strength distribution at a specified number of cycles is of interest.

V. INVESTIGATION OF TEST DESIGN USING THE RANDOM FATIGUE LIMIT MODEL

The purpose of this chapter is to investigate the use of different test strategies using the random fatigue limit (RFL) model when characterizing high cycle fatigue behavior. The goal of this analysis is to apply the findings to determine a small-sample test strategy to characterize $S-N$ behavior for a different material with little existing data (namely, a beta-annealed variant of Ti-6Al-4V), which is described in the next chapter. The first part of this chapter presents the case for using a method other than staircase testing for characterizing behavior over a range of cycles. Next, the necessary background of the RFL model is presented in more detail. Lastly, an investigation of different test designs is presented by applying the RFL model to simulated test results, concluding with a recommended test design for the subsequent experimental test phase.

Staircase Testing at Multiple Numbers of Cycles

In Chapter III, the staircase method was investigated in detail as a means of quantifying the fatigue strength distribution at a given number of cycles. This test was a quantal response method in which test results were binary – i.e., either a specimen survived the number of cycles or it failed. This approach was shown to be a viable means of characterizing the mean (or median) fatigue strength and its scatter at a specified number of cycles. An additional application which is of interest is determining the shape of the stress-life ($S-N$) curve in the very high cycle regime to determine if a fatigue limit exists. For example, a researcher may be interested in determining the fatigue strength at not one, but two or more, numbers of cycles. This type of investigation goes beyond the original application for which the staircase method was intended.

A possible approach to determining the fatigue strength at more than one specified number of cycles is use of a single staircase test with extrapolated results. An example of such an approach can be made using the 10^8 and 10^9 staircase data of Morrissey and Nicholas for Ti-6Al-4V specimens with stress-relief annealing using both cooling and no cooling during tests on the Air Force Research Laboratory's 20 kHz ultrasonic fatigue testing machine [4; 52]. These tests were conducted under fully-reversed loading ($R = -1$). Tests were initially conducted up to 10^8 cycles and the Dixon-

Mood method was used to estimate fatigue strength parameters at 10^8 cycles. Those specimens which survived 10^8 cycles were then rerun at a later time with a runout limit of 10^9 cycles. The data for these tests are shown in Table 15 and Table 16 (also shown in Appendix A). For the non-cooled specimens, no additional failures were observed going from 10^8 cycles to 10^9 cycles, and therefore the Dixon-Mood analysis is identical for both the 10^8 and 10^9 data. Thus, the calculated mean fatigue strength at both points is the same, in this case 415 MPa (stress amplitude). For the cooled data, there were three additional failures going from 10^8 to 10^9 cycles. Using Dixon-Mood for the 10^8 data yields a mean fatigue strength of 403 MPa. For the 10^9 cycles, the addition of the three failures violates the sequence of results dictated by staircase protocol, and hence a full staircase is no longer available in accordance with Dixon-Mood analysis. Thus, use of the Dixon-Mood equations results in estimates which are no longer mathematically valid with respect to the maximum likelihood method underlying the analysis. If one were to disregard the fact that the staircase is incomplete and perform the Dixon-Mood analysis anyway on the 10^9 data, the mean fatigue strength from the cooled samples is estimated to be 405 MPa. Obviously, this answer is illogical since changing any survivals to failures in a given group of data should not increase the fatigue strength, it should lower this estimate. Thus, unless some additional analysis (non-staircase) is performed on the 10^9 data, or additional data points are collected at 10^9 cycles to fill in the staircase holes in order to create a complete staircase, one cannot use Dixon-Mood analysis to quantify the slope in the $S-N$ curve from 10^8 to 10^9 cycles.

Table 15. Ti-6Al-4V (stress-relief annealed with no cooling, $R = -1$) fatigue data for 10^8 and 10^9 staircase tests from Morrissey and Nicholas [4; 52].

Specimen	Stress (MPa)	10^8 Result	Cycles	10^9 Result	Cycles
1	400	Survival	10^8	Survival	10^9
2	410	Survival	10^8	Survival	10^9
3	420	Failure	1.0×10^6	Failure	1.0×10^6
4	410	Survival	10^8	Survival	10^9
5	420	Failure	7.2×10^5	Failure	7.2×10^5
6	410	Failure	3.0×10^5	Failure	3.0×10^5
7	400	Survival	10^8	Survival	10^9
8	410	Survival	10^8	Survival	10^9
9	420	Survival	10^8	Survival	10^9
10	430	Failure	3.8×10^5	Failure	3.8×10^5

Table 16. Ti-6Al-4V (stress-relief annealed with cooling, $R = -1$) fatigue data for 10^8 and 10^9 staircase tests from Morrissey and Nicholas [4; 52].

Specimen	Stress (MPa)	10^8 Result	Cycles	10^9 Result	Cycles
1	410	Failure	5.7×10^6	Failure	5.7×10^6
2	400	Survival	10^8	Failure	1.6×10^8
3	410	Failure	6.1×10^6	Failure	6.1×10^6
4	400	Failure	9.0×10^6	Failure	9.0×10^6
5	390	Survival	10^8	Failure	1.1×10^8
6	400	Survival	10^8	Survival	10^9
7	410	Failure	2.9×10^7	Failure	2.9×10^7
8	400	Survival	10^8	Survival	10^9
9	410	Failure	7.1×10^6	Failure	7.1×10^6
10	400	Survival	10^8	Failure	6.0×10^8

In addition to the likely possibility that an incomplete staircase (and thus incomplete analysis) would result from an extrapolated staircase approach, there are very real concerns about the statistical validity of such a method. For one, such an approach raises the issue of multiple-weighting in the sense that a single specimen may create more than one S - N data point (even though the multiple points are consistent; i.e., a runout at a lower number of cycles and a failure at a higher number). In a quantal response approach, this condition may appear to be of no concern as S - N data points are only used in a pass/fail manner. If a specimen failed to survive X cycles, it must also have failed at Y cycles if $Y > X$. Conversely, if a specimen survives X cycles, it must also survive Y cycles if $Y < X$. However, from a statistical standpoint, if one is interested in the difference in material behavior at both X and Y cycles, then one needs to perform independent trials at X and Y cycles to test the hypothesis that the fatigue strength at X cycles is the same as the fatigue strength at Y cycles. Using the same data as results for different numbers of cycles clearly violates the independence of the data sets. It is certainly acceptable to use staircase results from tests conducted at a lower number of cycles, perform additional testing on the runout samples (assuming that no change in fatigue strength occurs from such interrupted testing), and fill in any staircase holes if they exist, in order to estimate fatigue strength parameters at a higher number of cycles. Likewise, one could use data from tests conducted at a higher number of cycles, reclassifying any failures between the lower number of cycles and higher number of cycles as survivals at the lower number of cycles, and perform a staircase analysis for the

lower number of cycles. There is nothing intrinsically wrong with this mix-and-match approach for reporting data at one of the numbers of cycles. However, it would be incorrect to then compare the results from the lower number of cycles to those from the higher number of cycles, thus making conclusions regarding differences in material behavior at the two numbers of cycles. Such an approach leads to dependency between the two sets of data, and thus differences in material response may be overlooked. For example, one could use the data from Table 15 to report the mean fatigue strength at 10^8 cycles as 415 MPa. Or, the data could be used to report the mean fatigue strength at 10^9 cycles as 415 MPa. But one should not use the data to say the difference between mean fatigue strengths at 10^8 and 10^9 cycles is 0 MPa, since the data sets are not independent. Thus, there is a bit of a paradox. If one were to report the findings together, the fact that the data sets are highly correlated would need to be clearly made and observed differences would have to be presented without statistical confidence. A solution to this dependency issue would be to conduct independent trials at each of the two numbers of specimens. The drawback to this approach is of course the need to do twice the number of tests, as well as the inefficiency in utilizing the available data.

In addition to this statistical dependence, the issue of staircase step size plays a role in masking differences as well. If one were to use a step too large compared to the difference in fatigue strength at the two numbers of cycles, then it is quite possible that runouts using the lower number of cycles will also run out at the higher number of cycles simply because the step is too large to observe any additional failures. The obvious solution would appear to be the use of step sizes which are small relative to the change in fatigue strength in order for this change in fatigue strength to appear in the results (as a survival at the lower number of cycles which is a failure at the higher number of cycles). For example, if one wanted to detect any changes in fatigue strength on the order of 5 MPa or less, a step size of 2-3 MPa may be considered. However, specifying step size based on the difference in fatigue strength between two numbers of cycles could potentially lead to seriously biased results. As the work of Chapter III showed, step sizes should be chosen rather carefully based on true standard deviation of the fatigue strength in order to minimize standard deviation bias inherent in the Dixon-Mood method. Although methods such as bias correction were shown to alleviate this bias, intentionally

basing step size on considerations other than true standard deviation would knowingly lead to greater errors in standard deviation estimates. If one is only concerned with the difference in mean fatigue strengths between the two numbers of cycles, this issue is not as relevant since the Dixon-Mood analysis of mean fatigue strength is much less dependent on step size.

An additional problem with using staircase testing to quantify fatigue strength differences at two or more numbers of cycles is the lack of data utilization inherent in such a method. If one were interested in the shape of the $S-N$ curve between two numbers of cycles (like 10^8 and 10^9), it would be a waste to use the $S-N$ data as merely pass/fail results rather than stress-life results. If the data are used in their stress-life format, $S-N$ curve-fitting methods may be used to better estimate the fatigue strength differences. As an analogy, use of the staircase method for this application would be like trying to quantify the mean differences in height between two groups by selecting a height and recording if a member from group A and a member from group B are taller or shorter than this height, and then repeating this approach for each member, selecting different heights for comparison against. A better approach would obviously be measuring each individual's height and then using a probability distribution to estimate the mean difference and associated confidence interval between the two groups.

This section provides some rationale for avoiding an extrapolated staircase test as a means of determining the differences between fatigue strength at two or more numbers of cycles. Note that the staircase test was not intended for such an application, but it is still well tailored for fatigue strength estimation at a single specified number of cycles using the methodology of the previous two chapters. With an extrapolated staircase test not a viable option for the characterization of the fatigue strength over a range of cycles, the use of the random fatigue limit (RFL) model was considered for such a purpose. The RFL model, another likelihood-based analysis method, was specifically developed to characterize $S-N$ behavior for fatigue data sets with runouts and thus seems a logical method to investigate for use in evaluating fatigue strength behavior in the ultra high cycle regime [66].

Methodology of the RFL Model

The RFL model was developed by Pascual and Meeker in 1999 [66]. Their method was “motivated by the need to develop and present quantitative fatigue-life information used in the design of jet engines” [66]. Although Pascual and Meeker specifically noted the staircase method as an “efficient and effective way of estimating the median fatigue limit,” they noted that “it is not used to estimate the stress-life relationship” [66]. This section provides a brief overview of the RFL model in order to lay the groundwork for the test design analysis performed in the next section.

Genealogy of the RFL Model

The genealogy of the model traces its lineage through Nelson’s work in 1984 [59]. Nelson modeled the fatigue life of a nickel-based superalloy, creating probabilistic S - N curves incorporating non-constant standard deviation in fatigue life and using censored data (runouts) through a maximum likelihood approach. Standard models for fatigue curves before Nelson’s work typically assumed a lognormal distribution in fatigue life for a given stress level. The standard deviation of this lognormal fatigue life was generally assumed to be constant (i.e., independent of the stress level), as illustrated in Figure 54. Thus, the distribution in fatigue life is the same for both low-cycle and high cycle regimes. However, fatigue-life data have shown generally more scatter in the high cycle (low stress) regime for many materials, leading to Nelson’s analysis.

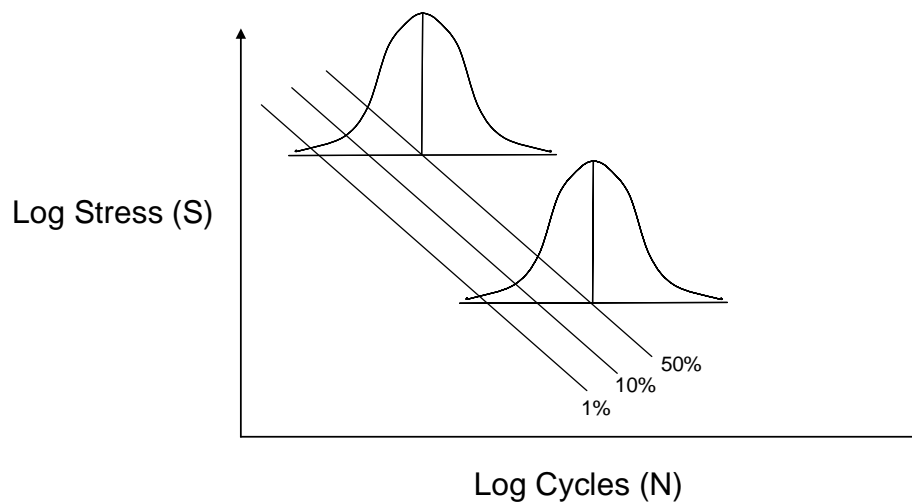


Figure 54. Probabilistic stress-life curve with constant standard deviation in fatigue life as a function of stress.

Nelson developed $S-N$ models using non-constant standard deviations as a function of the stress level. He assumed a linear form for μ , the mean fatigue life, as a function of stress (represented by the 50% line in Figure 54), with a log-linear standard deviation σ of fatigue life, as shown below where a and b are parameter constants used to fit the data, LPS is the log pseudo-stress (pseudo-stress being the effective stress used for the application), and LPS^* is the mean of the log pseudo-stress values [59]:

$$\sigma(S) = e^{\{a + b \cdot (LPS - LPS^*)\}} \quad (40)$$

In addition to the linear μ model, he used a quadratic form for μ , also in conjunction with the log-linear form for σ shown above. The quadratic form was more useful for $S-N$ data which exhibit curvature. An illustrated pictograph of the quadratic μ , non-constant σ , $P-S-N$ model is shown in Figure 55. The fatigue model based on these assumptions provided a generally better fit for the nickel-based superalloy data, although a problem was observed in that some percentiles of the $P-S-N$ curve may be greater (in terms of fatigue life) at intermediate stresses than at low stresses. This situation is of course impossible as fatigue life cannot increase as stress increases, but the increasing standard deviation as stress decreases may cause the modeled curves to “bend back” too far for some data sets (as depicted by Figure 56).

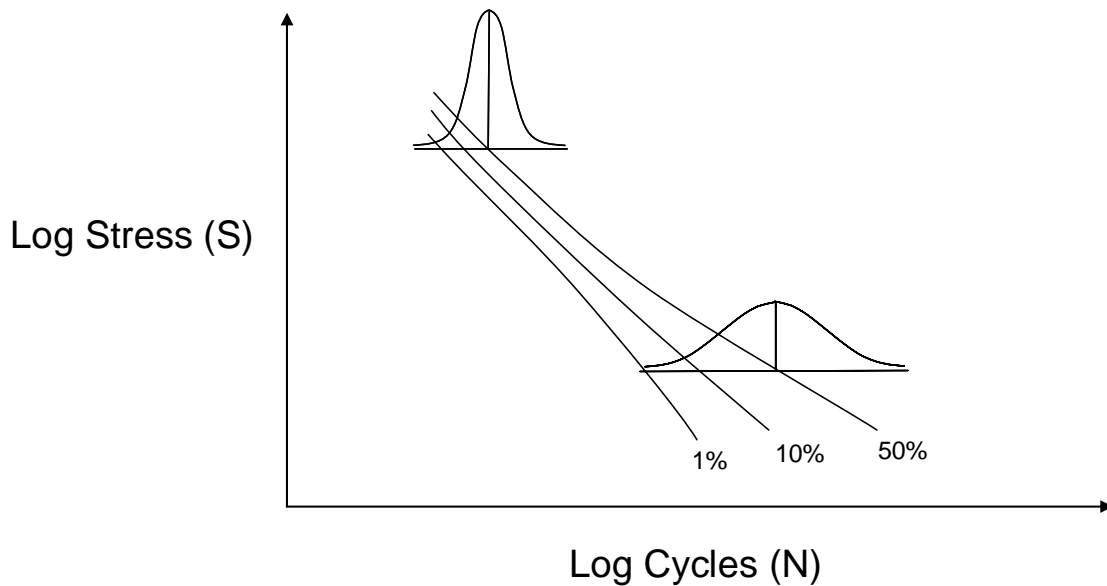


Figure 55. Probabilistic stress-life curve with non-constant standard deviation in fatigue life as a function of stress.

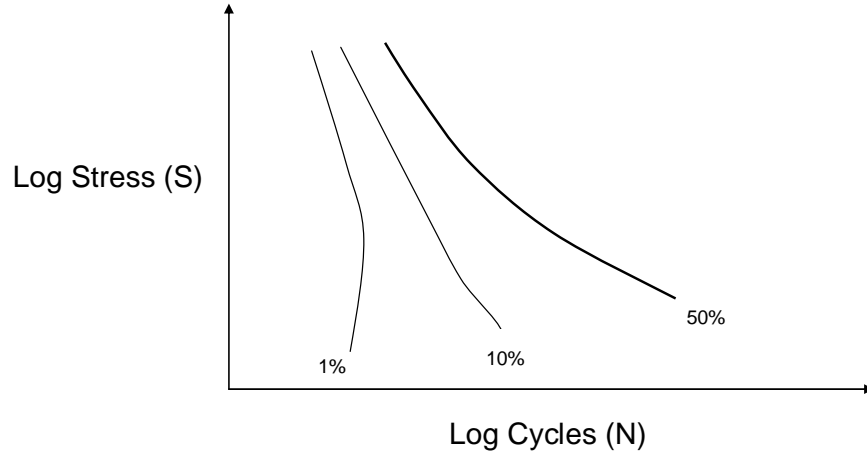


Figure 56. *P-S-N* curve exhibiting a bend-back effect.

The RFL development also built upon the work of Hirose in 1993 [37], who used maximum likelihood methods to estimate the fatigue limit of polyethylene terephthalate (PET) films as well as their mean life under service stress. Hirose fitted a Weibull inverse power relationship that included a fixed fatigue life parameter (constant). In addition, Nelson's text [58] suggested that the fatigue limit may be considered a random parameter, such that specimens have different fatigue limits which make up a "strength distribution." This suggestion would later generate interest in modeling using a random variable for fatigue limit.

Before developing the RFL model, Pascual and Meeker presented a model in 1997 [67] incorporating a constant fatigue limit parameter (similar to Hirose) using non-constant standard deviation of a lognormal fatigue life (similar to Nelson), applying this model to the nickel-based superalloy data of Nelson [59]. The fatigue data is described with x_1, x_2, \dots, x_n denoting pseudo-stress levels of n specimens, and Y_1, Y_2, \dots, Y_n denoting the associated numbers of cycles tested. The fatigue limit is denoted as γ . For $x_i > \gamma$, fatigue life Y_i was modeled as lognormally distributed such that $\log(Y_i)$ was distributed normally with mean $\mu(x_i)$ and standard deviation $\sigma(x_i)$. The form of the mean fatigue life and the standard deviation of fatigue life are thus given as [67]:

$$\mu(x_i) = E[\log(Y_i)] = \beta_0^{[\mu]} + \beta_1^{[\mu]} \log(x_i - \gamma), \quad x_i > \gamma \quad (41)$$

$$\sigma(x_i) = \sqrt{\text{Var}(\log(Y_i))} = \exp[\beta_0^{[\sigma]} + \beta_1^{[\sigma]} \log(x_i)], \quad x_i > \gamma \quad (42)$$

In this fixed fatigue limit model, $\beta_0^{[\mu]}$, $\beta_1^{[\mu]}$, $\beta_0^{[\sigma]}$, $\beta_1^{[\sigma]}$, and γ are unknown parameters to be estimated from the fatigue test data. The β constants are without restrictions, however $\beta_1^{[\sigma]} < 0$ corresponds to a decreasing standard deviation as stress increases (generally the case with most fatigue data). The size of the fatigue limit parameter (γ) determines the amount of curvature in the S - N plot. The plot approaches linearity as γ approaches zero. Large values of γ indicate significant curvature. The use of this fatigue limit parameter allows a “physically appealing alternative” to the quadratic form of Nelson’s model of S - N curvature, according to Pascual and Meeker [67]. This model still may exhibit the “bend back” problem for some data sets as seen with Nelson’s quadratic model, but Pascual and Meeker note that this effect was not observed in the range of the superalloy data, and is minimized compared to the quadratic model. The simulation work performed to evaluate this model used constant interval stress levels with one data point per stress level. The primary shortcoming of the model, as noted by Pascual and Meeker, was the assumption of a constant fatigue limit. By using a single-valued parameter to describe the fatigue limit, the model requires that γ is less than the lowest stress tested such that $\log(x_i - \gamma)$ is defined, regardless of whether the specimen at the lowest stress level failed or not. As Annis and Griffiths noted [11], this model thus caused the γ asymptote to be “so low as to produce an unrealistic material model that had to be continually revised downward to accommodate newer, low stress data.” The incorporation of a variable fatigue limit based on the concept of Nelson’s “strength distribution” led to the refinement of this model, which then became the RFL model proposed in 1999 [66].

RFL Model Formulation

The RFL model accounts for the two main trends observable in most S - N data using engineering materials; namely, the increase in fatigue life scatter as stress level is decreased, and the curvature associated with a fatigue limit. The formulation of the model is shown in Equation 43 using the notation of Annis and Griffiths from 2001 [11] rather than the original notation used by Pascual and Meeker [66], which is less conventional for fatigue analysis. The fatigue life for each specimen tested is denoted by

N and the associated stress level is denoted by S . Fatigue life for specimen i is then modeled by the following equation:

$$\log(N_i) = \beta_0 + \beta_1 \log(S_i - \gamma_i) + \varepsilon_i, \quad S_i > \gamma_i \quad (43)$$

In this equation, β_0 and β_1 are curve coefficients, γ_i is the fatigue limit of specimen i , ε_i is an error term associated with specimen i , and \log denotes natural logarithm. Unlike the constant fatigue limit formulation of Equation 41, the fatigue limit used in Equation 43 is a random variable. Note that the error term ε_i is the random life variable associated with scatter from specimens which have the same value for fatigue limit γ .

The logarithm of the random variable for fatigue limit γ is also a random variable, and if V is defined such that $V = \log(\gamma)$, then Pascual and Meeker assume V to be distributed with probability density function (pdf) given by [66]:

$$f_V(v, \mu_\gamma, \sigma_\gamma) = \frac{1}{\sigma_\gamma} \phi_V\left(\frac{v - \mu_\gamma}{\sigma_\gamma}\right) \quad (44)$$

In this equation, μ_γ and σ_γ are location and scale parameters for the distribution of γ , respectively, and ϕ_V may be the standardized smallest extreme value (sev) or normal pdf. Next, they let $x = \log(S)$ and $W = \log(N)$ so that x and W are the logarithms of the stress and fatigue life, respectively. Then for $V < x$ (i.e., the fatigue limit is less than the stress level tested), they assume that W given V (denoted as $W|V$) has a pdf of the form [66]:

$$f_{W|V}(w, \beta_0, \beta_1, \sigma, x, v) = \frac{1}{\sigma} \phi_{W|V}\left(\frac{w - [\beta_0 + \beta_1 \log(\exp(x) - \exp(v))]}{\sigma}\right) \quad (45)$$

In this equation, $\beta_0 + \beta_1 \log(\exp(x) - \exp(v))$ acts as a location parameter and σ acts as a scale parameter. $\phi_{W|V}$ may be the standardized sev or normal pdf. The marginal pdf of W is then given by [66]:

$$f_W(w, x, \theta) = \int_{-\infty}^x \frac{1}{\sigma \sigma_\gamma} \phi_{W|V}\left(\frac{w - \mu(x, v, \theta)}{\sigma}\right) \phi\left(\frac{v - \mu_\gamma}{\sigma_\gamma}\right) dv \quad (46)$$

where $\theta = (\beta_0, \beta_1, \sigma, \mu_\gamma, \sigma_\gamma)$ and $\mu(x, v, \theta) = \beta_0 + \beta_1 \log(\exp(x) - \exp(v))$. Finally, the marginal cumulative distribution function (cdf) of W (the logarithm of fatigue life) can be given by [66]:

$$F_W(w; x, \theta) = \int_{-\infty}^x \frac{1}{\sigma_\gamma} \Phi_{W|V} \left(\frac{w - \mu(x, v, \theta)}{\sigma} \right) \phi_V \left(\frac{v - \mu_\gamma}{\sigma_\gamma} \right) dv \quad (47)$$

where $\Phi_{W|V}$ is the cdf of W given V . This rather complicated formulation is the statistical representation of the RFL model. Pascual and Meeker note that there are no closed-form solutions for the density and distribution functions of the fatigue life, or specifically, $W = \log(N)$. However, numerical means can be used to evaluate these equations.

It is important to note that there are two random variables in the model described by Equations 43 through 47 which have been specified through a probability distribution. The error term ε which represents the scatter in fatigue life can be adequately modeled by the lognormal distribution for many engineering materials (and thus, the logarithm of fatigue life is normal). Then, the conditional distribution for cycles to failure ($W = \log(N)$) given γ ($V = \log(\gamma)$) will be a lognormal distribution with mean $\beta_0 + \beta_1 \log(S - \gamma)$ and standard deviation σ_ε , such that ε is lognormal(0, σ_ε) [11]. As for the distribution of the random variable γ , the Weibull distribution is an adequate choice for describing the skewed downward (towards lower stress levels) strength distribution of many engineering materials [11]. The Weibull distribution introduces two parameters, namely the location parameter η and the scale parameter β , which correspond to the location and scale parameters μ_γ and σ_γ , respectively, used by Pascual and Meeker. When the RFL model incorporates these assumptions, it includes five total parameters (β_0 , β_1 , σ_ε , η , and β).

Estimating the Model Parameters

Unlike conventional S - N analysis in which all specimens are tested until failure, an ordinary least-squares approach cannot be used to estimate the parameters of the probabilistic S - N model used in the RFL approach. Ordinary least-squares fitting, although popular amongst analysts since its formulation by Gauss and having a well-established place in statistical analysis of fatigue experiments, does not have the capability to account for partial information data points (runouts). In addition, an ordinary least-squares approach assumes constant variance, which of course may not be the case for S - N data [11].

The approach taken by Pascual and Meeker [66] to solve the parametric estimation problem is the use of maximum likelihood methods, as described by Nelson

for data with runouts [58]. First, the likelihood function is defined for data tested at stress levels $x_i = \log(S_i)$ and cycles of $w_i = \log(N_i)$ with n samples. The likelihood is given by:

$$L(\theta) = \prod_{i=1}^n [f_W(w_i; x_i, \theta)]^{\delta_i} [1 - F_W(w_i; x_i, \theta)]^{1-\delta_i}; \quad (48)$$

where

$$\delta_i = \begin{cases} 1 & \text{if } w_i \text{ is a failure} \\ 0 & \text{if } w_i \text{ is a runout.} \end{cases} \quad (49)$$

Thus, the likelihood function $L(\theta)$ can be interpreted as the probability of observing the experimental data given a set of model parameters θ . The set of parameters which maximizes this value of likelihood is taken as the best-fit set of parameters, and thus a curve fit is accomplished. In practice, a log-likelihood function is generally used so that terms may be added rather than multiplied. Maximizing the log-likelihood function produces the same set of parameters as maximizing the likelihood function, and thus either function may be used. The log-likelihood function is shown below:

$$\mathcal{L}(\theta) = \log[L(\theta)] = \sum_{i=1}^n \mathcal{L}_i(\theta) \quad (50)$$

The likelihood problem has already been modeled and solved by Pascual and Meeker for combinations of normal and sev distributions for the logarithm of fatigue life and the logarithm of the fatigue limit [66]. Annis developed a workbook using Microsoft Excel™ which runs on a personal computer (PC) to calculate the likelihood of a set of experimental data given user-controlled parameter settings for an underlying Weibull fatigue limit and lognormal fatigue life [12].

Test Design using the RFL Model

At this point, the inadequacy of the staircase method for analyzing the S - N behavior of a material over a specified range has been presented, along with the introduction and formulation of the RFL model which was specifically developed to analyze the S - N behavior of high cycle fatigue data. There remains one more question to address before an analysis of the HCF behavior of a material can be planned and executed using the RFL model. Namely, the problem of test design has not been

discussed to this point. Pascual and Meeker applied their model to existing data (the nickel-based superalloy data of Nelson) and an analysis of Ti-6Al-4V data using a Smith-Watson-Topper effective stress from the National HCF S&T Program was accomplished by Annis and Griffiths [11]. However, nothing has emerged in the literature since the RFL model's introduction in 1999 which suggests how one should plan a test to prepare for analysis using the RFL model. In fact, Pascual and Meeker addressed this void in their initial RFL paper as an area for further research with the following:

“There are important questions about how to design fatigue experiments under the random fatigue-limit model. Traditional methods will have to be extended to account for the nonlinear relationship between life and stress. Large-sample approximations would provide easy-to-compare evaluations of test plan properties with respect to the efficiency of estimating quantities of interest. Simulation studies require much more computer time but can be conducted to study the small-sample properties of the test plans. This is currently under investigation.” [66]

This section presents a simulation-based analysis of several test design strategies to determine their effectiveness in conjunction with an RFL analysis.

Scoping the Problem

To start an investigation of test design, it is important to set a baseline situation for which the test should be designed to address. For this study, the investigation of the HCF behavior of a beta annealed Ti-6Al-4V alloy was selected as the baseline situation. After completion of the Ti-6Al-4V tests from Chapter IV, a second material was considered for which to demonstrate the modified staircase technique. The choice of material was narrowed down to the beta annealed Ti-6Al-4V alloy as this material was already available and samples for use in the 20-kHz ultrasonic fatigue testing machine could be fabricated relatively quickly and cheaply. The specifics of this alloy are described in more detail in Chapter VI.

Although the initial objective was the demonstration of the modified staircase technique, it was decided that due to the little information available in the literature on beta annealed Ti-6Al-4V high cycle fatigue behavior, a test which yielded more information than just the fatigue strength distribution at a specified number of cycles

should be considered. In discussions with AFIT and AFRL representatives, several questions of interest emerged which included:

- What is the fatigue strength of the alloy in the 10^7 -cycle regime?
- What is the fatigue strength of the alloy in the 10^9 -cycle regime?
- What does the fatigue strength distribution look like in the gigacycle regime?
- Are subsurface crack initiations observable during long-life testing?

Based on these questions, the preferred test strategy must balance two objectives; namely, (1) address the slope of the S - N curve in the very high cycle regime, and (2) address the fatigue strength distribution at 10^9 cycles. These two objectives were the guidelines used in test design analysis. Test limitations included the ability to provide machined specimens, the availability of the 20-kHz fatigue testing apparatus, and the compressed test schedule due to work returning the machine to fully-operational status after a new power supply was installed. Due to these limitations as well as the objective of ensuring results were applicable to small-sample test programs, test designs incorporating 12 specimens were considered.

Three Approaches to Consider

In order to meet the two objectives, three test designs were considered. These three approaches stem from the fatigue strength strategies already in the literature. The first test design was a traditional staircase test starting at 400 MPa with a 20 MPa step and conducted for a 10^9 -cycle maximum duration using 12 specimens. The S - N data points from this test would be used in the RFL model to evaluate the S - N behavior in the very high cycle regime, and the quantal response data could also add information about the fatigue strength distribution at 10^9 cycles. The starting stress and step size are based on the results from the two-phase Ti-6Al-4V tests reported in Chapter IV. Specifically, the starting stress is near the true fatigue limit of the α - β variant, and the step size is on the order of 1.5 times the true standard deviation, which was shown in Chapter III to provide less standard deviation bias. This approach is termed the “traditional staircase.”

The second approach uses a balanced strategy of four stress levels with three specimens each. Again, the initial stress level is set at 400 MPa, and 20 MPa intervals are used. If the first three specimens at 400 MPa all fail to reach 10^9 cycles, then the next

three specimens are tested at 380 MPa. If the first three all survive, then the next three are at 420 MPa. If at least one failure and one survival are observed at 400 MPa, then both 420 MPa and 380 MPa stress levels are used. This process is repeated until four stress levels have been used. The advantage to using four stress levels with three specimens each rather than three stress levels with four specimens each is that the staircase bootstrapping technique may be used on the P - S data from such a test to give an assessment of the standard deviation of the fatigue strength at 10^9 cycles. Recall that the bootstrapping technique proved to be quite effective for four or more stress levels, but was rather ineffective with three-level staircase data. The 20 MPa step may be altered in this strategy if the data suggest the step is too large. For example, if the tests at 400 MPa were all failures and the tests at 380 MPa were all survivals, then the remaining two levels would be between 380 MPa and 400 MPa (i.e., 386.7 MPa and 393.3 MPa). Another example would be if all failures were observed at 400 MPa, two of three failed at 380 MPa, and then all survived at 360 MPa. In this case, the fourth stress level would be taken as 370 MPa. Thus, the step was constant in all cases except those in which the $P(\text{failure}) = 0$ and $P(\text{failure}) = 1$ stress levels are both found with less than three full steps between them. The advantage to changing the step in these cases is to get more data at stress levels with non-unity and non-zero probabilities of failure. The drawback to changing the step is that the staircase bootstrap analysis can no longer be used for those data sets since it requires constant step size. This approach is termed the “balanced strategy.”

The third approach uses an adaptive staircase strategy in which the starting stress is set at 400 MPa and the first step is 20 MPa, again with a runout limit of 10^9 cycles. If a change in result occurs, the step size is halved. The step may be halved up to two times (thus the smallest step possible is 5 MPa). This approach was considered in case the initial step was significantly larger than the true standard deviation in fatigue strength. The S - N data would be analyzed using the RFL model, but a Dixon-Mood analysis of staircase data would not be possible using this variable-step approach. This approach is termed the “adaptive approach.”

The test strategies are illustrated together in Figure 57.

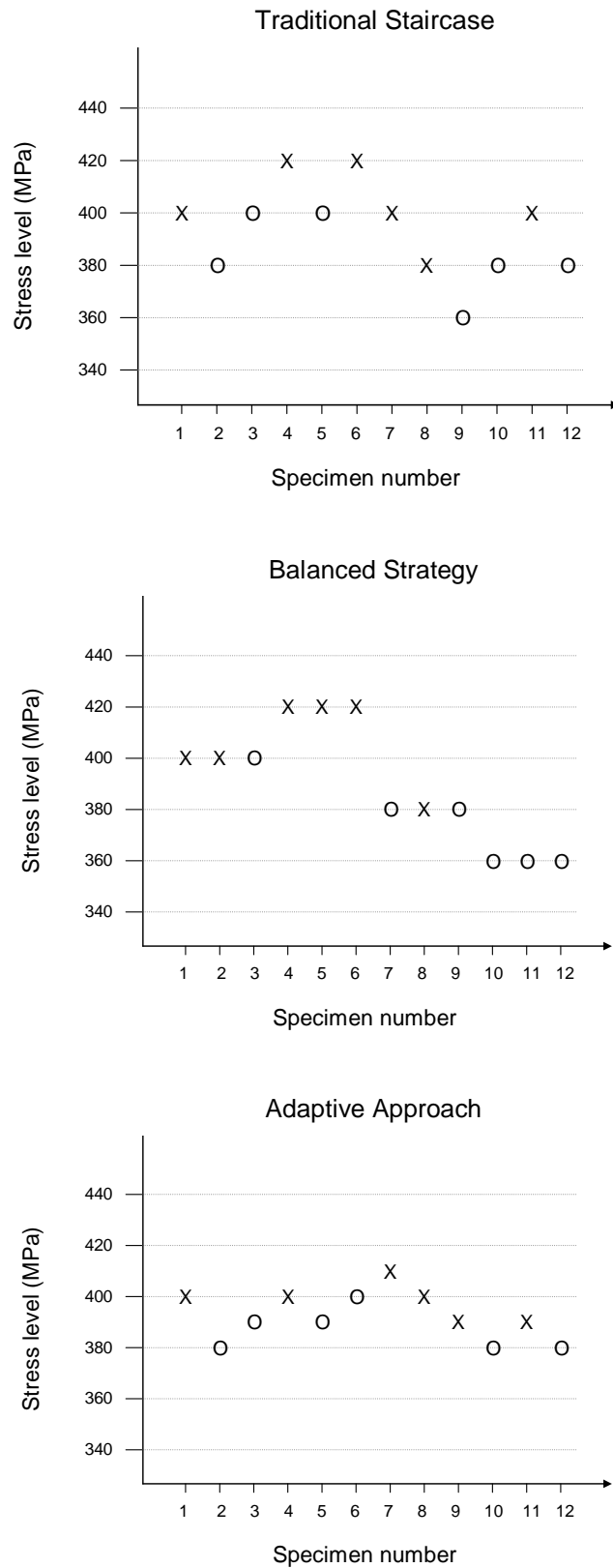


Figure 57. Illustration of test designs used with the RFL model.

Simulation Scenarios

In order to evaluate the three test approaches, three scenarios for underlying material behavior were considered. The curve shapes were created using the Nishijima hyperbolic S - N model as described by Hanaki *et al* [36]. This model allows a convenient way to describe S - N curves with varying degrees of curvature. The model is illustrated pictorially in Figure 58. There are four parameters: the fatigue limit E , a curvature constant C , and two location constants A and B contained in the term $(B - E)/A$ as shown.

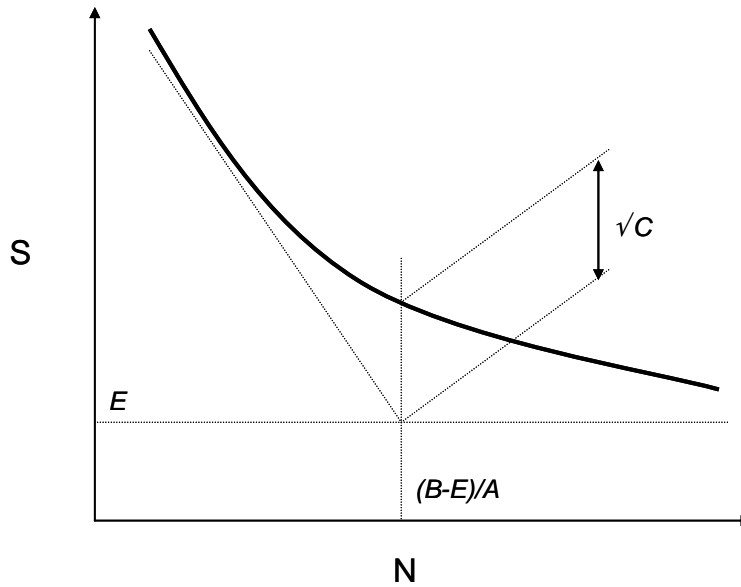


Figure 58. Nishijima S - N model.

The first scenario used an S - N curve with a linear region in the lower-cycle region which gradually transitioned to a fatigue limit between 10^5 and 10^7 cycles. The fatigue strength distribution for this scenario was modeled as normal with increasing standard deviation as the stress decreased. The second scenario assumed curved S - N behavior with less evidence of a fatigue limit before 10^9 cycles. The fatigue strength distribution was again modeled as normal with increasing standard deviation as stress decreased. For the third scenario, a bilinear S - N model was used which exhibited a more distinct transition from the sloped lower-cycle behavior to the flat fatigue-limit behavior starting near 10^6 cycles. Unlike the previous two scenarios, a skewed fatigue strength distribution was used, with the larger percentile differences towards lower stresses. Standard

deviation again increased as stress decreased. The Nishijima model constants for each of these three scenarios are shown in Table 17. The three scenario models are plotted in detail on the following pages (Figure 59 through Figure 64), where the top figure shows the $S-N$ behavior from 10^4 to 10^9 cycles, and the bottom figure zooms in to show the percentile curves in more detail. These three scenarios typify the possible characteristics of $S-N$ behavior for most materials.

Table 17. Nishijima $S-N$ model constants for the three $S-N$ scenarios.

Scenario	Descriptor	A	B	C	E
1	Flat $S-N$ from 10^7 to 10^9	-130	1000	3500	350
2	Sloped $S-N$ from 10^7 to 10^9	-100	960	18000	330
3	Linear $S-N$ with fatigue limit	-120	1100	500	400

Simulation Process

A scenario was analyzed by first generating 12 random numbers (corresponding to 12 specimens). The test protocol was used to select the starting stress (400 MPa in each case), and then the associated $P-S-N$ plot and the first random number were used to determine an associated number of cycles until failure (or runout if greater than 10^9 cycles) for the starting stress. This process was accomplished manually as scenarios were developed with fatigue strength distributions specified rather than fatigue life distributions. Thus, fatigue life sample points were determined using the fine $P-S-N$ plots (Figure 60, Figure 62, and Figure 64) by reading the N corresponding to the stress level and random number (represents percentile point). For example, using the 400 MPa starting stress with the fine $P-S-N$ plot of Figure 60 and a random number of 0.75, one would calculate a fatigue life of 2.0×10^5 cycles. Note that random numbers greater than 0.5 correspond to percentile lines higher than the median (50%) $S-N$ line, while random numbers less than 0.5 correspond to percentile lines lower than the median. The stress level for the next specimen is then selected according to the strategy protocol. Once 12 $S-N$ data points are generated in this manner, the PC-based RFL modeling tool of Annis [12] was used to determine the values of the five RFL parameters which result in the best curve fit (i.e., maximum log-likelihood). Maximizing the log-likelihood using five parameters is a very iterative process and may be quite time consuming in order to account for the significant interaction amongst some of the parameters.

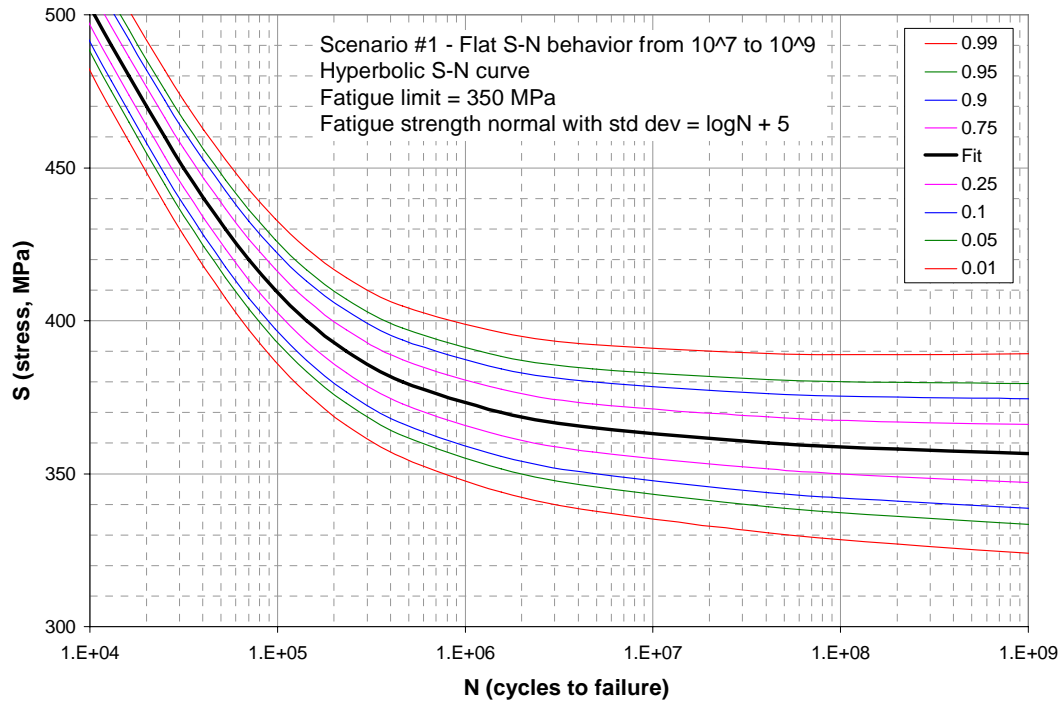


Figure 59. Coarse P - S - N plot of scenario #1 material behavior.

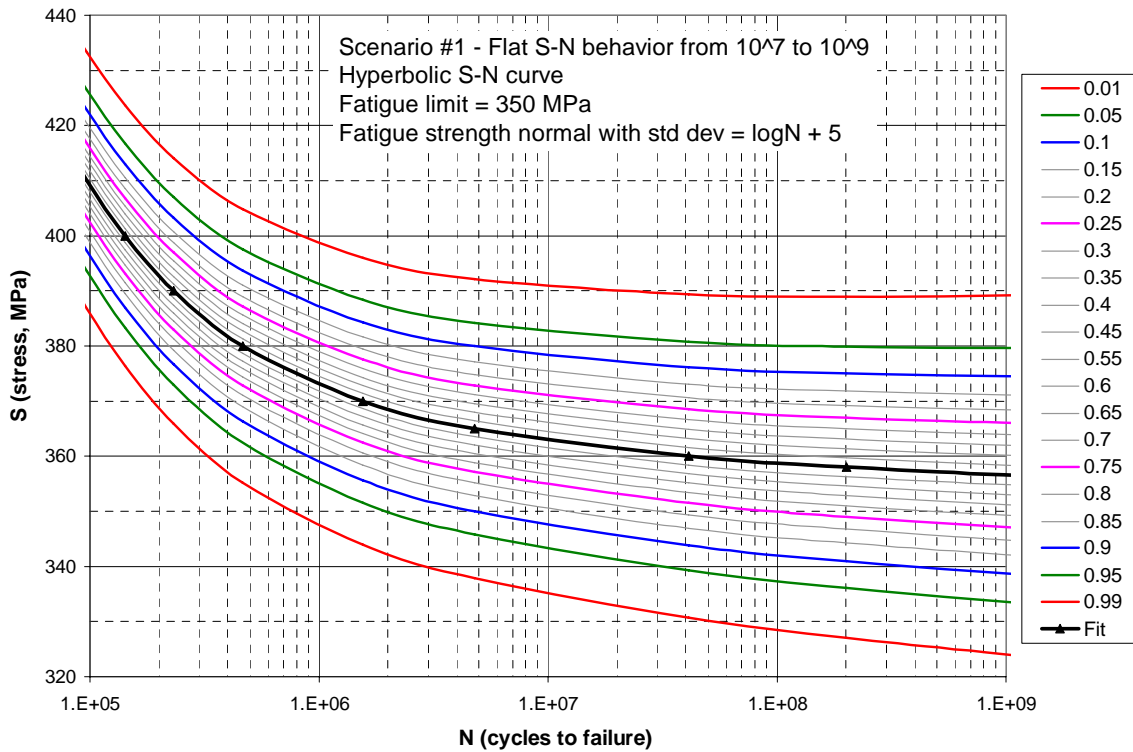


Figure 60. Fine P - S - N plot of scenario #1 material behavior.

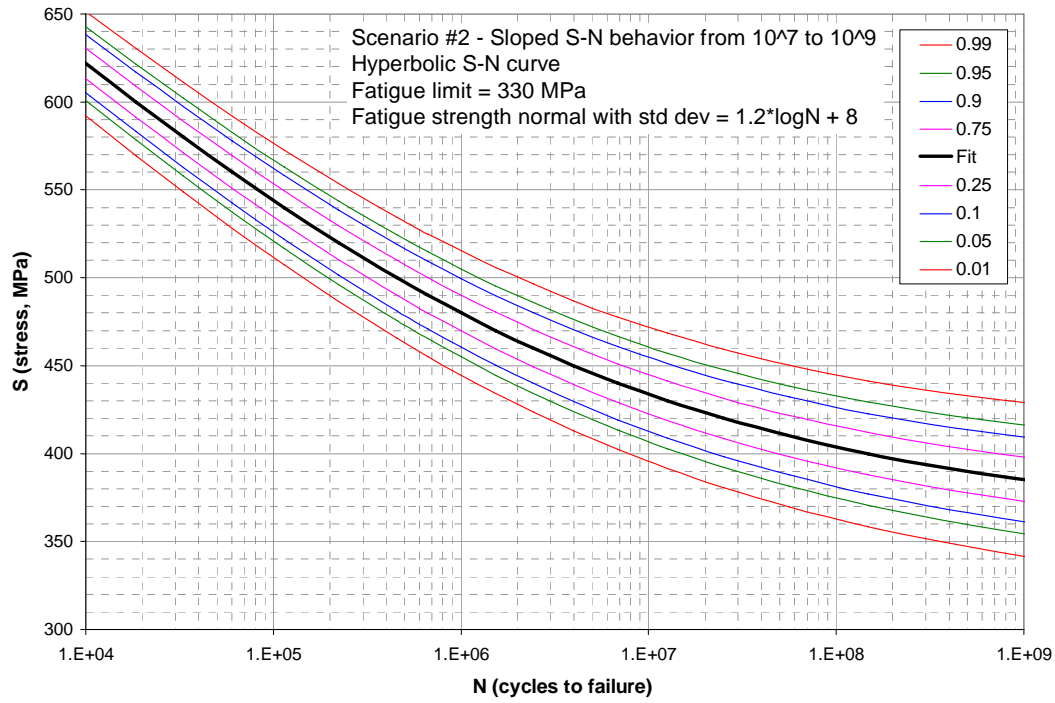


Figure 61. Coarse P - S - N plot of scenario #2 material behavior.

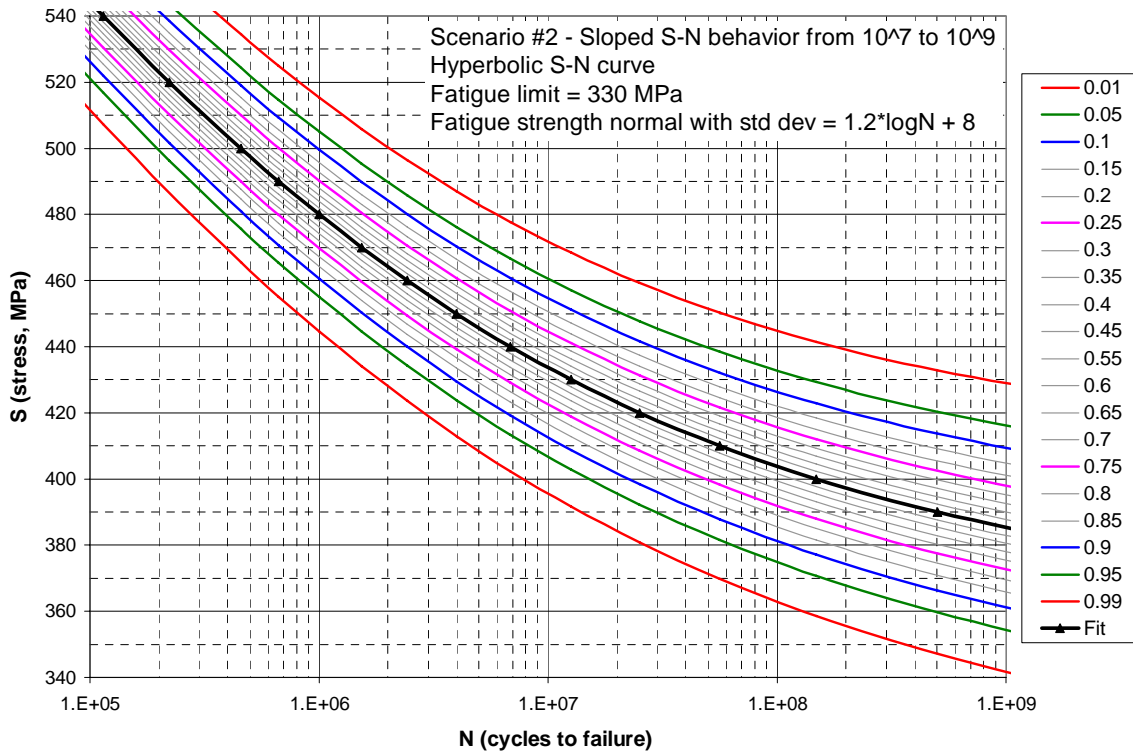


Figure 62. Fine P - S - N plot of scenario #2 material behavior.

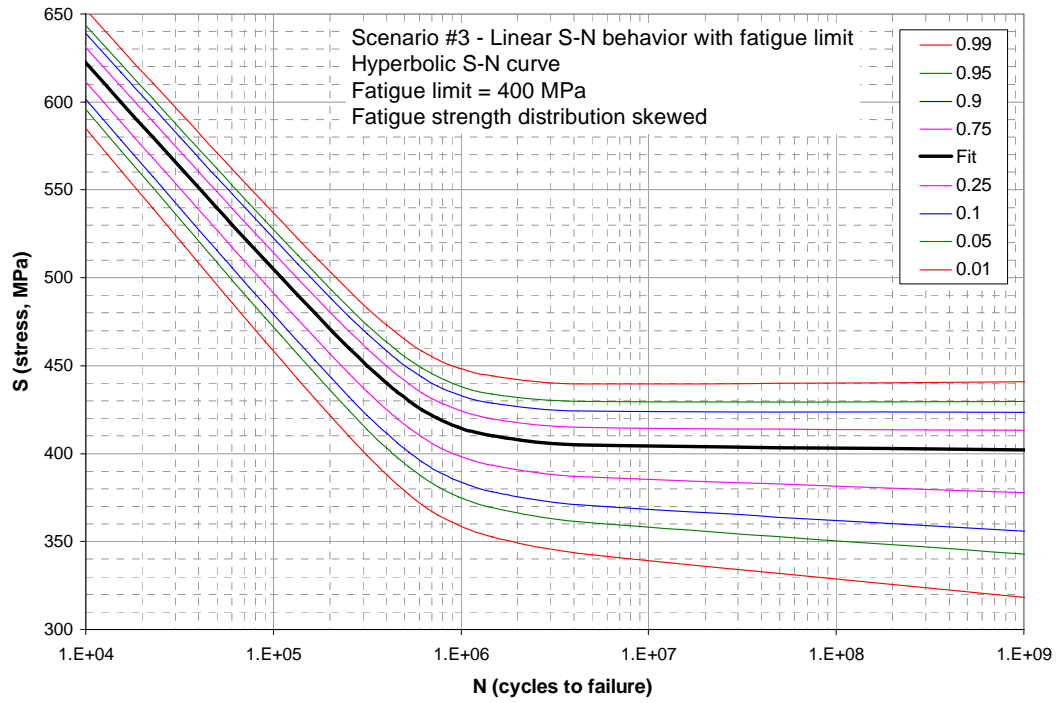


Figure 63. Coarse P - S - N plot of scenario #3 material behavior.

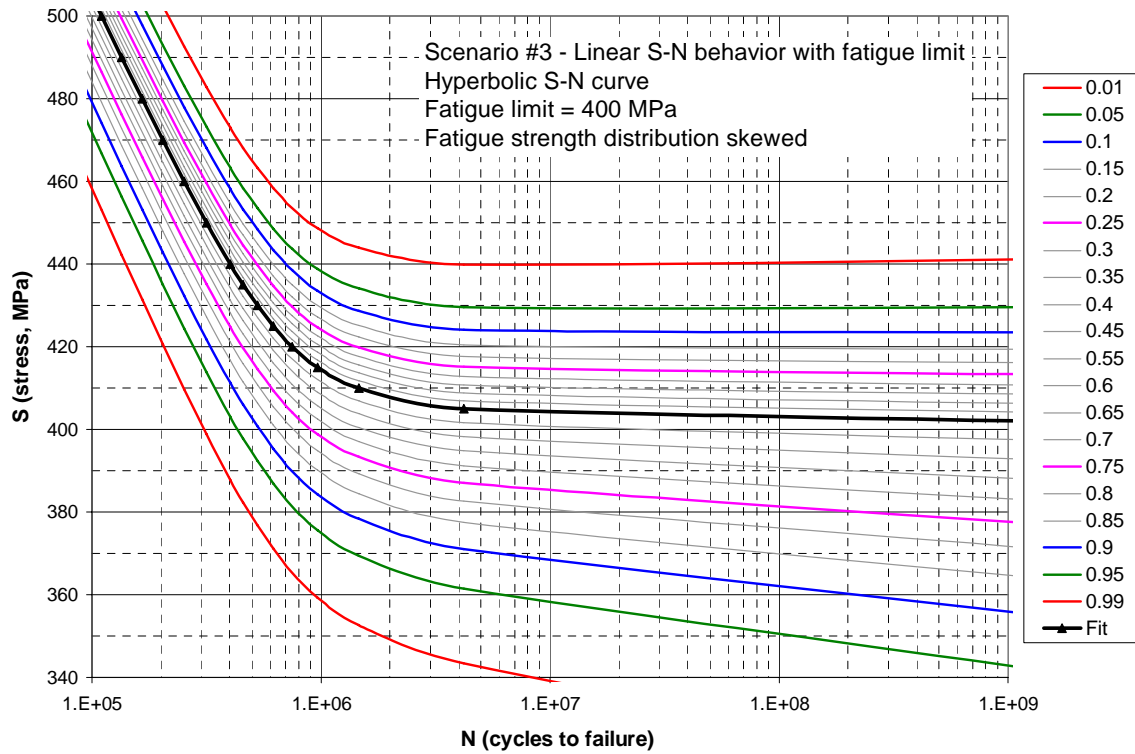


Figure 64. Fine P - S - N plot of scenario #3 material behavior.

The process described thus far represents analyzing one run for one scenario for one test strategy. Using the same random number values (in order to control variance in results), the other two test strategies are then accomplished for the current scenario. Then the process is repeated for the other two scenarios. Then the process is repeated in its entirety for another run with 12 new random number draws. In total, three complete runs were accomplished for each test design strategy and material scenario combination, yielding 27 runs in total (and thus 27 data sets to be analyzed using the RFL model). The simulation process was thus a very manually-intensive process, with each of these 27 runs requiring a manually simulated test followed by an iterative RFL analysis. A sample set of runs are shown in Table 18 for scenario #3 (using Figure 64).

Table 18. A set of sample simulation runs for scenario #3.

Specimen	Random Number	Traditional Staircase		Balanced Strategy		Adaptive Approach	
		S (MPa)	N (cycles)	S (MPa)	N (cycles)	S (MPa)	N (cycles)
1	0.581	400	10^9	400	10^9	400	10^9
2	0.466	420	7.0×10^5	400	2.0×10^8	420	7.0×10^5
3	0.614	400	10^9	400	10^9	410	3.0×10^6
4	0.119	420	3.3×10^5	380	1.4×10^6	400	5.7×10^5
5	0.435	400	7.0×10^6	380	10^9	390	10^9
6	0.352	380	10^9	380	10^9	400	1.7×10^6
7	0.534	400	10^9	420	8.0×10^5	395	10^9
8	0.220	420	4.1×10^5	420	4.1×10^5	400	8.0×10^5
9	0.998	400	10^9	420	10^9	395	10^9
10	0.207	420	8.0×10^5	440	1.6×10^5	390	1.4×10^6
11	0.853	400	10^9	440	6.3×10^5	385	10^9
12	0.253	420	4.4×10^5	440	1.8×10^5	390	2.1×10^6

Simulation Results

For each strategy/scenario combination, three data sets were generated with associated RFL curve fit analyses. In Appendix H, the RFL best-fit P - S - N curves are shown for each strategy/scenario combination. The scales for each scenario are identical, and thus the figures give a visual perspective on the differences in S - N output due to test strategy. For some runs, the random data sets provided quite similar results despite differing test designs, as shown in Figure 65 for a run with the traditional staircase and

balanced strategy. However, the test designs produced quite different RFL model results in other cases, with the extreme case shown in Figure 66.

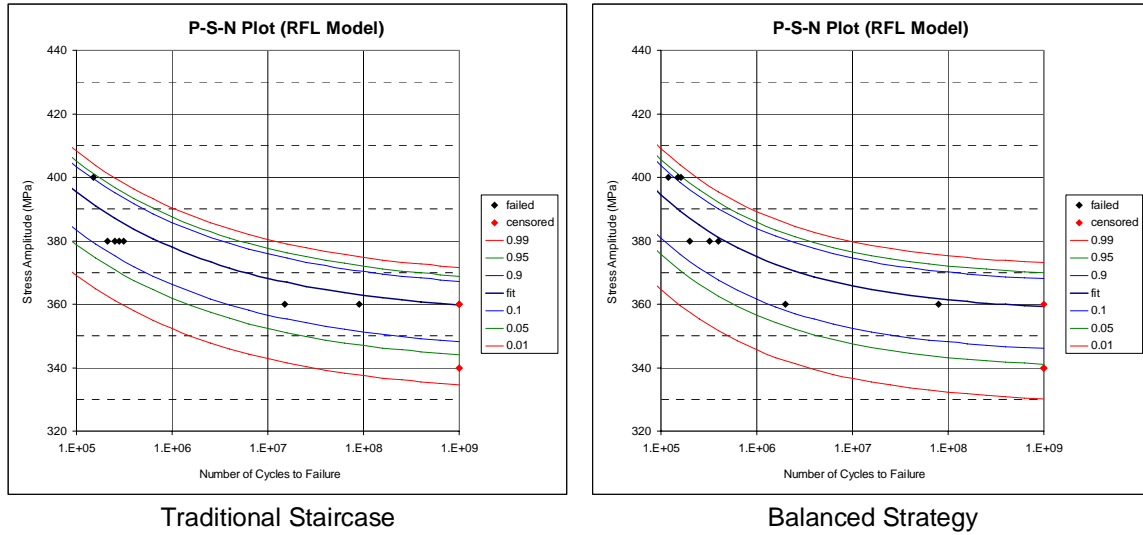


Figure 65. RFL analysis for scenario #1 using the traditional staircase and balanced strategy for random number set #1.

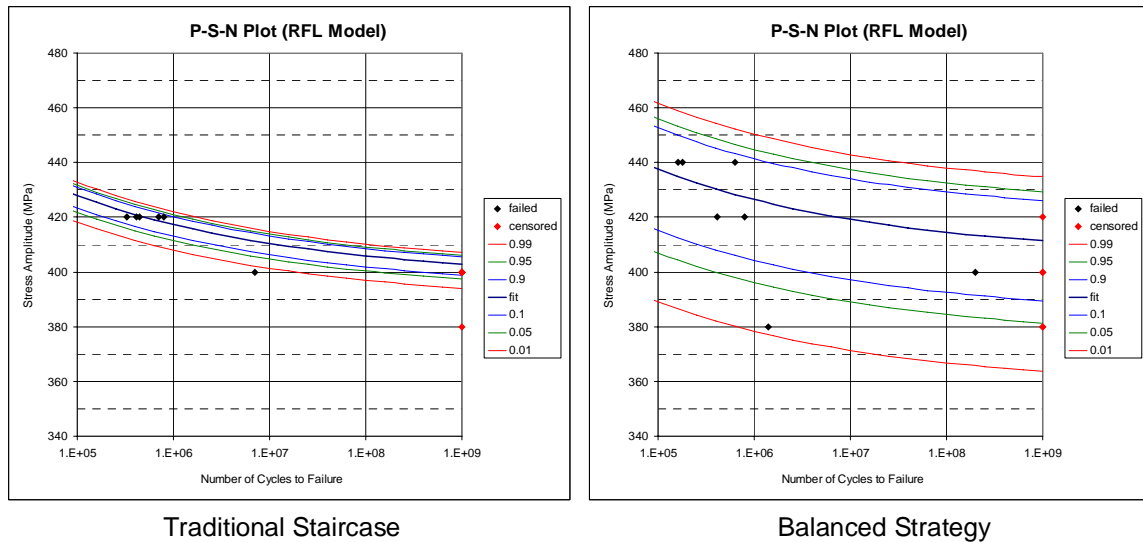


Figure 66. RFL analysis for scenario #3 using the traditional staircase and balanced strategy and random number set #1.

For each $P-S-N$ plot made using the RFL model, four statistics of interest were calculated: (1) the median fatigue strength at 10^7 cycles, (2) the median fatigue strength at 10^9 cycles, (3) the 10th-percentile fatigue strength at 10^7 cycles, and (4) the 10th-percentile fatigue strength at 10^9 cycles. These four statistics give a fair perspective on

how the test design characterizes $S-N$ behavior in the very high cycle regime. Table 19 summarizes the very high cycle statistics of interest calculated from the RFL best-fit curves for each strategy/scenario combination, with the mean value of fatigue strength over the three runs shown for each statistic.

Table 19. Summary of simulated results for each strategy/scenario combination.

Scenario #1 – Relatively flat $S-N$ behavior from 10^7 to 10^9				
Method	FS50@ 10^7	FS50@ 10^9	FS10@ 10^7	FS10@ 10^9
Staircase Mean	371.3	363.7	357.7	349.7
Balanced Mean	370.3	363.3	356.3	349.7
Adaptive Mean	364.0	355.3	346.0	337.7
True Value	363	357	347	339
Scenario #2 – Sloped $S-N$ behavior from 10^7 to 10^9				
Method	FS50@ 10^7	FS50@ 10^9	FS10@ 10^7	FS10@ 10^9
Staircase Mean	467.0	381.0	442.0	357.3
Balanced Mean	446.7	384.3	425.0	363.7
Adaptive Mean	464.3	384.3	436.0	357.0
True Value	434	385	412	361
Scenario #3 – Linear $S-N$ behavior with fatigue limit				
Method	FS50@ 10^7	FS50@ 10^9	FS10@ 10^7	FS10@ 10^9
Staircase Mean	430.3	404.3	419.3	389.0
Balanced Mean	427.6	403.0	410.3	385.0
Adaptive Mean	420.3	399.3	408.0	386.3
True Value	404	402	369	356
Note: FS50 = median fatigue strength, FS10 = 10^{th} -percentile fatigue strength				

Based on the simulation results, several observations can be made. First, the adaptive approach provided the best fit for scenarios #1 and #3 (as shown in Figure 67 and Figure 68, respectively). Both these scenarios incorporated a distinct fatigue limit beginning prior to 10^9 cycles. However, note that the traditional staircase and the balanced strategy were very similar for these scenarios in an average sense, with the balanced strategy providing a slightly better fit. Note that none of the strategies were particularly effective in characterizing the flat $S-N$ behavior in the 10^7 to 10^9 regime for scenario #3. The difference between 10^7 -cycle and 10^9 -cycle mean fatigue strengths ranged from 21 to 26 MPa, despite the true difference of just 2 MPa. Thus, the RFL model using any of the strategies was very ineffective in characterizing the bilinear $S-N$ model with little curvature in transition from sloped to flat behavior.

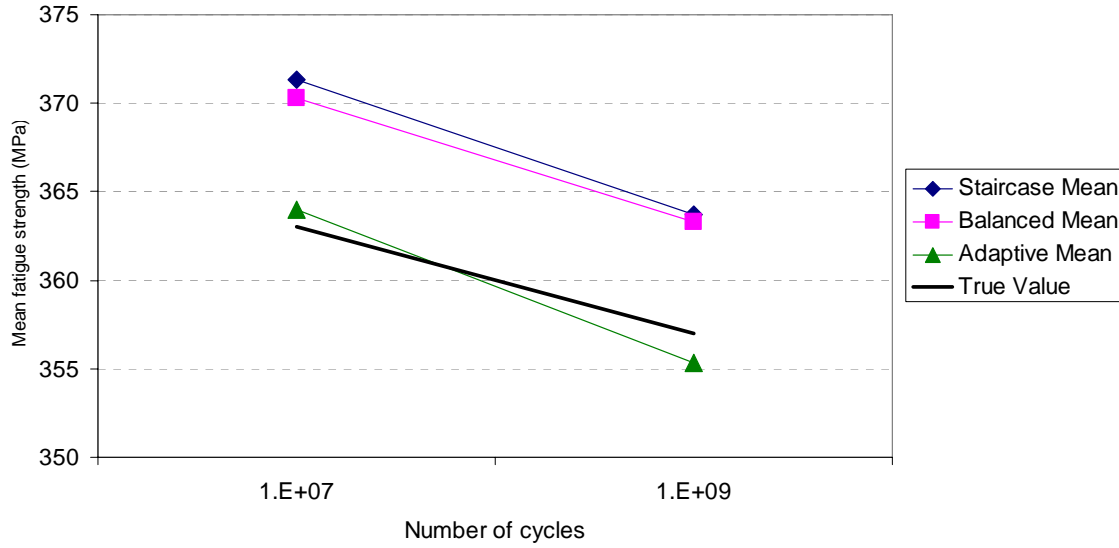


Figure 67. Comparison of mean fatigue strength results for scenario #1.

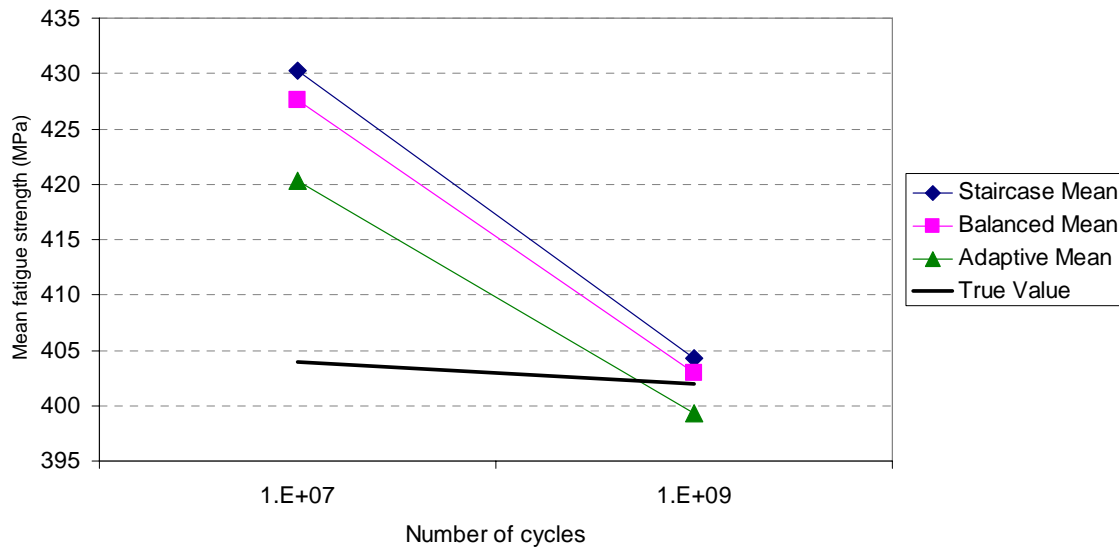


Figure 68. Comparison of mean fatigue strength results for scenario #3.

For the second scenario, in which there was significantly sloped $S-N$ behavior in the very high cycle regime, the balanced strategy performed better on average (shown by Figure 69). The balanced strategy showed a difference between 10^7 -cycle and 10^9 -cycle mean fatigue strengths equal to 62 MPa, compared to the true 49 MPa difference, while the two staircase-based methods were 80-86 MPa of difference. Once again, the RFL

model using any of the test designs resulted in more slope in the very high cycle regime than actually existed.

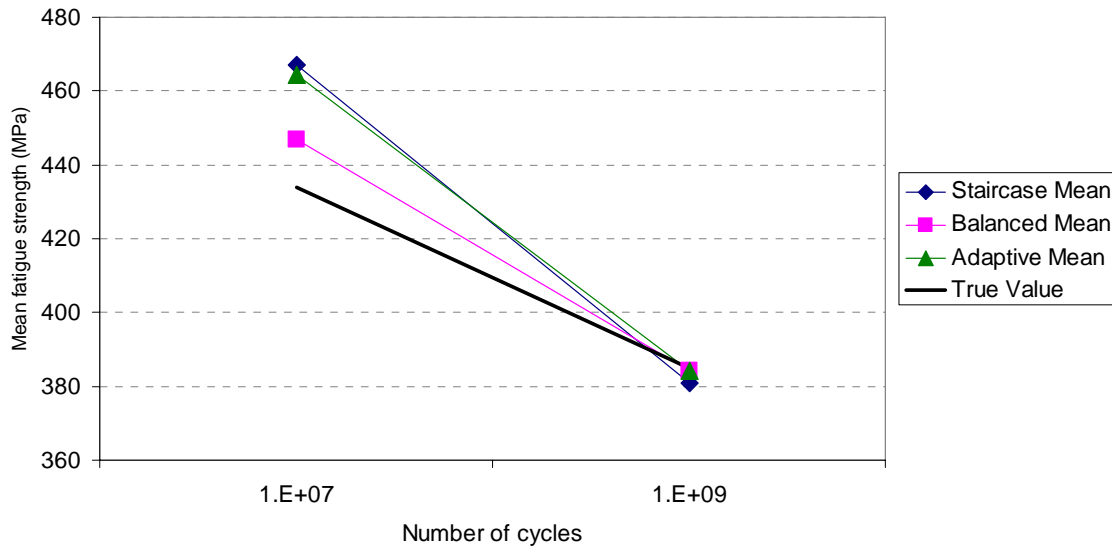


Figure 69. Comparison of mean fatigue strength results for scenario #2.

Based on this set of simulation data, the adaptive approach appears to do a better job of characterizing S - N behavior in the very high cycle regime when the curve is less sloped over this area, while the balanced strategy does a slightly better job when the curve is more sloped. These results are based on a small set of simulations, however, and should not be considered definitive just yet. Note that none of the test strategies using the RFL model did a very good job of representing a very flat region using a 12-specimen test. Additionally, the results of this analysis show that there is little observable difference in RFL results (for the very high cycle regime) for cases in which data sets are generated from a staircase approach or a balanced approach. This finding is significant in that one can choose either a staircase or probit-type strategy without affecting the RFL results too greatly. The adaptive approach, although it appeared to fit better in some cases, does not allow an alternative analysis of fatigue strength distribution at the maximum number of cycles as does a staircase or balanced approach, which may use Dixon-Mood (with bootstrapping) or probit analysis as a secondary means to characterize the fatigue strength distribution. In addition, the adaptive approach is more complicated in terms of test planning than the staircase or balanced approaches. It is also quite

possible that apparent advantages to the adaptive approach are simply due to the fact that some step sizes in this approach were smaller, and thus more data were grouped closer to the mean and this allowed slightly better modeling of flatter $S-N$ behavior. For these reasons, the balanced strategy was recommended for use on the second material.

Summary

In this chapter, the problems inherent with the use of the staircase method for characterizing the fatigue strength over a range of cycles were discussed. The RFL model was introduced for this application, and an overview of its formulation was presented. The problem of test design using the RFL model was addressed through a simulation-based study. The results of this study suggest that use of an adaptive staircase approach may provide better characterization of fatigue behavior in the very high cycle regime for materials which exhibit a definitive fatigue limit. However, the adaptive strategy does not allow an alternative means of characterizing the fatigue strength distribution. Since the balanced 4-level strategy performed as well or better than the traditional staircase approach for each simulation scenario, it may provide a preferred means of RFL test planning with small sample sizes. This finding is really the key result of this analysis—namely, that there was no obvious disadvantage to the use of the balanced approach compared to the traditional staircase. Thus, one could perform a balanced strategy with four fixed stress levels with three specimens each and use the $S-N$ data in the RFL model and the $P-S$ data in a staircase bootstrap, thus ensuring four stress levels of data. Thus, the balanced approach was recommended for use with the small-sample beta annealed Ti-6Al-4V fatigue tests. The results of this analysis show that further investigation of an adaptive approach to staircase testing may be of future benefit. The beta annealed Ti-6Al-4V tests are discussed in detail in the next chapter.

VI. ANALYSIS OF BETA ANNEALED Ti-6Al-4V TEST DATA USING RFL MODELING AND ALTERNATIVE MEANS

In this chapter, the investigation of a beta annealed Ti-6Al-4V alloy is detailed. In the first section, a description of the fatigue experiment is presented, in which a 20-kHz ultrasonic fatigue testing machine was used for tests up to 10^9 cycles. Next, the analysis of experimental data using the RFL model is detailed. Deficiencies of the model are discussed. Finally, alternative means of characterizing the stress-life behavior are presented. These alternative means include a bilinear S - N model with horizontal fatigue limit and a Nishijima S - N model, both using an extreme value distribution to represent the scatter in fatigue strength at a given number of cycles.

Experiment Objective

The goal of the beta annealed Ti-6Al-4V tests was to determine the S - N behavior of the titanium alloy in the HCF regime. In addition to estimating the shape of the S - N curve, a characterization of the fatigue strength distribution was sought in order to develop a probabilistic S - N curve from which probabilities of failure for given cycle times could be determined for given stress levels. Use of the beta annealed titanium alloy allowed an investigation of a material for which there are relatively few HCF data in the literature. The experiment thus provides a real-world scenario in which S - N behavior is sought for a material with few existing data using a small-sample testing program.

Experimental Background

This section provides an overview of the beta annealed Ti-6Al-4V experiments.

Material Microstructure

In Chapter II, an overview of the heat treatment of titanium alloys was presented. Chapter IV discussed the specific processing for the Ti-6Al-4V test material. For this next series of tests, the microstructure of this titanium alloy was altered in order to create the beta annealed microstructure. Processing included a 10-minute heat treatment at 1005°C, followed by a rapid quenching at 100°C -130°C per minute, and then a final

annealing at 705°C for two hours [4]. The resulting microstructure is one of lamellar design, as shown by the micrograph in Figure 70.

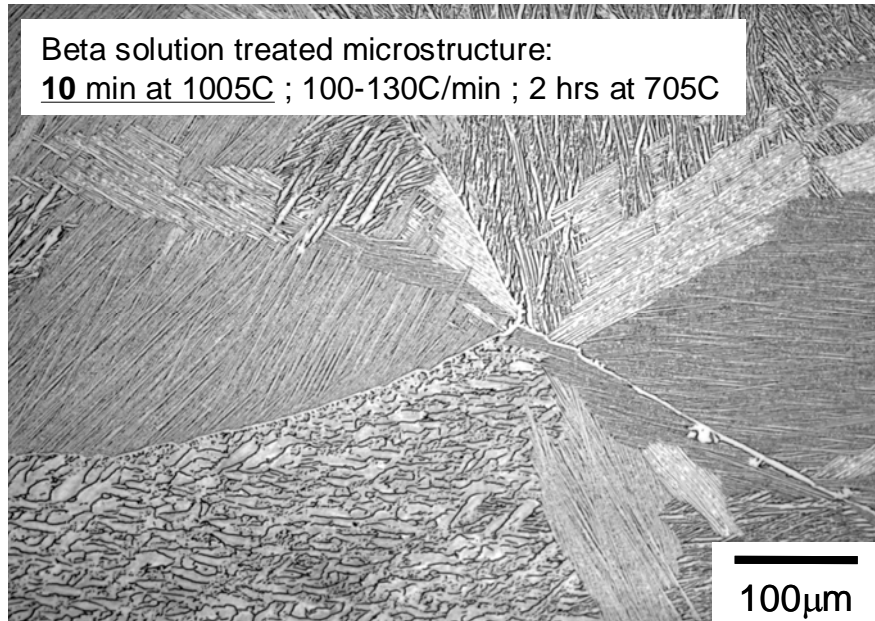


Figure 70. Microstructure for beta annealed Ti-6Al-4V specimens as used in 20-kHz fatigue testing (provided by AFRL/MLLM).

A comparison between the bimodal (α - β) and lamellar (beta annealed) Ti-6Al-4V microstructures was also conducted by Nalla *et al* [57]. Their experiments incorporated materials processing very similar to the AFRL/MLLM processing. The bimodal material for their experiments was solution heat treated for 1 hour at 925°C and stabilized at 700°C for 2 hours [57], as compared to the 1 hour heat treatment at 932°C and stabilization for 2 hours at 705°C for the AFRL/MLLM material. For the beta annealed material, the Nalla *et al* experiments used heat treatment at 1005°C for 10-30 minutes, followed by a rapid quench at 100°C per minute in helium gas, then a 2-hour stabilization at 700°C [57], also quite similar to the AFRL/MLLM processing. Micrographs of the microstructures used in their tests are shown in Figure 71. These pictures show the significant difference in the grain structures of the bimodal (α - β) and lamellar (beta annealed) Ti-6Al-4V.

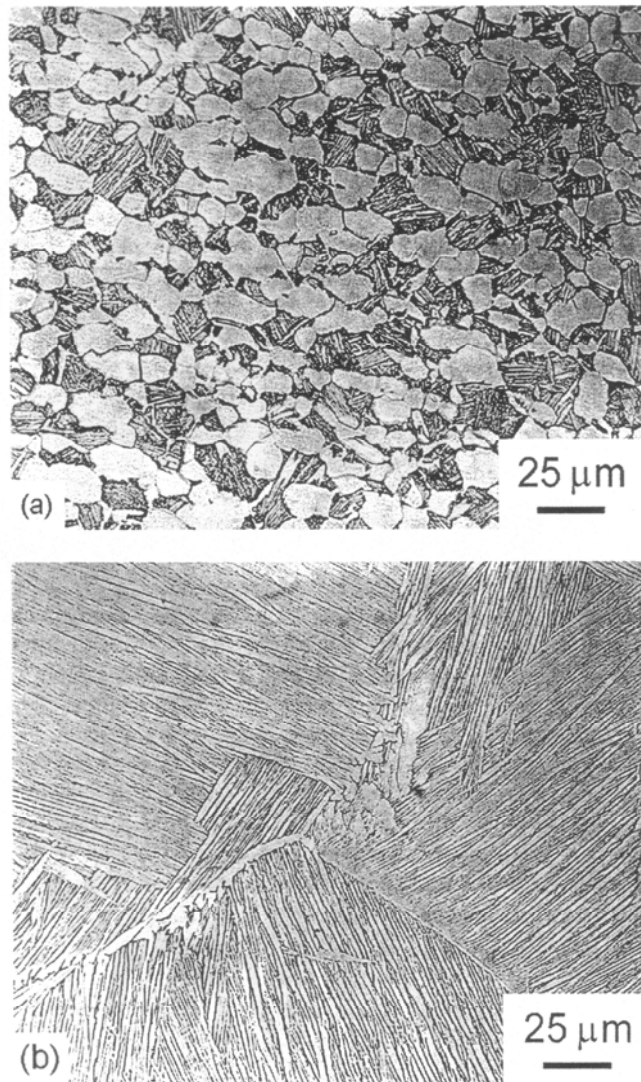


Figure 71. Comparison of microstructure for (a) an α - β (solution treated and overaged, STOA) Ti-6Al-4V alloy, and (b) a lamellar beta annealed Ti-6Al-4V alloy (from Nalla *et al* [57]).

Test Machine and Specimen Design

The same equipment used for the α - β Ti-6Al-4V tests described in Chapter IV was used for the beta annealed tests (see Figure 40). Thus, these tests were all conducted at a frequency of 20 kHz. Cylindrical specimens with a 20-kHz natural frequency similar to those used for the α - β Ti-6Al-4V tests were machined and used (see Figure 41).

Test Strategy

Based on the results of Chapter V, a balanced test strategy was chosen to investigate the S - N behavior of the beta annealed Ti-6Al-4V alloy. The experiment was limited to 12 specimens based on specimen availability, testing machine availability, and schedule constraints. This strategy incorporated four stress levels with three specimens tested at each level. The starting stress was set at 400 MPa, as this value was near the fatigue strength of the α - β Ti-6Al-4V at 10^9 cycles (actually 406.4 MPa as shown in Chapter IV). Thus, the fatigue strength of the bimodal α - β Ti-6Al-4V was used as an initial estimate for the beta annealed variant. The experiments of Nalla *et al* indicated that differences between the HCF behavior of the two Ti-6Al-4V variants are not large [57], and thus use of the bimodal fatigue strength characteristics as initial estimates for the lamellar material was justified. Interval spacing between stress levels was set at 20 MPa, which is approximately 1.6 times the standard deviation estimate for the α - β variant. This spacing was intended to provide at least two stress levels with non-zero or non-unity probabilities of failure. If the three specimens tested at 400 MPa resulted in all failures, then 400 MPa would be used as the upper limit for stress settings, and the next series of tests would be run at 380 MPa. If the 400 MPa tests were all runouts, then this stress level would be the lower limit and the next series of tests would be conducted at 420 MPa. If the 400 MPa tests resulted in at least one failure and one survival, then tests would be accomplished at both 380 MPa and 420 MPa. Tests would be conducted in this manner until four stress levels were tested with three specimens each. All tests were conducted under fully-reversed ($R = -1$) loading.

Experimental Data

The results of the beta annealed Ti-6Al-4V tests are shown in Table 20. The P - S data can be summarized by the vectors $\mathbf{P} = (0.3333, 0.3333, 0.6667, 1.0)$ and $\mathbf{S} = (360, 380, 400, 420)$ where P_i is the probability of failure at stress S_i measured in MPa. Indeed, more than two stress levels were tested with non-zero or non-unity probabilities of failure; these levels correspond to the tests at 360 MPa, 380 MPa, and 400 MPa. The stress-life (S - N) data for these tests are plotted in Figure 72, where the numbers in parentheses indicate the number of multiple runouts.

Table 20. Fatigue data for beta annealed Ti-6Al-4V tests at $R = -1$.

Specimen	Stress (MPa)	10^9 Result	Cycles
1	400	Failure	5.967E+05
2	400	Survival	1.000E+09
3	400	Failure	3.399E+05
4	420	Failure	2.483E+05
5	420	Failure	3.316E+05
6	420	Failure	4.026E+05
7	380	Failure	5.807E+05
8	380	Survival	1.000E+09
9	380	Survival	1.000E+09
10	360	Failure	4.755E+05
11	360	Survival	1.000E+09
12	360	Survival	1.000E+09

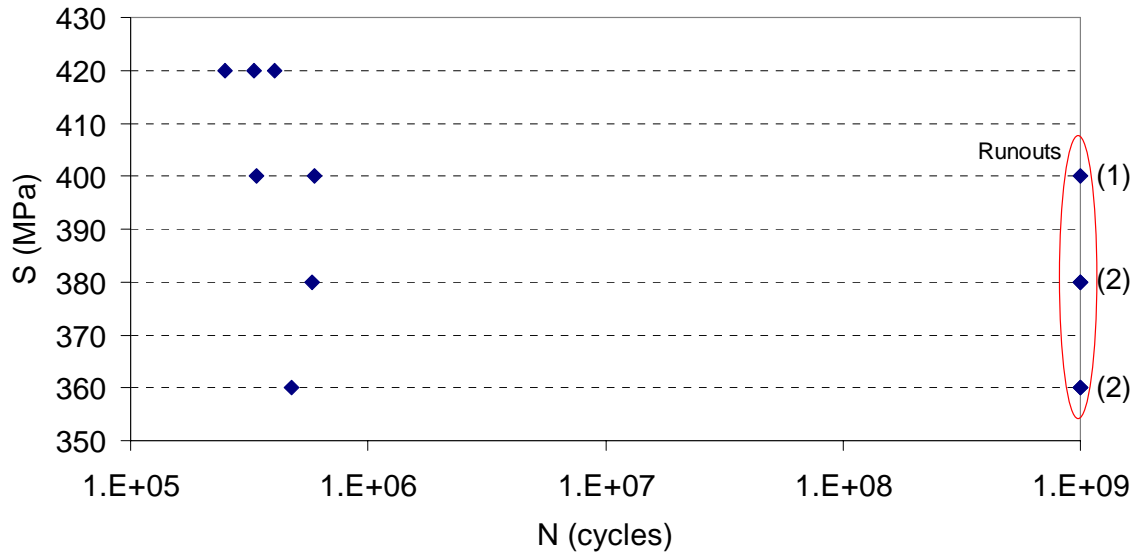


Figure 72. Stress-life data for beta annealed Ti-6Al-4V tests at $R = -1$.

This S - N data can be plotted along with the 68 data points from the α - β Ti-6Al-4V tests, as shown in Figure 73 (where “censored” implies a runout). This plot suggests that the beta annealed alloy has similar HCF properties to the bimodal alloy, with possibly slightly lower fatigue strength. Use of the α - β Ti-6Al-4V fatigue strength characteristics as initial estimates for the beta annealed tests appears justified.

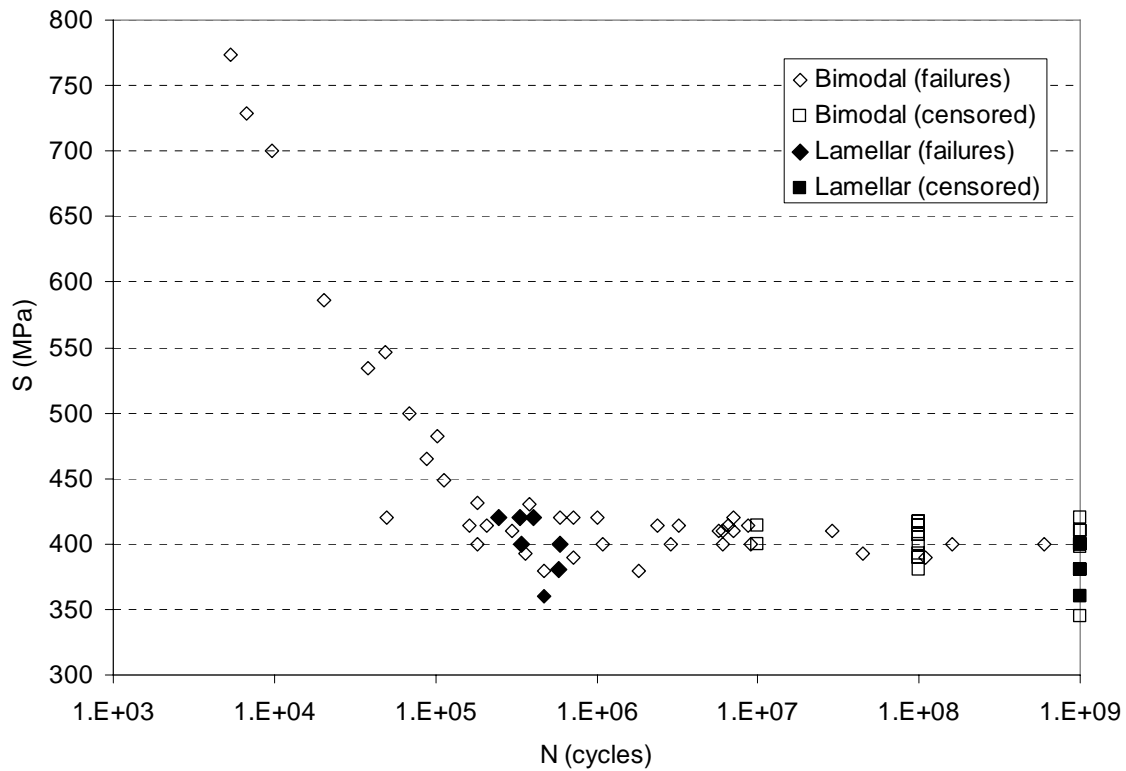


Figure 73. Stress-life data for Ti-6Al-4V α - β (bimodal) and beta annealed (lamellar) microstructures at $R = -1$.

Analysis with the RFL Model

The RFL model described in Chapter V was used to analyze the 12 S - N data points for the beta annealed Ti-6Al-4V tests. The PC-based RFL analysis tool of Annis [12] was used to determine the set of RFL parameters which provided the best fit to the beta annealed data. This best fit is shown in Figure 74. For this fit, the RFL model parameters are shown in Table 21. At first glance, the RFL model does not appear to give a very good fit to this data. It looks as though the S - N data should have a highly sloped S - N curve in the 10^5 to 10^6 regime with a horizontal fatigue limit which produces runouts to 10^9 cycles. This type of underlying fatigue behavior produce S - N data very similar to the actual beta annealed data. Recall the scenario #3 from Chapter V, in which a linear S - N curve with horizontal fatigue limit was modeled. One of the data sets for this scenario is shown in Figure 75 (simulated in Chapter V) for a test strategy with four stress levels using three specimens each. The simulated data set shows a similar pattern

to the experimental data set (Figure 72), lending credibility to the hypothesis that the true behavior of the beta annealed Ti-6Al-4V data more closely resembles scenario #3 rather than the curve shape depicted by the RFL analysis. Looking at the α - β Ti-6Al-4V data shown in Figure 73, it is clear that the bimodal variant of the alloy displays a sloped linear S - N curve followed by a flat fatigue limit region, rather than a gently sweeping shape similar to that shown in Figure 74. Thus, it appears that the beta annealed data are not well represented by the RFL model in its current form.

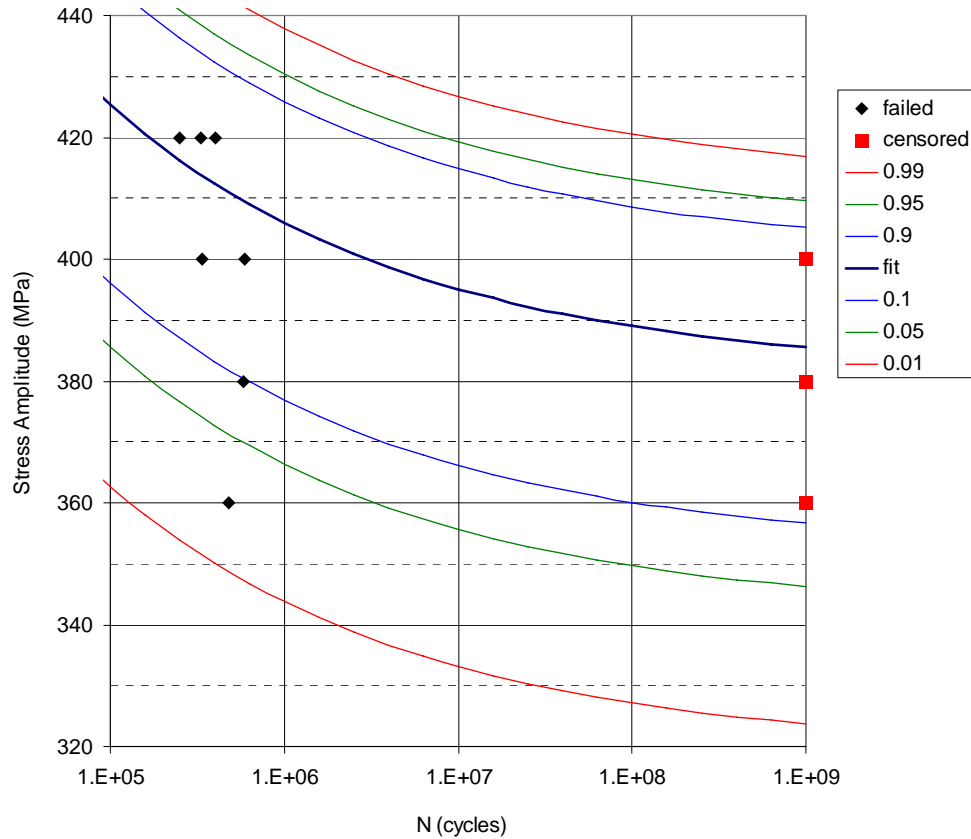


Figure 74. Analysis of beta annealed Ti-6Al-4V data using the RFL model.

Table 21. RFL model parameters for best fit to beta annealed Ti-6Al-4V data.

Parameter	Descriptor	Value
β_0	S - N curve coefficient	5.904
β_1	S - N curve coefficient	-3.988
σ_ε	Standard deviation in lognormal fatigue life	0.04
η	Weibull location parameter for fatigue limit	387
β	Weibull scale parameter for fatigue limit	24

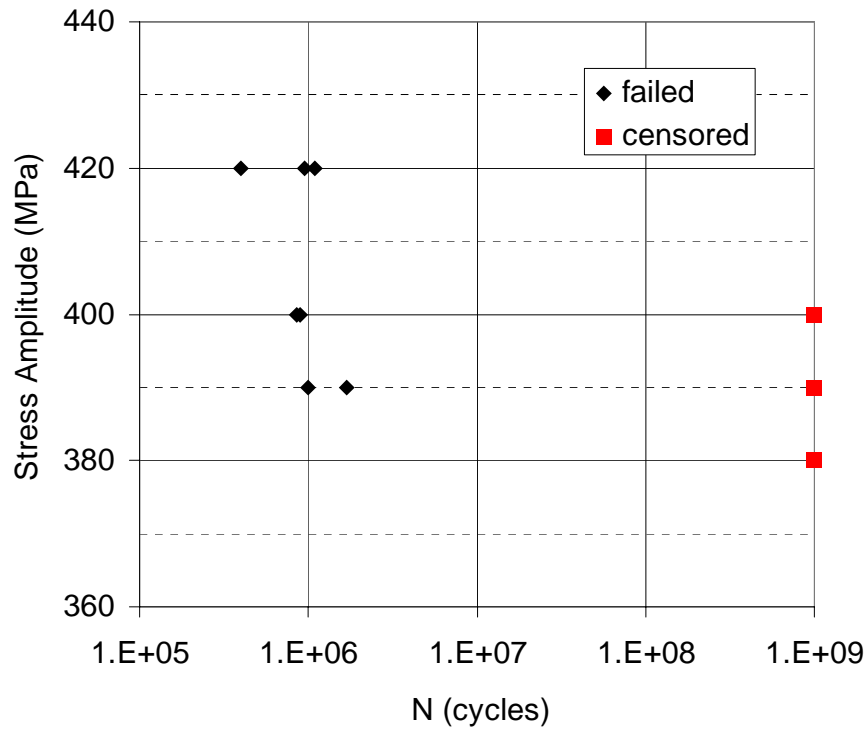


Figure 75. Simulated data set for a linear S - N curve with horizontal fatigue limit.

RFL Model Applied to α - β Ti-6Al-4V Data

Based on the analysis of the beta annealed Ti-6Al-4V data, the RFL model reveals a gently sweeping best-fit S - N curve. There was some question whether this result was a function of the model's inability to adequately fit a curve with a sharp "knee," or whether the best-fit curve just happened to be a gently sweeping shape. In order to determine if this seemingly poor fit was a limitation of the model itself (more specifically, a limitation of the assumptions used by the model in its current form), the RFL model was applied to the 68 α - β Ti-6Al-4V data points to check its adequacy using a larger data set with an obvious knee-shaped S - N curve. The results of this analysis are shown in Figure 76 and Table 22. Based on this analysis, the RFL model seems to do a very good job modeling the highly sloped region in the low-cycle regime, as well as the flat region in the very high cycle regime. This good fit is predicated on the existence of a large number of data points in these regimes for the larger data set (68 in this case). However, the middle of the curve where the sloped region transitions to a flat region is still not well represented by the model, which cannot account for such a discontinuous change in slope.

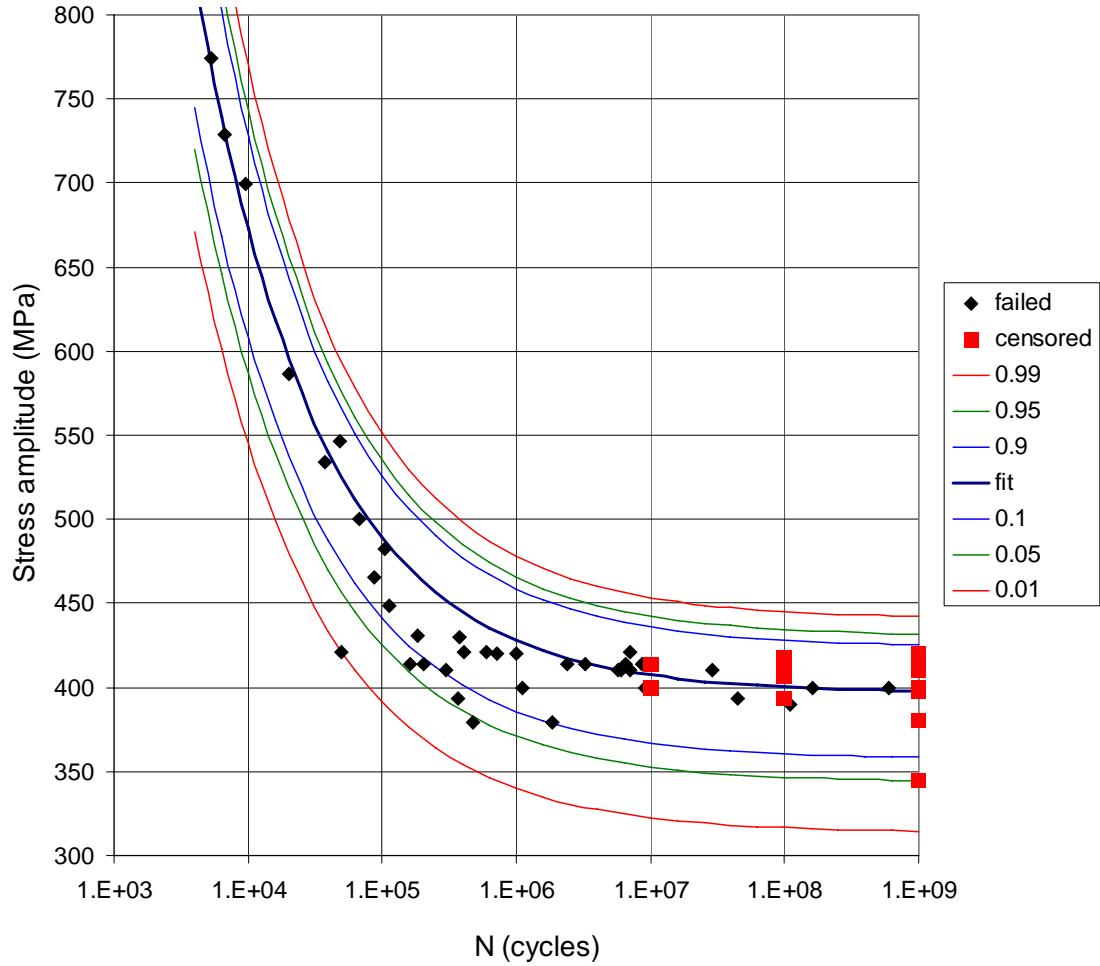


Figure 76. RFL model applied to the α - β Ti-6Al-4V data.

Table 22. RFL model parameters for best fit to α - β Ti-6Al-4V data.

Parameter	Descriptor	Value
β_0	S - N curve coefficient	4.950
β_1	S - N curve coefficient	-2.110
σ_ε	Standard deviation in lognormal fatigue life	0.16
η	Weibull location parameter for fatigue limit	405
β	Weibull scale parameter for fatigue limit	18

In order to better represent S - N curves with a discontinuous change in slope, a model with assumptions more closely representing the observed behavior of the fully-reversed Ti-6Al-4V tests must be specified for this application.

Alternative Models for Representing Knee-shaped S - N Curves

In this section, two models are developed and analyzed for representing the material behavior observed from the Ti-6Al-4V testing conducted in support of the National HCF S&T Program. The first model is termed the “hockey stick” model and is based on a bilinear shape with a horizontal fatigue limit. The second model goes beyond the linear constraints of the first model and is an adaptation of the Nishijima hyperbolic model introduced in Chapter V. Both models use fatigue strength distributions based on real Ti-6Al-4V data analysis and use maximum likelihood methods to generate best-fit parameters.

Bilinear “Hockey Stick” Model

The bilinear model assumes a constant slope for the S - N curve at lower cycles, followed by a transition to a horizontal fatigue limit at a specified number of cycles. Thus, there are three S - N model parameters: (1) m , the slope of the curve at lower cycles, which is a negative number and is expressed in units of stress/log(cycles), (2) FLS , the fatigue limit strength expressed in units of stress, and (3) N^* , the number of cycles at which the curve transitions from sloped to flat. The model is thus specified by the following equations (written for S - N curves with linear S axis and logarithmic N axis), and is represented by Figure 77:

$$S = -m \cdot (\log N^* - \log N) + FLS, \text{ for } N < N^* \quad (51)$$

$$S = FLS, \text{ for } N \geq N^* \quad (52)$$

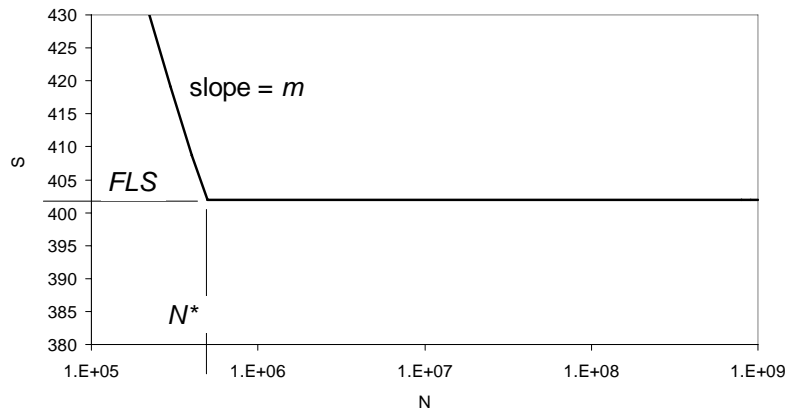


Figure 77. Bilinear (hockey stick) S - N model.

Nishijima Hyperbolic Model

A hyperbolic S - N model is presented by Nishijima [63] and described by Hanaki *et al* [36]. The model uses four parameters as shown in Figure 58 from Chapter V. These parameters can be varied to create S - N curves ranging from a curved form similar to that exhibited by the RFL model to the more bilinear form represented by the hockey stick model. The model is formulated using the following equation, where A , B , C , and E are model constants [36]:

$$(S - E)(S - A \log N - B) = C \quad (53)$$

Equation 6-3 can be solved in order to evaluate S as a function of $\log N$. Representation of S as a function of $\log N$ was necessary for use in the proposed model. After completing the multiplication on the left side of Equation 53 and then solving the resulting quadratic equation, the Nishijima model can be represented by the following:

$$S = \frac{A \log N + (B + E) + \sqrt{A^2 (\log N)^2 + 2A(\log N)(B - E) + (B - E)^2 + 4C}}{2} \quad (54)$$

Figure 78 illustrates several S - N curve shapes which can be modeled using the Nishijima hyperbolic form.

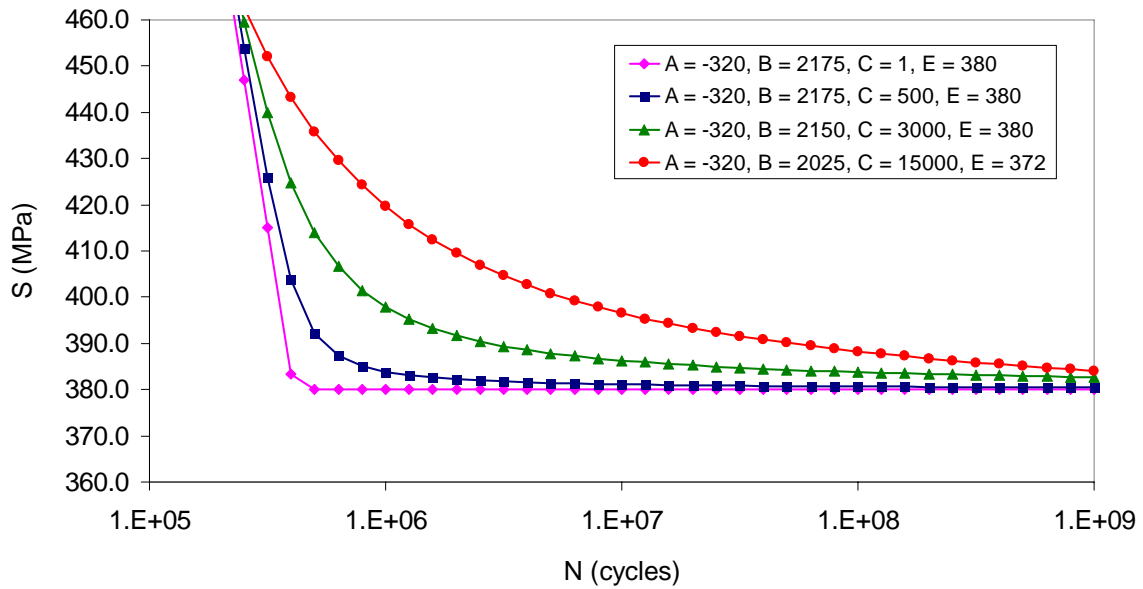


Figure 78. Sample S - N curve shapes using the Nishijima hyperbolic model.

Fatigue Strength Distribution

Unlike the RFL approach which specifies a distribution for the fatigue life at a given stress level as well as a distribution for the fatigue limit from which the curvature is based, the modeling approach developed for the analysis of the Ti-6Al-4V data (both α - β and beta annealed microstructures) used a single probability distribution. This distribution represented the fatigue strength at a specified number of cycles. The form of this distribution was based on the analysis of real Ti-6Al-4V data. As shown in Chapter IV, the residuals of a best-fit bilinear S - N model for the α - β Ti-6Al-4V data were well represented by an extreme value distribution. In order to evaluate these residuals as a single distribution, it was necessary to assume that the scatter in fatigue strength was constant as a function of cycles. The plot of the available Ti-6Al-4V data shown in Figure 73 supports the assertion that fatigue strength scatter can be adequately modeled as constant. No clear violation of this assumption is in evidence. The work of Hanaki *et al* supported the assertion that fatigue strength scatter is relatively constant for many engineering materials, and thus a distribution of residuals across various fatigue lives can be made [36].

At this point, it is necessary to discuss the mathematics of the extreme value distribution in more detail. The extreme value distribution is also known as the Fisher-Tippett distribution or log-Weibull distribution [2]. The distribution is governed by two parameters: a location parameter α and a scale parameter β . The probability density function (pdf) and cumulative distribution function (cdf) are shown below [2]:

$$P(x) = \frac{e^{\left(\left(\frac{\alpha - x}{\beta}\right) - e^{\left(\frac{\alpha - x}{\beta}\right)}\right)}}{\beta} \quad (\text{pdf}) \quad (55)$$

$$D(x) = e^{-e^{\left(\frac{\alpha - x}{\beta}\right)}} \quad (\text{cdf}) \quad (56)$$

A sample plot of these distribution functions is shown in Figure 79. The figure shows the skewed behavior, with the larger tail in the $+x$ direction.

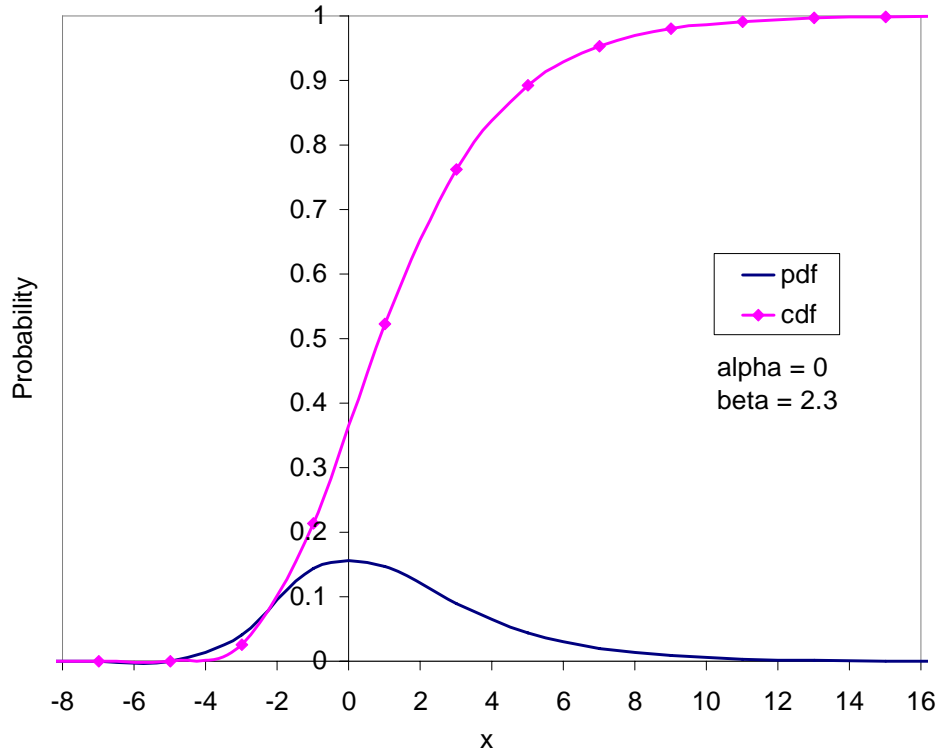


Figure 79. Probability functions for the extreme value distribution.

When using this distribution function for the fatigue strength distribution of the Ti-6Al-4V data, two considerations must be made. First, the extreme value distribution as defined has a longer tail in the $+x$ direction. However, residual analysis of the experimental data suggests that the fatigue strength distribution is skewed downwards towards lower values of stress (see Figure 47 from Chapter IV). This finding is consistent with the assumptions of the RFL model. Thus, the values from the extreme value distribution should be subtracted from (not added to) the S - N baseline model in order to represent the fatigue strength scatter about the S - N curve. The second consideration concerns the location parameter α . There is no need to have a non-zero location parameter if the baseline S - N curve is modeled as the mode (most likely outcome) and thus corresponds to the peak in fatigue strength pdf. For $\alpha = 0$, the extreme value pdf has a peak at $x = 0$. Thus, the fatigue strength distribution when modeled by the extreme value distribution is dependent on only one parameter: the scale parameter β . Because the Ti-6Al-4V data do not show a significant increase or decrease in fatigue

strength scatter as a function of cycles, this location parameter β can be considered a constant, independent of the number of cycles.

With the fatigue strength distribution modeled in this manner based on the analysis of real Ti-6Al-4V test data, there are now four parameters for the hockey stick model (m , FLS , N^* , and β) and five parameters for the hyperbolic model (A , B , C , E , and β). The next section discusses how these two models are fit to real test data.

Maximum Likelihood Method for Model Fitting

To determine the best fit for the hockey stick and hyperbolic models, a maximum likelihood approach was used. Each test point from the fatigue testing involves three pieces of data: (1) S_i , the stress level, (2) $\log N_i$, the logarithm (base 10) of the number of cycles tested, and (3) δ_i , a delta function which equals 1 if the specimen failed and 0 if the specimen did not fail (i.e., a runout, or censored data). The number of specimens tested is denoted by n . The model parameters are denoted by θ . Thus, for the hockey stick model, $\theta = (m, FLS, N^*, \beta)$, and for the hyperbolic model $\theta = (A, B, C, E, \beta)$. Each data point also has a corresponding \hat{S}_i which represents the point on the modeled S - N curve corresponding to $\log N_i$. Thus, given θ and $\log N_i$, Equations 51 and 52 are used to determine \hat{S}_i for each test point using the hockey stick model, and Equation 54 is used for the hyperbolic model. Now, x_i is defined by the following equation:

$$x_i = -\frac{S_i - \hat{S}_i}{\beta} \quad (57)$$

Thus, x_i represents a scaled residual between the true value of stress as tested (S_i) and the corresponding point on the modeled S - N curve given the specified parameters (\hat{S}_i). It is scaled by β , the scale parameter of the extreme value distribution representing fatigue strength scatter. The minus sign in Equation 57 is used because a stress value greater than its modeled companion represents a negative residual since the extreme value distribution is positively skewed downwards to lower stress values.

With the problem as defined thus far, the maximum likelihood method uses a likelihood function of the form:

$$L(\theta) = \prod_{i=1}^n [f_S(x_i, \theta)]^{\delta_i} [1 - F_S(x_i, \theta)]^{1-\delta_i} \quad (58)$$

where

$$\begin{aligned} f_S &= \text{fatigue strength pdf} = e^z - e^{z^2} \\ F_S &= \text{fatigue strength cdf} = e^{-e^z} \end{aligned} \quad (59)$$

and

$$z_i = -\frac{x_i}{\beta}. \quad (60)$$

By the property of logarithms, the likelihood function can be maximized by maximizing its logarithm, so that the following log-likelihood function is used:

$$\mathcal{L}(\theta) = \log[L(\theta)] = \log \left[\prod_{i=1}^n L_i(\theta) \right] = \sum_{i=1}^n \mathcal{L}_i(\theta) \quad (61)$$

where

$$\mathcal{L}_i(\theta) = \delta_i \log[f_S(x_i, \theta)] + (1 - \delta_i) \log[1 - F_S(x_i, \theta)]. \quad (62)$$

With this formulation in place, the test data can be plotted and initial estimates for the S - N baseline model parameters and distribution scale factor can be made based on a reasonable fit. The log-likelihood function is then maximized by methodically adjusting these parameters until improvements to the fit are no longer possible (or gains are so marginal that the fit is considered “good enough”).

Analysis of α - β Ti-6Al-4V Data

The 68 data points associated with the fully-reversed α - β tests were first investigated using the bilinear model with the extreme value distribution for fatigue strength. The maximum likelihood analysis is shown in Figure 80. The best-fit parameter settings are shown in the boxes at the top left of the figure. The log-likelihood function is shown at the top right. Using the results of this analysis, a P - S - N curve can be drawn based on the percentiles of the fatigue strength distribution at each given number of cycles. This P - S - N curve is shown in Figure 81. Sensitivity plots based on the final parameter settings are shown in Figure 82.

<div> <div>alpha = 0</div> <div>beta = 13.5</div> <div>FLS = 418</div> <div>N* = 1.80E+05</div> <div>m = -227</div> <div>logN* = 5.255</div> <div> <div>Sum of log-likelihoods</div> <div>base e base 1000</div> <div>-192.055 -27.8029</div> </div> </div>													
i	Si	Ni	LogNi	Runout	Ni >= N*	Model	Si_hat - Si	xi	pdf	cdf	pdf or cdf	Log(Likelihood)	
												base e	base 1000
1	774.03	5.319E+03	3.73	0	0	765.18	-8.85	-0.66	0.02079	0.14577	0.02079	-3.873	-0.561
2	729.08	6.737E+03	3.83	0	0	741.88	12.80	0.95	0.01948	0.67888	0.01948	-3.939	-0.570
3	699.84	9.700E+03	3.99	0	0	705.95	6.11	0.45	0.02494	0.52941	0.02494	-3.691	-0.534
4	586.49	2.020E+04	4.31	0	0	633.64	47.15	3.49	0.00219	0.97003	0.00219	-6.125	-0.887
5	546.29	4.854E+04	4.69	0	0	547.21	0.92	0.07	0.02719	0.39288	0.02719	-3.605	-0.522
6	534.36	3.777E+04	4.58	0	0	571.94	37.58	2.78	0.00430	0.94007	0.00430	-5.448	-0.789
7	499.89	6.823E+04	4.83	0	0	513.64	13.75	1.02	0.01864	0.69687	0.01864	-3.982	-0.576
8	482.65	1.034E+05	5.01	0	0	472.70	-9.95	-0.74	0.01915	0.12369	0.01915	-3.956	-0.573
9	465.41	8.830E+04	4.95	0	0	488.21	22.80	1.69	0.01138	0.83134	0.01138	-4.476	-0.648
10	448.17	1.125E+05	5.05	0	0	464.33	16.16	1.20	0.01655	0.73921	0.01655	-4.102	-0.594
11	430.94	1.833E+05	5.26	0	1	418.00	-12.94	-0.96	0.01424	0.07369	0.01424	-4.252	-0.616
12	430	3.800E+05	5.58	0	1	418.00	-12.00	-0.89	0.01582	0.08782	0.01582	-4.146	-0.600
13	420.6	4.963E+04	4.70	0	0	545.01	124.41	9.22	0.00001	0.99990	0.00001	-11.819	-1.711
14	420.6	4.069E+05	5.61	0	1	418.00	-2.60	-0.19	0.02672	0.29749	0.02672	-3.622	-0.524
15	420.6	5.913E+05	5.77	0	1	418.00	-2.60	-0.19	0.02672	0.29749	0.02672	-3.622	-0.524
16	420.6	7.050E+06	6.85	0	1	418.00	-2.60	-0.19	0.02672	0.29749	0.02672	-3.622	-0.524
17	420	7.200E+05	5.86	0	1	418.00	-2.00	-0.15	0.02694	0.31359	0.02694	-3.614	-0.523
18	420	1.000E+06	6.00	0	1	418.00	-2.00	-0.15	0.02694	0.31359	0.02694	-3.614	-0.523
19	413.7	2.058E+05	5.31	0	1	418.00	4.30	0.32	0.02603	0.48325	0.02603	-3.648	-0.528
20	413.7	3.248E+06	6.51	0	1	418.00	4.30	0.32	0.02603	0.48325	0.02603	-3.648	-0.528
21	413.7	6.554E+06	6.82	0	1	418.00	4.30	0.32	0.02603	0.48325	0.02603	-3.648	-0.528
22	413.7	1.610E+05	5.21	0	0	429.02	15.32	1.13	0.01727	0.72500	0.01727	-4.059	-0.588
23	413.7	8.746E+06	6.94	0	1	418.00	4.30	0.32	0.02603	0.48325	0.02603	-3.648	-0.528
24	413.7	2.400E+06	6.38	0	1	418.00	4.30	0.32	0.02603	0.48325	0.02603	-3.648	-0.528
25	410	3.000E+05	5.48	0	1	418.00	8.00	0.59	0.02356	0.57528	0.02356	-3.748	-0.543
26	410	5.700E+06	6.76	0	1	418.00	8.00	0.59	0.02356	0.57528	0.02356	-3.748	-0.543
27	410	6.100E+06	6.79	0	1	418.00	8.00	0.59	0.02356	0.57528	0.02356	-3.748	-0.543
28	410	7.100E+06	6.85	0	1	418.00	8.00	0.59	0.02356	0.57528	0.02356	-3.748	-0.543
29	410	2.900E+07	7.46	0	1	418.00	8.00	0.59	0.02356	0.57528	0.02356	-3.748	-0.543
30	400	9.000E+06	6.95	0	1	418.00	18.00	1.33	0.01500	0.76828	0.01500	-4.200	-0.608
31	400	1.600E+08	8.20	0	1	418.00	18.00	1.33	0.01500	0.76828	0.01500	-4.200	-0.608
32	400	6.000E+08	8.78	0	1	418.00	18.00	1.33	0.01500	0.76828	0.01500	-4.200	-0.608
33	400	2.900E+06	6.46	0	1	418.00	18.00	1.33	0.01500	0.76828	0.01500	-4.200	-0.608
34	400	1.800E+05	5.26	0	1	418.00	18.00	1.33	0.01500	0.76828	0.01500	-4.200	-0.608
35	400	6.000E+06	6.78	0	1	418.00	18.00	1.33	0.01500	0.76828	0.01500	-4.200	-0.608
36	399.91	1.099E+06	6.04	0	1	418.00	18.09	1.34	0.01493	0.76963	0.01493	-4.205	-0.609
37	393.02	3.634E+05	5.56	0	1	418.00	24.98	1.85	0.00995	0.85455	0.00995	-4.610	-0.667
38	393.02	4.490E+07	7.65	0	1	418.00	24.98	1.85	0.00995	0.85455	0.00995	-4.610	-0.667
39	390	1.100E+08	8.04	0	1	418.00	28.00	2.07	0.00821	0.88190	0.00821	-4.802	-0.695
40	390	7.100E+05	5.85	0	1	418.00	28.00	2.07	0.00821	0.88190	0.00821	-4.802	-0.695
41	379.23	4.750E+05	5.68	0	1	418.00	38.77	2.87	0.00396	0.94498	0.00396	-5.531	-0.801
42	379.23	1.835E+06	6.26	0	1	418.00	38.77	2.87	0.00396	0.94498	0.00396	-5.531	-0.801
43	420	1.000E+09	9.00	1	1	418.00	-2.00	-0.15	0.02694	0.31359	0.31359	-1.160	-0.168
44	417.15	1.000E+08	8.00	1	1	418.00	0.85	0.06	0.02720	0.39103	0.39103	-0.939	-0.136
45	417.15	1.000E+08	8.00	1	1	418.00	0.85	0.06	0.02720	0.39103	0.39103	-0.939	-0.136
46	413.7	1.000E+07	7.00	1	1	418.00	4.30	0.32	0.02603	0.48325	0.48325	-0.727	-0.105
47	413.7	1.000E+08	8.00	1	1	418.00	4.30	0.32	0.02603	0.48325	0.48325	-0.727	-0.105
48	413.7	1.000E+08	8.00	1	1	418.00	4.30	0.32	0.02603	0.48325	0.48325	-0.727	-0.105
49	410	1.000E+09	9.00	1	1	418.00	8.00	0.59	0.02356	0.57528	0.57528	-0.553	-0.080
50	410	1.000E+09	9.00	1	1	418.00	8.00	0.59	0.02356	0.57528	0.57528	-0.553	-0.080
51	410	1.000E+09	9.00	1	1	418.00	8.00	0.59	0.02356	0.57528	0.57528	-0.553	-0.080
52	406.8	1.000E+08	8.00	1	1	418.00	11.20	0.83	0.02089	0.64648	0.64648	-0.436	-0.063
53	406.8	1.000E+08	8.00	1	1	418.00	11.20	0.83	0.02089	0.64648	0.64648	-0.436	-0.063
54	400	1.000E+09	9.00	1	1	418.00	18.00	1.33	0.01500	0.76828	0.76828	-0.264	-0.038
55	400	1.000E+09	9.00	1	1	418.00	18.00	1.33	0.01500	0.76828	0.76828	-0.264	-0.038
56	400	1.000E+09	9.00	1	1	418.00	18.00	1.33	0.01500	0.76828	0.76828	-0.264	-0.038
57	400	1.000E+09	9.00	1	1	418.00	18.00	1.33	0.01500	0.76828	0.76828	-0.264	-0.038
58	400	1.000E+08	8.00	1	1	418.00	18.00	1.33	0.01500	0.76828	0.76828	-0.264	-0.038
59	399.91	1.000E+07	7.00	1	1	418.00	18.09	1.34	0.01493	0.76963	0.76963	-0.262	-0.038
60	398.19	1.000E+09	9.00	1	1	418.00	19.81	1.47	0.01356	0.79412	0.79412	-0.231	-0.033
61	393.02	1.000E+08	8.00	1	1	418.00	24.98	1.85	0.00995	0.85455	0.85455	-0.157	-0.023
62	390	1.000E+08	8.00	1	1	418.00	28.00	2.07	0.00821	0.88190	0.88190	-0.126	-0.018
63	390	1.000E+08	8.00	1	1	418.00	28.00	2.07	0.00821	0.88190	0.88190	-0.126	-0.018
64	380	1.000E+09	9.00	1	1	418.00	38.00	2.81	0.00418	0.94184	0.94184	-0.060	-0.009
65	380	1.000E+09	9.00	1	1	418.00	38.00	2.81	0.00418	0.94184	0.94184	-0.060	-0.009
66	380	1.000E+09	9.00	1	1	418.00	38.00	2.81	0.00418	0.94184	0.94184	-0.060	-0.009
67	380	1.000E+08	8.00	1	1	418.00	38.00	2.81	0.00418	0.94184	0.94184	-0.060	-0.009
68	344.75	1.000E+09	9.00	1	1	418.00	73.25	5.43	0.00032	0.99561	0.99561	-0.004	-0.001

Figure 80. Maximum likelihood analysis of fully-reversed α - β Ti-6Al-4V data using the bilinear model with extreme value distribution for fatigue strength.

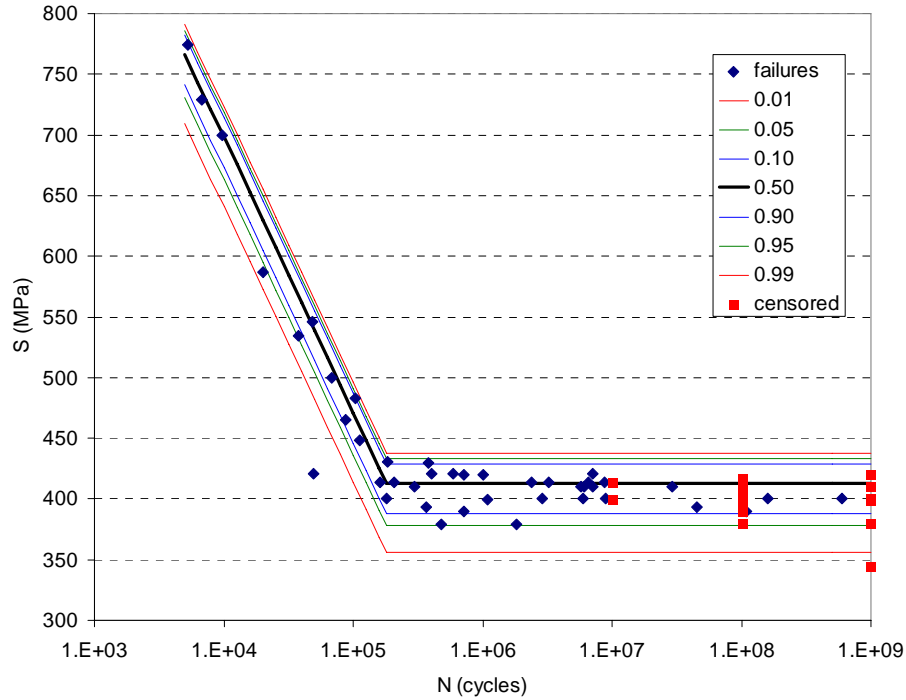


Figure 81. P - S - N plot of α - β Ti-6Al-4V data using the bilinear model with extreme value distribution for fatigue strength.

When compared to the RFL model fit shown in Figure 76, the P - S - N plot of Figure 81 appears to be a superior fit. The modeled fit accounts for most of the behavior observed from the Ti-6Al-4V testing. Namely, the model illustrates the highly sloped region at lower cycles, the flat region at higher cycles, the sharp transition between the two regions, along with the skewed scatter towards lower stresses, and the relatively constant scatter in fatigue strength as a function of fatigue life. If one looks at the failure points only, 34 of the 42 (81.0%) failure points lie within the 10th and 90th percentiles (an 80% band). Likewise, 39 of the points (92.9%) lie within the 5th and 95th percentiles (90% band). Finally, 41 of the points (97.6%) lie within the 1st and 99th percentiles (98% band). Thus, the modeled percentile bands match well with experimental data. One attribute of the RFL model which is not captured by this modeling approach is the lognormal distribution in fatigue life for a given stress level. Looking at a horizontal line through the sloped region of the curve, the percentile lines about the median fit are not symmetrical, thus indicating that the fatigue life is not normally distributed along the logarithmic axis.

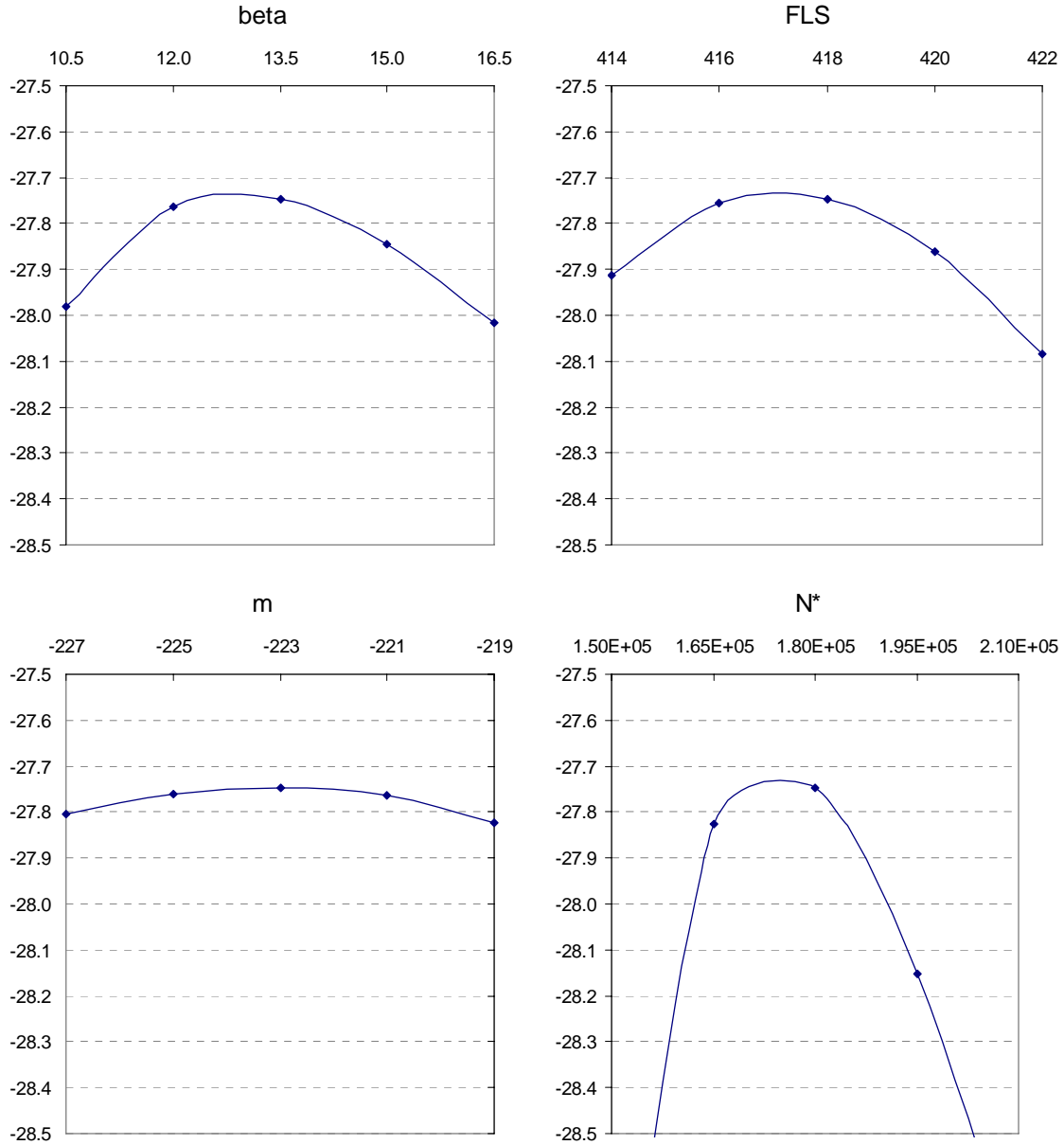


Figure 82. Sensitivity plots based on log-likelihood for parameter settings using the bilinear model for the α - β Ti-6Al-4V data.

The hyperbolic model was also applied to the α - β Ti-6Al-4V data in order to improve upon the fit using the bilinear model. Interestingly, the best fit accomplished resulted in a log-likelihood (base 1000) of -29.263, compared to the value of -27.746 using the bilinear model. Thus, the best fit with the 5-parameter hyperbolic model was not quite as good as that of the 4-parameter bilinear model. The results of the hyperbolic model analysis are shown in Figure 83. The P - S - N plot of the α - β Ti-6Al-4V data is

alpha =	0											
beta =	16.0											
A =	-311											
B =	1970											
C =	1950											
E =	414											
Sum of log-likelihoods												
base e base 1000												
-202.140 -29.2627												
Log(Likelihood)												
i	Si	Ni	LogNi	Runout	Model	Si_hat - Si	xi	pdf	cdf	pdf or cdf	base e	base 1000
1	774.03	5.319E+03	3.73	0	816.12	42.09	2.63	0.00419	0.93048	0.00419	-5.475	-0.793
2	729.08	6.737E+03	3.83	0	784.61	55.53	3.47	0.00188	0.96938	0.00188	-6.274	-0.908
3	699.84	9.700E+03	3.99	0	736.17	36.33	2.27	0.00582	0.90188	0.00582	-5.146	-0.745
4	586.49	2.020E+04	4.31	0	639.68	53.19	3.32	0.00217	0.96465	0.00217	-6.133	-0.888
5	546.29	4.854E+04	4.69	0	529.51	-16.78	-1.05	0.01028	0.05764	0.01028	-4.578	-0.663
6	534.36	3.777E+04	4.58	0	559.88	25.52	1.60	0.01035	0.81640	0.01035	-4.571	-0.662
7	499.89	6.823E+04	4.83	0	491.73	-8.16	-0.51	0.01968	0.18908	0.01968	-3.928	-0.569
8	482.65	1.034E+05	5.01	0	456.47	-26.18	-1.64	0.00189	0.00588	0.00189	-6.273	-0.908
9	465.41	8.830E+04	4.95	0	467.95	2.54	0.16	0.02272	0.42599	0.02272	-3.785	-0.548
10	448.17	1.125E+05	5.05	0	451.32	3.15	0.20	0.02258	0.43996	0.02258	-3.791	-0.549
11	430.94	1.833E+05	5.26	0	433.45	2.51	0.16	0.02273	0.42528	0.02273	-3.784	-0.548
12	430	3.800E+05	5.58	0	424.28	-5.72	-0.36	0.02139	0.23947	0.02139	-3.845	-0.557
13	420.6	4.963E+04	4.70	0	526.90	106.30	6.64	0.00008	0.99870	0.00008	-9.418	-1.363
14	420.6	4.069E+05	5.61	0	423.83	3.23	0.20	0.02256	0.44167	0.02256	-3.792	-0.549
15	420.6	5.913E+05	5.77	0	421.90	1.30	0.08	0.02292	0.39767	0.02292	-3.776	-0.547
16	420.6	7.050E+06	6.85	0	417.38	-3.22	-0.20	0.02250	0.29434	0.02250	-3.794	-0.549
17	420	7.200E+05	5.86	0	421.15	1.15	0.07	0.02293	0.39427	0.02293	-3.775	-0.547
18	420	1.000E+06	6.00	0	420.17	0.17	0.01	0.02299	0.37173	0.02299	-3.773	-0.546
19	413.7	2.058E+05	5.31	0	431.16	17.46	1.09	0.01500	0.71480	0.01500	-4.200	-0.608
20	413.7	3.248E+06	6.51	0	418.12	4.42	0.28	0.02220	0.46833	0.02220	-3.807	-0.551
21	413.7	6.554E+06	6.82	0	417.44	3.74	0.23	0.02242	0.45307	0.02242	-3.798	-0.550
22	413.7	1.610E+05	5.21	0	436.68	22.98	1.44	0.01172	0.78835	0.01172	-4.447	-0.644
23	413.7	8.746E+06	6.94	0	417.22	3.52	0.22	0.02248	0.44813	0.02248	-3.795	-0.549
24	413.7	2.400E+06	6.38	0	418.51	4.81	0.30	0.02207	0.47686	0.02207	-3.814	-0.552
25	410	3.000E+05	5.48	0	426.22	16.22	1.01	0.01578	0.69565	0.01578	-4.149	-0.601
26	410	5.700E+06	6.76	0	417.55	7.55	0.47	0.02089	0.53598	0.02089	-3.868	-0.560
27	410	6.100E+06	6.79	0	417.50	7.50	0.47	0.02092	0.53476	0.02092	-3.867	-0.560
28	410	7.100E+06	6.85	0	417.37	7.37	0.46	0.02098	0.53218	0.02098	-3.864	-0.5

Figure 83. Maximum likelihood analysis of fully-reversed α - β Ti-6Al-4V data using the hyperbolic model with extreme value distribution for fatigue strength.

shown in Figure 84. For this fit, 83.3% (35/42) of the failures fall within the 80% band, 90.5% (38/42) fall within the 90% band, and 95.2% (40/42) fall within the 98% band, as given by the percentile lines.

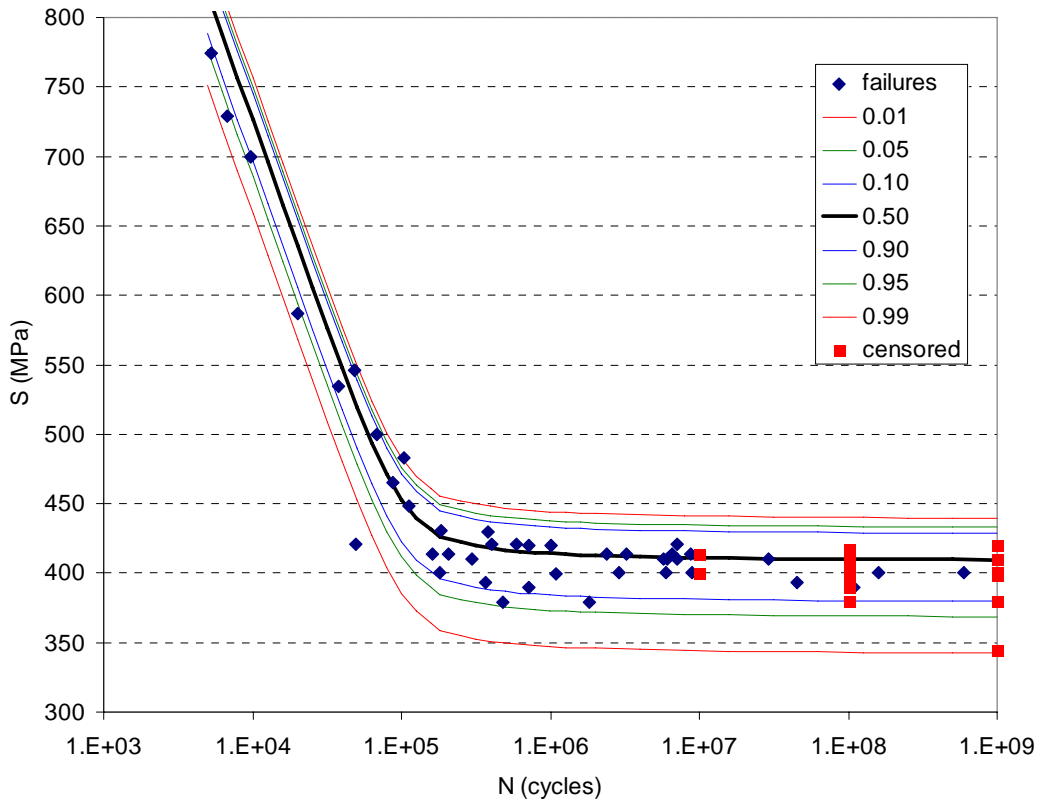


Figure 84. P - S - N plot of α - β Ti-6Al-4V data using the hyperbolic model with extreme value distribution for fatigue strength.

A comparison between the outputs for each model as applied to the α - β Ti-6Al-4V data is shown in Table 23. Recall that the modified staircase analysis of this alloy based on the small-sample testing from Chapter IV showed a median fatigue strength of 406.4 MPa at 10^9 cycles.

Table 23. Comparison of modeled output using the RFL, bilinear, and hyperbolic models for the α -B Ti-6Al-4V data.

Parameter (in MPa)	RFL	Bilinear	Hyperbolic
Median fatigue strength at 10^9	398	413	410
90% lower bound fatigue strength at 10^9	359	388	380
95% lower bound fatigue strength at 10^9	344	378	369
99% lower bound fatigue strength at 10^9	315	356	343

Beta Annealed Ti-6Al-4V Analysis

At this point, the bilinear and hyperbolic models have been shown to provide a better fit to the α - β Ti-6Al-4V data when compared to the RFL model. In addition, the beta annealed Ti-6Al-4V data has been shown to reasonably result from an S - N curve with a highly sloped region at lower cycles and fatigue limit at higher cycles (similar to the α - β behavior). This assertion is also supported by the work of Boyer *et al*, who showed that lamellar Ti-6Al-4V S - N curve shapes were quite similar in shape to those of the bimodal alloy [19]. Thus, the beta annealed data should also be fit better with the bilinear or hyperbolic models. These models were therefore applied to the beta annealed data in order to characterize the fatigue behavior.

Bilinear Model

The best-fit parameter settings for the bilinear model were: $m = -84$ MPa/log(cycle), $FLS = 402$ MPa, $N^* = 4.8 \times 10^5$ cycles, and $\beta = 12.1$. The P - S - N plot based on this model fit is shown in Figure 85. Based on this fit, the median fatigue strength at 10^9 cycles is 397.5 MPa, with a 95% lower bound of 366.0 MPa.

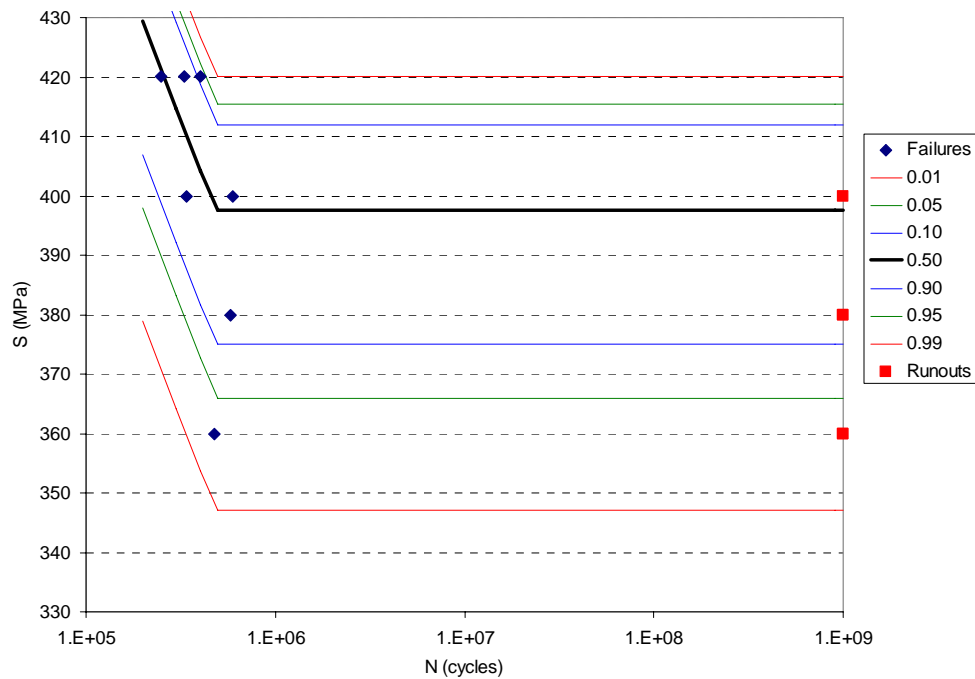


Figure 85. Bilinear model with extreme value distribution applied to beta annealed Ti-6Al-4V data.

Hyperbolic Model

The best-fit hyperbolic model resulted from parameter settings: $A = -325$, $B = 2170$, $C = 250$, $E = 401$, and $\beta = 13.5$. The P - S - N plot based on this model fit is shown in Figure 86. This fit yields a median fatigue strength at 10^9 cycles equal to 396.2 MPa, with a 95% lower bound at 361.2 MPa.

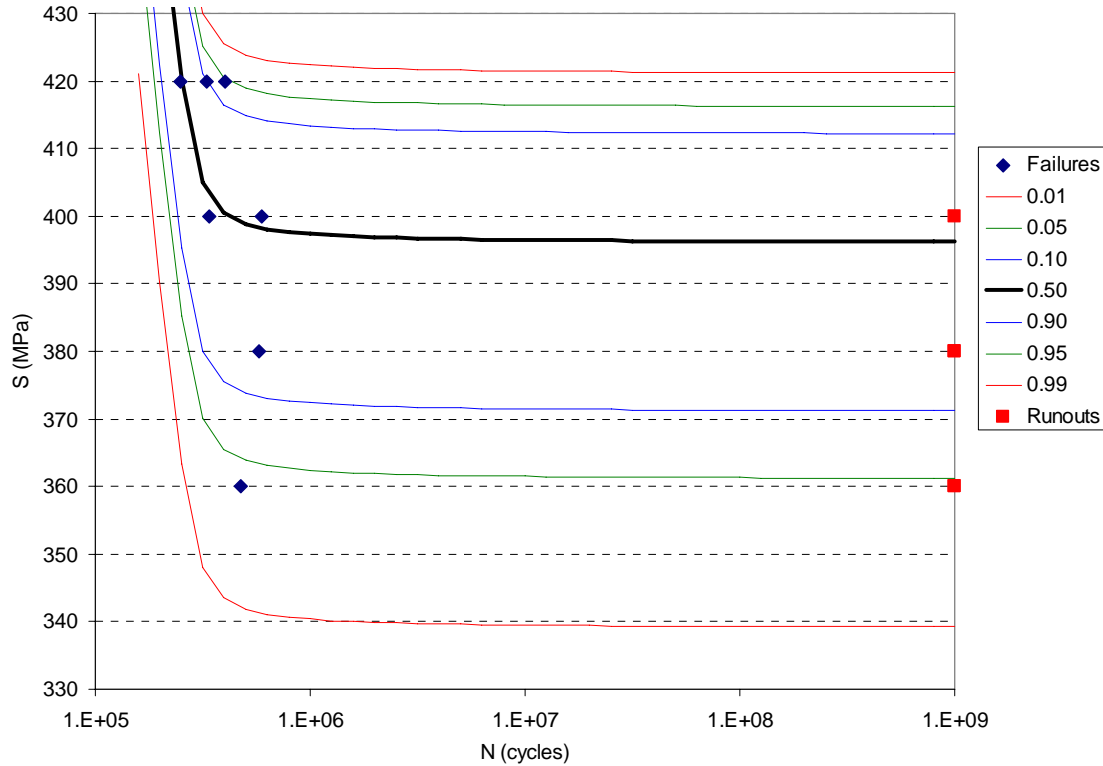


Figure 86. Hyperbolic model with extreme value distribution applied to beta annealed Ti-6Al-4V data.

Quantal Response Analysis

Another analysis avenue would be to use the P - S data from the beta annealed tests and bootstrap these results in accordance with the method proposed in Chapter III. However, there is no lower bound stress value for which only survivals resulted from testing, so an assumption must be made. Namely, the 340 MPa stress level must be assumed to have a probability of failure of 0. When this assumption is made, the P - S data can be summarized by the vectors $\mathbf{P} = (0, 0.3333, 0.3333, 0.6667, 1.0)$ and $\mathbf{S} = (340, 360, 380, 400, 420)$ where P_i is the probability of failure at stress S_i measured in MPa.

The staircase bootstrap algorithm was applied to this data. According to the results of Chapter III, the estimate for fatigue strength standard deviation using 5-level data should be based on the mean Svensson-Lorén standard deviation from the bootstrapped distribution. This estimate is 25.7 MPa based on this data set, along with a mean fatigue strength of 387.0 from the bootstrapped distribution. Assuming normality, this data correlates to a 95% lower bound of 344.7 MPa for fatigue strength at 10^9 cycles. Of course, the fatigue strength distribution was already shown to be better represented by an extreme value distribution for the α - β data, and thus an assumption of normality for the beta annealed data may lead to errors. The quantal response analysis is really not necessary given that the S - N data can be used by the models previously described to generate P - S - N plots from which P - S data can be gleaned.

Summary

The objective of this chapter was to characterize the fatigue behavior of the beta annealed Ti-6Al-4V alloy under fully-reversed loading at very high cycles. A 12-specimen experiment was conducted using the 20-kHz ultrasonic test machine, with a runout limit of 10^9 cycles. Stress-life data from this experiment was analyzed using the RFL model. The model did not appear to represent the small-sample data very well. The RFL tool was applied to the larger sample set of α - β Ti-6Al-4V data and was shown to poorly fit data with a sharp transition between sloped and flat S - N behavior. A simple bilinear model was proposed to better represent this S - N behavior. Analysis of residuals (i.e., differences between actual failure points and the mean curve fit) from α - β testing showed that the extreme value distribution represented the scatter in fatigue strength quite well. Thus, a probabilistic S - N model was proposed using the bilinear model as a baseline with fatigue strength distributed according to the extreme value distribution. Parameters for the best fit using this model were determined using the maximum likelihood method. This model provided a good fit to the α - β data. A second model using the Nishijima hyperbolic S - N model as a baseline was also proposed and analyzed, also providing a good fit to the α - β data. These models were then applied to the beta annealed data. Based on this analysis, the fatigue strength of the beta annealed alloy at 10^9 cycles is approximately 397 MPa, about 2.5% lower than the α - β alloy.

VII. SUMMARY AND CONCLUSIONS

In this chapter, the problem is restated and the methods and findings of this research are summarized. In addition, areas for further research are identified and discussed. Finally, the research conclusions are presented.

Problem Restatement

The primary goal of this research was to provide a means of characterizing the fatigue strength at a specified number of cycles. The method proposed for such a purpose was to demonstrate the following characteristics as best as possible:

- *Efficiency* – the capability of the test approach to estimate parameters with relatively few specimens.
- *Accuracy* – the capability of the test approach to estimate both fatigue strength central tendency and dispersion while minimizing errors.
- *Simplicity* – the ease of use of the method in terms of both experimental and analytical (or computational) requirements.
- *Objectivity* – the capability of the method to be defensible, repeatable, and unbiased through the mitigation of subjective inputs.
- *Robustness* – the ability of the method to be applied to various materials with differing underlying fatigue strength behaviors.

A method possessing these properties would be well-served for use in ultra high cycle fatigue testing where there is generally few data for many aerospace materials, and may be considered for use in the development of high cycle fatigue design guidance provided by the Department of Defense to engine manufacturers, or other such applications. Such a method would require experimental validation to demonstrate its utility, which would provide a testing opportunity to explore material behavior in the gigacycle regime. A survey of existing methods, to include recent research related to high cycle fatigue testing methods, was a prerequisite for such an effort and led to the investigations of the staircase test and random fatigue limit (RFL) model.

Summary of Findings

The primary findings of this research are broken into four sections: (1) the investigation of the staircase method, (2) the investigation of α - β Ti-6Al-4V in the gigacycle regime, (3) the investigation of test strategies using the random fatigue limit (RFL) model, and (4) the investigation of very high cycle fatigue behavior of beta annealed Ti-6Al-4V and development of analysis models to characterize Ti-6Al-4V behavior using maximum likelihood methods. These findings are discussed in each of the following four sections.

Investigation of the Staircase Method

The staircase method was selected as one of the most promising methods for analysis of high cycle fatigue data for several reasons. To start, the test is simple in terms of test protocol. It is also widely used in industry and academia and has been a part of testing guidance for some time. The test has also proven to be extremely accurate in characterizing the mean fatigue strength at a specified number of cycles using very few specimens. Although the analysis methods were developed in the 1950s for explosives testing, there has been a flurry of recent activity from 1998 to the present [20; 34; 41; 73; 84-85] in exploring the ability of the staircase test to characterize the scatter in fatigue strength. None of these recent efforts has appeared to result in a complete characterization of the staircase test's ability to estimate fatigue strength standard deviation as a function of staircase parameter settings (step size, starting stress, and number of specimens). In addition, these efforts have not as yet demonstrated an ability to both improve estimates in an average sense as well as minimize scatter in results.

A major part of this research effort was the simulation-based characterization of the staircase test's ability to estimate standard deviation. The staircase test was modeled and simulated using assumed normal distributions to represent true fatigue strength. Although this assumption seems overly restrictive, stress transformations may be used to better approach normality for those materials with non-normal fatigue strength behavior. The simulation work produced a complete picture of the bias inherent in standard deviation estimation using the Dixon-Mood analysis method for staircase test data (see Figure 25), as a function of step size ($s \geq 0.1\sigma$) and sample size ($N \geq 8$). This bias picture

showed an unbiased region in the $1.6\text{--}1.75\sigma$ region, which uses significantly larger steps than currently recommended in the literature. In addition, the results showed that starting a staircase test slightly below or above the true mean fatigue strength may mitigate some of the underestimating bias inherent in the analysis method. This result follows from the fact that starting too low or too high may allow more stress levels with non-zero or non-unity probabilities of failure, which tends to increase standard deviation estimates. The characterization of standard deviation bias led to the development of a non-linear correction factor (Equation 63) which accounted for both step size and the number of specimens. In an average sense, this correction factor produced less biased results than traditional staircase analysis. However, the correction factor also suffered from an increase in scatter of results.

$$\sigma_{PC} = A\sigma_{DM}\left(\frac{N}{N-3}\right)\left(B\frac{\sigma_{DM}}{s}\right)^m \quad (63)$$

where:

N is the number of specimens and s is the step size,

A , B , and m are constants dependent on sample size as shown in Table 7,

σ_{DM} is the fatigue strength standard deviation derived from Dixon-Mood analysis,

σ_{PC} is the corrected standard deviation estimate.

The increased scatter in staircase results due to bias correction was addressed through the use of bootstrapping. A data-based algorithm was proposed which would utilize the P - S data (probability of failure associated with each stress level) to perform repeated “virtual staircases” on the data, each with its own estimate of corrected fatigue strength standard deviation. In this manner, instead of a staircase test producing a single estimate for standard deviation, it would produce a distribution for standard deviation from which a relevant statistic could be used as the estimate for standard deviation. The bootstrapping algorithm was found to significantly reduce the scatter in both uncorrected and corrected standard deviation estimates. This bootstrapping algorithm thus allowed use of the proposed bias correction method without significantly increased scatter relative to the uncorrected method without bootstrapping. The code for the algorithm is found in

Appendix D. Rules for use of the bootstrapping distribution were developed based on an analysis of simulated staircase data. These rules are summarized as follows:

- P - S data must be bounded by stress levels with $P(\text{failure}) = 0$ and $P(\text{failure}) = 1$.
- If the staircase resulted in just two stress levels, then the staircase results are not meaningful and should not be used.
- If the test results in three stress levels, bootstrapping is generally ineffective and the non-bootstrapped Svensson-Lorén corrected standard deviation estimate may be used to estimate the true standard deviation. However, it is recommended that additional testing be conducted to ensure four or more stress levels.
- If the test results in four stress levels, the 60th- and 65th-percentile points of the bootstrap distribution using the proposed non-linear correction for standard deviation should be averaged to estimate the true standard deviation for larger step sizes. If the step size is known to be on the order of standard deviation or smaller, then the 60th- and 65th-percentile points of the bootstrap distribution for Svensson-Lorén corrected standard deviation should be averaged to estimate the true standard deviation.
- If the test results in five or more stress levels, then the mean of the Svensson-Lorén bootstrap distribution should be used to estimate the true standard deviation.

The use of an iterated staircase algorithm was also considered, in which a single staircase test would be divided into a series of smaller subtests and each subtest would use the results of the previous subtest as initial estimates. Investigation showed that such an approach did not reduce the scatter in results, but may in fact increase such scatter. Thus, the iterative staircase algorithm was not recommended for use.

Experimental Investigation of α - β Ti-6Al-4V

With a test method proposed for investigation of fatigue strength at a specified number of cycles, the next step was an experimental validation of this method. The National HCF Science & Technology Program collected a significant amount of data

points for two-phase Ti-6Al-4V specimens. In addition, AFRL/MLLM already had an ongoing Ti-6Al-4V test program using a 20-kHz ultrasonic fatigue testing machine capable of testing in the gigacycle regime. Thus, it was a fairly obvious choice to utilize these data and test program to provide validation of the modified staircase method.

Twenty data points from two separate 10-specimen staircase tests were collected by AFRL/MLLM as part of their research program. These staircases used a 10 MPa step under fully-reversed loading. Data from these tests are shown in Figure 87. The objective of this phase was to use these data points to apply the modified staircase method to a small-sample set, and then use the larger pool of Ti-6Al-4V data from the National HCF S&T Program to validate results. AFRL/MLLM's work already demonstrated that there were no observable differences between the two sets of data due to testing at different frequencies. Only tests conducted under fully-reversed conditions would be compared.

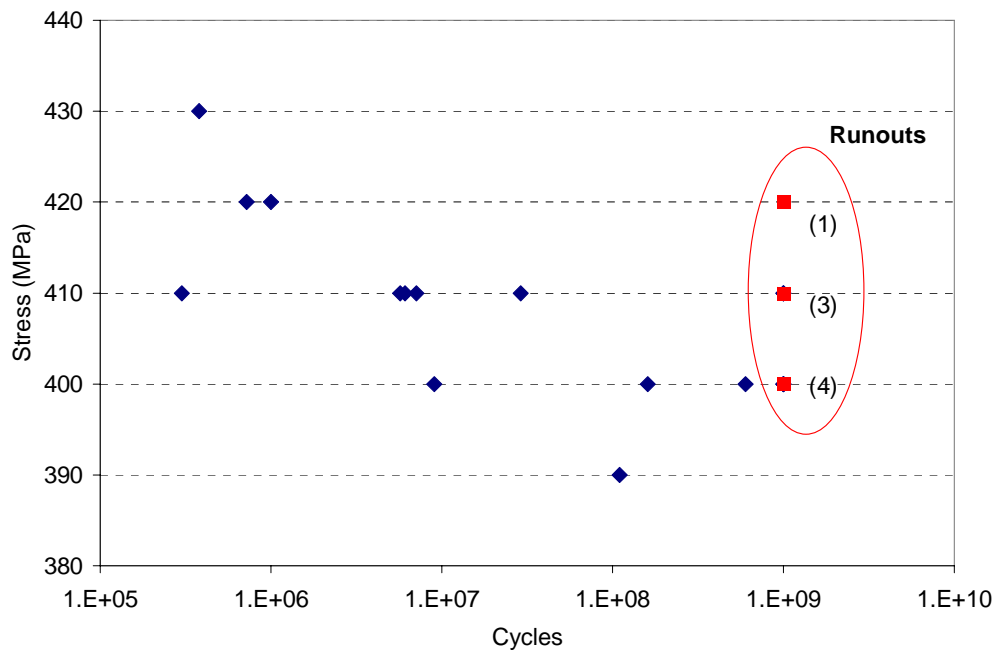


Figure 87. Initial staircase data for 10^9 -limited tests of α - β Ti-6Al-4V under $R = -1$ loading using the 20 stress-relief annealed (SRA) specimens (numbers in parentheses indicate number of runouts).

Investigation of the 20 data points showed that it would not be possible to create one seamless staircase using 10 MPa steps. The data was reworked using a 20 MPa step

size using the conditions that a failure at a particular stress level would also be a failure at any higher stress level, and a survival at a particular stress level would also be a survival at any lower stress level. This reorganization of the data also had the advantage of increasing the step size, which was shown in the staircase investigation to produce less biased results so long as more than three stress levels still result. In fact, the data did fit into four stress levels, although three additional tests were necessary to round out the complete staircase, as shown in Figure 88. These tests were subsequently conducted and resulted in runouts, thus completing a 23-specimen staircase with 20 MPa step.

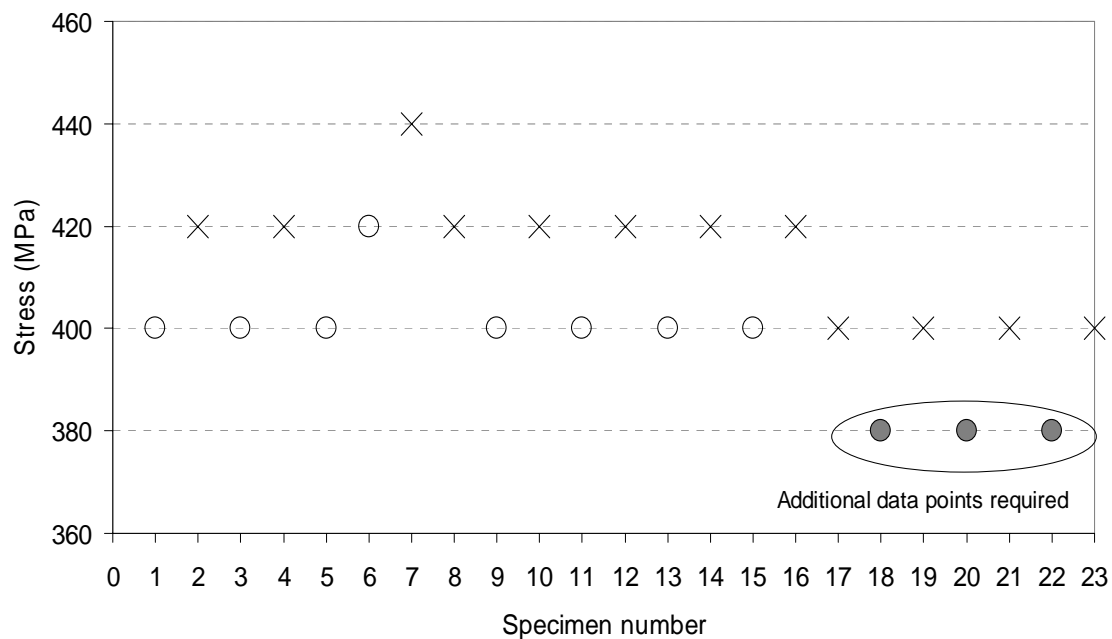


Figure 88. AFRL/MLLM's α - β Ti-6Al-4V data reworked into a single staircase.

The 23-specimen staircase data resulted in a mean fatigue strength of 406.4 MPa using Dixon-Mood analysis. Investigation of the normality assumption for fatigue strength distribution was accomplished using a residuals analysis based on a least squares curve fit (with bilinear S - N model) to the entire Ti-6Al-4V data set (68 data points). The fatigue strength distribution was shown to be adequately modeled by the extreme value distribution, but was not so grossly non-normal as to negate Dixon-Mood analysis. The modified analysis method was applied to the data. The standard deviation estimate using the proposed non-linear correction was 11.69 MPa. Bootstrapping the P - S data and using

the rules defined in the previous section, the bootstrapped estimate increased to 12.45 MPa. The standard deviation estimate for 10^9 -cycle fatigue strength using the modified staircase analysis method was thus 12.45 MPa.

Validation of this result was accomplished in two ways. The first manner was to use the residuals data from the entire Ti-6Al-4V data set (68 points). When modeled by a normal distribution, these residuals data resulted in a standard deviation of 13.38 MPa. It is important to note that this standard deviation estimate represents the actual physical scatter of the larger set of S - N data points about the best-fit bilinear S - N curve. The 12.45 MPa estimate obtained from the modified staircase analysis is within 7% of the value obtained by analyzing this physical scatter. The second manner of comparison was to perform a simulation-based “what if” study. Staircase results were simulated using calculated estimates as true fatigue strength parameters. Of the 30 simulated staircases, 26 resulted in standard deviation estimates within 18% of the assumed standard deviation, with a mean of 12.74 MPa. Simulated results using larger and smaller assumed standard deviations were worse compared to that from the real 23-specimen data. Thus, both validation approaches support the validity of the standard deviation estimate obtained through use of the modified staircase method developed in Chapter III.

As a final note in this section, none of the α - β Ti-6Al-4V tests under fully-reversed loading resulted in failures which were internally initiated. All failures were surface initiations.

Test Strategies and the Random Fatigue Limit (RFL) Model

The genesis of this investigation was the desire to perform a second experimental validation of the modified staircase method using a different material. A beta annealed variant of the Ti-6Al-4V alloy was available for use and capable of being quickly and inexpensively machined into specimens capable of resonance at 20 kHz to support ultrasonic testing. The microstructure of the beta annealed Ti-6Al-4V was so different from the α - β Ti-6Al-4V that it essentially constituted a different material. However, there were fewer data available on this material and it was decided that characterizing the S - N behavior over a range of cycles in the very high cycle regime was of more interest than just determining fatigue strength at a specific number of cycles. So, a better means of characterizing S - N behavior was needed as the staircase test is not suited for such a

purpose. The RFL model, a maximum likelihood method recently developed by Pascual and Meeker for such an application [66], was investigated for use. However, there was an absence of guidance in the literature on how to design tests for use with this model, as it was generally demonstrated only after-the-fact in the literature (i.e., it was used to analyze test data collected from other tests). Thus, the goal of this section was to determine a test strategy suitable for use with the RFL analysis method.

Three approaches were considered as possible avenues of test design using the RFL method: (1) traditional staircase protocol, (2) a balanced strategy with equal number of specimens at each stress level, and (3) an adaptive staircase in which the step size can be changed based on test result trends. Each test design incorporated 12 specimens, as this number represented a test limitation. For each test design, three scenarios were considered: (1) relatively flat $S-N$ behavior in the very high cycle regime with a fairly soft knee in the curve approaching the low cycle regime, (2) sloped $S-N$ behavior in the very high cycle regime, and (3) a bilinear $S-N$ curve. Each scenario was modeled using a probabilistic Nishijima hyperbolic $S-N$ model. For each test approach and scenario combination, random 12-specimen tests were simulated using the probabilistic $S-N$ model and test protocol. A PC-based RFL analysis tool was then used to analyze each data set to produce the $P-S-N$ curve with maximum likelihood.

Results of this analysis showed that the adaptive staircase strategy worked better for the scenarios with relatively flat $S-N$ behavior in the very high cycle regime, while the balanced strategy worked better when the behavior was more sloped. The adaptive approach may have proven more successful for flat $S-N$ behavior due to the use of some tests with smaller steps which reduced the spread in data and thus allowed better modeling of flat behavior. One disadvantage for the use of the adaptive approach is that the resulting data are unsuitable for analysis using the staircase method, probit method, or other common data analysis techniques. Thus, despite its seeming advantage, it was not recommended for use in the beta annealed tests. Note that more extensive simulation work would be required to make any concrete conclusions regarding the supremacy of any of these methods. But the key result of this analysis was that there was no obvious disadvantage to the use of the balanced approach compared to the traditional staircase. Thus, one could perform a balanced strategy with 4 fixed stress levels with 3 specimens

each and use the S - N data in the RFL model and the P - S data in a staircase bootstrap, thus ensuring four stress levels.

Beta Annealed Ti-6Al-4V Data Analysis

A balanced test strategy was carried out using four stress levels with three specimens each to investigate the behavior of beta annealed Ti-6Al-4V in the very high cycle regime. Results from these tests are shown in Figure 89. The behavior depicted by Figure 89 was shown to be possible when the underlying S - N curve was highly sloped with a relatively sharp transition to a horizontal fatigue limit. Unfortunately, the RFL model does not do a very good job of modeling this behavior as evidenced by the poor fit to this data (see Figure 74), as well as the poor fit (for the changing slope region) to the 68-point S - N data set from α - β Ti-6Al-4V testing (see Figure 76).

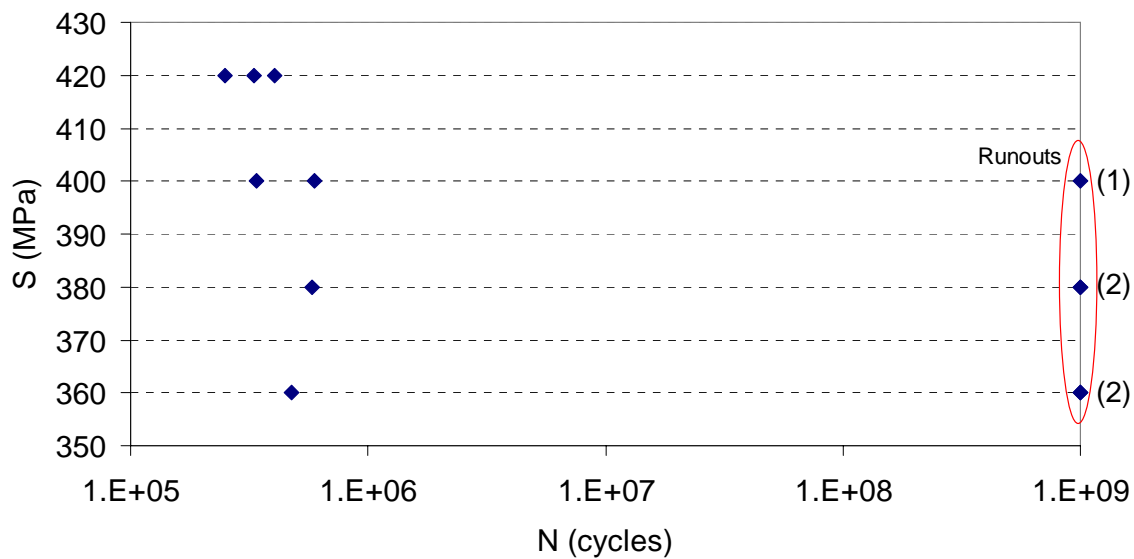


Figure 89. Experimental results for beta annealed Ti-6Al-4V tests at $R = -1$ (number of runouts in parentheses).

Two alternative models were developed to better analyze the beta annealed Ti-6Al-4V data. Since the beta annealed data appeared to behave similarly to the α - β variant in a qualitative sense, the larger α - β data set would be used to validate the models. The first model, called the bilinear (or hockey stick) model, represented the S - N behavior using a sloped line and a horizontal line (see Figure 77). The second model used the Nishijima hyperbolic model as a median S - N curve (see Figure 58). Both

models utilized the extreme value distribution as the fatigue strength distribution across all cycles, based on the results of the α - β Ti-6Al-4V residuals analysis which showed that the scatter about the S - N curve was well described by the extreme value distribution and also showed the scatter to be approximately constant as a function of number of cycles. Unlike more conventional P - S - N analysis approaches, this approach specified the fatigue strength distribution rather than the fatigue life distribution.

A maximum likelihood approach was used to estimate best-fit (most likely) model parameters for each model using the S - N data from the α - β Ti-6Al-4V data set. The results of these fits are shown in Figure 90 and Figure 91. These models appear to be in close agreement with the experimental data. Data points are spread with appropriate frequency given the probability levels. Based on the analysis of this α - β data, the proposed P - S - N models and associated maximum likelihood method provide a good fit for Ti-6Al-4V behavior. In terms of likelihood, the bilinear fit was a slightly better fit.

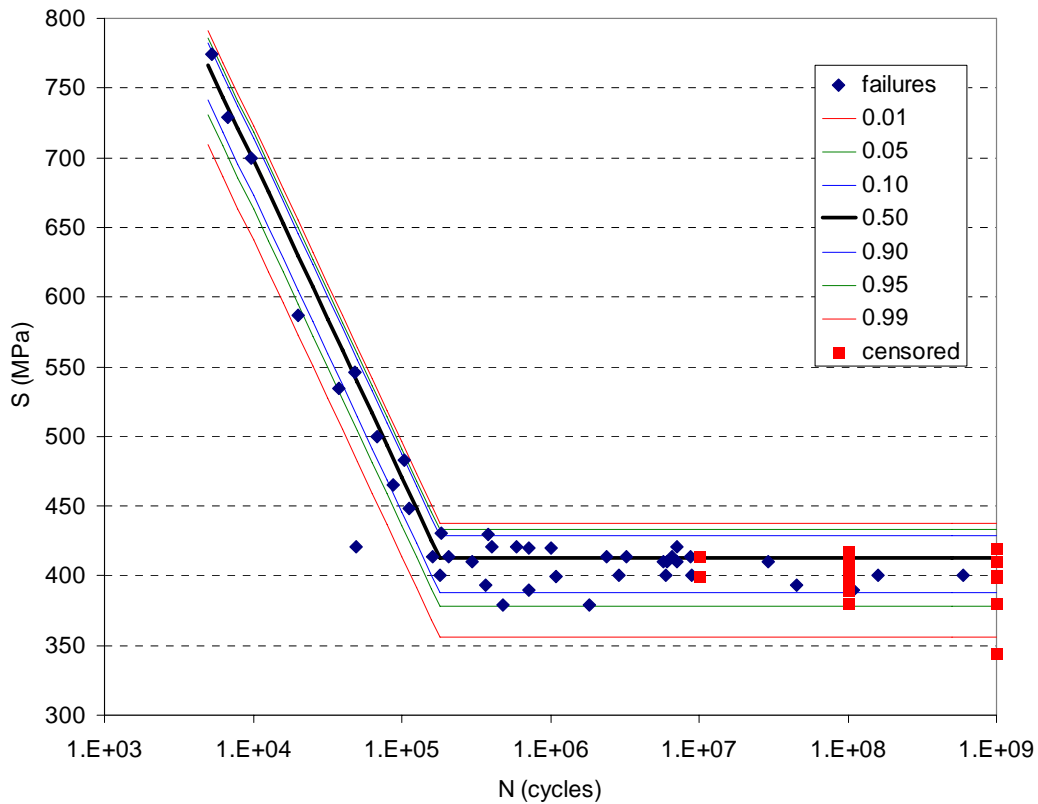


Figure 90. P - S - N plot of α - β Ti-6Al-4V data ($R = -1$) using the bilinear model with extreme value distribution for fatigue strength with constant standard deviation.

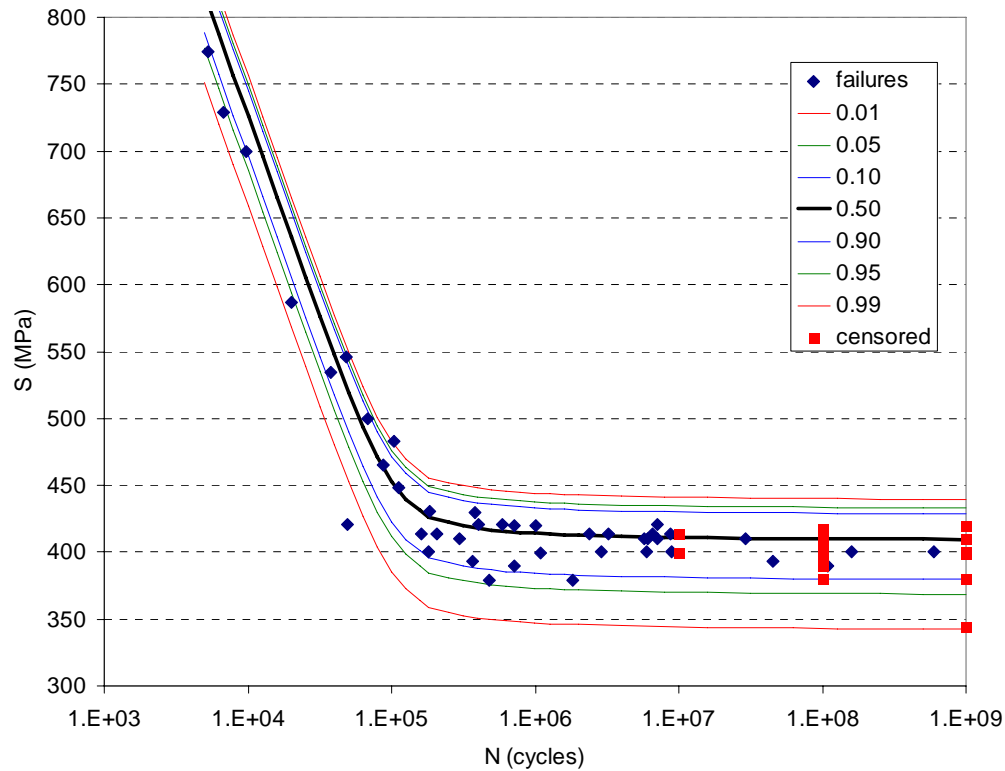


Figure 91. P - S - N plot of α - β Ti-6Al-4V data ($R = -1$) using the Nishijima model with extreme value distribution for fatigue strength with constant standard deviation.

With the proposed models validated using the larger α - β data set, the models were applied to the beta annealed Ti-6Al-4V data, with results shown in Figure 85 and Figure 86. Based on the bilinear fit, the median fatigue strength at 10^9 cycles is 397.5 MPa, with a 95% lower bound of 366.0 MPa. Based on the Nishijima fit, the median fatigue strength at 10^9 cycles is equal to 396.2 MPa, with a 95% lower bound of 361.2 MPa.

Despite a very small sample size, difficult to analyze S - N data, and the inability of the RFL model to provide a satisfying fit, the probabilistic stress-life analysis of beta annealed Ti-6Al-4V was still able to be accomplished. This analysis led to the development of two models which may be of use for future test programs with similarly behaving materials. The approach also demonstrated the utility of a maximum likelihood approach with fatigue strength, rather than fatigue life, as the primary distribution. One drawback to such an approach is that the fatigue life distribution is dependent rather than independent and may not represent real fatigue life behavior as well.

Areas for Further Research

This research effort has addressed a number of significant issues, but of course additional research opportunities still remain unaddressed. This section provides a brief overview of areas for further research which may be of interest.

Staircase Investigation

An interesting extension to the staircase analysis presented herein would be a more detailed investigation of the combined use of the proposed non-linear correction for standard deviation, the bootstrapping algorithm, and a screening test (similar to a short iteration). Due to the manual labor required by such an approach given the state of the staircase algorithm code developed for this research, investigation along these lines was rather limited. However, with the “parts” now in place (i.e., an understanding of the standard deviation bias, development of a bias correction factor, formulation of a bootstrap algorithm, and investigation of iteration behavior), the interaction of these parts may possibly be exploited to produce a more powerful staircase algorithm in the future.

Bootstrapped P-S-N Plots

Bootstrapping was shown to significantly reduce scatter in standard deviation estimates by allowing a distribution of standard deviation points to be generated from the *P-S* data generated by staircase tests. In a similar manner, bootstrapping may be applied to generate a distribution of *P-S-N* plots based on maximum likelihood analysis from a single set of *S-N* data. Relevant statistics taken from this distribution of *P-S-N* plots can then be used to provide a bootstrapped *P-S-N* plot which theoretically may be less prone to variance and a better model of true behavior despite small sample data. Such an approach may be mathematically cumbersome but once automated could provide an improved means of analyzing *S-N* behavior, specifically for tests with limited samples.

Mean Stress Effects

In this research, only fully-reversed test data were used for experimental validation and investigation. Use of mean loads to generate test data at stress ratios other than -1 could be investigated to determine if internal initiation can be observed in the α - β or beta annealed Ti-6Al-4V material. The methods developed in this research are independent of stress ratio and may be applied to testing at these other stress ratios.

Residual Stress Effects

Another means to possibly observe internally-initiated failures in Ti-6Al-4V would be to use residual stresses at the surface. Residual stresses may be induced through shot peening (or other methods such as laser shock peening or low plasticity burnishing). The compressive surface stresses have the effect of increasing the fatigue strength, and thus may allow an internally-initiated failure mode to be observed once the surface-initiated failure mode is no longer the life-controlling mechanism.

Conclusions

The research presented in this dissertation provides the designer or researcher with real analysis tools to apply to materials testing with limited samples. The modified staircase test allows a fairly straightforward, more reliable, and robust means (compared to conventional quantal response tests) of estimating fatigue strength at a given number of cycles. Thus, this method may be directly applied to address 10^9 -cycle HCF requirements outlined by the Engine Structural Improvement Program and defined in MIL-HDBK-1783B. The method utilizes quantal response data and thus would also be applicable to any application for which pass/fail responses are based on a variable input (may be a load, stress, dosage, height, etc.). In addition, the maximum likelihood models developed for the Ti-6Al-4V stress-life behavior may be applied to other materials of interest, so long as assumptions are validated. One class of materials which may benefit from such a model includes titanium matrix composites, such as the Ti-6Al-4V matrix with silicon carbide fibers currently being tested by AFRL/MLLM. In summary, this research should have real-world impact in improving current testing approaches for small-sample tests typical of high cycle and very high cycle materials programs.

APPENDIX A. EXPERIMENTAL STRESS-LIFE DATA COLLECTED FROM Ti-6Al-4V TESTS

In this appendix, the experimental results for Ti-6Al-4V fatigue tests are tabulated for easy reference. All data are part of the National HCF S&T Program [4] and all tests are conducted under fully-reversed ($R = -1$) loading under ambient air conditions.

Table 24. Fatigue data for α - β Ti-6Al-4V using conventional fatigue machines.

Specimen	Stress (MPa)	Cycles (bold = runout)
1	774.03	5.319E+03
2	729.08	6.737E+03
3	699.84	9.700E+03
4	586.49	2.020E+04
5	546.29	4.854E+04
6	534.36	3.777E+04
7	499.89	6.823E+04
8	482.65	1.034E+05
9	465.41	8.830E+04
10	448.17	1.125E+05
11	430.94	1.833E+05
12	420.60	4.963E+04
13	420.60	4.069E+05
14	420.60	5.913E+05
15	420.60	7.050E+06
16	417.15	1.000E+08
17	417.15	1.000E+08
18	413.70	2.058E+05
19	413.70	3.248E+06
20	413.70	6.554E+06
21	413.70	1.000E+07
22	413.70	1.610E+05
23	413.70	8.746E+06
24	413.70	1.000E+08
25	413.70	1.000E+08
26	413.70	2.400E+06
27	406.80	1.000E+08
28	406.80	1.000E+08
29	399.91	1.000E+07
30	399.91	1.099E+06
31	398.19	1.000E+09
32	393.02	3.634E+05
33	393.02	4.490E+07
34	393.02	1.000E+08
35	379.23	4.750E+05
36	379.23	1.835E+06
37	344.75	1.000E+09

Table 25. Fatigue data for α - β Ti-6Al-4V with stress-relief annealing and no cooling for 10^8 and 10^9 staircase tests using 20 kHz ultrasonic machine.

Specimen	Stress (MPa)	10^8 Result	Cycles	10^9 Result	Cycles
1	400	Survival	1.0E+08	Survival	1.0E+09
2	410	Survival	1.0E+08	Survival	1.0E+09
3	420	Failure	1.0E+06	Failure	1.0E+06
4	410	Survival	1.0E+08	Survival	1.0E+09
5	420	Failure	7.2E+05	Failure	7.2E+05
6	410	Failure	3.0E+05	Failure	3.0E+05
7	400	Survival	1.0E+08	Survival	1.0E+09
8	410	Survival	1.0E+08	Survival	1.0E+09
9	420	Survival	1.0E+08	Survival	1.0E+09
10	430	Failure	3.8E+05	Failure	3.8E+05

Table 26. Fatigue data for α - β Ti-6Al-4V with stress-relief annealing and with cooling for 10^8 and 10^9 staircase tests using 20 kHz ultrasonic machine.

Specimen	Stress (MPa)	10^8 Result	Cycles	10^9 Result	Cycles
1	410	Failure	5.7E+06	Failure	5.7E+06
2	400	Survival	1.0E+08	Failure	1.6E+08
3	410	Failure	6.1E+06	Failure	6.1E+06
4	400	Failure	9.0E+06	Failure	9.0E+06
5	390	Survival	1.0E+08	Failure	1.1E+08
6	400	Survival	1.0E+08	Survival	1.0E+09
7	410	Failure	2.9E+07	Failure	2.9E+07
8	400	Survival	1.0E+08	Survival	1.0E+09
9	410	Failure	7.1E+06	Failure	7.1E+06
10	400	Survival	1.0E+08	Failure	6.0E+08

Table 27. Fatigue data for α - β Ti-6Al-4V without stress-relief annealing and no cooling for 10^8 staircase tests using 20 kHz ultrasonic machine.

Specimen	Stress (MPa)	10^8 Result	Cycles
1	400	Failure	2.9E+06
2	400	Failure	1.8E+05
3	390	Failure	7.1E+05
4	380	Survival	1.0E+08
5	390	Survival	1.0E+08
6	400	Failure	6.0E+06
7	390	Survival	1.0E+08
8	400	Survival	1.0E+08

Table 28. Fatigue data for additional α - β Ti-6Al-4V tests used to supplement the stress-relief annealed staircase data.

Specimen	Stress (MPa)	10 ⁹ Result	Cycles
1	380	Survival	1.0E+09
2	380	Survival	1.0E+09
3	380	Survival	1.0E+09

Table 29. Fatigue data for beta annealed Ti-6Al-4V using 20-kHz ultrasonic machine.

Specimen	Stress (MPa)	10 ⁹ Result	Cycles
1	420	Failure	2.483E+05
2	420	Failure	3.316E+05
3	420	Failure	4.026E+05
4	400	Failure	3.399E+05
5	400	Failure	5.967E+05
6	400	Survival	1.000E+09
7	380	Failure	5.807E+05
8	380	Survival	1.000E+09
9	380	Survival	1.000E+09
10	360	Failure	4.755E+05
11	360	Survival	1.000E+09
12	360	Survival	1.000E+09

APPENDIX B. DETAILED RESULTS FOR COMPARISON OF METHODS FOR MEAN FATIGUE STRENGTH ESTIMATION

In this appendix, the various methods for calculating mean fatigue strength using staircase data are compared for tests in which the starting stress differs from the true mean, thus leading to a string of survivals or failures at the beginning of the staircase test. The methods compared include the traditional Dixon-Mood analysis [27], the modified method of Brownlee *et al* [21], Dixon's modified method for small samples [26], and Little's methods (using both maximum likelihood estimation and minimum chi-square analysis) [42]. The goal of this comparison was to determine which method provided the best estimates for mean fatigue strength for a small-sample test which starts significantly off the true mean.

A total of 40 unique simulated data sets were generated for an underlying fatigue strength distribution Normal(400,5) using a step size of 1σ . Ten of the data sets used a starting stress 4 steps below the true mean, 10 were 3 steps below, 10 were 3 steps above, and 10 were 4 steps above. Each staircase was terminated once four trials were accomplished after the initial string of survivals or failures. Survivals are denoted by "O" and failures by "X". Thus, a result may look like OOOXOXX. The data for each of the four starting stress scenarios are shown in the tables below.

Table 30. Comparison of various methods of determining fatigue strength mean for simulated data sets with true mean of 400 MPa starting 4 steps below the true mean.

	Sequence of Results	Dixon-Mood	Brownlee <i>et al</i>	Dixon	Little (MLE)	Little (min χ^2)
Run 1	OOXOOO	387.5	392.0	394.2	394.3	393.7
Run 2	OOXOOX	390.0	390.0	390.5	390.7	390.5
Run 3	OOOXOXO	392.5	393.0	393.7	393.7	393.3
Run 4	OOOXOOO	392.5	397.0	399.2	399.3	398.7
Run 5	OOOXOOX	395.0	395.0	395.7	395.7	395.5
Run 6	OOOOXXOO	395.0	396.0	396.9	396.9	396.9
Run 7	OOOOXOXX	395.8	396.0	395.9	395.9	396.2
Run 8	OOOOXOOX	400.0	400.0	400.7	400.7	400.5
Run 9	OOOOOXXOX	399.2	399.0	399.3	399.3	399.0
Run 10	OOOOOXOXX	400.8	401.0	400.9	400.9	401.2
Average		394.8	395.9	396.7	396.7	396.6

Table 31. Comparison of various methods of determining fatigue strength mean for simulated data sets with true mean of 400 MPa starting 3 steps below the true mean.

	Sequence of Results	Dixon-Mood	Brownlee <i>et al</i>	Dixon	Little (MLE)	Little (min χ^2)
Run 1	OOXOOX	395.0	395.0	395.7	395.7	395.5
Run 2	OOXOXO	392.5	393.0	393.7	393.7	393.3
Run 3	OOXOOO	392.5	397.0	399.2	399.3	398.7
Run 4	OOOXXOO	395.0	396.0	396.9	396.9	396.9
Run 5	OOOXOOX	400.0	400.0	400.7	400.7	400.5
Run 6	OOOXOXO	397.5	398.0	398.7	398.7	398.3
Run 7	OOOXOOO	397.5	402.0	404.2	404.3	403.7
Run 8	OOOOXXOO	400.0	401.0	401.9	401.9	401.9
Run 9	OOOOXOOX	405.0	405.0	405.7	405.7	405.5
Run 10	OOOOXOXX	400.8	401.0	400.9	400.9	401.2
Average		397.6	398.8	399.8	399.8	399.6

Table 32. Comparison of various methods of determining fatigue strength mean for simulated data sets with true mean of 400 MPa starting 3 steps above the true mean.

	Sequence of Results	Dixon-Mood	Brownlee <i>et al</i>	Dixon	Little (MLE)	Little (min χ^2)
Run 1	XXOXXX	407.5	403.0	400.8	398.9	401.8
Run 2	XXOOXX	410.0	409.0	408.1	408.1	408.1
Run 3	XXOXXO	405.0	403.0	404.3	404.3	404.6
Run 4	XXXOXOX	402.5	402.0	401.3	401.3	401.7
Run 5	XXXOXXX	402.5	398.0	395.8	393.9	396.8
Run 6	XXXOOXX	405.0	404.0	403.1	403.1	403.1
Run 7	XXXXOOXO	400.8	401.0	400.7	400.7	401.0
Run 8	XXXXOXOO	400.0	399.0	399.1	398.9	399.2
Run 9	XXXXOOXX	400.0	399.0	398.1	397.0	398.8
Run 10	XXXXOXOX	397.5	397.0	396.3	395.2	396.9
Average		403.8	401.5	400.8	400.1	401.2

Table 33. Comparison of various methods of determining fatigue strength mean for simulated data sets with true mean of 400 MPa starting 4 steps above the true mean.

	Sequence of Results	Dixon-Mood	Brownlee <i>et al</i>	Dixon	Little (MLE)	Little (min χ^2)
Run 1	XXOXXO	410.0	410.0	409.3	409.3	409.6
Run 2	XXOXXX	412.5	408.0	405.8	405.8	406.3
Run 3	XXOXOX	412.5	412.0	411.3	411.3	411.8
Run 4	XXXOOXX	410.0	407.0	408.1	408.1	408.1
Run 5	XXXOXXX	407.5	403.0	400.8	400.8	401.3
Run 6	XXXOXOX	407.5	407.0	406.3	406.3	406.7
Run 7	XXXOXXO	405.0	405.0	404.3	404.3	404.6
Run 8	XXXXOXXX	402.5	398.0	395.8	395.8	396.3
Run 9	XXXXOXXO	400.0	400.0	399.3	399.3	399.6
Run 10	XXXXOOOX	405.0	406.0	403.1	403.1	403.1
Average		407.3	405.6	404.4	404.4	404.7

In general, both the Little and Dixon MLE-based methods provide a better estimate (compared to the other methods) for mean fatigue strength for a small set of staircase data with leading string of same-result data points. However, when the Dixon-Mood estimate is slightly too high (if starting below) or too low (if starting high), the corrected means may actually make the result slightly worse. Note, however, that these results are statistically less probable. In other words, when starting low, it is far more likely that the result will be low rather than high (and vice versa). Thus, on average, the corrections work quite well.

APPENDIX C. OVERVIEW OF RABB'S USE OF SIZE EFFECT FOR ESTIMATING FATIGUE STRENGTH STANDARD DEVIATION

In this appendix, a brief overview of Rabb's approach to using size effect as a means of standard deviation is presented [73].

Rabb noted that it is well known that a size factor influences the fatigue limit for a given specimen – specimens stressed over larger areas have lower fatigue limits than those stressed over smaller areas. Rabb used the concept of a size factor to develop a method of evaluating the standard deviation of the fatigue strength. His premise is summarized by the following:

“The statistical size factor is basically determined by the effective stress area, or in some cases, the effective stress volume, and the standard deviation of the fatigue limit. ... It is therefore possible to evaluate a reliable estimate of the standard deviation by calculating it from the observed statistical size effect from two staircase tests with different specimen sizes.” [73]

The standard deviation of the material's fatigue strength is determined using the following approach. First, the ratio η is obtained (Rabb used n to denote this ratio as it represents the number of links from the theory of weakest link developed by Rabb and Makkonen, but it will be denoted as η to avoid confusion with sample sizes). An approximation for η is found as the ratio of effective stress areas, where A_1 is the effective stress area of the specimens with larger stress area and A_2 is the effective stress area of the specimens with smaller stress area, so that:

$$\eta = \frac{A_1}{A_2} \quad (64)$$

Unfortunately, calculation of the effective stress areas appears to be no trivial task. Rabb states that the effective stress area can be estimated by dividing the surface of the specimen into a number of subareas A_i , each with average stress σ_i . He then uses the following relations, where s_r is the relative standard deviation of the fatigue strength of the material (i.e., $s_r = \sigma/\mu$) which obviously must be approximated since σ (the true

standard deviation of the fatigue strength, not to be confused with stress) is the unknown which the method seeks to determine:

$$A_{eff} = \sum_i \frac{\log R_i}{\log 0.5} A_i, \text{ with } R_i = \frac{1}{\sqrt{2\pi}} \cdot \int_{\lambda_i}^{\infty} \exp\left(-\frac{x^2}{2}\right) dx, \text{ and } \lambda_i = \frac{1}{s_r} \left(\frac{\sigma_i}{\sigma_{\max}} - 1 \right) \quad (65)$$

Assuming that effective stress areas can be found using the relations above or some other theoretical or numerical method, the next step is to conduct staircase tests for each specimen size, yielding estimates for mean fatigue strength ($\hat{\mu}_1$ and $\hat{\mu}_2$) using any reliable method to analyze staircase data. Now, the statistical size factor K_{size} is found simply as the ratio of the two mean fatigue strengths:

$$K_{size} = \frac{\hat{\mu}_2}{\hat{\mu}_1} \quad (66)$$

Note that K_{size} should be greater than 1 since specimens with larger effective stress areas (denoted by subscript 1) should have lower fatigue strengths compared to specimens with smaller stress areas (denoted by subscript 2). Next, the value λ of the standard normal variable is determined iteratively from the following equation, where η is already defined:

$$R = \eta \sqrt{0.5} = \frac{1}{\sqrt{2\pi}} \cdot \int_{\lambda}^{\infty} \exp\left(-\frac{x^2}{2}\right) dx \quad (67)$$

Finally, with K_{size} and λ known, the relative standard deviation s_r is given by the following equation:

$$s_r = \frac{1}{\lambda} \left(\frac{1}{K_{size}} - 1 \right) \quad (68)$$

Rabb's paper presents details for determining the statistical confidence bounds of the relative standard deviation using the chi-square distribution.

This novel method has one distinct advantage. Namely, the standard deviation estimate is derived primarily from the statistical size factor K_{size} which is determined as the ratio of two mean fatigue strengths. Since the staircase test is both accurate and efficient in calculating mean fatigue strength, this ratio is not prone to the kinds of errors inherent with standard deviation estimation using the Dixon-Mood method. Nowhere in

the analysis is the generally unreliable standard deviation estimate from staircase analysis necessary. However, the method does require a reliable means to estimate effective stress areas. This problem may be quite difficult in itself.

Although this method may have merit, it is not explored further in this study. Use of the method would require the machining and testing of test specimens of different sizes which would still produce resonance at 20 kHz for tests conducted on the AFRL/MLLM ultrasonic fatigue testing machine.

APPENDIX D. STAIRCASE SIMULATION CODE

The MATLAB™ code used for each element of the staircase simulation is presented in this appendix. Some elements were modified as needed to address specific questions.

Master Simulation File (fls_sim_master.m)

This code was used to run a batch of simulations using a text file for input data and calls a staircase analysis module (fls_sim_calcs.m) to analyze the staircase data for each trial. Output data is stored in a text file and may be shown graphically in summary format or detailed results for each iteration (should only be selected if running a few iterations or it will take a very long time to complete).

```
% Purpose: Run a series of staircase sim cases based on input file.
% Input:   input.dat -- data file of simulation cases.
% Required: fls_sim_calcs.m -- runs staircase sim for each case.
% Output:  output.dat -- data file of statistics of interest.

clear all; clc;

% Read input file (each row is a different simulation case).

% Parameters for each case are listed in 6 columns:
%   truedist = ID for underlying FLS distribution (1 = normal).
%   truemean = mean of underlying FLS distribution.
%   truestdv = std dev of underlying FLS distribution.
%   initstress = initial stress used to start staircase test.
%   step_s = step used in staircase test in units of true std deviations.
%   n = number of specimens to be used for each staircase simulation.

datafile = load('input.dat');
for s = 1:size(datafile,1)
    truedist_v(s) = round(datafile(s,1));
    truemean_v(s) = datafile(s,2);
    truestdv_v(s) = datafile(s,3);
    step_v(s) = datafile(s,4)*truestdv_v(s);
    initstress_v(s) = datafile(s,5);
    n_v(s) = round(datafile(s,6));
end

% Set simulation parameters.

m = 1000;           % Number of iterations used for each simulation case.
graphics = 0;       % 0 = graphics off, 1 = case summary, 2 = each iteration.
                    % Unless running only a couple cases, turn graphics off.
alpha = 0.05;       % Significance level used for confidence intervals.
maxtime = 1000;     % Sets the max time before simulation times out.
trouble = 0;        % Sets trouble-shooting display indicator to NO.

% Run all the simulation cases. Note that a "while" loop (rather than a
% "for" loop) was used in order to terminate the simulation after a specified
% time. Note, however, that this time only affects whether another case is
% started or not. If there is a delay due to internal calculations in a
% particular case, the program will not timeout until the case is complete
% (but, at least another case will not be started).

tic % Start timer.
```

```

s = 1; % Initialize simulation case counter.
timeout = 0;
fid = fopen('output.dat','w+'); % Opens output data file.
while s <= size(datafile,1)
    truedist = truedist_v(s);
    truemean = truemean_v(s);
    truestdv = truestdv_v(s);
    step = step_v(s);
    initstress = initstress_v(s);
    n = n_v(s);
    fls_sim_calcs;
    output(s,1) = mean(sigma);
    output(s,2) = std(sigma);
    output(s,3) = prctile(sigma, 10);
    output(s,4) = prctile(sigma, 20);
    output(s,5) = prctile(sigma, 30);
    output(s,6) = prctile(sigma, 40);
    output(s,7) = prctile(sigma, 50);
    output(s,8) = prctile(sigma, 60);
    output(s,9) = prctile(sigma, 70);
    output(s,10) = prctile(sigma, 80);
    output(s,11) = prctile(sigma, 90);
    time = toc;
    totalcases = s;
    fprintf(fid,'%7.4f \t %7.4f \t %7.4f \t %7.4f \t %7.4f \t %7.4f \t %7.4f \t %7.4f \t %7.4f \t %7.4f \n',output(s,:));
    if time > maxtime
        timeout = 1;
        s = size(datafile,1) + 1;
    else
        s = s + 1;
    end
end
fclose(fid); % Close output data file.

% At this point, we have an R x 10 matrix of output data, where R is the
% number of completed cases. Each row corresponds to a simulation case
% with the mean, std dev, median, LCB, and UCB for both mu and sigma.
% Here, mu is the calculated FLS mean and sigma is the calculated FLS std
% dev using the Dixon-Mood method. LCB and UCB are the lower and upper
% confidence bounds.

% Display input and output on screen.

datafile
output
if timeout == 1
    disp(['Simulation timed out.']);
end
disp(['Cases completed: ', int2str(totalcases), ' of ', int2str(size(datafile,1))]);
disp([' ']);

```

Staircase Simulator and Analyzer (fls_sim_calcs.m)

This code was used to simulate a staircase test given input parameters provided by the fls_sim_master.m program, or it can be used as stand-alone if comment markers on variable identities are removed. The fatigue strength statistics given the simulated data are determined using the Dixon-Mood method.

```

% Purpose: Run a specified staircase simulation to determine fatigue limit stress
%          (FLS) mean and std dev.
% Input:   Parameters preset when called by fls_sim_master.m.
% Output:  Results stored in variables mu and sigma (vectors of values for

```

```

%           FLS mean and standard deviation).

clear fls stresses result stresslevel P S mu sigma count fail live k;

% Input parameters are set within fls_sim_master.m before this file is
% called. However, if this file is used as stand-alone, then the following
% input dialogue can be used (must remove comment markers).

% disp(['*** FATIGUE LIMIT DISTRIBUTION PARAMETERS ***']);
% truedist = input('Enter distribution (1 = normal): ');
% truemmean = input('Enter mean of distribution: ');
% truestdv = input('Enter standard deviation of distribution: ');
% disp(['*** STAIRCASE TEST PARAMETERS ***']);
% initstress = input('Enter initial stress level: ');
% step = input('Enter step size (interval): ');
% n = input('Enter number of specimens for testing: ');
% disp(['*** SIMULATION PARAMETERS ***']);
% m = input('Enter number of iterations: ');
% graphics = input('Graphics (0 = off, 1 = summary only, 2 = each iteration): ');
% trouble = input('Troubleshooting (0 = off, 1 = display variables): ');

% Begin the staircase test simulation.

for i = 1:m % Outer loop based on number of specified iterations.

% This portion generates a random FLS and compares it to current stress
% level to determine if the specimen failed or survived. If it failed, the
% stress level is reduced. If it survived, the stress level is increased.

    stress = initstress; % Initial stress level for staircase test.
    sumfail = 0; % Initialize number of failures to zero.
    sumlive = 0; % Initialize number of survivals to zero.
    for j = 1:n % "j" loops will always correspond to number of specimens.
        if truedist == 1
            fls(j) = normrnd(truemmean,truestdv);
        else
            disp(['ERROR: User did not select a supported distribution.']);
        end
        stresses(j) = stress; % Stress at which specimen j was tested.
        if stress > fls(j)
            result(j) = 1; % Specimen failed.
            sumfail = sumfail + 1;
            stress = stress - step;
        else
            result(j) = 0; % Specimen survived.
            sumlive = sumlive + 1;
            stress = stress + step;
        end
    end
end

% This portion finds the stress corresponding to i = 0 using the Dixon-Mood
% notation. This stress level is dependent on whether most specimens failed
% (then it is the lowest stress level corresponding to a survival) or
% survived (then it is the lowest stress level corresponding to a failure).

    stress0 = 1.0e+12; % Initialize stress0 to outrageously high number.
    if sumfail <= sumlive
        for j = 1:n
            if (result(j) == 1) & (stresses(j) < stress0)
                stress0 = stresses(j);
            end
        end
    else
        for j = 1:n
            if (result(j) == 0) & (stresses(j) < stress0)
                stress0 = stresses(j);
            end
        end
    end

end

% This portion determines the number of occurrences and failures at each

```



```

% stress level. Note that the index identifying stress level must be
% adjusted so that all vector indices are >= 1 as required by MATLAB.
% Data for P-S plot are also generated.

kmax = 0; % Maximum stress level tested relative to stress0.
kmin = 0; % Minimum stress level tested relative to stress0.
for j = 1:n % Determines the max and min stress levels.
    stresslevel(j) = round((stresses(j) - stress0)/step);
    if stresslevel(j) > kmax
        kmax = stresslevel(j);
    elseif stresslevel(j) < kmin
        kmin = stresslevel(j);
    end
end
for k = 1:(kmax - kmin + 1)
    count(k) = 0; % Initialize count of occurrences at each level.
    fail(k) = 0; % Initialize count of failures at each level.
    live(k) = 0; % Initialize count of survivals at each level.
end
for j = 1:n % Count number of stress level occurrences and failures.
    adjstresslevel = stresslevel(j) - kmin + 1; % Adjusted to be >= 1.
    count(adjstresslevel) = count(adjstresslevel) + 1;
    if result(j) == 1
        fail(adjstresslevel) = fail(adjstresslevel) + 1;
    else
        live(adjstresslevel) = live(adjstresslevel) + 1;
    end
    P(adjstresslevel) = fail(adjstresslevel)/count(adjstresslevel);
end
for k = 1:(kmax - kmin + 1)
    h = k + kmin - 1; % Readjusts stress level back to 0:kmax scale.
    S(k) = stress0 + h*step;
end

% This portion calculates mean and standard deviation of FLS for each
% iteration using the statistics of the Dixon-Mood method. Note that this
% analysis assumes a normal distribution for FLS. Also, note that the
% summation over k = (- kmin + 1):(kmax - kmin + 1) corresponds to the
% summation over i = 0:i_max using the Dixon-Mood method's notation.

sum_mi = 0; % Initialize summations used in Dixon-Mood statistics.
sum_imi = 0;
sum_iimi = 0;

for k = (- kmin + 1):(kmax - kmin + 1)
    h = k + kmin - 1; % Readjusts stress level back to 0:kmax scale.
    if sumfail > sumlive
        mi = live(k);
    else
        mi = fail(k);
    end
    sum_mi = sum_mi + mi;
    sum_imi = sum_imi + h*mi;
    sum_iimi = sum_iimi + h*h*mi;
end

if sumfail > sumlive
    mu(i) = stress0 + step*(sum_imi/sum_mi + 0.5);
else
    mu(i) = stress0 + step*(sum_imi/sum_mi - 0.5);
end
uglyterm = (sum_mi*sum_iimi - sum_imi*sum_imi)/(sum_mi^2);
if uglyterm > 0.3
    sigma(i) = 1.62*step*(uglyterm + 0.029);
else
    sigma(i) = 0.53*step;
end

% Troubleshooting. Remove semicolons to investigate variables.

if trouble == 1

```

```

disp(['DATA BY SPECIMEN']);
fls
stresses
result
sumfail
sumlive
stresslevel
disp(['DATA BY STRESS LEVEL']);
count
fail
live
disp(['DATA USED IN CALCS']);
kmin
kmax
sum_mi
sum_imi
sum_iimi
uglyterm
mu
sigma
end

% This portion displays results for each iteration if so selected by user.
% Intermediate results allow the user to visualize results, sanity check,
% and troubleshoot.

if graphics == 2
    subplot(2,2,1);
    hist(fls)
    title('Actual fatigue limit strengths generated');
    xlabel('Stress');
    ylabel('Frequency');
    subplot(2,2,2);
    plot(stresses, 'r-x')
    axis([1 n min(stresses) max(stresses)]);
    title('Staircase test results');
    xlabel('Specimen');
    ylabel('Stress');
    subplot(2,2,3);
    plot(S,P, '-o')
    title('P-S data');
    xlabel('Stress');
    ylabel('Percent failures');
    subplot(2,2,4);
    bar(stresslevel)
    title('Staircase test results');
    axis([1 n kmin kmax]);
    xlabel('Specimen');
    ylabel('Stress level (steps)');
    disp([' ']);
    disp(['Iteration: ', int2str(i)]);
    mu
    sigma
    pause = input('Press <Enter> to continue to next iteration: ');
end

end

% At this point, we have two vectors "mu" and "sigma", each of m elements
% (the number of iterations). So, we have created a distribution for both
% the mean and standard deviation of FLS based on simulated iterations of a
% staircase test program. Summary output is displayed if selected by user.

if graphics > 0
    newplot
    subplot(1,2,1);
    hist(mu)
    title('Distribution of FLS mean');
    xlabel('Stress');
    ylabel('Frequency');
    subplot(1,2,2);

```

```

hist(sigma)
title('Distribution of FLS std dev');
xlabel('Stress');
ylabel('Frequency');
disp([' ']);
disp(['*** SUMMARY RESULTS ***']);
disp([' ']);
p = 100*[0 0.05 0.1 0.25 0.5 0.75 0.9 0.95 1];
disp(['Results for mean of FLS (distribution of mu): ']);
disp([' Mean = ', num2str(mean(mu))]);
disp([' Std Dev = ', num2str(std(mu))]);
if m > 1
    y = prctile(mu,p);
    percentiles_for_mu = transpose([p;y])
end
disp(['Results for std dev of FLS (distribution of sigma): ']);
disp([' Mean = ', num2str(mean(sigma))]);
disp([' Std Dev = ', num2str(std(sigma))]);
if m > 1
    z = prctile(sigma,p);
    percentiles_for_sigma = transpose([p;z])
end
end
end

```

Detailed Staircase Simulator and Analyzer (stair.m)

This code was used to simulate a staircase test and calculate fatigue strength statistics using Dixon-Mood analysis, Svensson-Lorén correction, and the proposed correction. The P - S data from the simulated staircase is stored in variables $Pstar$ and $Sstar$, which can be used by the bootstrapping algorithm to provide bootstrapped results. Note that Pollak correction constants are hardcoded based on the number of specimens.

```

% Purpose:  Generate a simulated staircase test given an initial stress,
%           step size, and number of specimens.

clear all; clc;

% Input parameters.

truedist = 1;
truemean = 400;      % Must specify.
truestdv = 10;       % Must specify.
step = 5;            % Must specify.
initstress = 400;    % Must specify.
n = 15;              % Must specify.
m = 1;              % Number of iterations.

% Simulate a staircase test based on these parameters.

% This portion generates a random FLS and compares it to current stress
% level to determine if the specimen failed or survived.  If it failed, the
% stress level is reduced.  If it survived, the stress level is increased.

stress = initstress; % Initial stress level for staircase test.
sumfail = 0; % Initialize number of failures to zero.
sumlive = 0; % Initialize number of survivals to zero.
for j = 1:n % "j" loops will always correspond to number of specimens.
    if truedist == 1
        fls(j) = normrnd(truemean,truestdv);
    else
        disp(['ERROR:  User did not select a supported distribution.']);
    end
end

```

```

    stresses(j) = stress; % Stress at which specimen j was tested.
    if stress > fls(j)
        result(j) = 1; % Specimen failed.
        sumfail = sumfail + 1;
        stress = stress - step;
    else
        result(j) = 0; % Specimen survived.
        sumlive = sumlive + 1;
        stress = stress + step;
    end
end

% This portion finds the stress corresponding to i = 0 using the Dixon-Mood
% notation. This stress level is dependent on whether most specimens failed
% (then it is the lowest stress level corresponding to a survival) or
% survived (then it is the lowest stress level corresponding to a failure).

stress0 = 1.0e+12; % Initialize stress0 to outrageously high number.
if sumfail <= sumlive
    for j = 1:n
        if (result(j) == 1) & (stresses(j) < stress0)
            stress0 = stresses(j);
        end
    end
else
    for j = 1:n
        if (result(j) == 0) & (stresses(j) < stress0)
            stress0 = stresses(j);
        end
    end
end

% This portion determines the number of occurrences and failures at each
% stress level. Note that the index identifying stress level must be
% adjusted so that all vector indices are >= 1 as required by MATLAB.
% Data for P-S plot are also generated.

kmax = 0; % Maximum stress level tested relative to stress0.
kmin = 0; % Minimum stress level tested relative to stress0.
for j = 1:n % Determines the max and min stress levels.
    stresslevel(j) = round((stresses(j) - stress0)/step);
    if stresslevel(j) > kmax
        kmax = stresslevel(j);
    elseif stresslevel(j) < kmin
        kmin = stresslevel(j);
    end
end
for k = 1:(kmax - kmin + 1)
    count(k) = 0; % Initialize count of occurrences at each level.
    fail(k) = 0; % Initialize count of failures at each level.
    live(k) = 0; % Initialize count of survivals at each level.
end
for j = 1:n % Count number of stress level occurrences and failures.
    adjstresslevel = stresslevel(j) - kmin + 1; % Adjusted to be >= 1.
    count(adjstresslevel) = count(adjstresslevel) + 1;
    if result(j) == 1
        fail(adjstresslevel) = fail(adjstresslevel) + 1;
    else
        live(adjstresslevel) = live(adjstresslevel) + 1;
    end
    P(adjstresslevel) = fail(adjstresslevel)/count(adjstresslevel);
end
for k = 1:(kmax - kmin + 1)
    h = k + kmin - 1; % Readjusts stress level back to 0:kmax scale.
    S(k) = stress0 + h*step;
end

% This portion calculates mean and standard deviation of FLS for each
% iteration using the statistics of the Dixon-Mood method. Note that this
% analysis assumes a normal distribution for FLS. Also, note that the
% summation over k = (- kmin + 1):(kmax - kmin + 1) corresponds to the

```

```

% summation over i = 0:i_max using the Dixon-Mood method's notation.

i = 1;

sum_mi = 0; % Initialize summations used in Dixon-Mood statistics.
sum_imi = 0;
sum_iimi = 0;

for k = (- kmin + 1):(kmax - kmin + 1)
    h = k + kmin - 1; % Readjusts stress level back to 0:kmax scale.
    if sumfail > sumlive
        mi = live(k);
    else
        mi = fail(k);
    end
    sum_mi = sum_mi + mi;
    sum_imi = sum_imi + h*mi;
    sum_iimi = sum_iimi + h*h*mi;
end

if sumfail > sumlive
    mu(i) = stress0 + step*(sum_imi/sum_mi + 0.5);
else
    mu(i) = stress0 + step*(sum_imi/sum_mi - 0.5);
end
uglyterm = (sum_mi*sum_iimi - sum_imi*sum_imi)/(sum_mi^2);
if uglyterm > 0.3
    sigma(i) = 1.62*step*(uglyterm + 0.029);
else
    sigma(i) = 0.53*step;
end

Pstar = P
Sstar = S
sigmaDM = sigma % D-M std dev.
sigmaSV = sigma*(n/(n-3)) % Svensson-Loren std dev.
sigmaPO = 0.97*sigma*(n/(n-3))*((1.2*sigma/step)^0.55) % Pollak-corrected std dev.
ratio1 = sigmaDM/step
ratio2 = sigmaPO/sigmaSV

```

Bootstrap Controller (bootcontrol.m)

This code was used to set the staircase parameters and define the staircase results used for a bootstrap analysis. The program uses the bootsim.m code to perform the actual staircase analysis for each bootstrap iteration. Note that bootcontrol.m is the command the user must type to run the bootstrap algorithm, not bootsim.m (which is just called by bootcontrol.m internally).

```

% Purpose: Perform staircase study with bootstrap.

clear all;
alpha = 0.05; % Significance level used for confidence intervals.

% Specify staircase parameters:
initstress = 400;
step = 6.5;
n = 12;

% Specify staircase results:
Pstar = [0 0.333 0.667 1]; % P data from lowest to highest stress level.
Sstar = [380.5 387 393.5 400]; % S data from lowest to highest stress level.

```

```

i = 1;
while i <= 5000
    bootsim;
    i = i + 1;
end

sigmaBT = mean(sigma)           % Dixon-Mood.
sigmaBT_SV = mean(sigma2)       % Svensson-Loren.
sigmaBT_PO = mean(sigma3)       % Pollak correction.

```

Bootstrap Simulator (bootsim.m)

This code is called just a function called by bootcontrol.m to perform a single iteration of the bootstrap algorithm. The program is not explicitly run but is called by bootcontrol.m to perform the required analysis. Note that Pollak correction constants are hardcoded based on the number of specimens.

```

% Purpose: Generate a simulated staircase test using bootstrap.

clear P S x stresses result stresslevel count fail live k;

% "offset" corresponds to the number of steps up the initial stress level is from
% the lowest stress level for which P-S data is available.

offset = round((initstress-Sstar(1))/step);
index = offset + 1; % Sets the initial index for P-S data.

% Simulate a staircase test based on these parameters.

% This portion generates a random FLS and compares it to current stress
% level to determine if the specimen failed or survived. If it failed, the
% stress level is reduced. If it survived, the stress level is increased.

stress = initstress; % Initial stress level for staircase test.
sumfail = 0; % Initialize number of failures to zero.
sumlive = 0; % Initialize number of survivals to zero.
for j = 1:n % "j" corresponds to number of specimens.
    x(j) = rand; % Random number.
    stresses(j) = stress; % Stress at which specimen j was tested.
    if x(j) <= Pstar(index)
        result(j) = 1; % Specimen failed.
        sumfail = sumfail + 1;
        stress = stress - step;
        index = index - 1;
    else
        result(j) = 0; % Specimen survived.
        sumlive = sumlive + 1;
        stress = stress + step;
        index = index + 1;
    end
end
end

% This portion finds the stress corresponding to i = 0 using the Dixon-Mood
% notation. This stress level is dependent on whether most specimens failed
% (then it is the lowest stress level corresponding to a survival) or
% survived (then it is the lowest stress level corresponding to a failure).

stress0 = 1.0e+12; % Initialize stress0 to outrageously high number.
if sumfail <= sumlive
    for j = 1:n
        if (result(j) == 1) & (stresses(j) < stress0)
            stress0 = stresses(j);
        end
    end
end

```

```

        end
    else
        for j = 1:n
            if (result(j) == 0) & (stresses(j) < stress0)
                stress0 = stresses(j);
            end
        end
    end
end

% This portion determines the number of occurrences and failures at each
% stress level. Note that the index identifying stress level must be
% adjusted so that all vector indices are >= 1 as required by MATLAB.
% Data for P-S plot are also generated.

kmax = 0; % Maximum stress level tested relative to stress0.
kmin = 0; % Minimum stress level tested relative to stress0.
for j = 1:n % Determines the max and min stress levels.
    stresslevel(j) = round((stresses(j) - stress0)/step);
    if stresslevel(j) > kmax
        kmax = stresslevel(j);
    elseif stresslevel(j) < kmin
        kmin = stresslevel(j);
    end
end
for k = 1:(kmax - kmin + 1)
    count(k) = 0; % Initialize count of occurrences at each level.
    fail(k) = 0; % Initialize count of failures at each level.
    live(k) = 0; % Initialize count of survivals at each level.
end
for j = 1:n % Count number of stress level occurrences and failures.
    adjstresslevel = stresslevel(j) - kmin + 1; % Adjusted to be >= 1.
    count(adjstresslevel) = count(adjstresslevel) + 1;
    if result(j) == 1
        fail(adjstresslevel) = fail(adjstresslevel) + 1;
    else
        live(adjstresslevel) = live(adjstresslevel) + 1;
    end
    P(adjstresslevel) = fail(adjstresslevel)/count(adjstresslevel);
end
for k = 1:(kmax - kmin + 1)
    h = k + kmin - 1; % Readjusts stress level back to 0:kmax scale.
    S(k) = stress0 + h*step;
end

% This portion calculates mean and standard deviation of FLS for each
% iteration using the statistics of the Dixon-Mood method. Note that this
% analysis assumes a normal distribution for FLS. Also, note that the
% summation over k = (- kmin + 1):(kmax - kmin + 1) corresponds to the
% summation over i = 0:i_max using the Dixon-Mood method's notation.

sum_mi = 0; % Initialize summations used in Dixon-Mood statistics.
sum_imi = 0;
sum_iimi = 0;

for k = (- kmin + 1):(kmax - kmin + 1)
    h = k + kmin - 1; % Readjusts stress level back to 0:kmax scale.
    if sumfail > sumlive
        mi = live(k);
    else
        mi = fail(k);
    end
    sum_mi = sum_mi + mi;
    sum_imi = sum_imi + h*mi;
    sum_iimi = sum_iimi + h*h*mi;
end

if sumfail > sumlive
    mu(i) = stress0 + step*(sum_imi/sum_mi + 0.5);
else
    mu(i) = stress0 + step*(sum_imi/sum_mi - 0.5);
end
end

```

```

        uglyterm = (sum_mi*sum_iimi - sum_imi*sum_imi)/(sum_mi^2);
        if uglyterm > 0.3
            sigma(i) = 1.62*step*(uglyterm + 0.029);
        else
            sigma(i) = 0.53*step;
        end

% CORRECTION TERMS.
sigma2(i) = sigma(i)*(n/(n-3)); % Svensson-Loren.
sigma3(i) = 1.04*sigma(i)*(n/(n-3))*((1.2*sigma(i)/step)^0.78); % Pollak.

```

Advanced Staircase Simulator with Iteration (advstrat.m)

This code allows the user to analyze a desired sequence of iterative staircases with or without bootstrapping. The parameters of each staircase within each iteration may be varied. The user can set the parameter setting within the code to adjust the starting parameters (initial stress and step) and the parameters within each subsequence (number of specimens, step, bootstrapping). This is the command typed by the user, while the programs advstair.m, advcalcs.m, and advboot.m are called by this program internally.

```

% Run a simulation of a complete staircase test program strategy.
% R. Pollak, AFIT/ENY, Nov 2004.

clear all; clc;

% Set variable values.

truedist = 1; % True underlying FLS distribution, 1 = normal.
truemean = 400; % True mean of underlying FLS distribution.
truestdv = 1; % True std dev of underlying FLS distribution.
initmean = 400; % Initial estimate for mean.
initstdv = 0.5; % Initial estimate for std dev.
nv = [8 0 0 0 0 0 0 0 0 0 0 0]; % Number of specimens for each subtest (up to 12).
sv = [0.5 1.0 1.7 1.7 1.7 1.7 1.7 1.7 1.7 1.7 1.7 1.7]; % Step sizes (/s) for each subtest.
boot = [1 0 0 0 0 0 0 0 0 0 0 0]; % If boot(t) = 1, then bootstrap for subtest t.
mtot = 500; % Number of total iterations to simulate.
mboot = 500; % Number of iterations used for bootstrap routine.

% Index "i" corresponds to simulation iteration (1 through mtot).
% Index "t" corresponds to subtest number (1 through subs).
% Index "j" corresponds to specimen number (1 through nplus(t)).
% Index "b" corresponds to bootstrap iteration (1 through mboot).
% A failure is denoted by result = 1 (success is result = 0).

subs = 0;
for c = 1:12
    if nv(c) > 0
        subs = subs + 1; % Quick loop to calculate # of subtests used.
    end
end
for i = 1:mtot
    initstress = initmean;
    stdv = initstdv;
    nplus(i,:) = [0 0 0 0 0 0 0 0 0 0 0 0];
    ntot(i) = 0;
    for t = 1:subs
        step = stdv * sv(t); % Sets step size for subtest staircase.
    end
end

```



```

        n = nv(t);                % Sets specimen size for subtest staircase.
        advstair;                 % Runs a simulated subtest staircase.
        n = j;                   % Updates n based on simulated subtest.
        nplus(i,t) = j;          % Stores actual n for each subtest.
        advcalcs;                % DM method to calculate mu and sigma.
        musub(i,t) = mu;         % Mean estimate.
        sigmasub(i,t) = sigma;   % Std dev estimate.
        if boot(t) == 1
            Pstar = P;           % Stores P vector for use in bootstrap.
            Sstar = S;           % Stores S vector for use in bootstrap.
            advboot;              % Bootstrap used to improve sigma estimate.
            sigmaboostsub(i,t) = newsigma; % Updated std dev estimate.
            stdv = newsigma;      % Sets std dev estimate for next subtest.
        else
            sigmaboostsub(i,t) = 0;
            stdv = sigma;        % Sets std dev estimate for next subtest.
        end
        initstress = mu;         % Sets mean estimate for next subtest.
        ntot(i) = ntot(i) + nplus(i,t);
    end
end

% Display results.

for t = 1:subs
    disp(['RESULTS FOR SUBTEST #', int2str(t)]);
    disp([' Mean of sigma = ', num2str(mean(sigmasub(:,t)))]);
    disp([' StDv of sigma = ', num2str(std(sigmasub(:,t)))]);
    disp([' Mean of sigmaboost = ', num2str(mean(sigmaboostsub(:,t)))]);
    disp([' StDv of sigmaboost = ', num2str(std(sigmaboostsub(:,t)))]);
    disp([' Median of sigmaboost = ', num2str(median(sigmaboostsub(:,t)))]);
    disp([' 95% LCB of sigmaboost = ', num2str(prctile(sigmaboostsub(:,t),5))]);
    disp([' 95% UCB of sigmaboost = ', num2str(prctile(sigmaboostsub(:,t),95))]);
end
disp(['AVG SPECIMENS: ', num2str(mean(ntot(:)))]);

% Save results to file.

fid = fopen('output2.dat','w+'); % Opens output data file.
for i=1:mtot
    for t=1:subs
        fprintf(fid,'%7.4f \t', musub(i,t));
        fprintf(fid,'%7.4f \t', sigmasub(i,t));
        fprintf(fid,'%7.4f \t', sigmaboostsub(i,t));
    end
    fprintf(fid,' \n');
end
fclose(fid); % Close output data file.

```

Staircase Simulator (advstair.m)

This code is used by the advstrat.m program to create a virtual staircase based on specified parameter settings.

```

clear fls stresses result;

stress = initstress; % Initial stress level for staircase test.
sumfail = 0; % Initialize number of failures to zero.
sumlive = 0; % Initialize number of survivals to zero.
done = 0; % Used to indicate when to end staircase. (All specimens
           % tested with at least one failure and one success, and we
           % have P = 0 and P = 1 stress levels).
j = 1; % Specimen counter.
while done == 0
    if truedist == 1
        fls(j) = normrnd(truemean, truestdv);
    else

```

```

        disp(['ERROR: User did not select a supported distribution.']);
    end
    stresses(j) = stress; % Stress at which specimen j was tested.
    if stress > fls(j)
        result(j) = 1; % Specimen failed.
        sumfail = sumfail + 1;
        stress = stress - step;
    else
        result(j) = 0; % Specimen survived.
        sumlive = sumlive + 1;
        stress = stress + step;
    end
    if and(j >= n, and(sumlive > 0, sumfail > 0))
        if or(and(stresses(j) == min(stresses), result(j) == 1), and(stresses(j) ==
max(stresses), result(j) == 0))
            j = j + 1;
        else
            done = 1;
        end
    elseif and(j >= n, or(sumlive == 0, sumfail == 0))
        j = j + 1;
    else
        j = j + 1;
    end
end
end

```

Staircase Calculator (advcalcs.m)

This code is used by the advstrat.m program to compute the fatigue strength statistics using the Dixon-Mood method based on the staircase data simulated by the advstair.m routine. Note that Pollak correction constants are hardcoded based on the number of specimens.

```

clear j stresslevel P S count fail live k;

stress0 = 1.0e+12; % Initialize stress0 to outrageously high number.
if sumfail <= sumlive
    for j = 1:n
        if (result(j) == 1) & (stresses(j) < stress0)
            stress0 = stresses(j);
        end
    end
else
    for j = 1:n
        if (result(j) == 0) & (stresses(j) < stress0)
            stress0 = stresses(j);
        end
    end
end

% This portion determines the number of occurrences and failures at each
% stress level. Note that the index identifying stress level must be
% adjusted so that all vector indices are >= 1 as required by MATLAB.
% Data for P-S plot are also generated.

kmax = 0; % Maximum stress level tested relative to stress0.
kmin = 0; % Minimum stress level tested relative to stress0.
for j = 1:n % Determines the max and min stress levels.
    stresslevel(j) = round((stresses(j) - stress0)/step);
    if stresslevel(j) > kmax
        kmax = stresslevel(j);
    elseif stresslevel(j) < kmin
        kmin = stresslevel(j);
    end
end
for k = 1:(kmax - kmin + 1)

```

```

        count(k) = 0;    % Initialize count of occurrences at each level.
        fail(k) = 0;     % Initialize count of failures at each level.
        live(k) = 0;     % Initialize count of survivals at each level.
    end
    for j = 1:n    % Count number of stress level occurrences and failures.
        adjstresslevel = stresslevel(j) - kmin + 1; % Adjusted to be >= 1.
        count(adjstresslevel) = count(adjstresslevel) + 1;
        if result(j) == 1
            fail(adjstresslevel) = fail(adjstresslevel) + 1;
        else
            live(adjstresslevel) = live(adjstresslevel) + 1;
        end
        P(adjstresslevel) = fail(adjstresslevel)/count(adjstresslevel);
    end
    for k = 1:(kmax - kmin + 1)
        h = k + kmin - 1; % Readjusts stress level back to 0:kmax scale.
        S(k) = stress0 + h*step;
    end

% This portion calculates mean and standard deviation of FLS for each
% iteration using the statistics of the Dixon-Mood method. Note that this
% analysis assumes a normal distribution for FLS. Also, note that the
% summation over k = (- kmin + 1):(kmax - kmin + 1) corresponds to the
% summation over i = 0:i_max using the Dixon-Mood method's notation.

    sum_mi = 0;    % Initialize summations used in Dixon-Mood statistics.
    sum_imi = 0;
    sum_iimi = 0;

    for k = (- kmin + 1):(kmax - kmin + 1)
        h = k + kmin - 1; % Readjusts stress level back to 0:kmax scale.
        if sumfail > sumlive
            mi = live(k);
        else
            mi = fail(k);
        end
        sum_mi = sum_mi + mi;
        sum_imi = sum_imi + h*mi;
        sum_iimi = sum_iimi + h*h*mi;
    end

    if sumfail > sumlive
        mu = stress0 + step*(sum_imi/sum_mi + 0.5);
    else
        mu = stress0 + step*(sum_imi/sum_mi - 0.5);
    end
    uglyterm = (sum_mi*sum_iimi - sum_imi*sum_imi)/(sum_mi^2);
    if uglyterm > 0.3
        sigma = 1.62*step*(uglyterm + 0.029);
        % sigma = 1.3*sigma*(n/(n-3))*((1.2*sigma/step)^1.72); % Pollak correction.
        sigma = sigma*(n/(n-3)); % Svensson correction.
    else
        sigma = 0.53*step;
        % sigma = 1.3*sigma*(n/(n-3))*((1.2*sigma/step)^1.72); % Pollak correction.
        sigma = sigma*(n/(n-3)); % Svensson correction.
    end
end

```

Staircase Bootstrap (advboot.m)

This code is used by the advstrat.m program to run the bootstrap algorithm based on the staircase data simulated by the advstair.m routine. Note that Pollak correction constants are hardcoded based on the number of specimens.

```

for b = 1:mboot

clear P S x stresses result stresslevel count fail live k;

```

```

% "offset" corresponds to the number of steps up the initial stress level
% is from the lowest stress level for which P-S data is available.

offset = round((initstress-Sstar(1))/step);
index = offset + 1; % Sets the initial index for P-S data.

% Simulate a staircase test based on these parameters.

% This portion generates a random FLS and compares it to current stress
% level to determine if the specimen failed or survived. If it failed, the
% stress level is reduced. If it survived, the stress level is increased.

stress = initstress; % Initial stress level for staircase test.
sumfail = 0; % Initialize number of failures to zero.
sumlive = 0; % Initialize number of survivals to zero.
for j = 1:n % "j" corresponds to number of specimens.
    x(j) = rand; % Random number.
    stresses(j) = stress; % Stress at which specimen j was tested.
    if x(j) <= Pstar(index)
        result(j) = 1; % Specimen failed.
        sumfail = sumfail + 1;
        stress = stress - step;
        index = index - 1;
    else
        result(j) = 0; % Specimen survived.
        sumlive = sumlive + 1;
        stress = stress + step;
        index = index + 1;
    end
end

% This portion finds the stress corresponding to i = 0 using the Dixon-Mood
% notation. This stress level is dependent on whether most specimens failed
% (then it is the lowest stress level corresponding to a survival) or
% survived (then it is the lowest stress level corresponding to a failure).

stress0 = 1.0e+12; % Initialize stress0 to outrageously high number.
if sumfail <= sumlive
    for j = 1:n
        if (result(j) == 1) & (stresses(j) < stress0)
            stress0 = stresses(j);
        end
    end
else
    for j = 1:n
        if (result(j) == 0) & (stresses(j) < stress0)
            stress0 = stresses(j);
        end
    end
end

% This portion determines the number of occurrences and failures at each
% stress level. Note that the index identifying stress level must be
% adjusted so that all vector indices are >= 1 as required by MATLAB.
% Data for P-S plot are also generated.

kmax = 0; % Maximum stress level tested relative to stress0.
kmin = 0; % Minimum stress level tested relative to stress0.
for j = 1:n % Determines the max and min stress levels.
    stresslevel(j) = round((stresses(j) - stress0)/step);
    if stresslevel(j) > kmax
        kmax = stresslevel(j);
    elseif stresslevel(j) < kmin
        kmin = stresslevel(j);
    end
end
for k = 1:(kmax - kmin + 1)
    count(k) = 0; % Initialize count of occurrences at each level.
    fail(k) = 0; % Initialize count of failures at each level.
    live(k) = 0; % Initialize count of survivals at each level.
end

```

```

for j = 1:n % Count number of stress level occurrences and failures.
    adjstresslevel = stresslevel(j) - kmin + 1; % Adjusted to be >= 1.
    count(adjstresslevel) = count(adjstresslevel) + 1;
    if result(j) == 1
        fail(adjstresslevel) = fail(adjstresslevel) + 1;
    else
        live(adjstresslevel) = live(adjstresslevel) + 1;
    end
    P(adjstresslevel) = fail(adjstresslevel)/count(adjstresslevel);
end
for k = 1:(kmax - kmin + 1)
    h = k + kmin - 1; % Readjusts stress level back to 0:kmax scale.
    S(k) = stress0 + h*step;
end

% This portion calculates mean and standard deviation of FLS for each
% iteration using the statistics of the Dixon-Mood method. Note that this
% analysis assumes a normal distribution for FLS. Also, note that the
% summation over k = (- kmin + 1):(kmax - kmin + 1) corresponds to the
% summation over i = 0:i_max using the Dixon-Mood method's notation.

sum_mi = 0; % Initialize summations used in Dixon-Mood statistics.
sum_imi = 0;
sum_iimi = 0;

for k = (- kmin + 1):(kmax - kmin + 1)
    h = k + kmin - 1; % Readjusts stress level back to 0:kmax scale.
    if sumfail > sumlive
        mi = live(k);
    else
        mi = fail(k);
    end
    sum_mi = sum_mi + mi;
    sum_imi = sum_imi + h*mi;
    sum_iimi = sum_iimi + h*h*mi;
end

if sumfail > sumlive
    muboot(b) = stress0 + step*(sum_imi/sum_mi + 0.5);
else
    muboot(b) = stress0 + step*(sum_imi/sum_mi - 0.5);
end
uglyterm = (sum_mi*sum_iimi - sum_imi*sum_imi)/(sum_mi^2);
if uglyterm > 0.3
    sigmaboot(b) = 1.62*step*(uglyterm + 0.029);
    % sigmaboot(b) = 1.3*sigmaboot(b)*(n/(n-3))*((1.2*sigmaboot(b)/step)^1.72); %
    Pollak correction.
    sigmaboot(b) = sigmaboot(b)*(n/(n-3)); %
    Svensson correction.
else
    sigmaboot(b) = 0.53*step;
    % sigmaboot(b) = 1.3*sigmaboot(b)*(n/(n-3))*((1.2*sigmaboot(b)/step)^1.72); %
    Pollak correction.
    sigmaboot(b) = sigmaboot(b)*(n/(n-3)); %
    Svensson correction.
end

end

newmu = mean(muboot);
newsigma = prctile(sigmaboot,60); % Adjust this term to view the effect of various
percentile settings on computed bootstrap results.

```

Identical Iteration Program (iterations.m)

This code was used to analyze the effects of iterating staircase results such that a large series of identical staircases were run, each using the results of the previous staircase as new starting points (initial stress equal to mean fatigue strength and step based on

previous standard deviation estimate). The program used `fls_sim_calcs.m` to provide simulated staircase data and statistical analysis.

```
% Purpose: Run a series of staircase sim cases based on prev results.
% Required: fls_sim_calcs.m -- runs staircase sim for each case.

clear all; clc;

truedist = 1;
truemean = 400;
truestdv = 5;
n = 15;
series = 100;
startmean = 400; % initial mean estimate
startstdv = 2.5; % initial stdv estimate
ks = 1.70; % step size constant

% Set simulation parameters.

m = 1; % Number of iterations used for each simulation case.
graphics = 0; % 0 = graphics off, 1 = case summary, 2 = each iteration.
% Unless running only a couple cases, turn graphics off.
trouble = 0; % Troubleshooting: 0 = off, 1 = on.
alpha = 0.05; % Significance level used for confidence intervals.
maxtime = 1000; % Sets the max time before simulation times out.

for t = 1:1000
    initstress = startmean;
    step = ks*startstdv;
    for s = 1:series
        fls_sim_calcs;
        initstress = mu;
        step = ks*sigma;
    end
    mu_v(t) = mu;
    sigma_v(t) = sigma;
end

% At this point, we have an R x 10 matrix of output data, where R is the
% number of completed cases. Each row corresponds to a simulation case
% with the mean, std dev, median, LCB, and UCB for both mu and sigma.
% Here, mu is the calculated FLS mean and sigma is the calculated FLS std
% dev using the Dixon-Mood method. LCB and UCB are the lower and upper
% confidence bounds.

mu_bar = mean(mu_v)
mu_LCB = prctile(mu_v, 5)
mu_UCB = prctile(mu_v, 95)
sigma_bar = mean(sigma_v)
sigma_LCB = prctile(sigma_v, 5)
sigma_UCB = prctile(sigma_v, 95)

fid = fopen('output1.dat','w+'); % Opens output data file.
for t=1:1000
    fprintf(fid,'%7.4f \n',sigma_v(t));
end
fclose(fid); % Close output data file.
```

APPENDIX E. STAIRCASE SIMULATION DATA FOR MEAN FATIGUE STRENGTH USING THE DIXON-MOOD METHOD

This appendix shows the results of the mean fatigue strength analysis for the simulation-based staircase investigation.

The first part of this sub-investigation centered on the effect of starting stress on calculated mean fatigue strengths using the Dixon-Mood method. As discussed in Chapter III, there are already adequate methods for accounting for offset starting stresses (i.e., initial stress level differs from the mean fatigue strength). These methods include those of Brownlee *et al* [21], Dixon [26], and Little [42]. Nonetheless, the capability of the Dixon-Mood method of starting stress on mean fatigue strength was analyzed. These validation simulations used an underlying Normal($\mu = 400, \sigma = 5$) fatigue strength distribution. The number of specimens varied from 6 to 200 specimens, with the step size held constant as 1σ . Three levels of starting stress were used: μ (the true mean), $\mu + 2\sigma$ (2 steps above true), and $\mu - 2\sigma$ (2 steps below true). Each test point was simulated for 1000 iterations.

Figure 92 shows the mean for fatigue strength mean (i.e., $\bar{\mu}_{DM}$) over the 1000 simulations at each point, and Figure 93 shows the standard deviation for fatigue strength mean (i.e., μ_{DM}^{σ}) over the 1000 simulations. As one would expect, the fatigue strength estimates are slightly high when the starting stress is too high, and slightly low when starting too low; and as more specimens are used, the dependence on starting stress becomes negligible. Also, the variance in fatigue strength mean is less when starting near the true mean rather than two steps above or below. Again, this effect is reduced as more specimens are used. It should be noted that even with as few as 6 specimens and an offset starting stress, the Dixon-Mood method provides quite accurate estimates for fatigue strength mean.

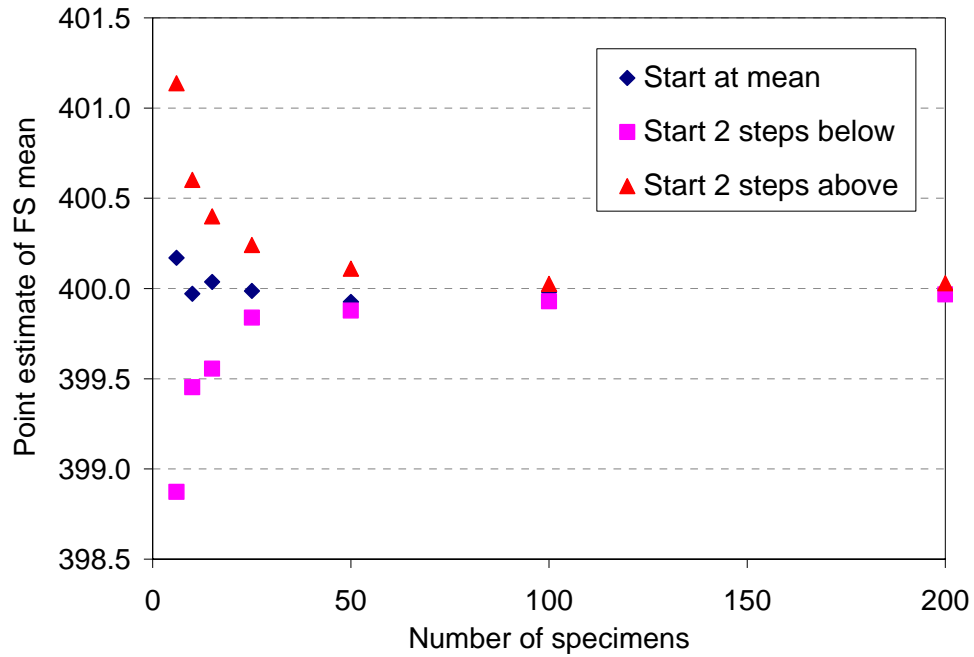


Figure 92. Effect of starting stress on calculated fatigue strength mean for a Normal(400,5) underlying fatigue strength distribution.

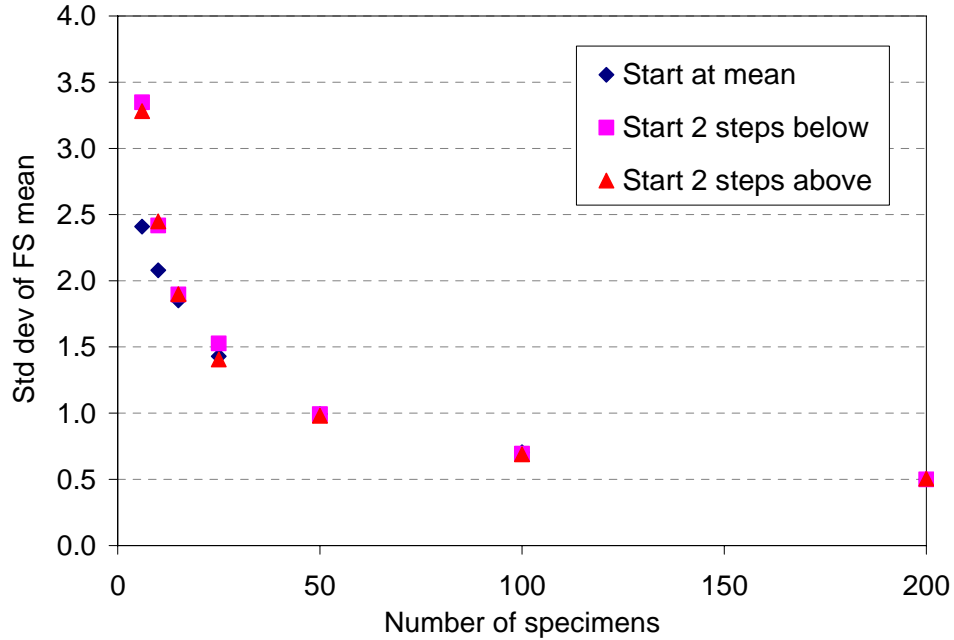


Figure 93. Effect of starting stress on scatter of fatigue strength mean for a Normal(400,5) underlying fatigue strength distribution.

The next part of this sub-investigation analyzed the effect of step size on estimates for mean fatigue strength. For these simulations, step size varied from 0.1σ to 2.0σ . The underlying distribution and the number of iterations remained unchanged from the previous sub-investigation. Figure 94 shows the effect of step size on the point estimates of mean fatigue strength, whereas Figure 95 shows the scatter in these estimates. These figures confirm that step size does not play a major role in mean fatigue strength estimates using the Dixon-Mood method, although scatter in mean fatigue strength estimates is reduced with the use of smaller steps (as one would expect since the data are thus more concentrated near the true mean value) or larger sample sizes.

The bottomline of this analysis is that the mean fatigue strengths calculated by the Dixon-Mood method can be used without further modification (beyond the starting stress offset corrections already described). Fatigue strength means calculated from staircase data are generally robust to step size and the number of specimens used.

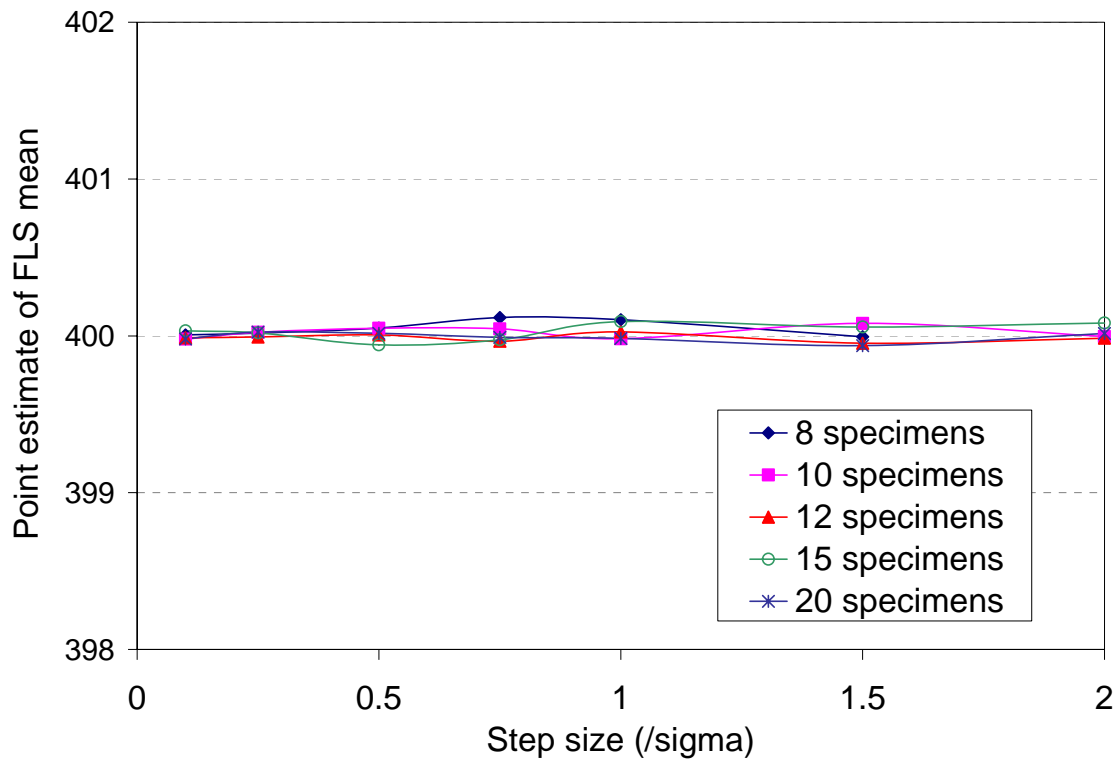


Figure 94. Effect of step size on calculated mean fatigue strength using the Dixon-Mood method for a Normal(400,5) underlying fatigue strength distribution.

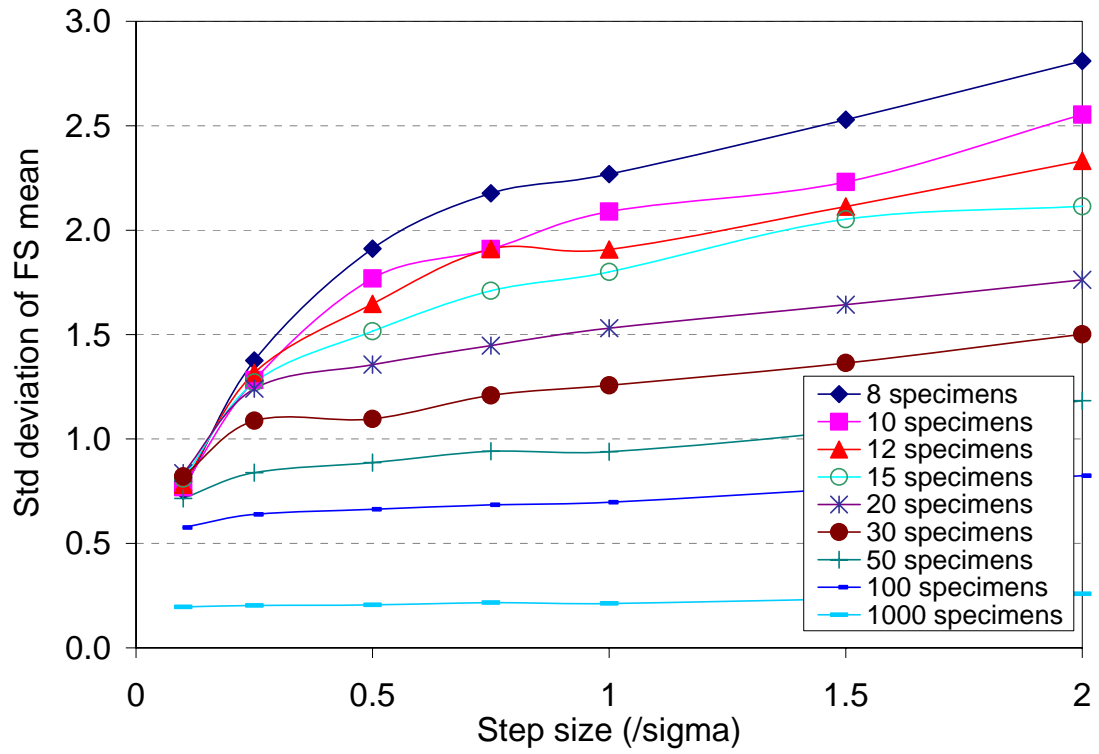


Figure 95. Effect of step size on scatter of mean fatigue strength using the Dixon-Mood method for a Normal(400,5) underlying fatigue strength distribution.

APPENDIX F. SIMULATION RESULTS FOR STAIRCASE PARAMETER INVESTIGATION

In this appendix, the detailed results for the staircase parametric analysis are displayed in detail for a number of the simulation runs. Specifically, this appendix enumerates the results for the standard deviation bias analysis which is summarized in Chapter III (see Figure 25 and Figure 26). The results for the following cases were simulated and summarized in Chapter III:

- Step sizes ranged from 0.1σ to 2σ , where σ is the true standard deviation of the fatigue strength distribution. Specifically, the following step sizes were used: $s/\sigma = 0.1, 0.25, 0.5, 0.75, 1, 1.5, \text{ and } 2$.
- Number of specimens ranged from 8 to 1000, with the following sample sizes: $N = 8, 10, 12, 15, 20, 30, 50, 100, 1000$.
- Starting stress equaled the true mean fatigue strength in all cases.
- True fatigue strength distribution was modeled as Normal(400,5) and Normal(400,15).
- A total of 126 cases were simulated with 1000 replications each.

In this appendix, only 21 of the 126 cases are shown in detail. Namely, the results for each step interval for $N = 8, 20, \text{ and } 100$ are shown for the Normal(400,5) distribution. For each case, the histogram of the simulated standard deviation estimates using the Dixon-Mood method are shown along with a statistical summary of results.

Case 1. $s/\sigma = 0.1$, $N = 8$ specimens

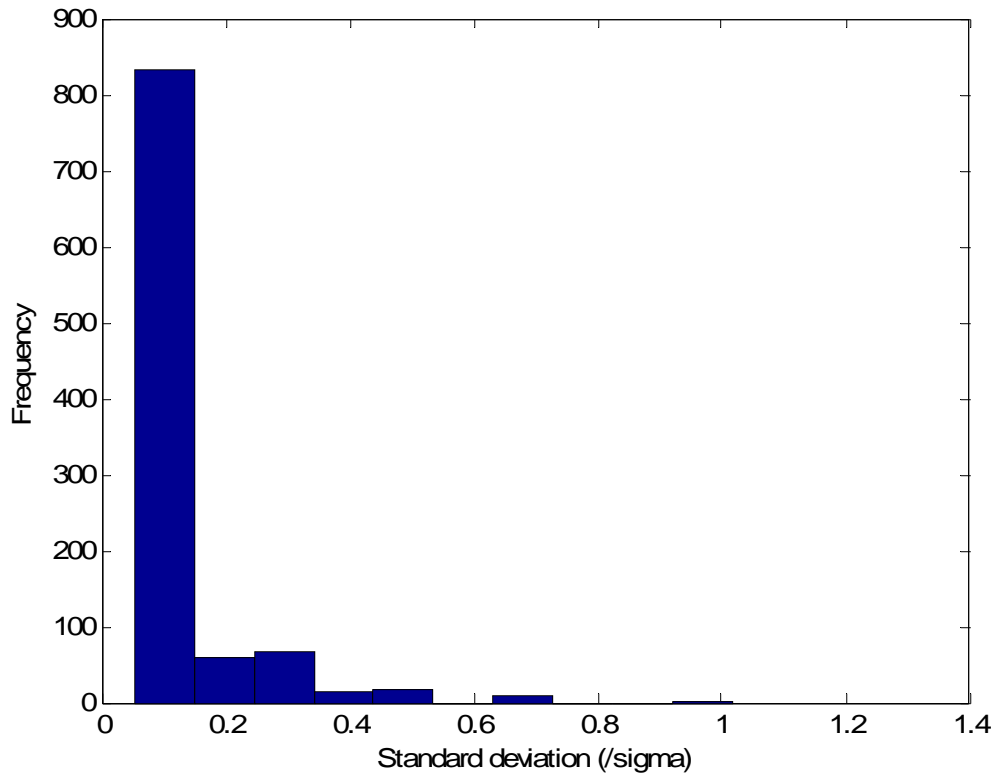


Figure 96. Histogram of staircase simulation results for 0.1σ step and 8 specimens.

Table 34. Summary statistics for simulation with 0.1σ step and 8 specimens.

Statistic for the simulated standard deviation distribution (using Dixon-Mood method)	Value ($/\sigma$)
Mean	0.1125
Standard deviation	0.1013
1 st percentile	0.0530
5 th percentile	0.0530
10 th percentile	0.0530
50 th percentile (median)	0.0857
90 th percentile	0.2567
95 th percentile	0.3287
99 th percentile	0.4727

Case 2. $s/\sigma = 0.25$, $N = 8$ specimens

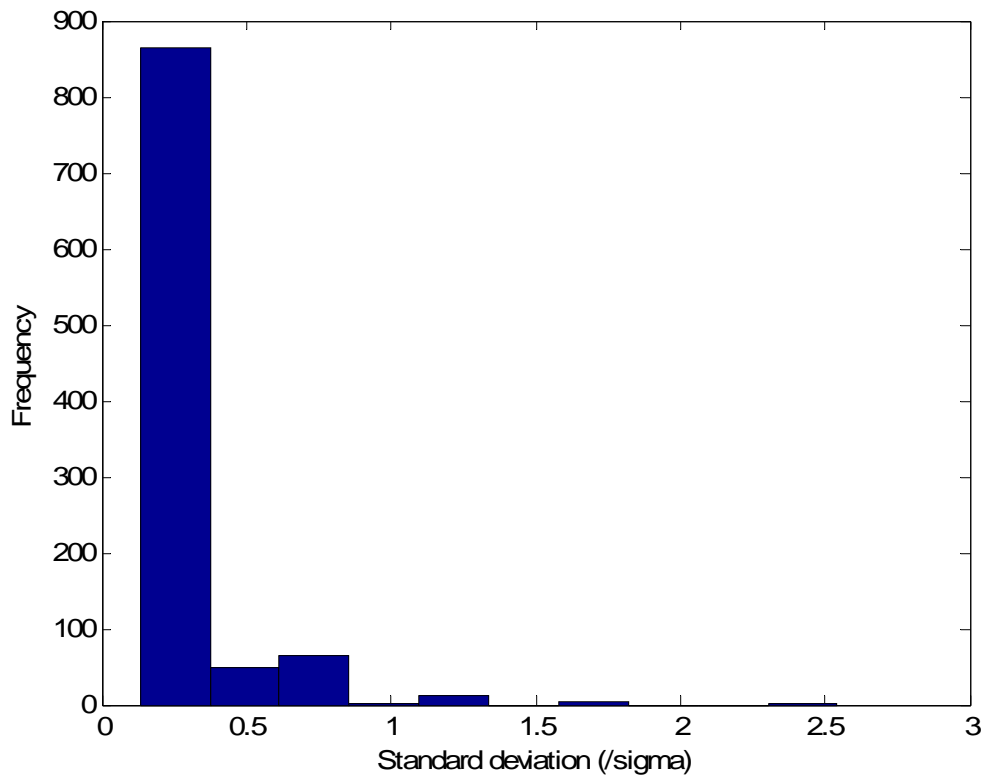


Figure 97. Histogram of staircase simulation results for 0.25σ step and 8 specimens.

Table 35. Summary statistics for simulation with 0.25σ step and 8 specimens.

Statistic for the simulated standard deviation distribution (using Dixon-Mood method)	Value ($/\sigma$)
Mean	0.2652
Standard deviation	0.2362
1 st percentile	0.1325
5 th percentile	0.1325
10 th percentile	0.1325
50 th percentile (median)	0.1734
90 th percentile	0.5180
95 th percentile	0.6417
99 th percentile	1.1817

Case 3. $s/\sigma = 0.5$, $N = 8$ specimens

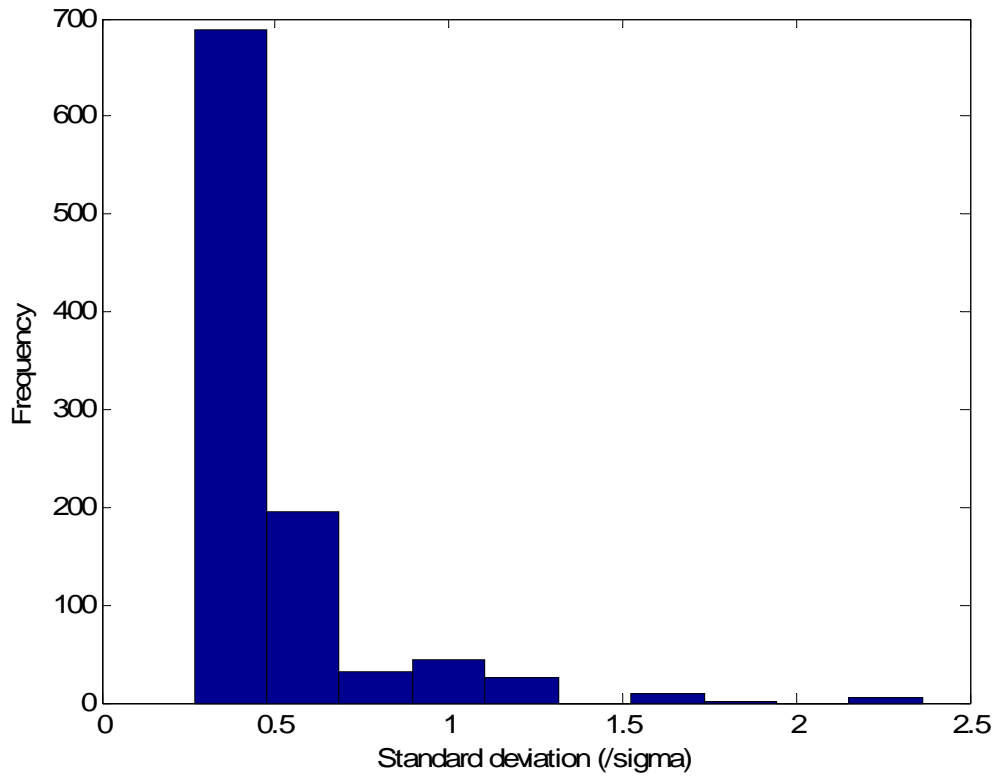


Figure 98. Histogram of staircase simulation results for 0.5σ step and 8 specimens.

Table 36. Summary statistics for simulation with 0.5σ step and 8 specimens.

Statistic for the simulated standard deviation distribution (using Dixon-Mood method)	Value ($/\sigma$)
Mean	0.4483
Standard deviation	0.3014
1 st percentile	0.2650
5 th percentile	0.2650
10 th percentile	0.2650
50 th percentile (median)	0.2650
90 th percentile	0.7435
95 th percentile	1.0360
99 th percentile	1.6435

Case 4. $s/\sigma = 0.75$, $N = 8$ specimens

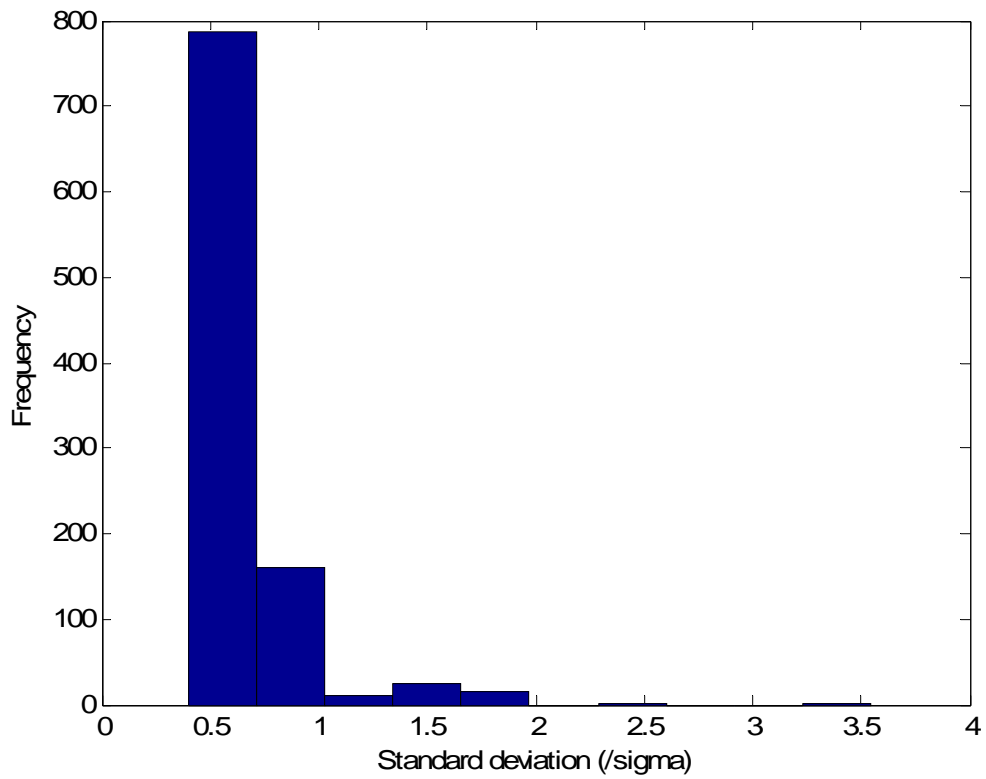


Figure 99. Histogram of staircase simulation results for 0.75σ step and 8 specimens.

Table 37. Summary statistics for simulation with 0.75σ step and 8 specimens.

Statistic for the simulated standard deviation distribution (using Dixon-Mood method)	Value (/σ)
Mean	0.5770
Standard deviation	0.3306
1 st percentile	0.3975
5 th percentile	0.3975
10 th percentile	0.3975
50 th percentile (median)	0.3975
90 th percentile	0.8705
95 th percentile	1.1152
99 th percentile	1.9252

Case 5. $s/\sigma = 1.0$, $N = 8$ specimens

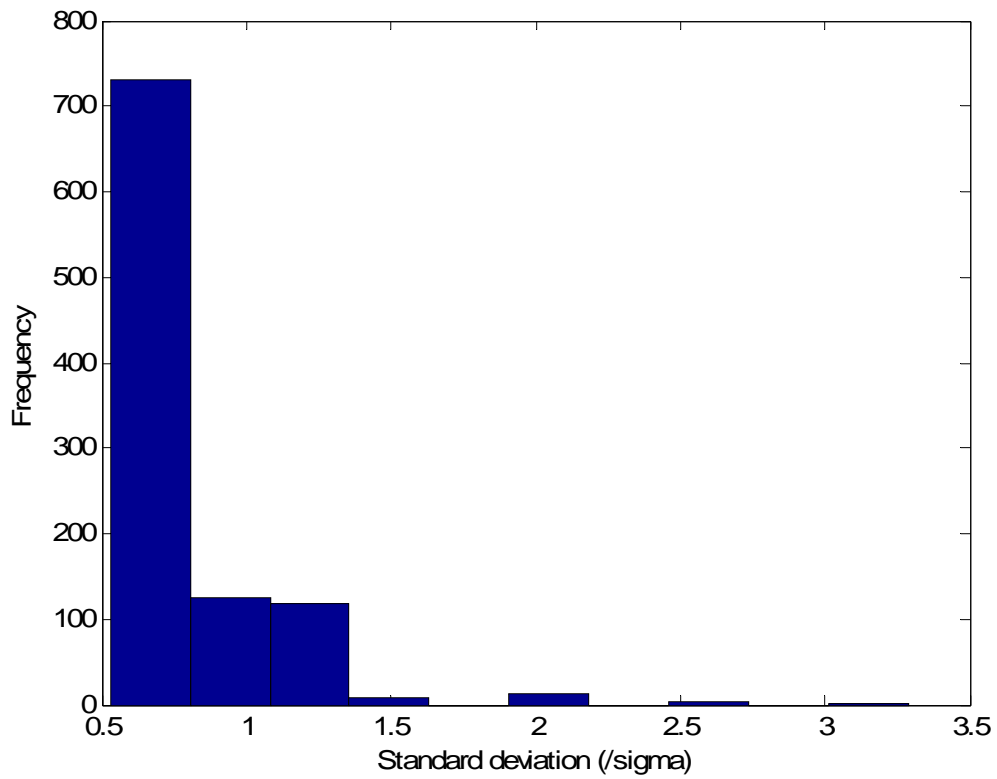


Figure 100. Histogram of staircase simulation results for 1.0σ step and 8 specimens.

Table 38. Summary statistics for simulation with 1.0σ step and 8 specimens.

Statistic for the simulated standard deviation distribution (using Dixon-Mood method)	Value (/σ)
Mean	0.6847
Standard deviation	0.3175
1 st percentile	0.5300
5 th percentile	0.5300
10 th percentile	0.5300
50 th percentile (median)	0.5300
90 th percentile	1.1607
95 th percentile	1.1607
99 th percentile	2.0720

Case 6. $s/\sigma = 1.5$, $N = 8$ specimens

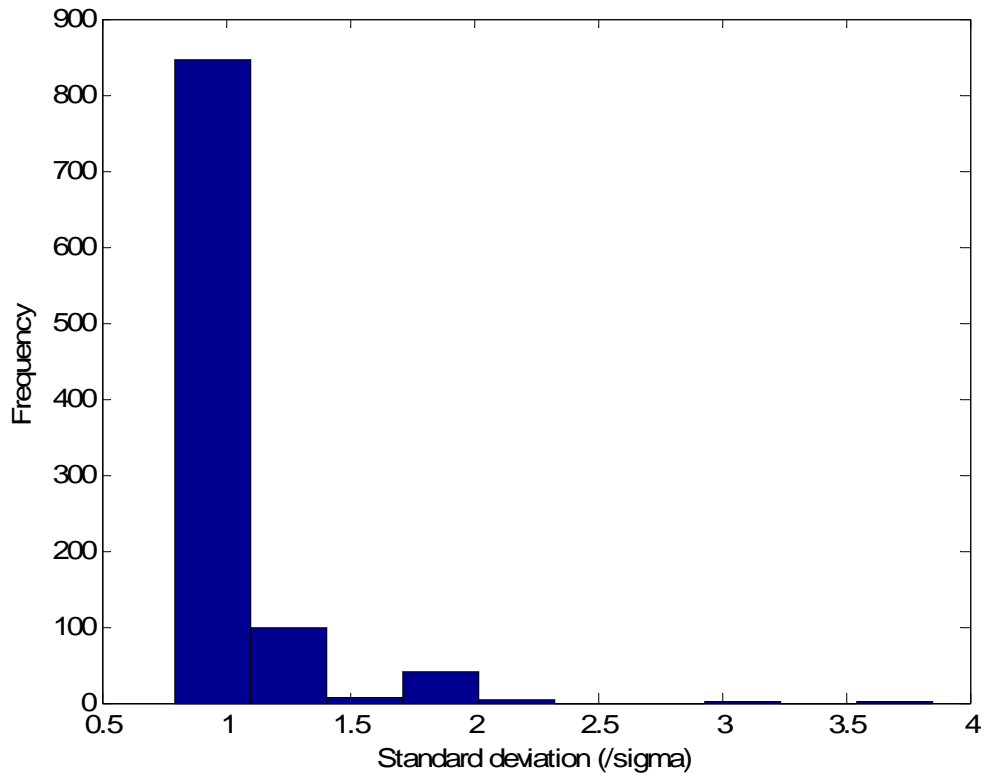


Figure 101. Histogram of staircase simulation results for 1.5σ step and 8 specimens.

Table 39. Summary statistics for simulation with 1.5σ step and 8 specimens.

Statistic for the simulated standard deviation distribution (using Dixon-Mood method)	Value ($/\sigma$)
Mean	0.9033
Standard deviation	0.2950
1 st percentile	0.7950
5 th percentile	0.7950
10 th percentile	0.7950
50 th percentile (median)	0.7950
90 th percentile	1.2855
95 th percentile	1.6905
99 th percentile	1.7411

Case 7. $s/\sigma = 2.0$, $N = 8$ specimens

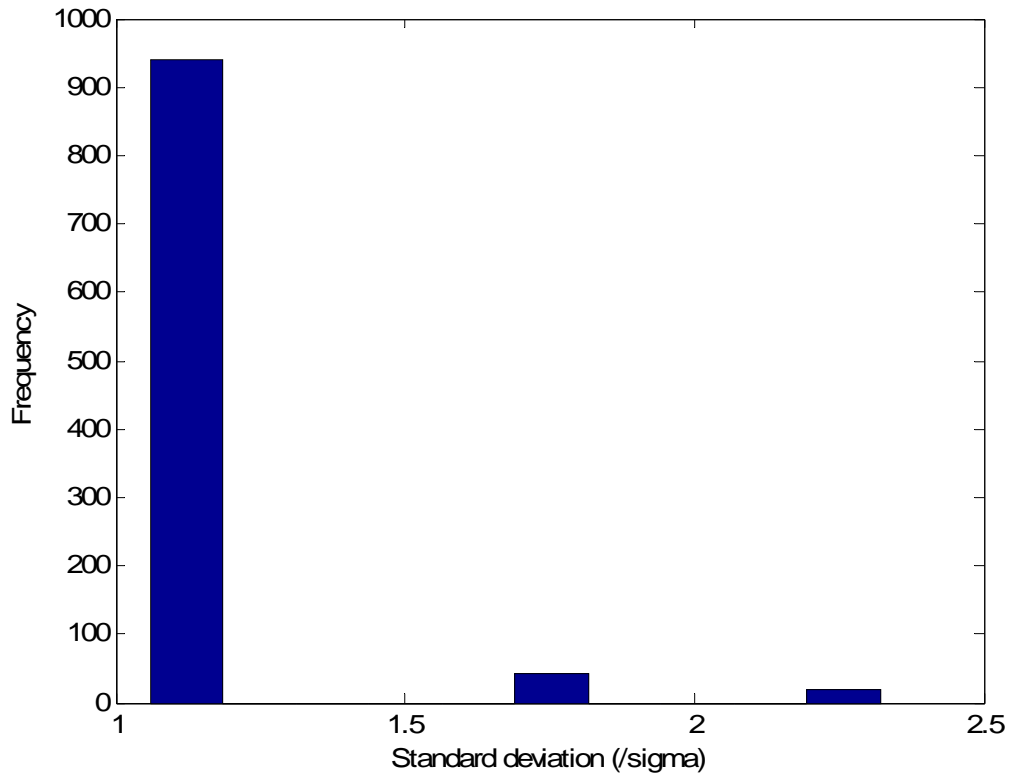


Figure 102. Histogram of staircase simulation results for 2.0σ step and 8 specimens.

Table 40. Summary statistics for simulation with 2.0σ step and 8 specimens.

Statistic for the simulated standard deviation distribution (using Dixon-Mood method)	Value (/σ)
Mean	1.1094
Standard deviation	0.2084
1 st percentile	1.0600
5 th percentile	1.0600
10 th percentile	1.0600
50 th percentile (median)	1.0600
90 th percentile	1.0600
95 th percentile	1.7140
99 th percentile	2.3215

Case 8. $s/\sigma = 0.1$, $N = 20$ specimens

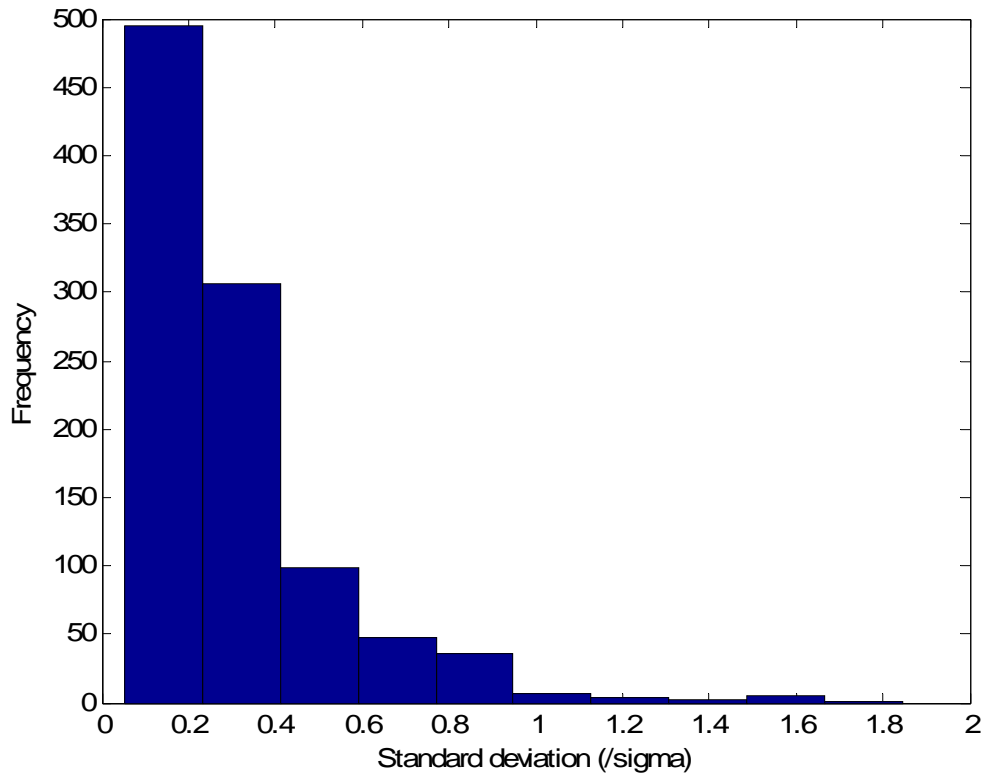


Figure 103. Histogram of staircase simulation results for 0.1σ step and 20 specimens.

Table 41. Summary statistics for simulation with 0.1σ step and 20 specimens.

Statistic for the simulated standard deviation distribution (using Dixon-Mood method)	Value ($/\sigma$)
Mean	0.3000
Standard deviation	0.2356
1 st percentile	0.0530
5 th percentile	0.0756
10 th percentile	0.0857
50 th percentile (median)	0.2367
90 th percentile	0.5944
95 th percentile	0.7811
99 th percentile	1.2171

Case 9. $s/\sigma = 0.25$, $N = 20$ specimens

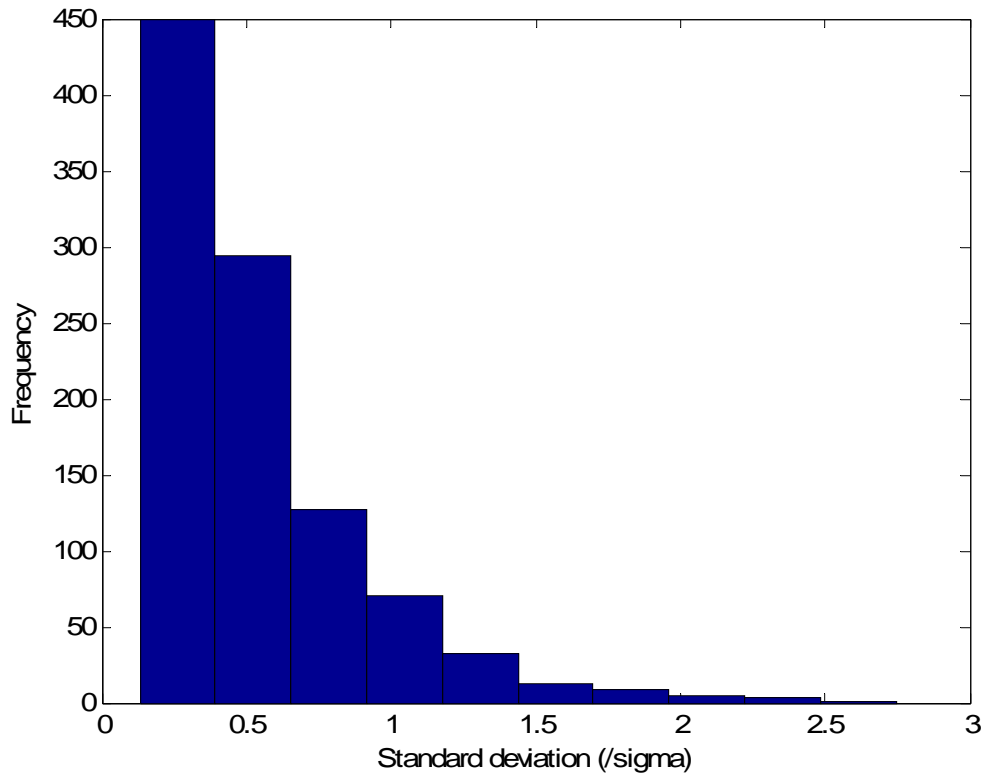


Figure 104. Histogram of staircase simulation results for 0.25σ step and 20 specimens.

Table 42. Summary statistics for simulation with 0.25σ step and 20 specimens.

Statistic for the simulated standard deviation distribution (using Dixon-Mood method)	Value ($/\sigma$)
Mean	0.5350
Standard deviation	0.3629
1 st percentile	0.1325
5 th percentile	0.1717
10 th percentile	0.1917
50 th percentile (median)	0.4208
90 th percentile	1.0117
95 th percentile	1.2517
99 th percentile	1.9065

Case 10. $s/\sigma = 0.5$, $N = 20$ specimens

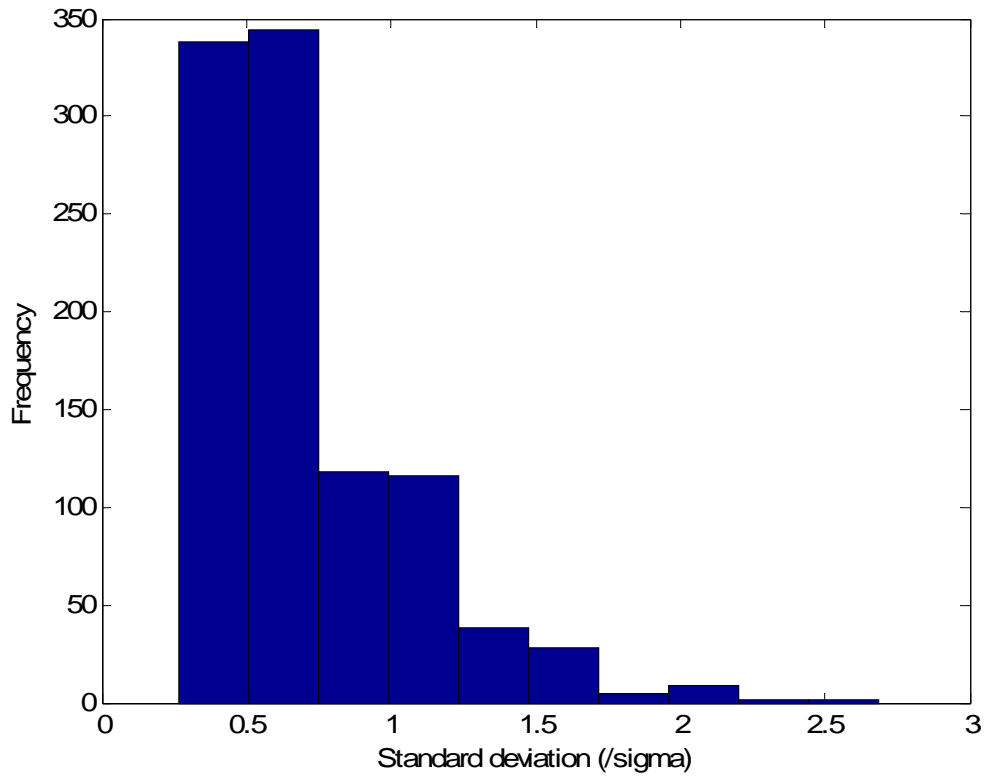


Figure 105. Histogram of staircase simulation results for 0.5σ step and 20 specimens.

Table 43. Summary statistics for simulation with 0.5σ step and 20 specimens.

Statistic for the simulated standard deviation distribution (using Dixon-Mood method)	Value ($/\sigma$)
Mean	0.6992
Standard deviation	0.3745
1 st percentile	0.2650
5 th percentile	0.2650
10 th percentile	0.3151
50 th percentile (median)	0.6391
90 th percentile	1.1835
95 th percentile	1.4635
99 th percentile	2.0017

Case 11. $s/\sigma = 0.75$, $N = 20$ specimens

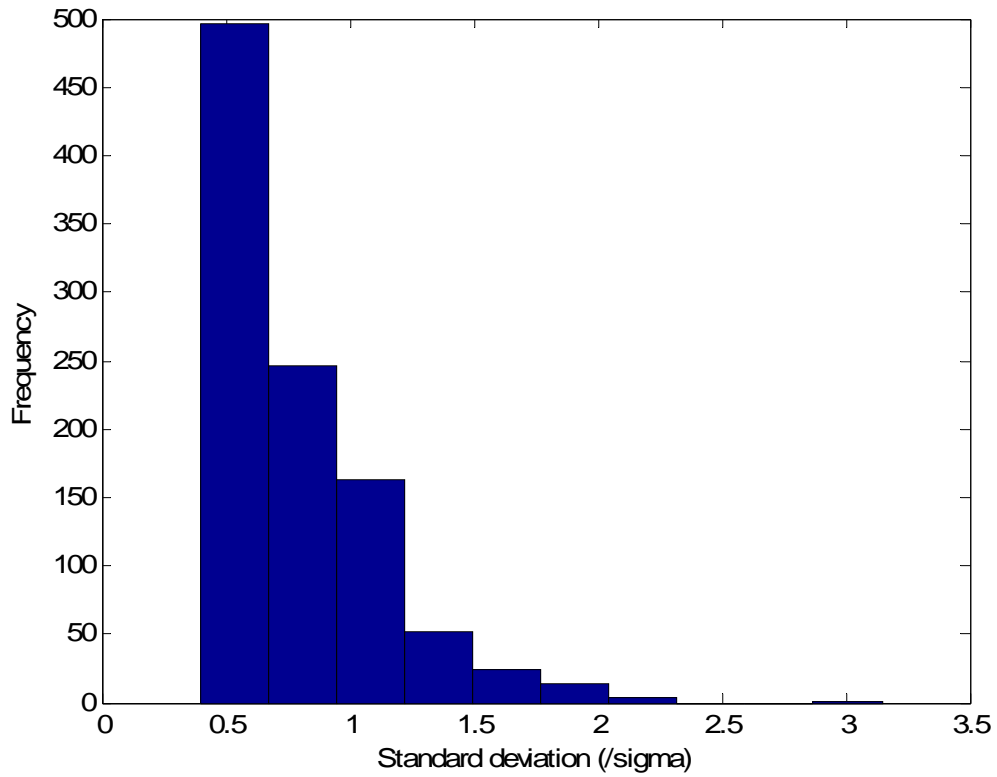


Figure 106. Histogram of staircase simulation results for 0.75σ step and 20 specimens.

Table 44. Summary statistics for simulation with 0.75σ step and 20 specimens.

Statistic for the simulated standard deviation distribution (using Dixon-Mood method)	Value ($/\sigma$)
Mean	0.7654
Standard deviation	0.3451
1 st percentile	0.3975
5 th percentile	0.3975
10 th percentile	0.3975
50 th percentile (median)	0.6952
90 th percentile	1.2016
95 th percentile	1.4446
99 th percentile	2.0339

Case 12. $s/\sigma = 1.0$, $N = 20$ specimens

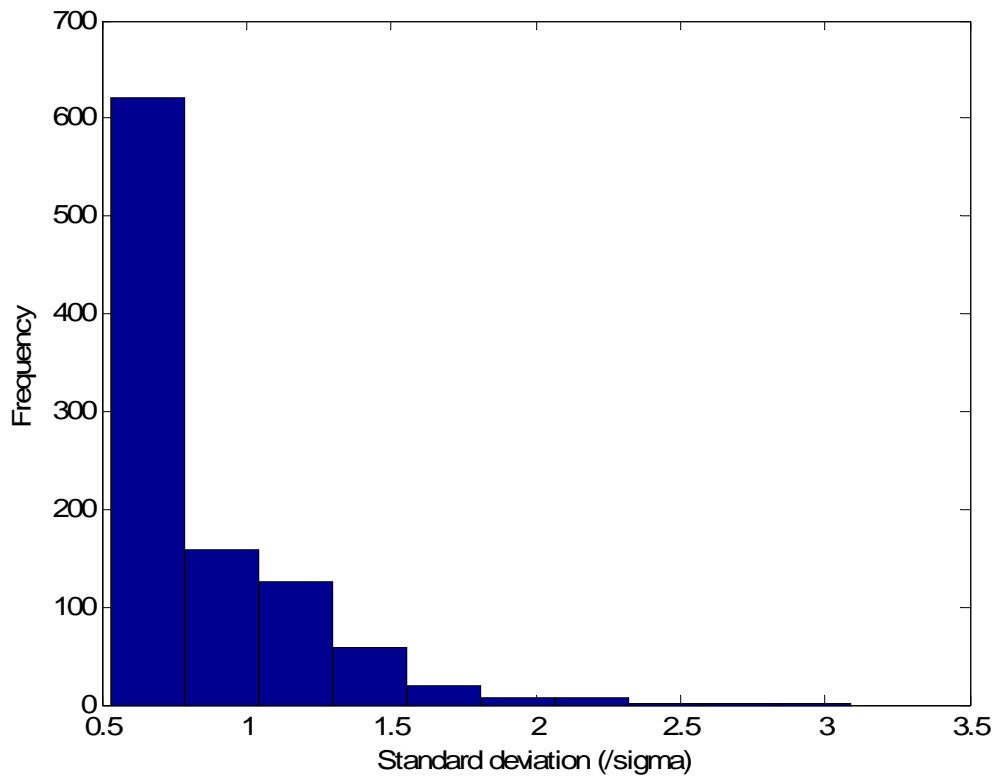


Figure 107. Histogram of staircase simulation results for 1.0σ step and 20 specimens.

Table 45. Summary statistics for simulation with 1.0σ step and 20 specimens.

Statistic for the simulated standard deviation distribution (using Dixon-Mood method)	Value ($/\sigma$)
Mean	0.8387
Standard deviation	0.3324
1 st percentile	0.5300
5 th percentile	0.5300
10 th percentile	0.5300
50 th percentile (median)	0.7598
90 th percentile	1.2782
95 th percentile	1.4870
99 th percentile	2.0995

Case 13. $s/\sigma = 1.5$, $N = 20$ specimens

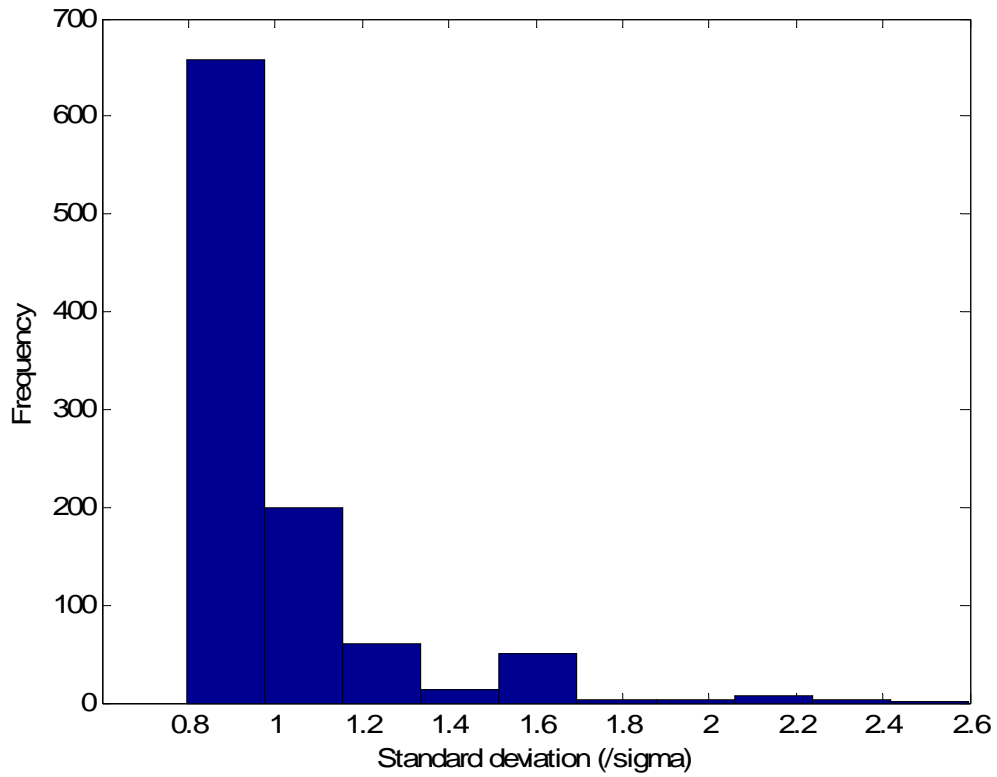


Figure 108. Histogram of staircase simulation results for 1.5σ step and 20 specimens.

Table 46. Summary statistics for simulation with 1.5σ step and 20 specimens.

Statistic for the simulated standard deviation distribution (using Dixon-Mood method)	Value ($/\sigma$)
Mean	0.9621
Standard deviation	0.2678
1 st percentile	0.7950
5 th percentile	0.7950
10 th percentile	0.7950
50 th percentile (median)	0.7950
90 th percentile	1.1640
95 th percentile	1.6257
99 th percentile	2.1111

Case 14. $s/\sigma = 2.0$, $N = 20$ specimens

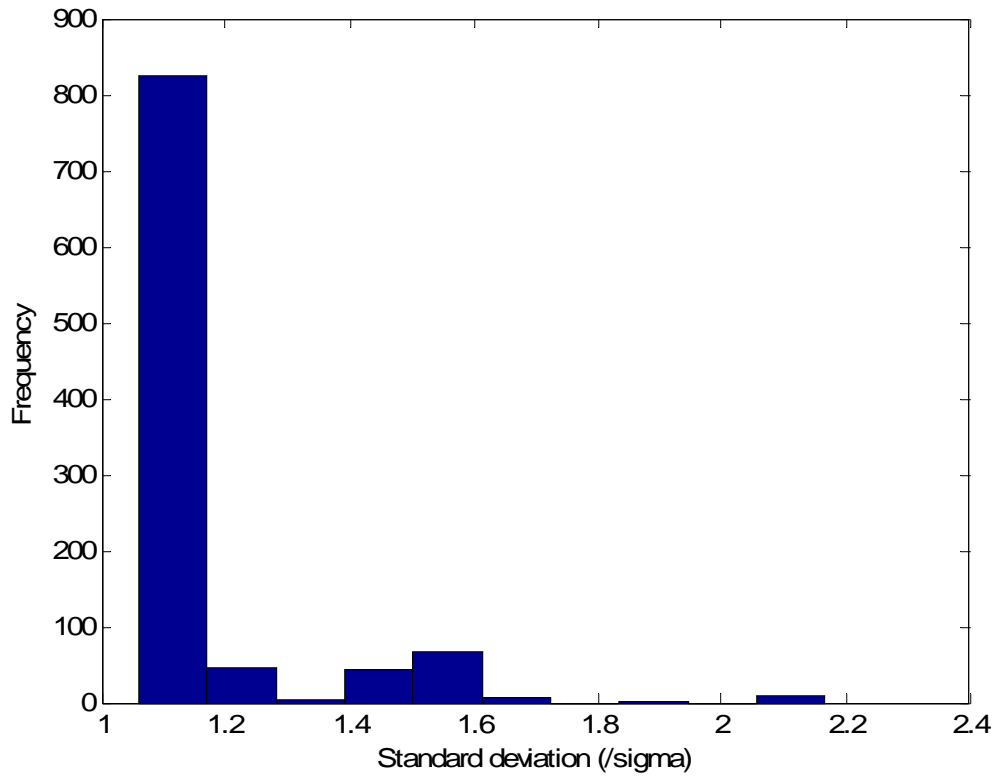


Figure 109. Histogram of staircase simulation results for 2.0σ step and 20 specimens.

Table 47. Summary statistics for simulation with 2.0σ step and 20 specimens.

Statistic for the simulated standard deviation distribution (using Dixon-Mood method)	Value (/σ)
Mean	1.1309
Standard deviation	0.1736
1 st percentile	1.0600
5 th percentile	1.0600
10 th percentile	1.0600
50 th percentile (median)	1.0600
90 th percentile	1.4224
95 th percentile	1.5196
99 th percentile	1.6816

Case 15. $s/\sigma = 0.1$, $N = 100$ specimens

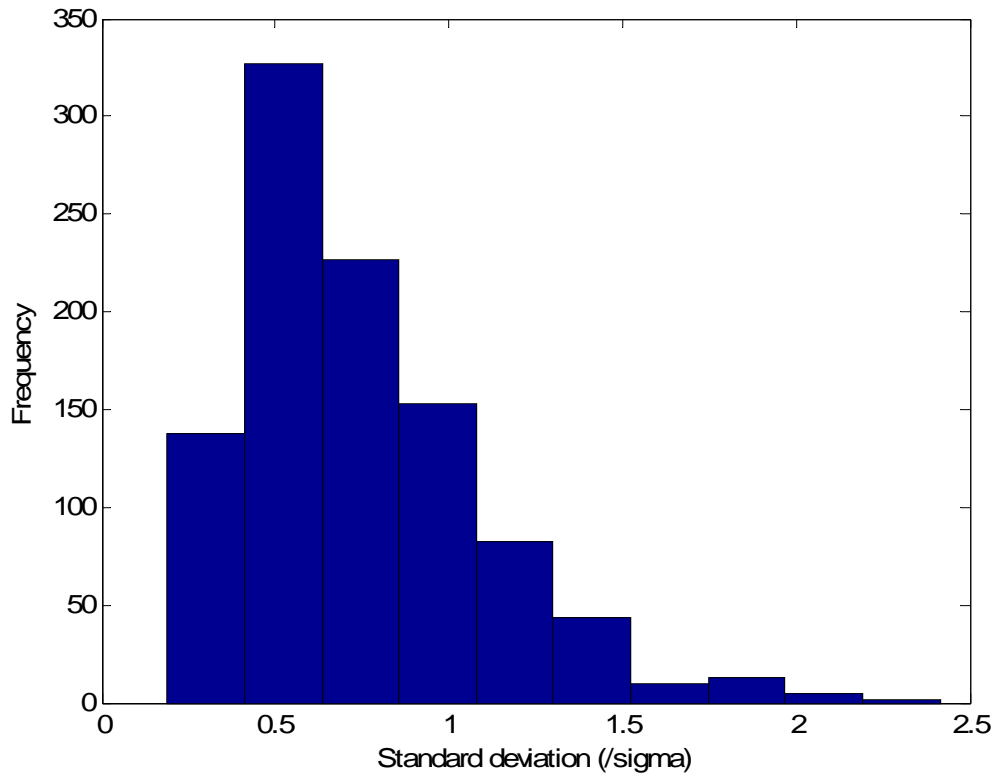


Figure 110. Histogram of staircase simulation results for 0.1σ step and 100 specimens.

Table 48. Summary statistics for simulation with 0.1σ step and 100 specimens.

Statistic for the simulated standard deviation distribution (using Dixon-Mood method)	Value ($/\sigma$)
Mean	0.7428
Standard deviation	0.3473
1 st percentile	0.2466
5 th percentile	0.3198
10 th percentile	0.3757
50 th percentile (median)	0.6590
90 th percentile	1.2156
95 th percentile	1.3759
99 th percentile	1.9084

Case 16. $s/\sigma = 0.25$, $N = 100$ specimens

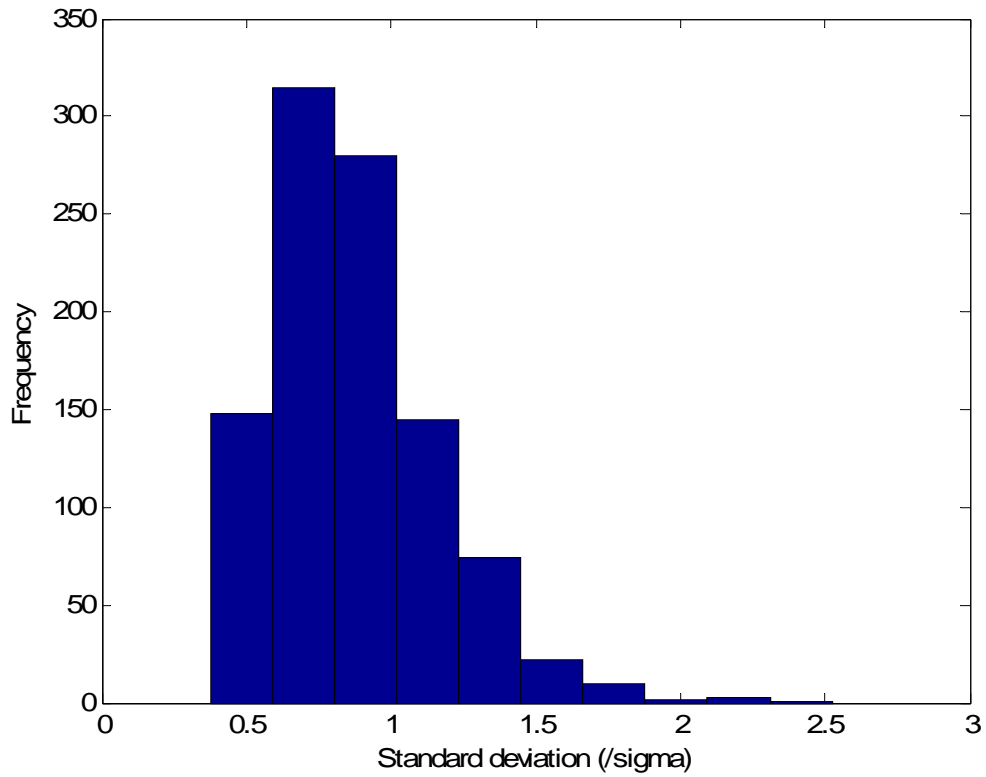


Figure 111. Histogram of staircase simulation results for 0.25σ step and 100 specimens.

Table 49. Summary statistics for simulation with 0.25σ step and 100 specimens.

Statistic for the simulated standard deviation distribution (using Dixon-Mood method)	Value ($/\sigma$)
Mean	0.8706
Standard deviation	0.2902
1 st percentile	0.4078
5 th percentile	0.4872
10 th percentile	0.5573
50 th percentile (median)	0.8280
90 th percentile	1.2442
95 th percentile	1.3656
99 th percentile	1.8111

Case 17. $s/\sigma = 0.5$, $N = 100$ specimens

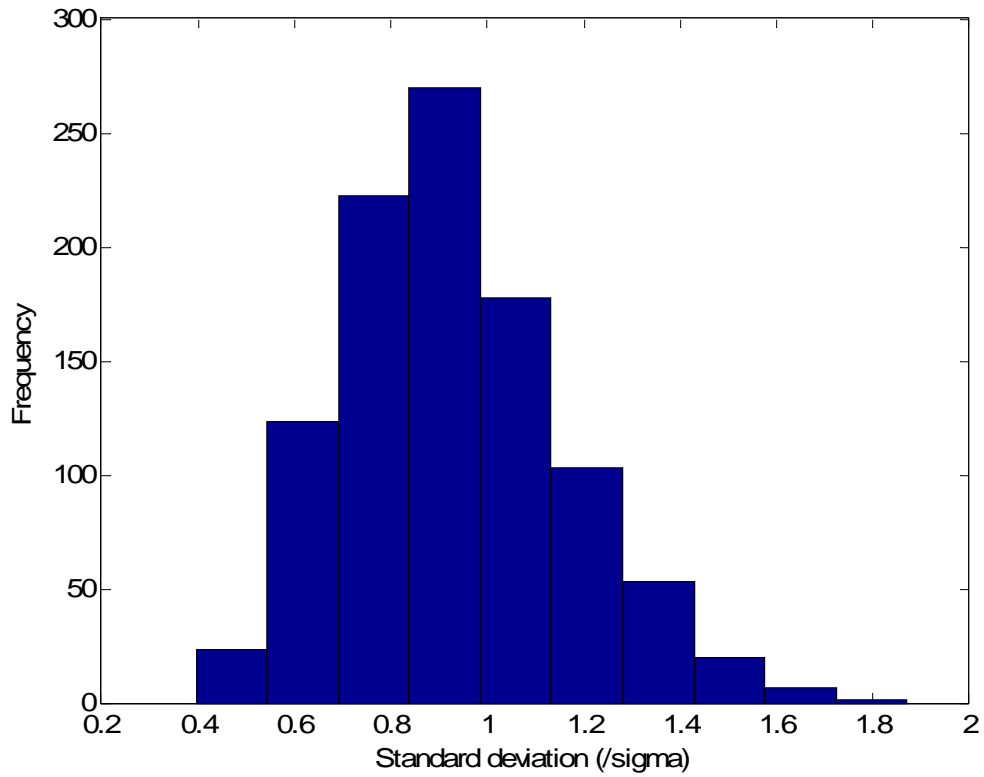


Figure 112. Histogram of staircase simulation results for 0.5σ step and 100 specimens.

Table 50. Summary statistics for simulation with 0.5σ step and 100 specimens.

Statistic for the simulated standard deviation distribution (using Dixon-Mood method)	Value ($/\sigma$)
Mean	0.9293
Standard deviation	0.2297
1 st percentile	0.4971
5 th percentile	0.5837
10 th percentile	0.6420
50 th percentile (median)	0.9062
90 th percentile	1.2288
95 th percentile	1.3506
99 th percentile	1.5714

Case 18. $s/\sigma = 0.75$, $N = 100$ specimens

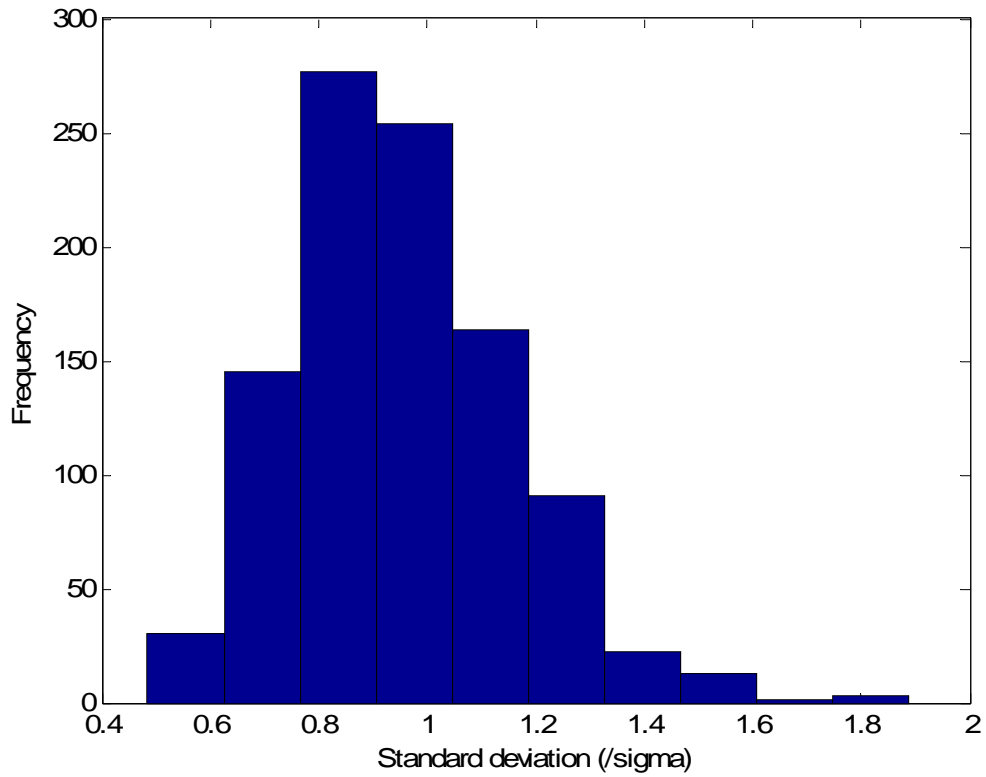


Figure 113. Histogram of staircase simulation results for 0.75σ step and 100 specimens.

Table 51. Summary statistics for simulation with 0.75σ step and 100 specimens.

Statistic for the simulated standard deviation distribution (using Dixon-Mood method)	Value ($/\sigma$)
Mean	0.9493
Standard deviation	0.2040
1 st percentile	0.5642
5 th percentile	0.6488
10 th percentile	0.6877
50 th percentile (median)	0.9222
90 th percentile	1.2153
95 th percentile	1.2998
99 th percentile	1.5236

Case 19. $s/\sigma = 1.0$, $N = 100$ specimens

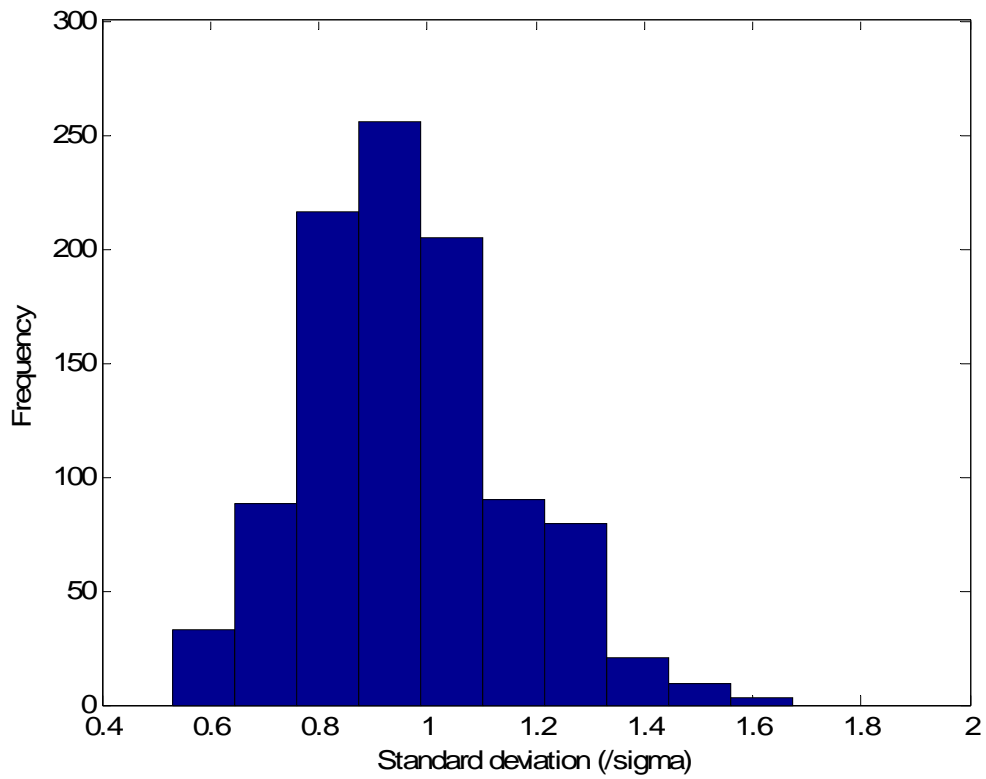


Figure 114. Histogram of staircase simulation results for 1.0σ step and 100 specimens.

Table 52. Summary statistics for simulation with 1.0σ step and 100 specimens.

Statistic for the simulated standard deviation distribution (using Dixon-Mood method)	Value ($/\sigma$)
Mean	0.9606
Standard deviation	0.1899
1 st percentile	0.5816
5 th percentile	0.6794
10 th percentile	0.7143
50 th percentile (median)	0.9533
90 th percentile	1.2270
95 th percentile	1.2899
99 th percentile	1.4677

Case 20. $s/\sigma = 1.5$, $N = 100$ specimens

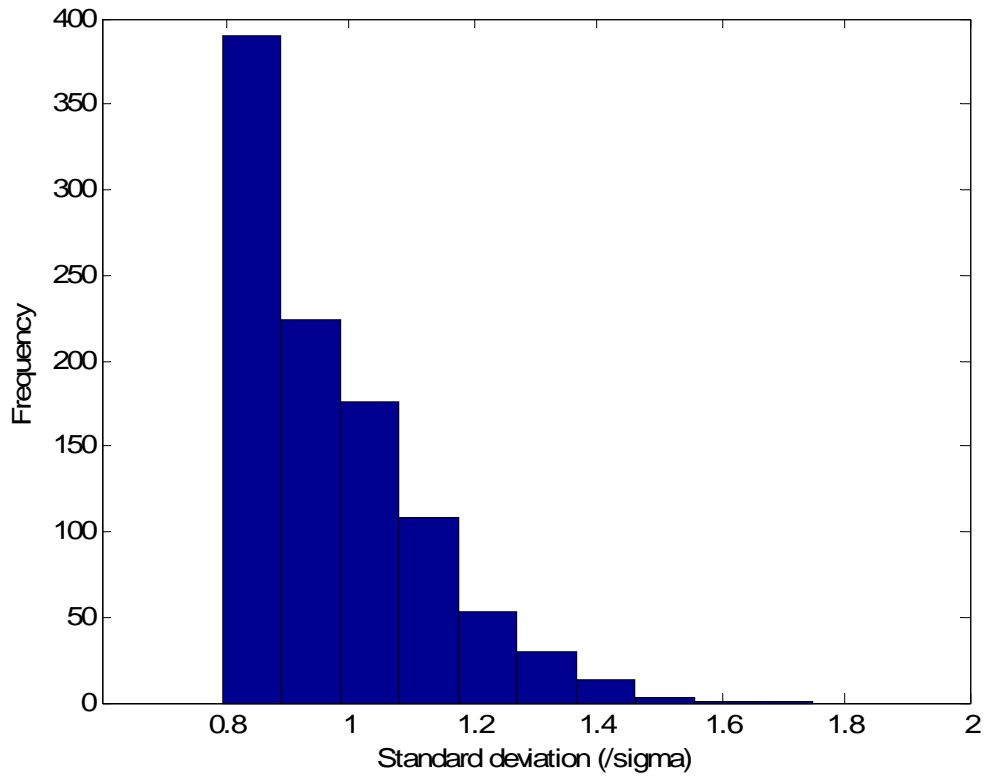


Figure 115. Histogram of staircase simulation results for 1.5σ step and 100 specimens.

Table 53. Summary statistics for simulation with 1.5σ step and 100 specimens.

Statistic for the simulated standard deviation distribution (using Dixon-Mood method)	Value ($/\sigma$)
Mean	0.9797
Standard deviation	0.1593
1 st percentile	0.7950
5 th percentile	0.7950
10 th percentile	0.7950
50 th percentile (median)	0.9608
90 th percentile	1.1824
95 th percentile	1.2640
99 th percentile	1.4400

Case 21. $s/\sigma = 2.0$, $N = 100$ specimens

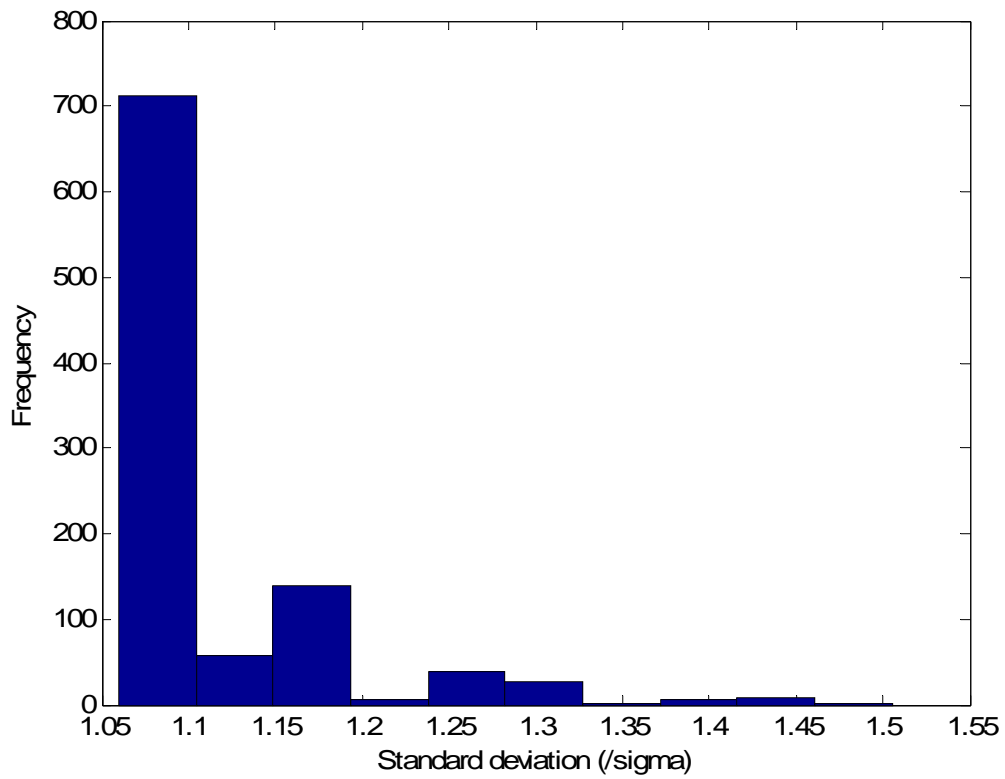


Figure 116. Histogram of staircase simulation results for 2.0σ step and 100 specimens.

Table 54. Summary statistics for simulation with 2.0σ step and 100 specimens.

Statistic for the simulated standard deviation distribution (using Dixon-Mood method)	Value ($/\sigma$)
Mean	1.0996
Standard deviation	0.0739
1 st percentile	1.0600
5 th percentile	1.0600
10 th percentile	1.0600
50 th percentile (median)	1.0600
90 th percentile	1.1632
95 th percentile	1.2811
99 th percentile	1.4139

APPENDIX G. SIMULATION RESULTS FOR STAIRCASE BOOTSTRAPPING ANALYSIS

In this appendix, the bootstrap results for several representative staircase scenarios are presented. For each case, the mean results and the standard deviation are given for each statistic taken from the simulated distribution of results.

Scenario #1: 15-specimen staircase with step 1σ . Data taken from 4-level tests only.

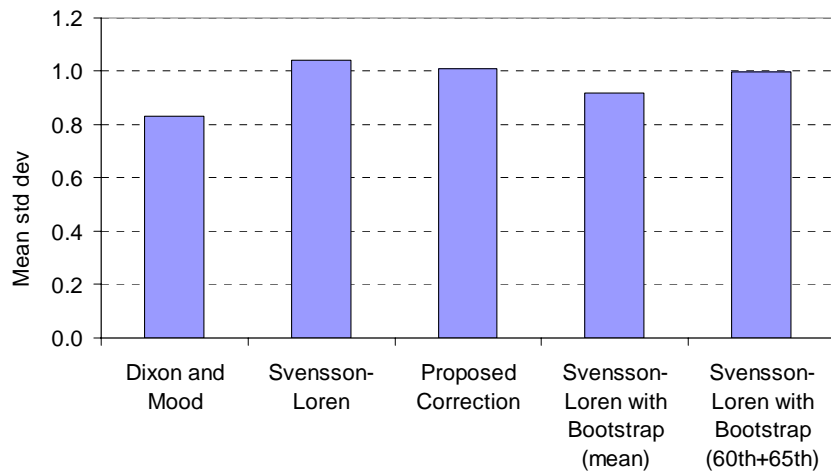


Figure 117. Mean standard deviation estimates for 15-specimen staircase test with step 1σ resulting in 4 stress levels.

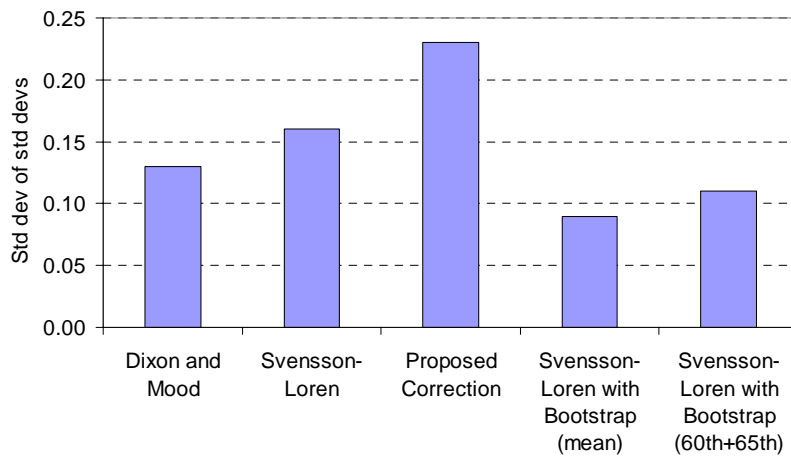


Figure 118. Standard deviation of standard deviation estimates for 15-specimen staircase test with step 1σ resulting in 4 stress levels.

Scenario #2: 20-specimen staircase with step 0.75σ . Data taken from 4-level tests only.

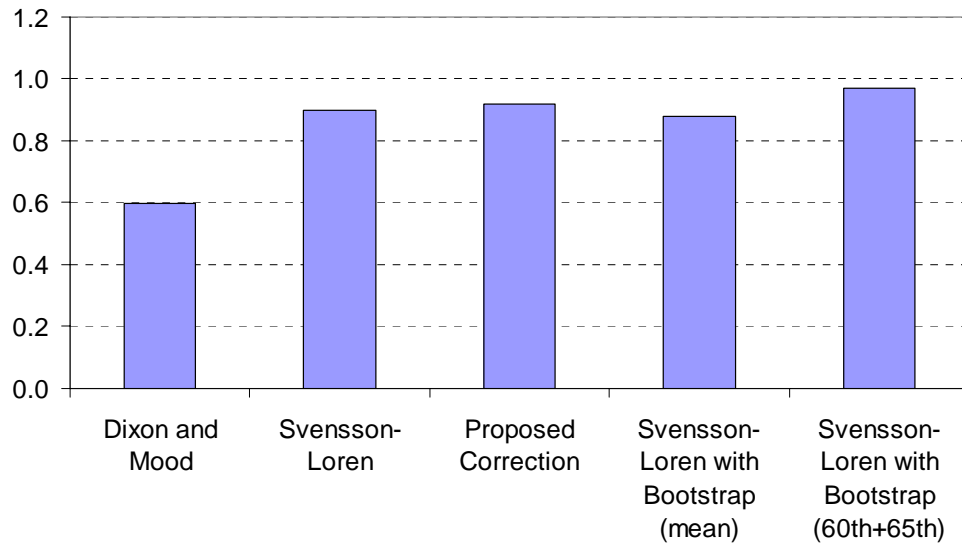


Figure 119. Mean standard deviation estimates for 20-specimen staircase test with step 0.75σ resulting in 4 stress levels.

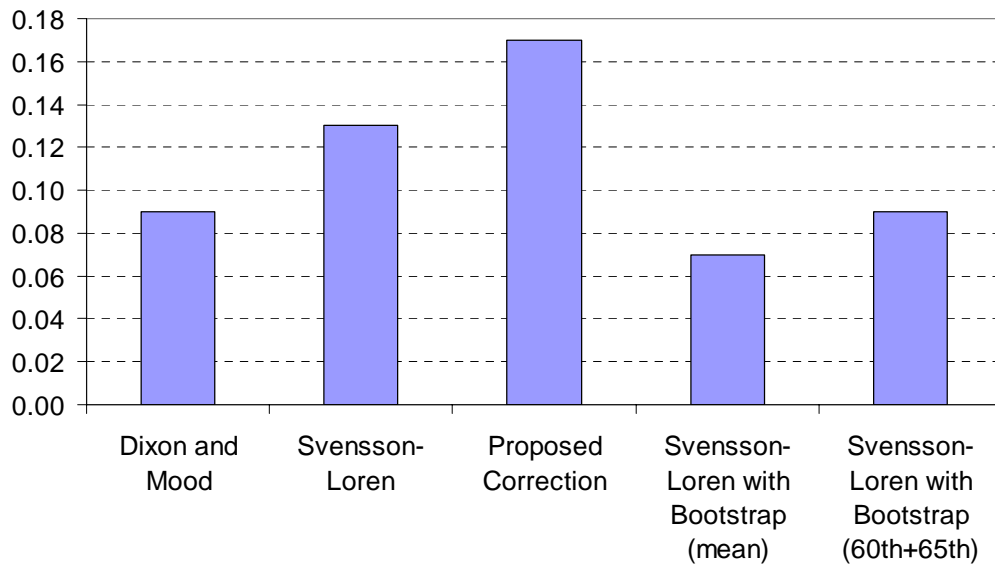


Figure 120. Standard deviation of standard deviation estimates for 20-specimen staircase test with step 0.75σ resulting in 4 stress levels.

APPENDIX H. PROBABILISTIC STRESS-LIFE CURVES USING THE RANDOM FATIGUE LIMIT MODEL BASED ON SIMULATED DATA

In this appendix, some of the P - S - N curves used for the test design investigation of Chapter V are presented. Only three runs for each strategy/scenario combination are detailed. These scenarios are specified as:

1. Scenario #1: An S - N curve with a linear region in the lower-cycle region which gradually transitioned to a fatigue limit between 10^5 and 10^7 cycles. The fatigue strength distribution for this scenario was modeled as normal with increasing standard deviation as the stress decreased. (Figure 59)
2. Scenario #2: A more curved S - N behavior with less evidence of a fatigue limit before 10^9 cycles. The fatigue strength distribution was again modeled as normal with increasing standard deviation as stress decreased. (Figure 61)
3. Scenario #3: A bilinear S - N model which exhibited a more distinct transition from the sloped lower-cycle behavior to the flat fatigue-limit behavior starting near 10^6 cycles. Unlike the previous two scenarios, a skewed fatigue strength distribution was used, with the larger percentile differences towards lower stresses. Standard deviation again increased as stress decreased. (Figure 63)

For each run of each scenario, three test design strategies were simulated. These strategies include (1) a traditional staircase approach, (2) a balanced strategy of four stress levels with three specimens each, and (3) an adaptive staircase approach with variable step size depending on outcomes. Each test design used 12 specimens.

The following pages show the P - S - N plots computed using best-fit RFL model analysis using the simulated data sets.

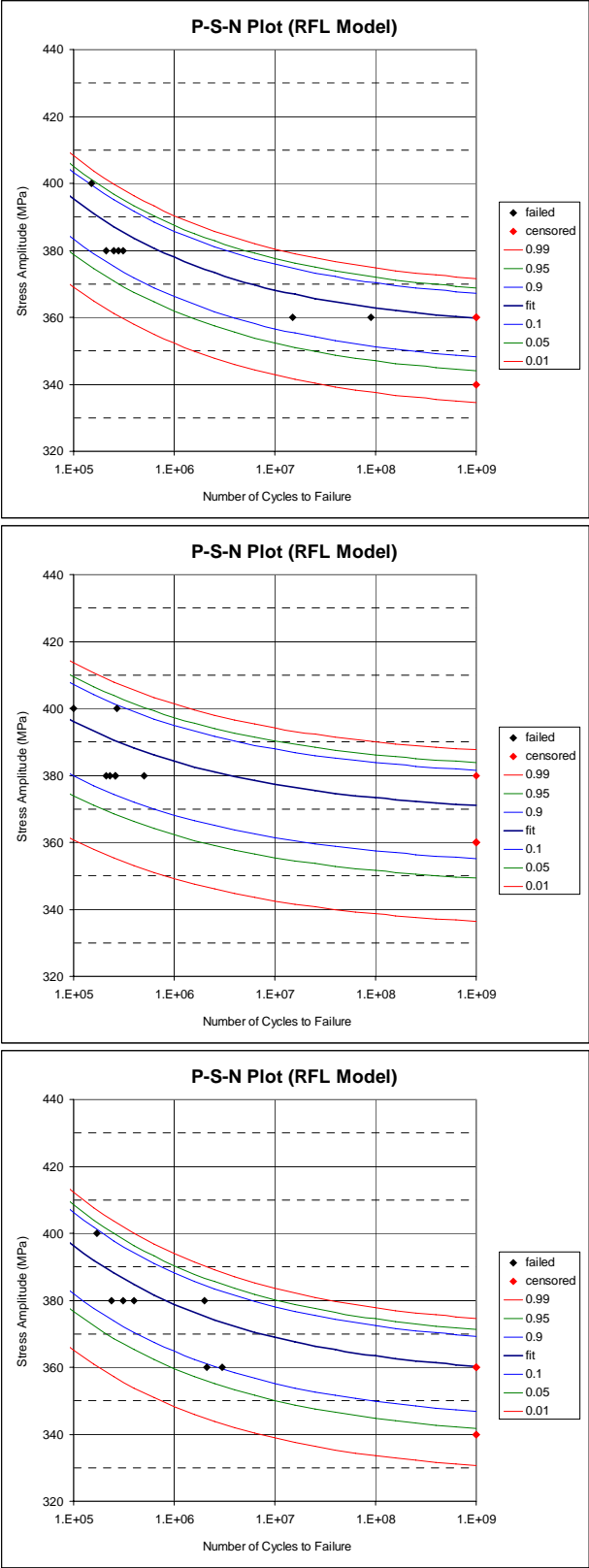


Figure 121. Scenario #1 using traditional staircase.

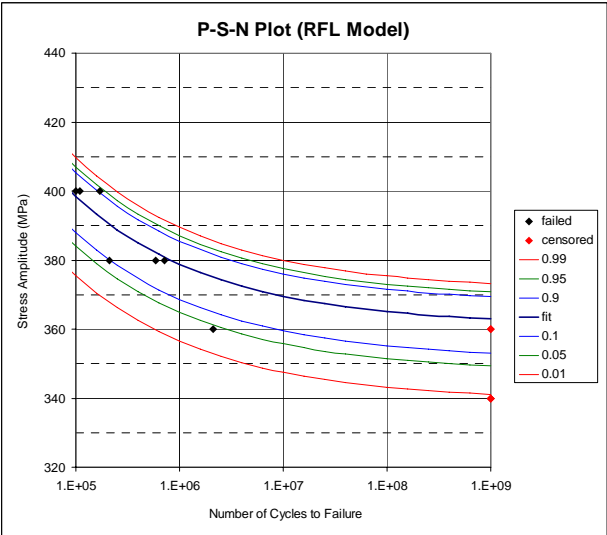
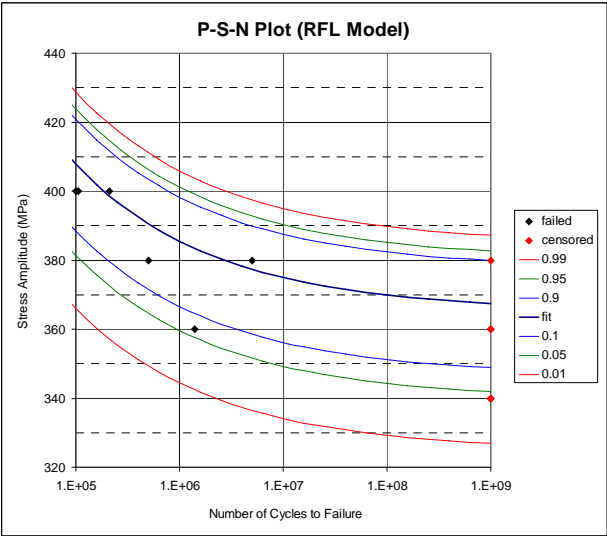
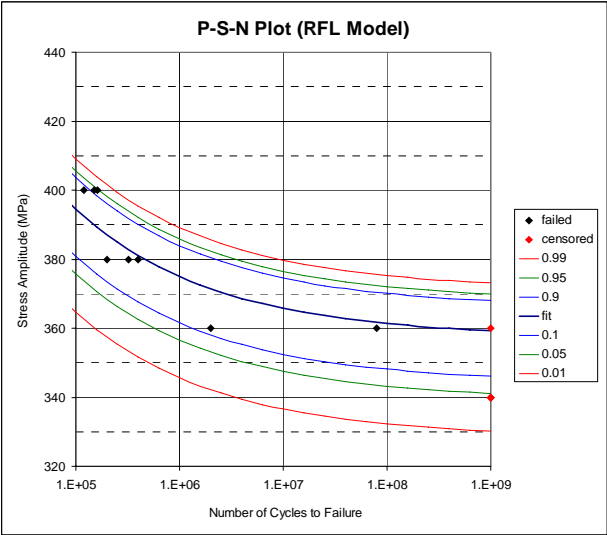


Figure 122. Scenario #1 using balanced strategy.

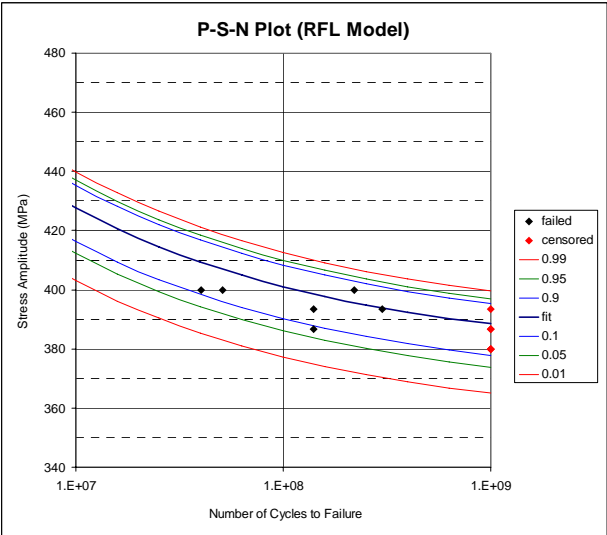
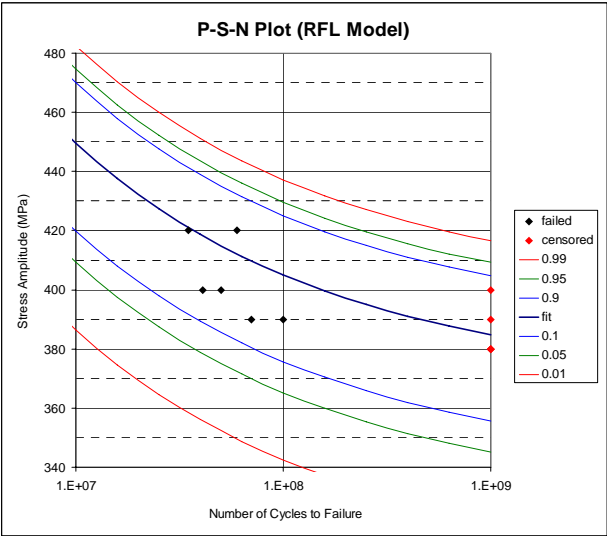
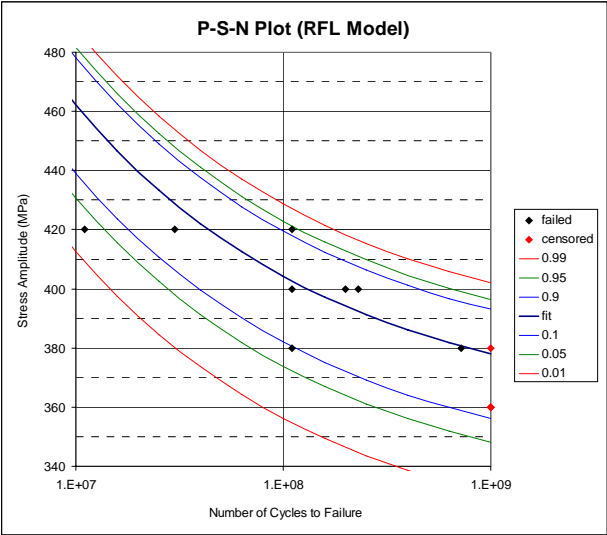


Figure 125. Scenario #2 using balanced strategy.

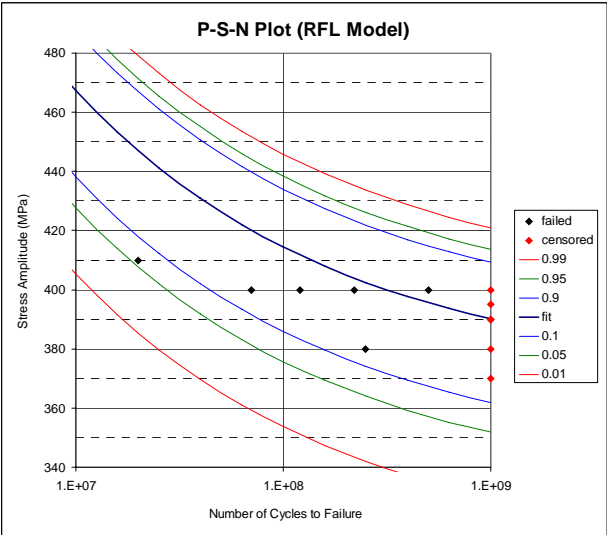
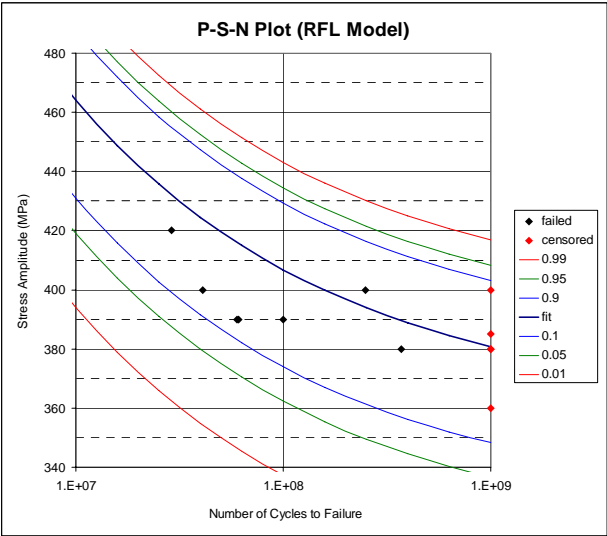
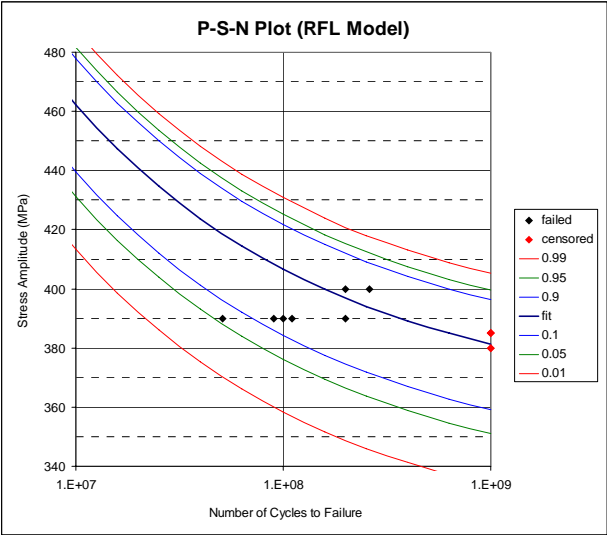


Figure 126. Scenario #2 using adaptive approach.

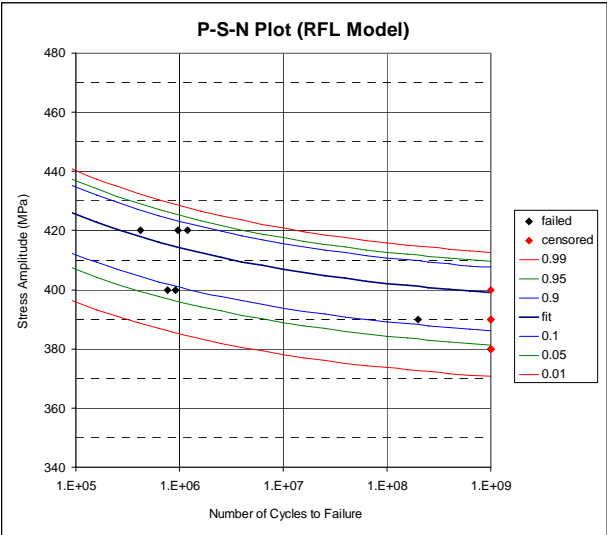
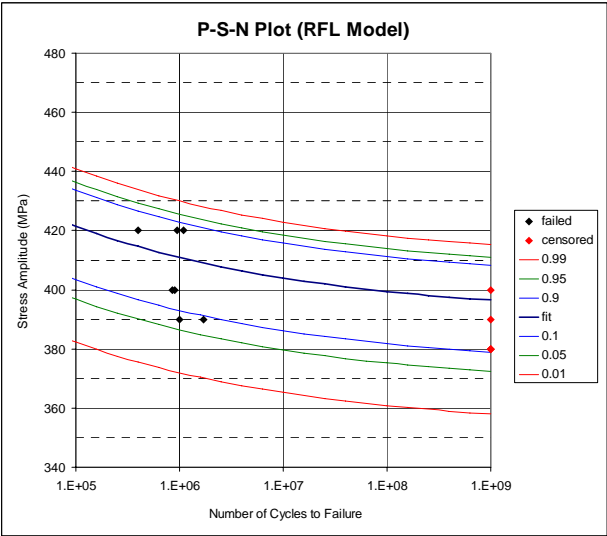
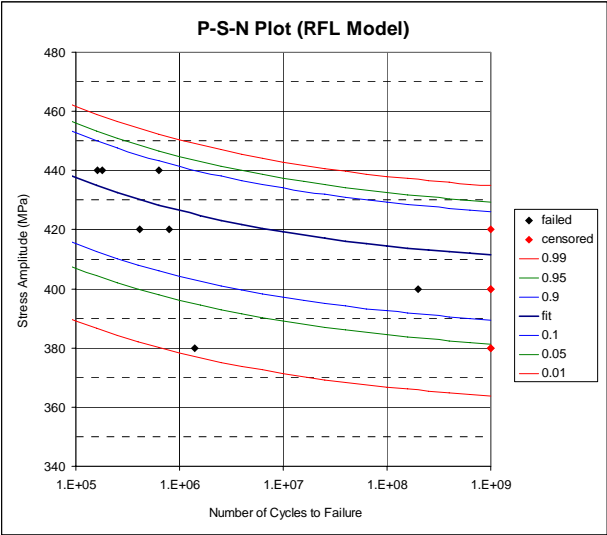


Figure 128. Scenario #3 using balanced strategy.

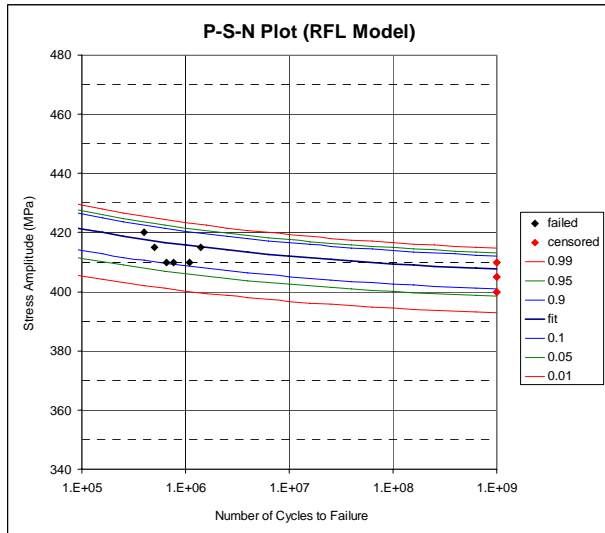
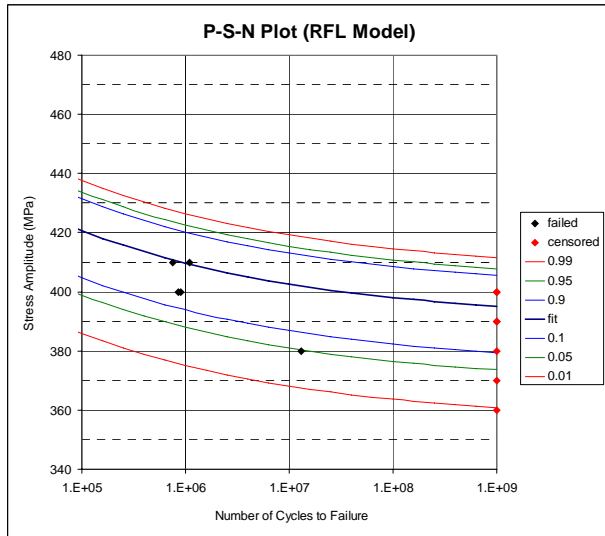
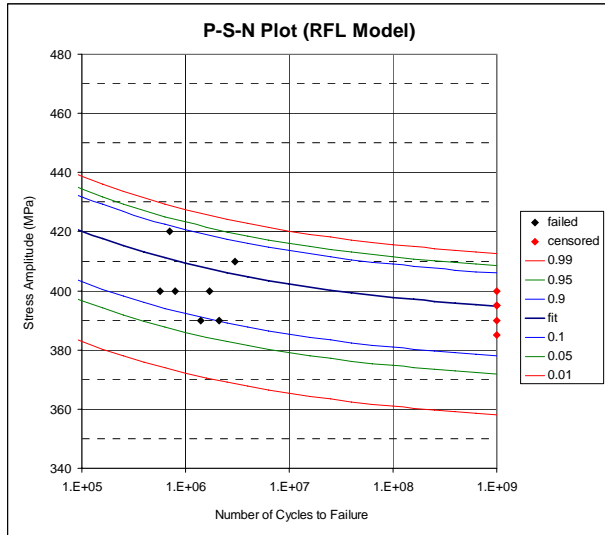


Figure 129. Scenario #3 using adaptive approach.

BIBLIOGRAPHY

1. Abe, T., Furuya, Y. and S. Matsuoka. "Gigacycle Fatigue Properties of 1800 MPa Class Spring Steels," *Fatigue and Fracture of Engineering Materials and Structures*, 27:159-167, 2004.
2. Abramowitz, M. and I. A. Stegun (Ed.). *Handbook of Mathematical Functions with Formulas, Graphs, and Mathematical Tables*, Dover (New York), 1972.
3. Aeronautical Systems Center (ASC/ENOI), "Engine Structural Integrity Program," MIL-HDBK-1783B (Wright-Patterson AFB, OH), 15 Feb 2002.
4. Air Force Research Laboratory, Materials and Manufacturing Directorate, Metals Branch (AFRL/MLLM). Ti-6Al-4V stress-life data collected in support of the National High Cycle Fatigue Science & Technology Program (Wright-Patterson AFB, OH), 1996-2004,
5. Air Force Research Laboratory, Propulsion Directorate. "HCF 2002 Annual Report," National High Cycle Fatigue Science & Technology Program (Wright-Patterson AFB, OH), Aug 2003.
6. Albert, W. A. J. "Über Treibsele am Harz," *Archive für Mineralogie, Geognosie, Bergbau und Hüttenkunde*, 10:215-234, 1838.
7. American Society for Testing and Materials. "A Guide for Fatigue Testing and the Statistical Analysis of Fatigue Data," ASTM STP 91-A, 2nd Ed., 1963.
8. American Society for Testing and Materials. "Standard Practice for Statistical Analysis of Linear or Linearized Stress-Life ($S-N$) and Strain-Life ($\epsilon-N$) Fatigue Data," ASTM Standard E739-80, Aug 1980.
9. Annis, Charles. "Discussion – Estimating Fatigues Curves with the Random Fatigue-Limit Model," *Technometrics*, 41:292-293, 1999.
10. Annis, Charles. "Runouts: Analyzing Fatigue Data with Runouts," StatisticalEngineering.com (website), 2004.
11. Annis, Charles, and James Griffiths. "Staircase Testing and the Random Fatigue Limit," Presented at the 6th National Turbine Engine High Cycle Fatigue Conference (Jacksonville, FL), Mar 2001.
12. Annis, Charles. Statistical Engineering, Inc., personal communication, 1 Jun 2004.
13. Atrens, A., Hoffelner, W., Duerig, T. W. and J. E. Allison. "Subsurface Crack Initiation in High Cycle Fatigue in Ti-6Al-4V and in a Typical Martensitic Stainless Steel," *ScriptaMet*, 17:601-606, 1983.

14. Bastenaire, F. A. "New Method for the Statistical Evaluation of Constant Stress Amplitude Fatigue-Test Results," *Probabilistic Aspects of Fatigue*, American Society for Testing and Materials, STP 511, 1972.
15. Bathias, C. "There is no Infinite Fatigue Life in Metallic Materials," *Fatigue and Fracture of Engineering Materials and Structures*, 22:559-565, 1999.
16. Bathias, C. and Jingang Ni. "Determination of Fatigue Limit Between 10^5 and 10^9 Cycles Using an Ultrasonic Fatigue Device," *Advances in Fatigue Lifetime Predictive Technique: Second Volume*, American Society for Testing and Materials, STP 1211, 1993.
17. Bathias, C. and P. Paris. *Gigacycle Fatigue in Mechanical Practice*, Marcel Dekker (New York), 2004.
18. Bathias, C., Miller, K. J. and Stefanie Stanzl-Tschegg. "Editorial: Gigacycle Fatigue," *Fatigue and Fracture of Engineering Materials and Structures*, 22:543, 1999.
19. Boyer, R., Welsch, G., and E. W. Collings (Ed.). *Material Properties Handbook*, ASM International (Materials Park, Ohio), 1994.
20. Braam, J. J. and S. van der Zwaag, "A Statistical Evaluation of the Staircase and the ArcSin \sqrt{P} Methods for Determining the Fatigue limit," *Journal of Testing and Evaluation*, 26:125-131, 1998.
21. Brownlee, K. A., Hodges, J. L., Jr. and Murray Rosenblatt. "The Up-and-Down Method with Small Samples," *Journal of the American Statistical Association*, 48:262-277, 1953.
22. Chandran, K. S. Ravi. "Duality of Fatigue Failures of Materials Caused by Poisson Defect Statistics of Competing Failure Modes," *Nature Materials*, 4:303-308, 2005.
23. Collins, J. A. *Failure of Materials in Mechanical Design*, Wiley (New York), 1993.
24. Corten, H. T., Dimoff, T. and T. J. Dolan. "An Appraisal of the Prot Accelerated Fatigue Test," *Proceedings of the American Society for Testing and Materials*, 54:875-894, 1954.
25. Dieter, G. E. *Mechanical Metallurgy*, McGraw-Hill (New York), 1976.
26. Dixon, W. J. "The Up-and-Down Method for Small Samples," *Journal of the American Statistical Association*, 60:967-978, 1965.
27. Dixon, W. J. and A. M. Mood, "A Method for Obtaining and Analyzing Sensitivity Data," *Journal of the American Statistical Association*, 43:109-126, 1948.

28. Donachie, M. J., Jr. (Ed.). *Titanium and Titanium Alloys: Source Book*, ASM International (Materials Park, OH), 1982.
29. Donachie, M. J., Jr. (Ed.). *Titanium: A Technical Guide*, ASM International (Materials Park, OH), 1988.
30. Dowling, Norman E. *Mechanical Behavior of Materials*, Prentice Hall (Upper Saddle River, NJ), 1999.
31. Efron, Bradley and Robert J. Tibshirani. *An Introduction to the Bootstrap*, Chapman & Hall (New York), 1993.
32. Elsayed, E. A. *Reliability Engineering*, Addison Wesley Longman (Reading, MA), 1996.
33. Epremian, E. and R. F. Mehl. "Investigation of the Statistical Nature of Fatigue Properties," NACA-TN-2719, Jun 1952.
34. Fang, Q. Z., Zhang, S. S., Zhao, M. H., and Y. J. Liu. "A New Method to Deal with the Staircase Fatigue Test," *Key Engineering Materials*, 183-187:951-956, 2000.
35. Finney, D. J. *Probit Analysis*, 3rd Ed., Cambridge University Press (Cambridge), 1971.
36. Hanaki, S., Yamashita, M., Uchida, H., Zako, M., and T. Kurashiki. "On Decision of S-N Curve Based on Evaluation of Fatigue Strength Distribution in Ultra High Cycle Fatigue Region," *Proceedings of the 3rd International Conference on Very High Cycle Fatigue*, Kusatsu, Japan, Sep 2004.
37. Hirose, H. "Estimation of Threshold Stress in Accelerated Life-Testing," *IEEE Transactions on Reliability*, 42:650-657, 1993.
38. Iversen, Gudmund R. *Bayesian Statistical Inference*, Sage Publications (London), 1984.
39. Johnson, V. E., Fitzgerald, M. and H. F. Martz. "Discussion – Estimating Fatigues Curves with the Random Fatigue-Limit Model," *Technometrics*, 41:294-296, 1999.
40. Kuzmenko, A. "Fatigue Strength of Structural Materials at Sonic and Ultrasonic Loading Frequencies," *Ultrasonics*, Jan 1975.
41. Lin, S. K., Lee, Y. L., and M. W. Lu. "Evaluation of the Staircase and the Accelerated Test Methods for Fatigue Limit Distributions," *International Journal of Fatigue*, 23:75-83, 2001.
42. Little, R. E. "Estimating the Median Fatigue Limit for Very Small Up-and-Down Quantal Response Tests and for S-N Data with Runouts," *Probabilistic Aspects of Fatigue*, American Society for Testing and Materials, STP 511, 1972.

43. Little, R.E. "The Up-and-Down Method for Small Samples with Extreme Value Response Distributions," *Journal of the American Statistical Association*, 69:803-806, 1974.
44. Little, R. E. *Manual on Statistical Planning and Analysis*, American Society for Testing and Materials, STP 588, 1975.
45. Little, R. E. "Optimal Stress Amplitude Selection in Estimating Median Fatigue Limits Using Small Samples," *Journal of Testing and Evaluation*, 18:115-122, 1990.
46. Little, R. E. and E. H. Jebe. *Statistical Design of Fatigue Experiments*, John Wiley & Sons (New York), 1975.
47. Madayag, A. F. (ed.) *Metal Fatigue: Theory and Design*, John Wiley & Sons (New York), 1969.
48. Mall, S., Nicholas, T., and T. W. Park. "Effect of Predamage from Low Cycle Fatigue on High Cycle Fatigue Strength of Ti-6Al-4V," *International Journal of Fatigue*, 25:1109-1116, 2003.
49. Mason, W. P. *Piezoelectric Crystals and Their Application in Ultrasonics*, Van Nostrand (New York), 1950.
50. Meeker, William Q. and Luis A. Escobar. *Statistical Methods for Reliability Data*, John Wiley & Sons (New York), 1998.
51. Miller, K. J. and W. J. O'Donnell. "The Fatigue Limit and its Elimination," *Fatigue and Fracture of Engineering Materials and Structures*, 22:545-557, 1999.
52. Morrissey, R. and T. Nicholas. "Staircase Testing of a Titanium Alloy in the Gigacycle Regime," *Proceedings of the 3rd International Conference on Very High Cycle Fatigue*, Kusatsu, Japan, Sep 2004.
53. Moshier, M. A., Nicholas, T., and B. M. Hillberry. "High Cycle Fatigue Threshold in the Presence of Naturally Initiated Small Surface Cracks," *Fatigue and Fracture Mechanics*, 33:129-146, 2002.
54. Mughrabi, H. "On 'Multi-Stage' Fatigue Life Diagrams and the Relevant Life-Controlling Mechanisms in Ultrahigh-Cycle Fatigue," *Fatigue and Fracture of Engineering Materials and Structures*, 25:755-764, 2002.
55. Mughrabi, H. "On the Life-Controlling Microstructural Fatigue Mechanisms in Ductile Metals and Alloys in the Gigacycle Regime," *Fatigue and Fracture of Engineering Materials and Structures*, 22:633-641, 1999.
56. Nakazawa, Hajime and Shotaro Kodama. "Statistical S-N Testing Method with 14 Specimens: JSME Standard Method for Determination of S-N Curves," *Statistical*

Research on Fatigue and Fracture, Japan Society of Materials Science, Elsevier (New York), 1987.

57. Nalla, R. K., Boyce, B. L., Campbell, J. P., Peters, J. O., and R. O. Ritchie. "Influence of Microstructure on High-Cycle Fatigue of Ti-6Al-4V: Bimodal vs. Lamellar Structures," *Metallurgical and Materials Transactions*, 33A:899-906, 2002.
58. Nelson, Wayne. *Accelerated Testing: Statistical Models, Test Plans, and Data Analyses*, John Wiley & Sons (New York), 1990.
59. Nelson, Wayne. "Fitting of Fatigue Curves with Nonconstant Standard Deviation to Data with Runouts," *Journal of Testing and Evaluation*, 12:69-77, Mar 1984.
60. Neter, J., Wasserman, W., and M. H. Kutner. *Applied Linear Statistical Models: Regression, Analysis of Variance, and Experimental Designs*, Irwin (Homewood, IL), 1990.
61. Nicholas, Theodore. "Step Loading for Very High Cycle Fatigue," *Fatigue & Fracture of Engineering Materials & Structures*, 25:861-869, 2002.
62. Nishijima, Satoshi. "Statistical Analysis of Small Sample Fatigue Data," *Statistical Research on Fatigue and Fracture*, Japan Society of Materials Science, Elsevier (New York), 1987.
63. Nishijima, Satoshi. *Transactions of Japanese Society Mechanical Engineering*, 50:451, 1984.
64. Nishijima, S. and K. Kanazawa. "Stepwise S-N Curve and Fish-Eye Failure in Gigacycle Fatigue," *Fatigue and Fracture of Engineering Materials and Structures*, 22:601-607, 1999.
65. Ochi, Y., Matsumura, T., Masaki, K. and S. Yoshida. "High-Cycle Rotating Bending Fatigue Property in Very Long-Life Regime of High-Strength Steels," *Fatigue and Fracture of Engineering Materials and Structures*, 25:823-830, 2002.
66. Pascual, Francis G. and William Q. Meeker. "Estimating Fatigue Curves with the Random Fatigue-Limit Model," *Technometrics*, 41:277-289, Nov 1999.
67. Pascual, Francis G. and William Q. Meeker. "Analysis of Fatigue Data with Runouts Based on a Model with Nonconstant Standard Deviation and a Fatigue Limit Parameter," *Journal of Testing and Evaluation*, 25:292-301, 1997.
68. Pollak, R., Palazotto, A., and T. Nicholas. "Investigation of the Staircase Method using Numerical Simulation," presented at the 10th National Turbine Engine High Cycle Fatigue Conference, New Orleans, LA, 8-11 Mar 2005.

69. Pollak, R., Palazotto, A., and T. Nicholas. "A Simulation-based Investigation of the Staircase Method for Fatigue Strength Testing," *Mechanics of Materials*, accepted for publication, Sep 2005.
70. Poncelet, J. V. *Introduction à la Mécanique, Industrille, Physique our Expérimentale*, Imprimerie de Gauthier-Villars (Paris), 1839.
71. Press, S. James. *Bayesian Statistics: Principles, Models, and Applications*, John Wiley & Sons (New York), 1989.
72. Prot, M. "Un Nouveau Type de Machine D'Essai des Metaux a la Fatigue par Flexion Rotative," *Rev. Metall.*, 34:440, 1937.
73. Rabb, B. R. "Staircase Testing – Confidence and Reliability," *Transactions on Engineering Sciences*, 40:447:464, 2003.
74. Ransom, J. T. and R. F. Mehl. "The Statistical Nature of the Endurance Limit," *Metals Transactions*, 185:364-365, 1949.
75. Rice, John A. *Mathematical Statistics and Data Analysis*, Duxbury Press (Belmont, CA), 1995.
76. Ritchie, R. O., Davidson, D. L., Boyce, B. L., Campbell, J. P., and O. Roder, "High-Cycle Fatigue of Ti-6Al-4V," *Fatigue and Fracture of Engineering Materials and Structures*, 22:621-631, 1999.
77. Shiozawa, K., Lu, L. and S. Ishihara. "S-N Curve Characteristics and Subsurface Crack Initiation Behavior in Ultra-Long Life Fatigue of a High Carbon-Chromium Bearing Steel," *Fatigue and Fracture of Engineering Materials and Structures*, 24:781-790, 2001.
78. Sinclair, G. M. and T. J. Dolan, "Effect of Stress Amplitude on Statistical Variability in Fatigue Life of 75S-T6 Aluminum Alloy," *Transactions of the American Society of Mechanical Engineers*, 75:867-872, 1953.
79. Sirian, C. R., Conn, A. F., Mignogna, R. B. and R. E. Green. "Method of Measuring Elastic Strain Distribution in Specimens Used for High Frequency Fatigue Testing," *Proceedings of the International Conference on Ultrasonics*, Oct 1981.
80. Sobczyk, K. and B. F. Spencer, Jr. *Random Fatigue: From Data to Theory*, Academic Press (San Diego), 1992.
81. Spindel, J. E. and E. Haibach. "Some Considerations in the Statistical Determination of the Shape of S-N Curves," *Statistical Analysis of Fatigue Data*, American Society for Testing and Materials, STP 744, 1981.

82. Stanzl-Tschegg, Stefanie. "Editorial: Special Double Issue on the International Conference 'Fatigue in the Very High Cycle Regime,' held in Vienna on 2-4 July 2001," *Fatigue and Fracture of Engineering Materials and Structures*, 25:725, 2002.
83. Suresh, S. *Fatigue of Materials*, Cambridge University Press (Cambridge), 1991.
84. Svensson, Thomas, and Jacques de Maré. "Random Features of the Fatigue Limit," *Extremes*, 2:165-176, 1999.
85. Svensson, T., Wadman, B., de Maré, J., and S. Lorén. "Statistical Models of the Fatigue Limit," Online Project Paper, Swedish National Testing and Research Institute, 2000.
86. Tanaka, K. and Y. Akiniwa. "Fatigue Crack Propagation Behavior Derived from *S-N* Data in Very High Cycle Regime," *Fatigue and Fracture of Engineering Materials and Structures*, 25:775-784, 2002.
87. Titanium Industries, Inc. "Titanium & Titanium Alloys," <http://www.titanium.com>, current as of Sep 2005.
88. Tóth, László. "Fatigue Crack Growth Laws and their Material Parameters," VII Summer School of Fracture Mechanics – Current Research on Fatigue and Fracture (Pokrzwyna, Poland), 2001.
89. Wackerly, Dennis D., Mendenhall, William, III and Richard L. Scheaffer. *Mathematical Statistics with Applications*, 5th ed., Duxbury Press (New York), 1996.
90. Ward, E. J., Schwartz, R. T. and D. C. Schwartz. "An Investigation of the Prot Accelerated Fatigue Test," *Proceedings of the American Society for Testing and Materials*, 53:885-891, 1953.
91. Wöhler, August. "Über die Festigkeits-Versuche mit Eisen und Stahl [On Strength Tests of Iron and Steel]," *Zeitschrift für Bauwesen*, 20:73-106, 1870.

VITA

Major Randall ‘Ty’ Pollak graduated Highest Honors with a B.S. in Aeronautical and Astronautical Engineering from the University of Illinois at Urbana-Champaign in 1994. He was commissioned a second lieutenant that same year and began his service as a cruise missile flight test engineer. He then attended the Air Force Institute of Technology, receiving his M.S. in Systems Engineering as a Distinguished Graduate in 1999. Following an assignment as an operations analyst, he returned to the Air Force Institute of Technology for his Ph.D. work in Materials Science and Engineering. His follow-on assignment is to the Air Force Research Laboratory’s Materials and Manufacturing Directorate.

REPORT DOCUMENTATION PAGE					<i>Form Approved OMB No. 0704-0188</i>	
<small>The public reporting burden for this collection of information is estimated to average 1 hour per response, including the time for reviewing instructions, searching existing data sources, gathering and maintaining the data needed, and completing and reviewing the collection of information. Send comments regarding this burden estimate or any other aspect of this collection of information, including suggestions for reducing the burden, to the Department of Defense, Executive Services and Communications Directorate (0704-0188). Respondents should be aware that notwithstanding any other provision of law, no person shall be subject to any penalty for failing to comply with a collection of information if it does not display a currently valid OMB control number.</small>						
PLEASE DO NOT RETURN YOUR FORM TO THE ABOVE ORGANIZATION.						
1. REPORT DATE (DD-MM-YYYY) Oct 2005		2. REPORT TYPE Doctoral Dissertation			3. DATES COVERED (From - To) Jan 2004 - Oct 2005	
4. TITLE AND SUBTITLE Analysis of Methods for Determining High Cycle Fatigue Strength of a Material with Investigation of Ti-6Al-4V Gigacycle Fatigue Behavior					5a. CONTRACT NUMBER 5b. GRANT NUMBER 5c. PROGRAM ELEMENT NUMBER 5d. PROJECT NUMBER 5e. TASK NUMBER 5f. WORK UNIT NUMBER	
6. AUTHOR(S) Pollak, Randall D., Major, USAF					8. PERFORMING ORGANIZATION REPORT NUMBER AFIT/DS/ENY/06-07	
7. PERFORMING ORGANIZATION NAME(S) AND ADDRESS(ES) Air Force Institute of Technology Graduate School of Engineering and Management (AFIT/ENY) 2950 Hobson Way, WPAFB OH 45433-7765					10. SPONSOR/MONITOR'S ACRONYM(S) 11. SPONSOR/MONITOR'S REPORT NUMBER(S)	
9. SPONSORING/MONITORING AGENCY NAME(S) AND ADDRESS(ES) N/A					12. DISTRIBUTION/AVAILABILITY STATEMENT APPROVED FOR PUBLIC RELEASE; DISTRIBUTION UNLIMITED.	
13. SUPPLEMENTARY NOTES						
14. ABSTRACT This research utilized the benefits of numerical simulation to investigate the staircase method for use in fatigue strength testing. The staircase method is a commonly used fatigue strength test, but its ability to characterize fatigue strength variability is extremely suspect. A modified staircase approach was developed and shown to significantly reduce bias and scatter in estimates for fatigue strength variance. Experimental validation of this proposed test strategy was accomplished using a dual-phase Ti-6Al-4V alloy. The HCF behavior of a second material with a very different microstructure (beta annealed Ti-6Al-4V) was also investigated. The random fatigue limit (RFL) model was investigated to characterize stress-life behavior. Two alternative models (bilinear and hyperbolic) were developed based on maximum likelihood methods to characterize the Ti-6Al-4V fatigue life behavior. Based on this research, designers should be better able to make reliable estimates of fatigue strength parameters using small-sample testing.						
15. SUBJECT TERMS Fatigue, Fatigue Tests, Simulation, Maximum Likelihood Estimation, Fatigue Strength, Probabilistic Fatigue, Titanium Alloys						
16. SECURITY CLASSIFICATION OF:			17. LIMITATION OF ABSTRACT		18. NUMBER OF PAGES	
a. REPORT U	b. ABSTRACT U	c. THIS PAGE U	UU		19a. NAME OF RESPONSIBLE PERSON Anthony N. Palazotto, AFIT/ENY 19b. TELEPHONE NUMBER (Include area code) (937) 255-3636 x4599, anthony.palazotto@afit.edu	